Electronic Supporting Information (ESI)

Synthesis and characterization of a novel [^{52}Mn]Mn-labelled affibody based radiotracer for HER2+ targeting

Balázs Váradi,[a,b,c] Károly Brezovcsik,[c] Zoltán Garda,[a] Enikő Madarasi,[a,b] Horea Szedlacsek,[d] Rodica-Aura Badea,[d] Andrei-Mihai Vasilescu,[d] Adina-Gabriela Puiu,[d] Aura Elena Ionescu,[d] Livia-Elena Sima,[d] Cristian V. A. Munteanu,[d] Simona Călăraș,[d] Adrienn Vágner,[e] Dezső Szikra,[e] Ngô Minh Toàn,[e] Tibor Nagy,[f] Zoltán Szűcs,[c*] Stefan Szedlacsek,[d*] Gábor Nagy,[e*] and Gyula Tircsó[a*]

[a.] *Department of Physical Chemistry, Faculty of Science and Technology, University of Debrecen, Egyetem tér 1, Debrecen, H-4032, Hungary.* gyula.tircso@science.unideb.hu

[b.] *Doctoral School of Chemistry, University of Debrecen, Egyetem tér 1, Debrecen, H-4032, Hungary.*

[c.] *Institute for Nuclear Research, Bem tér 18/C, Debrecen, H-4026, Hungary.* zszucs@atomki.hu

[d.] *Institute of Biochemistry, 296 Splaiul Independentei, Bucharest, 060031, Romania.* szedlacs@yahoo.co.uk

[e.] *Scanomed Ltd., Nagyeredei krt 98, Debrecen, H-4032, Hungary.* Nagy.Gabor@scanomed.hu

[f.] *Department of Applied Chemistry, Faculty of Science and Technology, University of Debrecen, Egyetem tér 1, Debrecen, H-4032, Hungary.*

* Corresponding authors

Table of content

Table of content....2
1. Synthesis of the ligands for analytical studies....4
Reagents and materials....4
General experimental procedures....4
Synthesis of the 3,9-PC2ABn^{pNO2} (L^0)....5
Diethyl 2,2'-(6-(*tert*-butoxycarbonyl)-3,6,9-triaza-1(2,6)-pyridinacyclodecaphane-3,9-diyl)diacetate (2)....6
Diethyl 2,2'-(3,6,9-triaza-1(2,6)-pyridinacyclodecaphane-3,9-diyl)diacetate (3)....9
Diethyl 2,2'-(6-(4-(tert-butoxycarbonyl)benzyl)-3,6,9-triaza-1(2,6)-pyridinacyclodecaphane-3,9-diyl)diacetate (4)....13
2,2'-(6-(4-Carboxybenzyl)-3,6,9-triaza-1(2,6)-pyridinacyclodecaphane-3,9-diyl)diacetic acid (L^1)....17
Diethyl 2,2'-(6-(*tert*-butoxycarbonyl)-3,6,9-triaza-1(2,6)-pyridinacyclodecaphane-3,9-diyl)(2R,2'R)-dipropionate (5)....21
Diethyl 2,2'-(3,6,9-triaza-1(2,6)-pyridinacyclodecaphane-3,9-diyl)(2R,2'R)-dipropionate (6)....25
Diethyl 2,2'-(6-(4-(*tert*-butoxycarbonyl)benzyl)-3,6,9-triaza-1(2,6)-pyridinacyclodecaphane-3,9-diyl)(2R,2'R)-dipropionate (7)....28
(2R,2'R)-2,2'-(6-(4-carboxybenzyl)-3,6,9-triaza-1(2,6)-pyridinacyclodecaphane-3,9-diyl)dipropionic acid (L^2)32
2,2'-(3,6,9-triaza-1(2,6)-pyridinacyclodecaphane-3,9-diyl)bis(1-(piperidin-1-yl)ethan-1-one) (8)....36
Tert-butyl 4-((3,9-bis(2-oxo-2-(piperidin-1-yl)ethyl)-3,6,9-triaza-1(2,6)-pyridinacyclodecaphane-6-yl)methyl)benzoate (9)....40
4-((3,9-bis(2-oxo-2-(piperidin-1-yl)ethyl)-3,6,9-triaza-1(2,6)-pyridinacyclodecaphane-6-yl)methyl)benzoic acid (L^3)....44
2. Physicochemical characterization of the Mn(II) complexes formed by the BFCs: stability and speciation, dissociation and relaxivity....49
3. [^{52}Mn]Mn labelling of the ligands....54
Radiochemistry experiments....54
General....54
Production and purification of ^{52}Mn radioisotope in the laboratory of Institute for Nuclear Research....54
^{52}Mn labelling of 3,9-PC2ABn^{pCO2H}, 3,9-PC2MABn^{pCO2H}, 3,9-PC2AM^{pip}Bn^{pCO2H}....54
trans-CDTA challenge of [^{52}Mn][Mn(3,9-PC2ABn^{pCO2H})], [^{52}Mn][Mn(3,9-PC2MABn^{pCO2H})], [^{52}Mn][Mn](3,9-PC2AM^{pip}Bn^{pCO2H})]....55
Production of ^{52}Mn in the laboratory of Scanomed Ltd....59
Labelling optimization of 3,9-PC2ABn^{pCO2H}....60
4. Synthesis of the bifunctional chelator (BFC)....62
3,9-bis((4-nitrophenyl)sulfonyl)-3,6,9-triaza-1(2,6)-pyridinacyclodecaphane (11)....62
Tert-butyl 4-((3,9-bis((4-nitrophenyl)sulfonyl)-3,6,9-triaza-1(2,6)-pyridinacyclodecaphane-6-yl)methyl)benzoate (12)....65
Tert-butyl 4-(3,6,9-triaza-1(2,6)-pyridinacyclodecaphane-6-ylmethyl)benzoate (13)....69
4-(3,6,9-Triaza-1(2,6)-pyridinacyclodecaphane-6-ylmethyl)benzoic acid (14)....73
4-((3,9-Bis(2-(*tert*-butoxy)-2-oxoethyl)-3,6,9-triaza-1(2,6)-pyridinacyclodecaphane-6-yl)methyl)benzoic acid (15)....76

Di-*tert*-butyl 2,2'-(6-(4-((2-(2,5-dioxo-2,5-dihydro-1H-pyrrol-1-yl)ethyl)carbamoyl)benzyl)-3,6,9-triaza-1(2,6)-pyridinacyclodecaphane-3,9-diyl)diacetate (16) 80
2,2'-(6-(4-((2-(2,5-dioxo-2,5-dihydro-1H-pyrrol-1-yl)ethyl)carbamoyl)benzyl)-3,6,9-triaza-1(2,6)-pyridinacyclodecaphane-3,9-diyl)diacetic acid (17) 83
2,2'-(6-(4-nitrobenzyl)-3,6,9-triaza-1(2,6)-pyridinacyclodecaphane-3,9-diyl)diacetic acid (L^0) 86
5. Expression and purification of the anti-HER2 affibody 91
Materials and Methods 91
Analysis of anti-HER2 affibody dimerization state 91
Mass spectrometry analyses 91
Materials 91
Methods 92
Mass spectrometry identification of proteins using the bottom-up approach 95
In-gel digestion 95
LC-MS/MS analysis 95
Protein identification 95
Mass spectrometry analysis of purified anti-HER2 affibody 96
Sample preparation 96
nLC-MS/MS analysis of anti-HER2 affibody 96
Data analysis 96
Results 96
6. Coupling and labelling of the BFC with anti-HER2 affibody 101
Conjugation of 3,9-PC2ABn^{pMA}-Cys-HER2-affibody (18) 101
Production of [[^{52}Mn]Mn(3,9-PC2ABn^{pMA})(H_2O)]-Cys-HER2-affibody (19) 105
7. HER2+ cells labelling with affibody-AlexaFluor 555 conjugate 108
Conjugation of AlexaFluor 555 to Anti-HER2-Affibody (23) 108
Cell lines 112
Flow cytometry analysis 112
8. Small-Animal PET/MRI imaging with [^{52}Mn]Mn-labelled Anti-HER2-affibody 113
Materials and methods 113
Cell line and animal models 113
PET imaging and in vivo measurements 113
MDA-MB HER2+ 114
4T1 HER2- (1. mouse) 123
4T1 HER2- (2. mouse) 132
References 142

1. Synthesis of the ligands for analytical studies

Reagents and materials

Starting reagents/solvents were purchased from Sigma-Aldrich (St. Louis, MO, USA), Tokyo Chemical Industry (Tokyo, Japan) and Fluorochem (Hadfield, Glossop, UK) and were used without further purification unless otherwise stated. Deionized Milli-Q® water was used for the preparation of all aqueous solutions (equilibrium/kinetic/relaxometric studies).

General experimental procedures

NMR spectra (^{1}H and ^{13}C-JMOD) were recorded at 298.0 K using a Bruker Avance DRX 360 MHz (360.13 MHz - ^{1}H, 90.55 MHz - ^{13}C) or Avance I 400 MHz (400.13 MHz - ^{1}H, 100.62 MHz - ^{13}C) spectrometer. The chemical shifts (δ) were calibrated against reference solvent peaks (^{1}H, δ = 7.26 ppm and ^{13}C, δ = 77.16 ppm for $CDCl_3$; ^{1}H, δ = 4.79 ppm for D_2O; ^{1}H, δ =-3.31 ppm and ^{13}C, δ = 49.00 ppm for CD_3OD, ^{1}H, δ = 1.32 ppm and ^{13}C, δ = 118.26 ppm for CD_3CN, 1H, δ = 2.50 ppm and ^{13}C, δ = 39.52 ppm for DMSO-d_6).[1]

In ^{13}C-JMOD (J-modulated) spectrum the multiplicity of the ^{13}C signals (methyl: quartet, methylene: triplet, methine: doublet, quaternary: singlet) is reflected in the phase of the fully ^{1}H decoupled ^{13}C spectrum using the SEFT (Spin-Echo Fourier Transform) technique. In the spectrum, the methyl and methine signals (odd number of hydrogen atoms) give signals with positive phase, while the methylene and quaternary carbon atoms (even number and lacking hydrogen atoms) give negative phase signals.

High resolution (ESI) mass spectra were measured on a Bruker maXis II UHR ESI-QTOF mass spectrometer (Bruker, Bremen, Germany) using a capillary electrophoresis - electrospray ionization (CE-ESI) Sprayer interface (G1607B, Agilent). Sample introduction was carried out with an Agilent 7100 model capillary electrophoresis (CE) instrument (Agilent, Waldbronn, Germany) using a 70 cm x 75 µm id. capillary (Polymicro, Phoenix, AZ, USA). MS instrument was controlled by otofControl version 4.1 (build: 3.5, Bruker), spectra were processed by Compass DataAnalysis version 4.4 (build: 200.55.2969, Bruker). MS measurements were performed in positive ionization mode; 0.8 bar nebulizer pressure, 200 °C dry gas temperature, 4.5 L/min dry gas flow rate, 3500 V capillary voltage, 500 V end plate offset, 1 Hz spectra rate, 100-1400 m/z mass range were applied. Sodium formate calibrant enabled internal m/z calibration.

Analytical high-performance liquid chromatography (HPLC) was performed with a Waters Alliance 2690 HPLC (Waters Inc., Milford, MA, USA) system equipped with a Waters 996 photodiode array detector with an Alliance series column heater at 25 °C temperature equipped with a Luna C18(2) column (150 mm × 4.6 mm, 100 Å, 3 µm or 5 µm, Phenomenex Inc., Torrance, CA, USA) with a flow rate of 1.00 mL/min. Results were analysed with Waters Empower software.

The reactions requiring microwave irradiation were performed in a CEM Discover microwave synthesis reactor, using dynamic (constant temperature) mode and strong stirring during the reaction.

Flash normal-phase chromatography was performed using a CombiFlash® EZ Prep compact flash preparative chromatography system (Teledyne Isco Inc., Lincoln, NE, USA) with integrated photodiode array detector equipped with a Redi*SepR*f® Gold silica gel disposable flash column (40 gram, 60 Å, 20 - 40 µm, Teledyne Isco Inc., Lincoln, NE, USA).

Preparative reverse-phase HPLC was performed using a YL9100 (YoungIn Chromass, Anyang-si Korea) system with YL91110s quaternary pump with YL9120s UV/Vis detector equipped with a Luna C18(2) Prep column (250 mm × 21.2 mm, 100 Å, 5 µm or 10 µm, Phenomenex Inc., Torrance, CA, USA). The solvent flow rate in this case was 25.00 mL/min using gradient elution as follows: eluent A (5 mM TFA in water) and B (acetonitrile).

Proteins and conjugates were analysed on XBridge Peptide BEH C18 OBD column (150 mm × 4.6 mm, 300 Å, 5 µm, Waters Inc., Milford, MA, USA) and separated on XBridge Peptide BEH C18 OBD Prep column (150 mm × 10.0 mm, 300 Å, 5 µm, Waters Inc., Milford, MA, USA).

Synthesis of the 3,9-PC2ABn^{pNO2} (L^0)

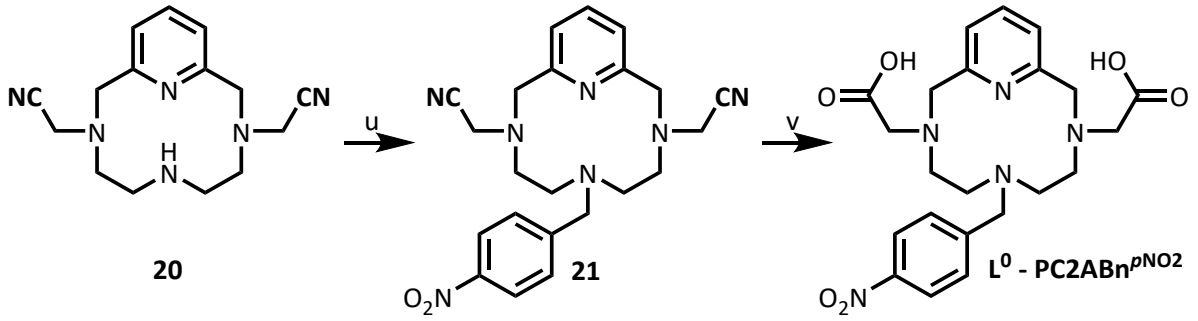

Scheme S001. Synthesis of the 3,9-PC2ABn^{pNO2} (**L^0**) ligand; (u) 1-(bromomethyl)-4-nitrobenzene, NaI, DIPEA, ACN, 60 °C, 72 h; (v) 12 M HCl, 110 °C, 3 h (66%).

For the synthesis of **L^0** (Scheme S01) we applied the previously reported synthesis of Won D. Kim et al. which is based on the use of 3,9-Bis(methylenenitrile)-3,6,9,15-tetraazabicyclo[9.3.1]pentadeca1(15),11,13-triene (**20**) as a starting material.[2, 3] Alkylation of compound **20** with 1-(bromomethyl)-4-nitrobenzene in acetonitrile in the presence of *N,N*-diisopropylethylamine and sodium iodide gave the compound **21**. The **L^0** ligand studied was obtained following the hydrolysis of the nitrile groups by concentrated hydrochloric acid.

Diethyl 2,2'-(6-(*tert*-butoxycarbonyl)-3,6,9-triaza-1(2,6)-pyridinacyclodecaphane-3,9-diyl)diacetate (2)

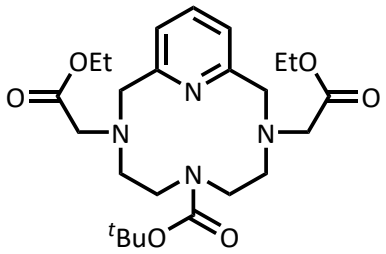

The alkylation of 6-Boc-Pyclen (*tert*-butyl 3,6,9-triaza-1(2,6)-pyridinacyclodecaphane-6-carboxylate, **1**) in acetonitrile under an argon atmosphere using sodium acetate trihydrate as a weak base. 500 mg (1.63 mmol) of 6-Boc-Pyclen was dissolved in 200 mL of acetonitrile following the addition of 910 mg (6.69 mmol) of sodium acetate trihydrate. The reaction mixture was then heated to 65 °C and a solution of ethyl bromoacetate (510 mg, 3.05 mmol) in dissolved in 50 mL of acetonitrile was added to the reaction mixture dropwise while stirred vigorously. The reaction mixture was kept stirred at 65 °C for an additional 48 h followed by the removal of the solvent under vacuum to afford the crude product **2** as a brownish oil (687 mg, yield 88%).

^{1}H NMR (360.13 MHz, MeOD-d_4) δ 1.32 (t, J = 7.1 Hz, 6H), 1.41 (s, 9H), 2.66 (t, J = 6.4 Hz, 4H), 3.24 (m, 4H), 3.63 (s, 4H), 3.99 (s, 4H), 4.26 (q, J = 7.1 Hz, 4H), 4.87 (s, 2H), 7.35 (d, J = 7.7 Hz, 2H), 7.85 (t, J = 7.7, 1H) ppm; **^{13}C-JMOD NMR** (90.56 MHz, MeOD-d_4) δ 14.61, 28.55, 48.69, 53.60, 57.55, 61.17, 62.13, 81.55, 123.80, 139.95, 157.87, 158.14, 173.90 ppm; **UHRMS** (ESI+) *m/z* calculated for $C_{24}H_{38}N_4O_6$ $[M+H]^+$ 479.2864; found 479.2863; **HPLC** purity (260 nm): 85.67%; retention time: 8.482 min; gradient: 0.00→15.00 min 5→95% B; eluent: mixture of 5 mM TFA in MQ-water (A) and acetonitrile (B); flow: 1.00 mL/min; injection volume: 10.00 µL; sample: 0.70 mg/mL 50% ACN in H_2O; column: Phenomenex Luna C18(2) 100 Å, 3 µm, 150 × 4.60 mm; column ID: H20-260762.

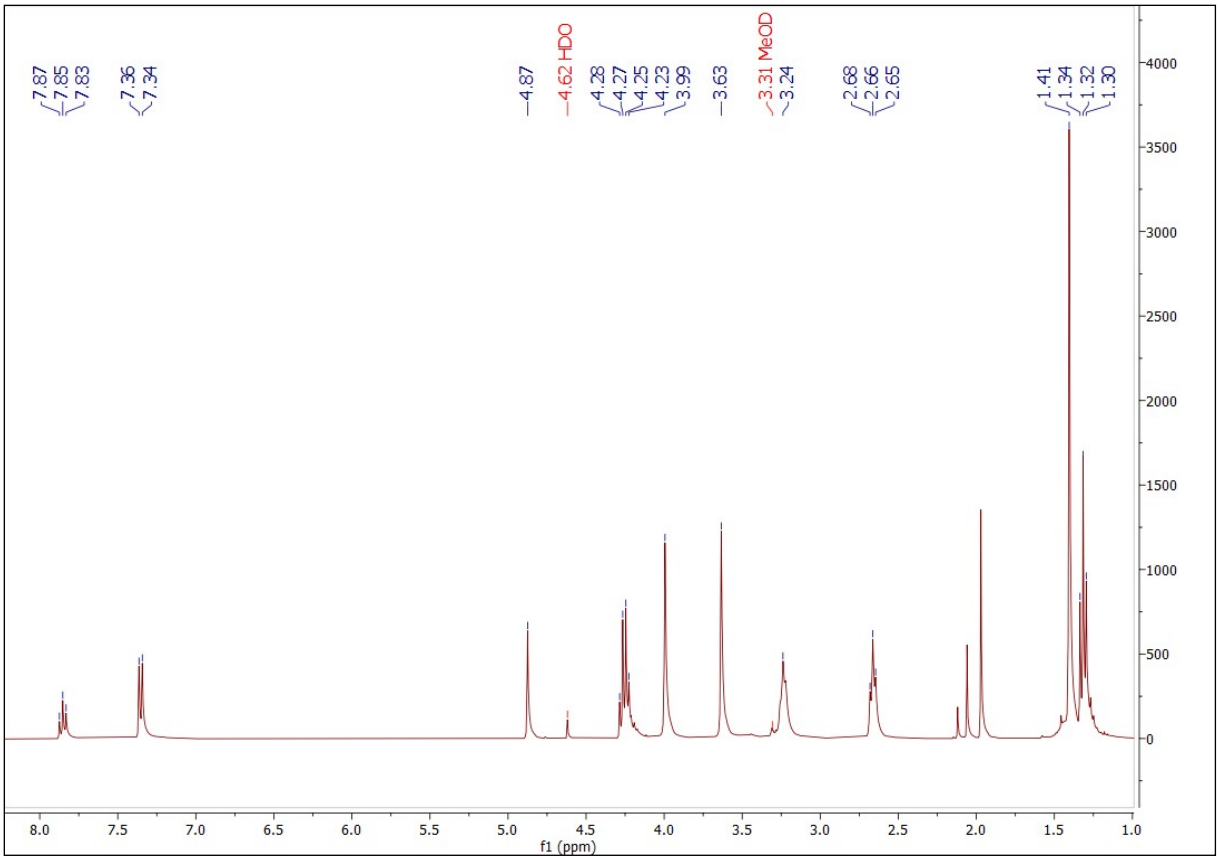

Figure S001. ^{1}H NMR (360.13 MHz, 298.0 K, MeOD-*d4*) spectra of compound **2**.

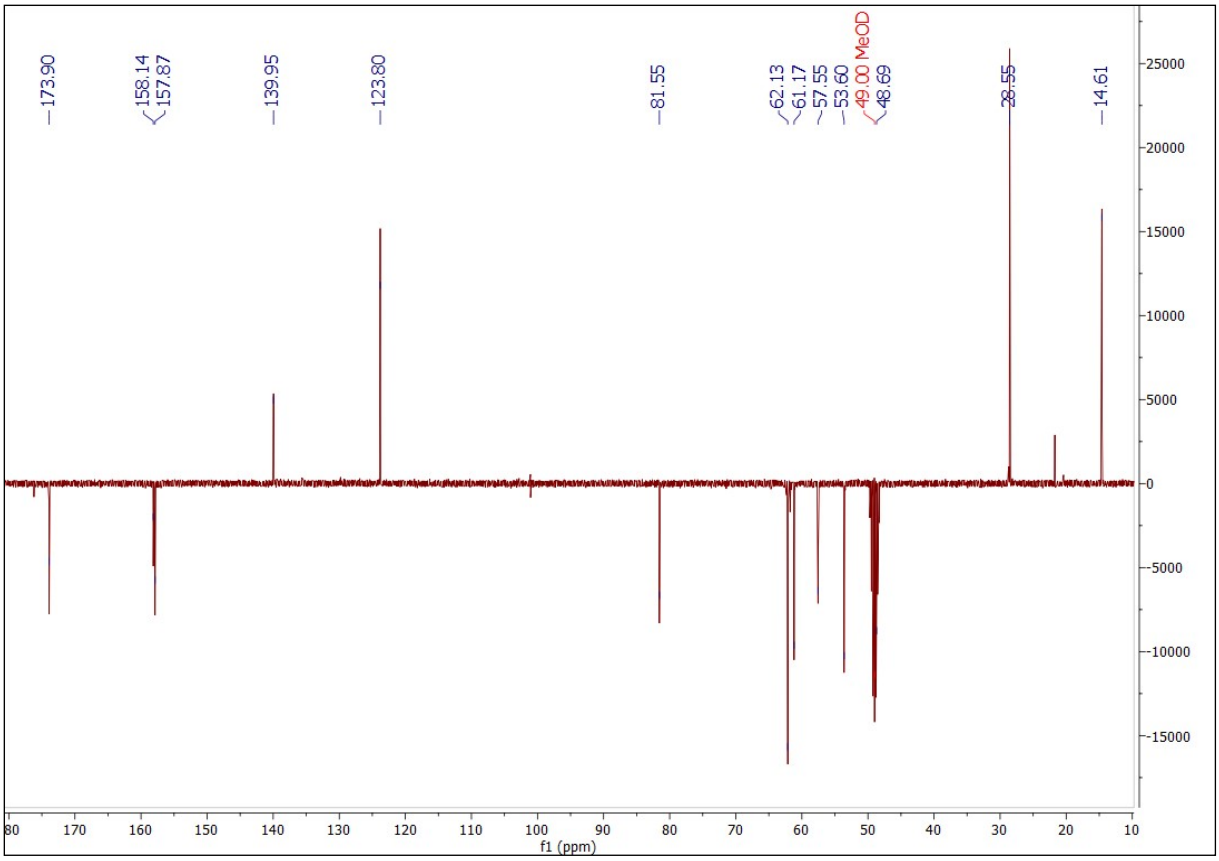

Figure S002. ^{13}C-JMOD NMR (90.56 MHz, 298.0 K, MeOD-*d4*) spectra of compound **2**.

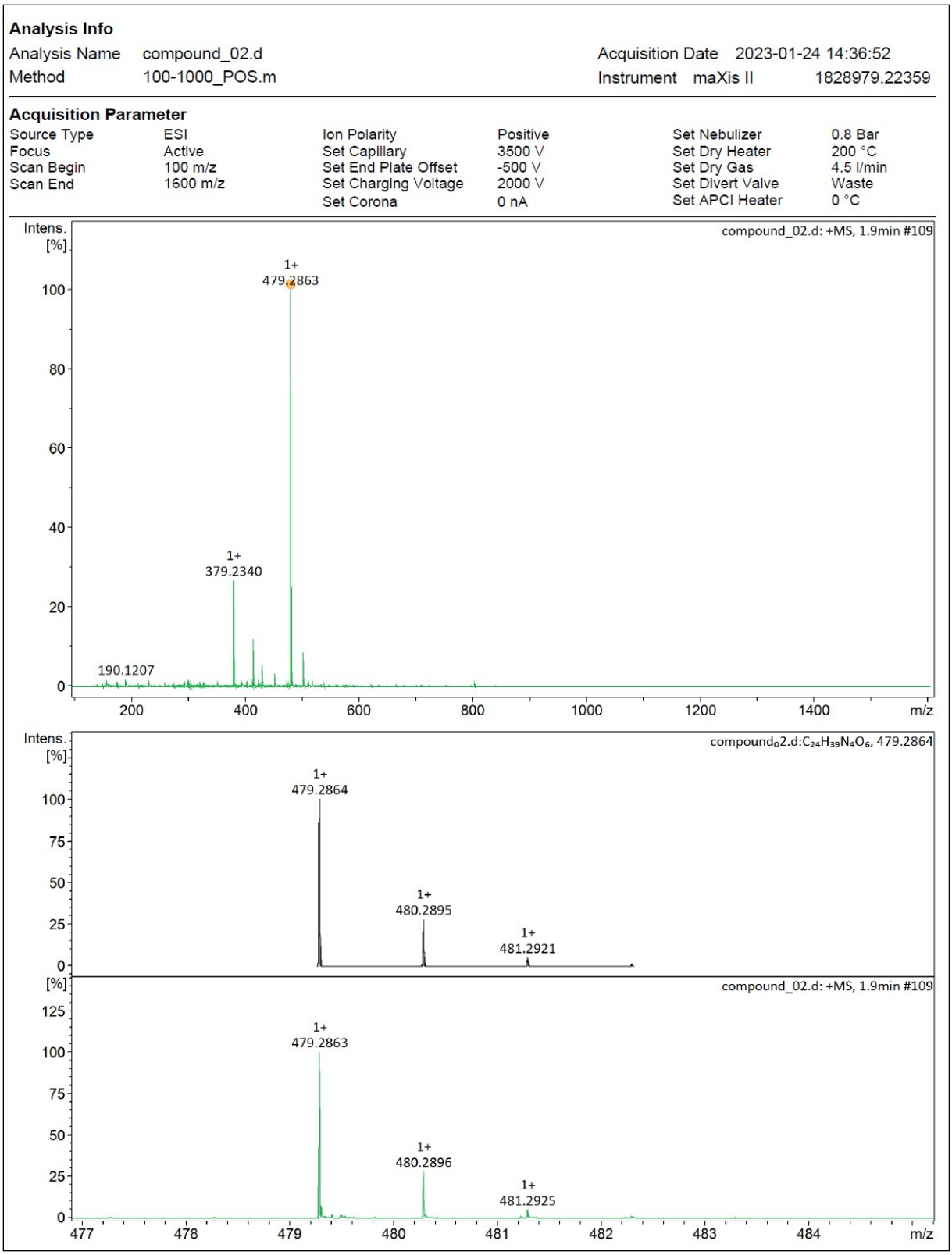

Figure S003. UHRMS spectra (ESI+) of compound **2**.

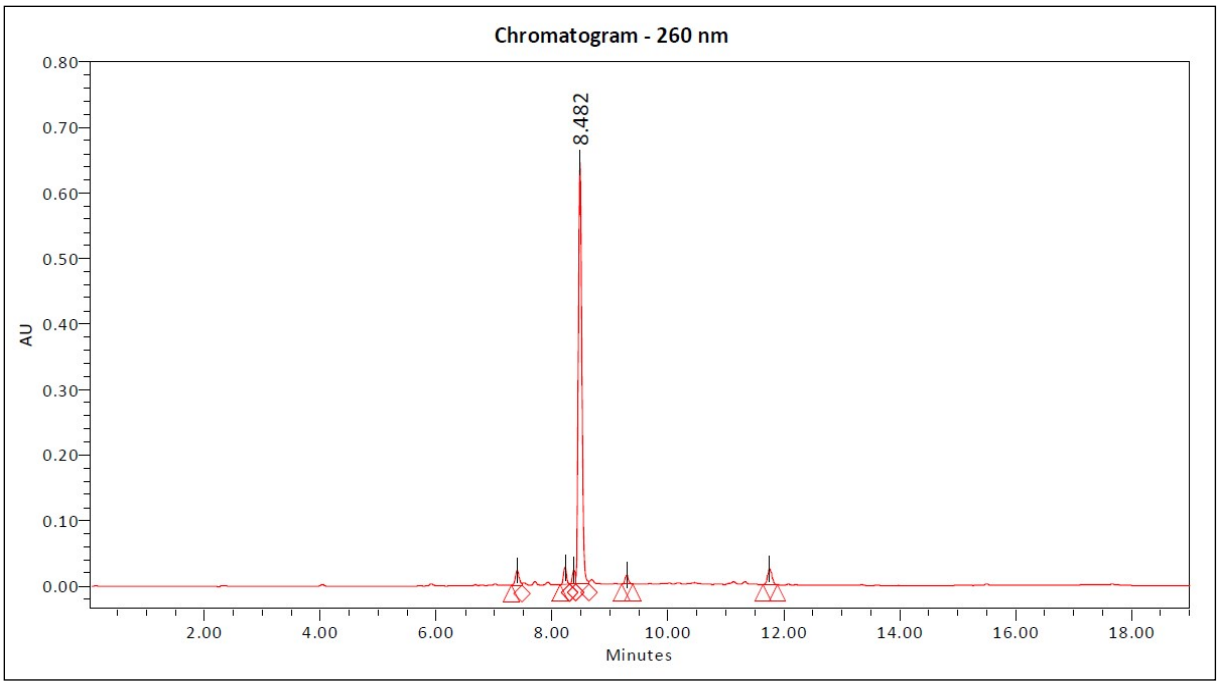

Figure S004. Analytical HPLC chromatogram (260 nm) of compound **2**.

Diethyl 2,2'-(3,6,9-triaza-1(2,6)-pyridinacyclodecaphane-3,9-diyl)diacetate (3)

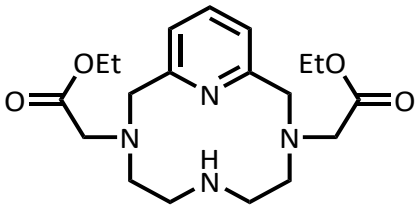

750 mg (1.57 mmol) diethyl-2,2'-(6-(*tert*-butoxycarbonyl)-3,6,9-triaza-1(2,6)-pyridinacyclodecaphane-3,9-diyl)diacetate (**2**) was dissolved in 30 mL CH_2Cl_2 14 mL of trifluoroacetic acid was added to this solution dropwise at 0 °C. The reaction mixture was further stirred for 24 hours at room temperature and the solvent was evaporated off under reduced pressure to afford the crude product, which was purified by preparative HPLC. Lyophilization of the pure fractions returned the product **3** as a white solid (553 mg, yield 93%).

Preparative HPLC: UV-Vis detection: 210 and 260 nm; retention time: 8.45 min; gradient: 0.00→15.00 min 5→95% B; eluent: mixture of 5 mM TFA in MQ-water (A) and acetonitrile (B); flow: 25.00 mL/min; injection volume: 500.00 µL; sample: 590 mg / 3.00 mL 50% ACN in H_2O; column: Phenomenex Luna Prep C18(2) 100 Å, 5 µm, 250 x 21.20 mm; column ID: H18-268346.

^{1}H NMR (400.13 MHz, MeOD-d_4) δ 1.25 (t, J = 7.2 Hz, 6H), 3.14 (m, 4H), 3.25 (m, 4H), 3.66 (s, 4H), 4.13 (s, 4H), 4.17 (q, J = 7.2 Hz, 4H), 7.25 (d, J = 7.7 Hz, 2H), 7.79 (t, J = 7.7, 1H) ppm; **^{13}C-JMOD NMR** (100.62 MHz, MeOD-d_4) δ 14.50, 46.89, 52.87, 57.80, 58.50, 61.78, 122.02, 140.03, 160.34, 173.01 ppm; **UHRMS** (ESI+) *m/z* calculated for $C_{19}H_{30}N_4O_4$ $[M+H]^+$ 379.2340; found 379.2340; **HPLC** purity (260 nm): 95.39%; retention time: 7.598 min; gradient: 0.00→15.00 min 5→95% B; eluent: mixture of 5 mM TFA in MQ-water (A) and acetonitrile (B); flow: 1.00 mL/min; injection volume: 10.00 µL; sample: 1.00 mg/mL 50 %

ACN in H_2O; column: Phenomenex Luna C18(2) 100 Å, 3 µm, 150 × 4.60 mm; column ID: H20-260762.

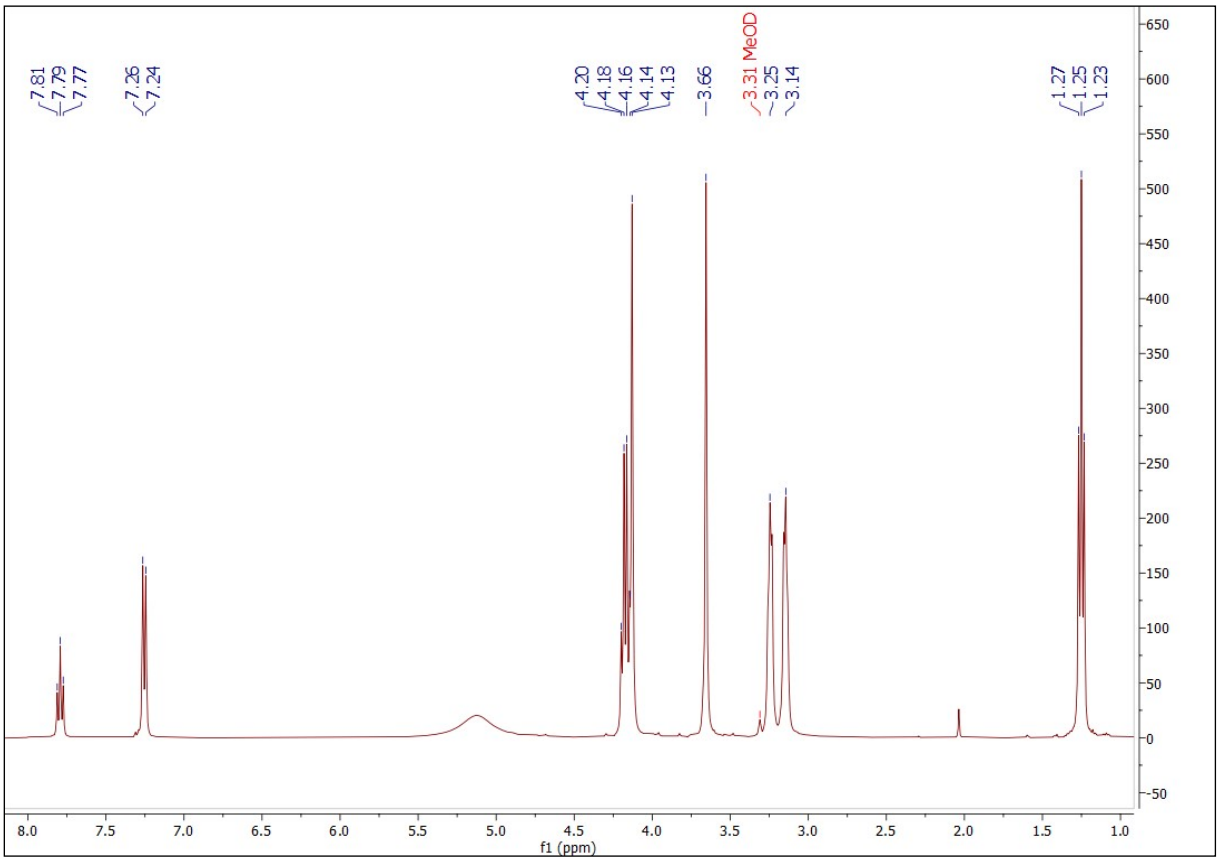

Figure S005. ^{1}H NMR (400.13 MHz, 298.0 K, MeOD-*d4*) spectra of compound **3**.

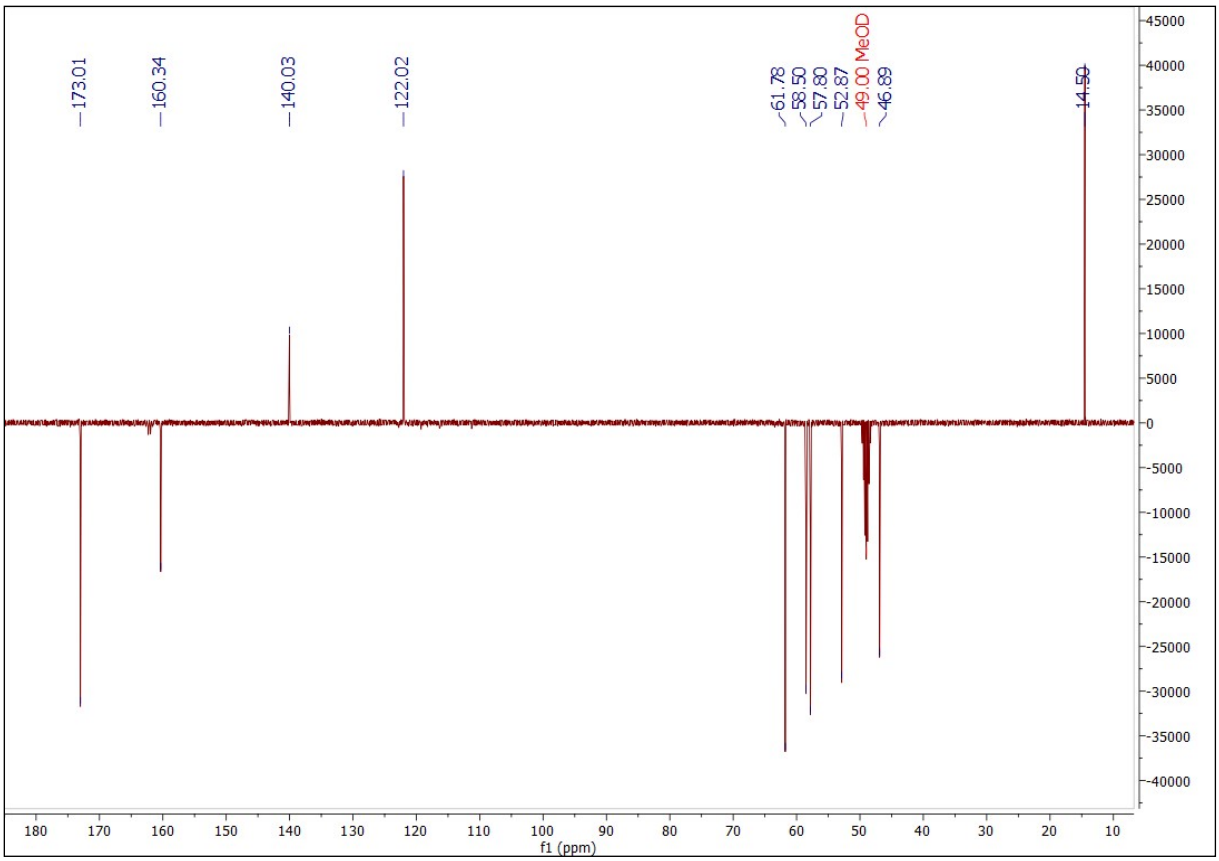

Figure S006. ^{13}C-JMOD NMR (100.62 MHz, 298.0 K, MeOD-d_4) spectra of compound **3**.

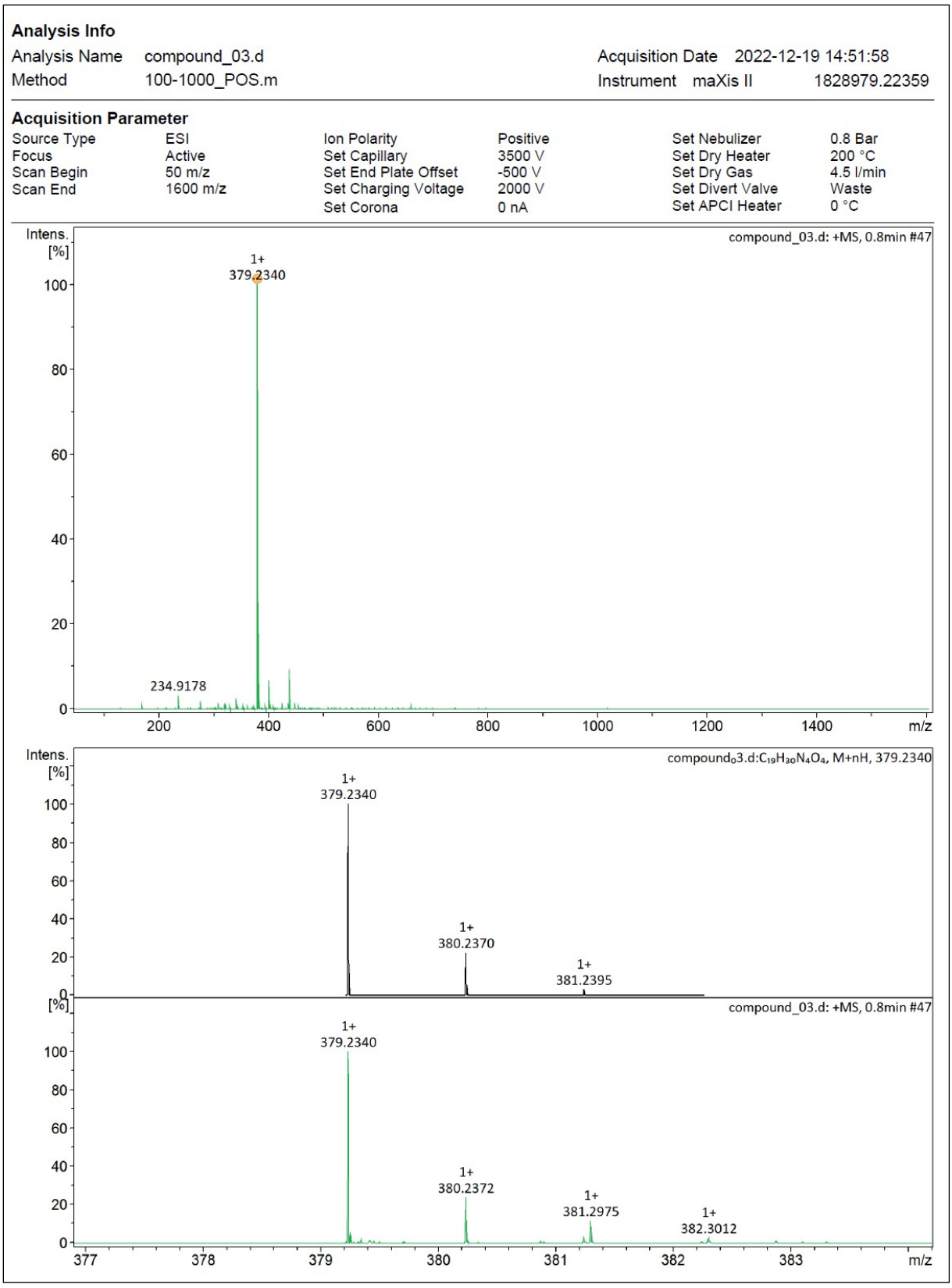

Figure S007. UHRMS spectra (ESI+) of compound **3**.

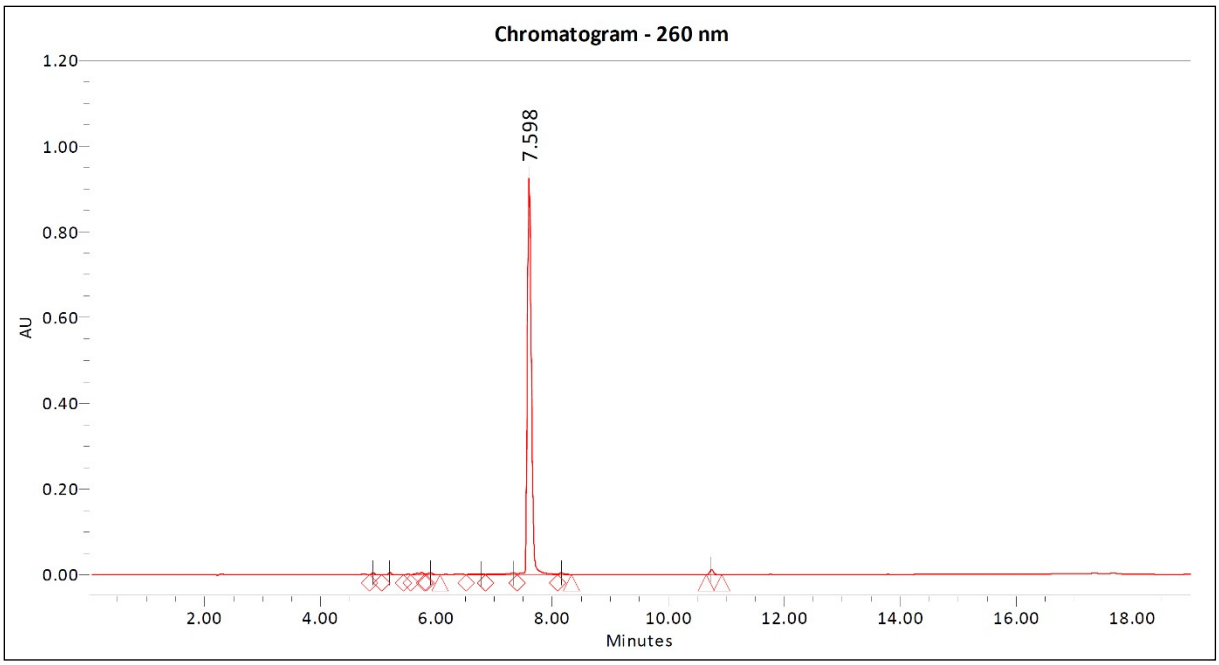

Figure S008. Analytical HPLC chromatogram (260 nm) of compound **3**.

Diethyl 2,2'-(6-(4-(tert-butoxycarbonyl)benzyl)-3,6,9-triaza-1(2,6)-pyridinacyclodecaphane-3,9-diyl)diacetate (4)

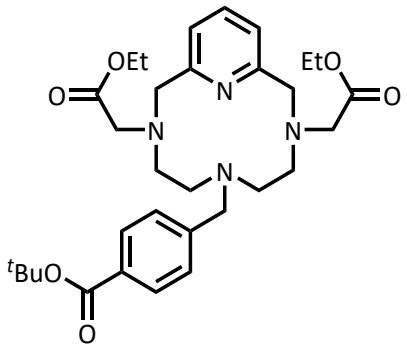

To a solution of 150 mg (0.396 mmol) diethyl 2,2'-(3,6,9-triaza-1(2,6)-pyridinacyclodecaphane-3,9-diyl)diacetate (**3**) in 150 mL acetonitrile, 380 µL (1.84 mmol) of *N,N*-diisopropylethylamine and 21.0 mg (0.198 mmol) sodium iodide was added at room temperature under an argon atmosphere. The reaction mixture was then heated up to 80 °C and the solution of 170 mg (0.627 mmol) *tert*-butyl 4-(bromomethyl)benzoate dissolved in 70 mL acetonitrile was added dropwise over the course of 30 min. The reaction mixture was stirred at 80 °C for an additional 72 h, cooled to room temperature and the solvent was then evaporated off under reduced pressure. The crude product obtained was purified by preparative HPLC. The combined fractions containing the pure substance were combined and lyophilized. Freezer-drying returned the product **4** as a white solid (209 mg, yield 93%).

Preparative HPLC: UV-Vis detection: 210 and 260 nm; retention time: 4.98 min; gradient: 0.00→9.00 min 36→90% B; eluent: mixture of 5 mM TFA in MQ-water (A) and acetonitrile (B); flow: 25.00 mL/min; injection volume: 200.00 µL; sample: 375 mg/mL 50% can in H_2O; column: Phenomenex Luna Prep C18(2) 100 Å, 5 µm, 250 × 21.20 mm; column ID: H18-268346.

^{1}H NMR (360.13 MHz, $CDCl_3$) δ 1.38 (t, *J* = 7.0 Hz, 6H), 1.74 (s, 9H), 3.–2 - 3.40 (m, 8H), 3.–2 - 3.67 (m, 4H), 4.–2 - 4.20 (m, 4H), 4.28 (q, *J* = 7.2 Hz, 4H) 4.72 (s, 2H), 7.25 (d, *J* = 7.7 Hz, 2H), 7.69 (d, *J* = 7.9 Hz, 2H), 7.85 (t, *J* = 7.7 Hz, 1H), 8.14 (d, J = 7.9 Hz, 2H) ppm; **^{13}C-JMOD NMR** (90.56 MHz, $CDCl_3$) δ 14.10, 28.12, 49.91, 54.21, 54.44, 56.66, 58.33, 60.96, 81.77, 121.04, 130.14, 130.41, 133.19, 134.62, 138.50, 158.74, 164.81, 170.54 ppm; **UHRMS** (ESI+) *m/z* calculated for $C_{31}H_{44}N_4O_6$ $[M+H]^+$ 569.3334; found 569.3334. **HPLC** purity (260 nm): 99.50%; retention time: 10.949 min; gradient: 0.00→15.00 min 5→95 %B; eluent: mixture of 5 mM TFA in MQ-water (A) and acetonitrile (B); flow: 1.00 mL/min; injection volume: 10.00 µL; sample: 0.80 mg/mL 50% ACN in H_2O; column: Phenomenex Luna C18(2) 100 Å, 3 µm, 150 × 4.60 mm; column ID: H20-260762.

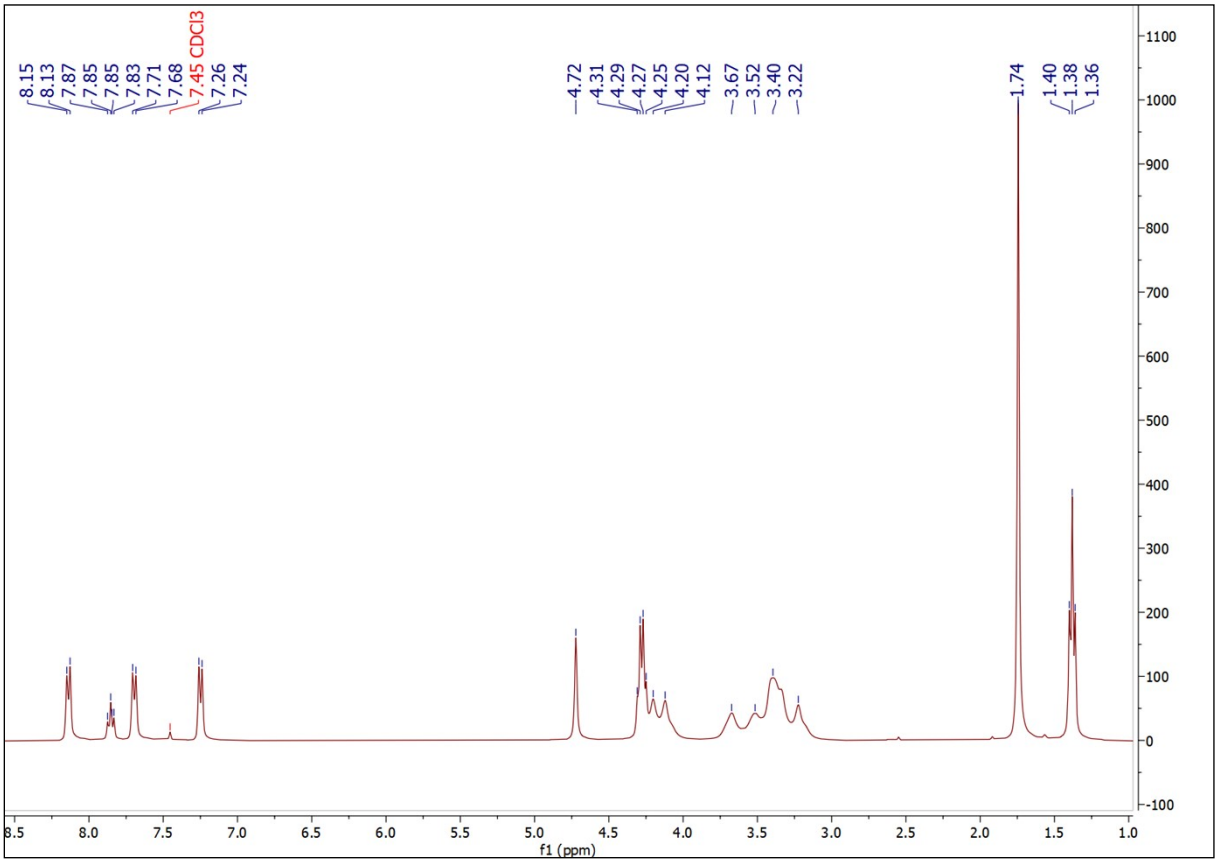

Figure S009. ^{1}H NMR (360.13 MHz, 298.0 K, $CDCl_3$) spectra of compound **4**.

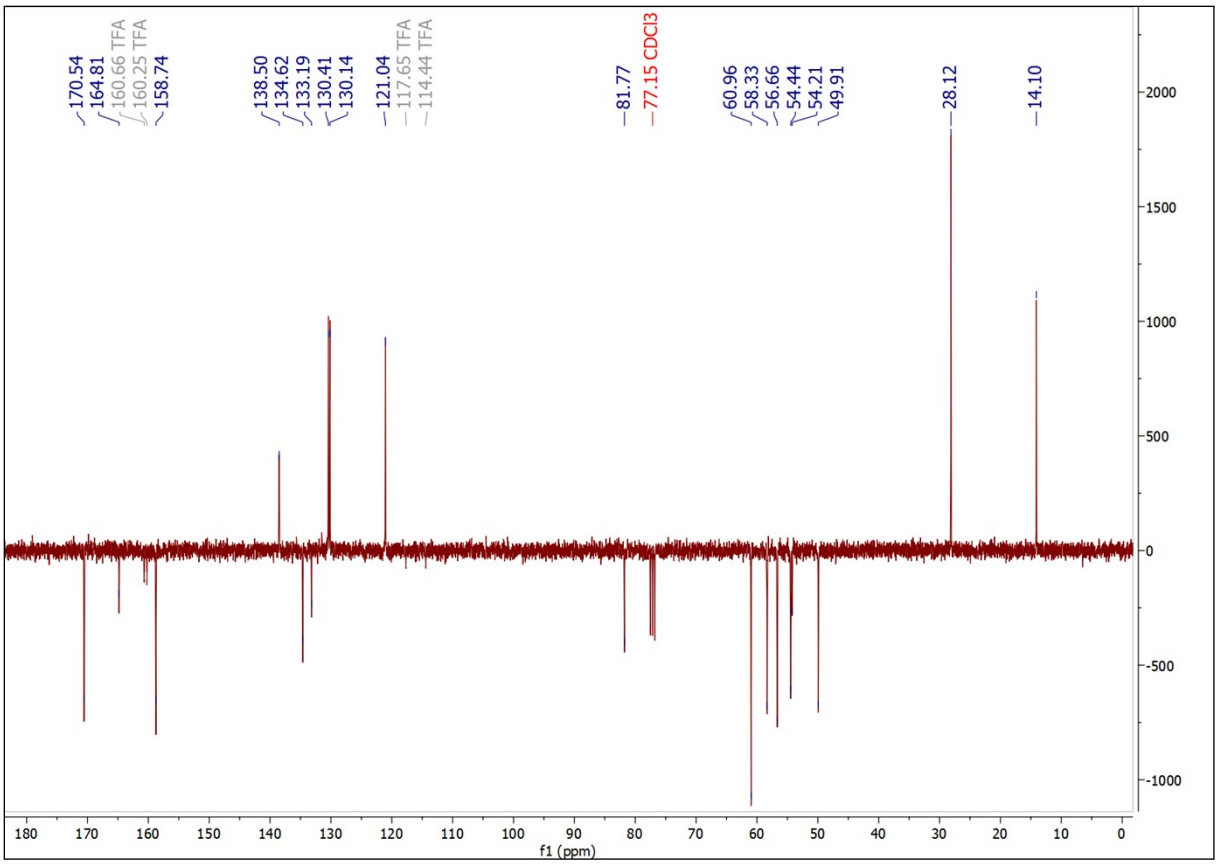

Figure S010. ^{13}C-JMOD NMR (90.56 MHz, 298.0 K, $CDCl_3$) spectra of compound **4**.

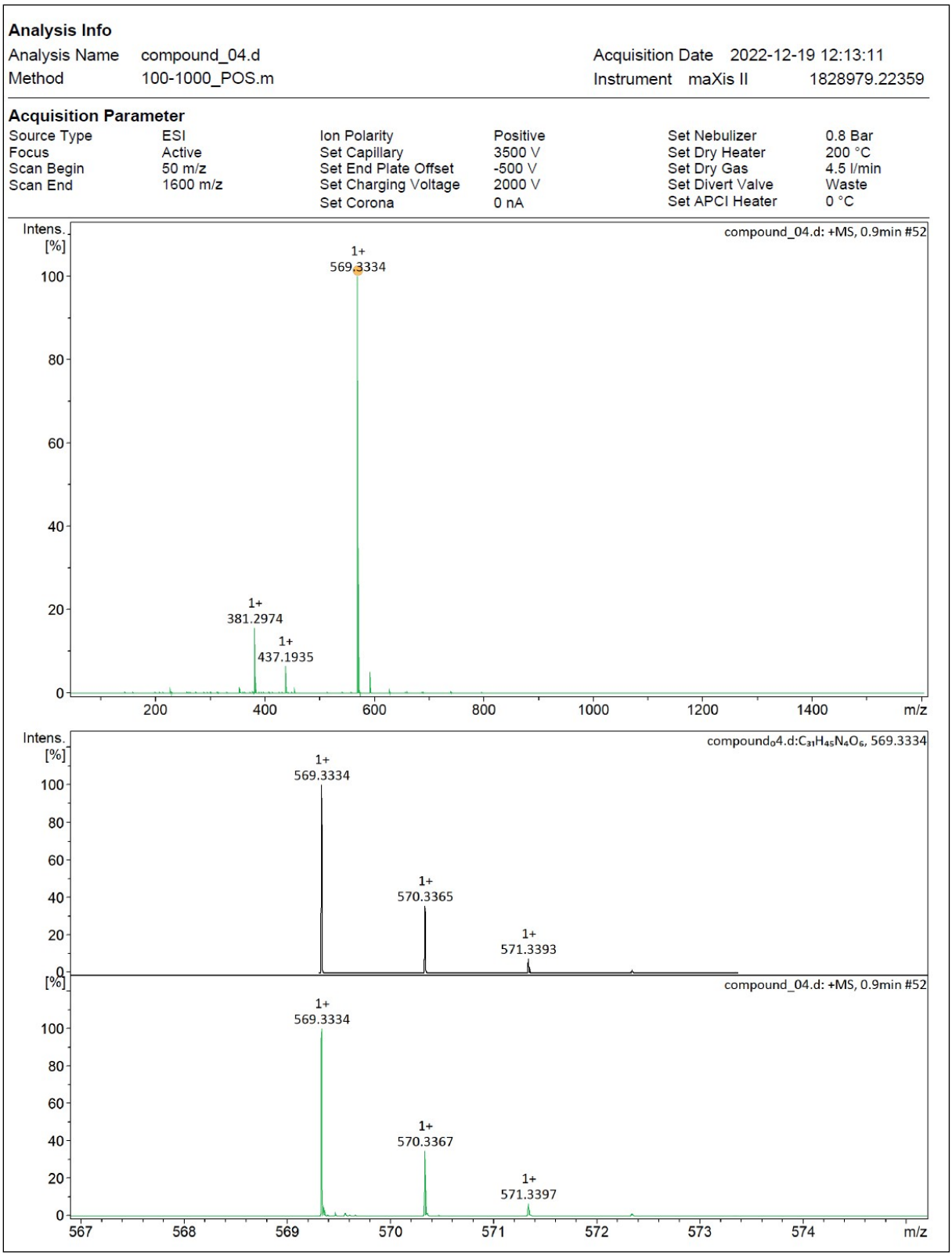

Figure S011. UHRMS spectra (ESI+) of compound **4**.

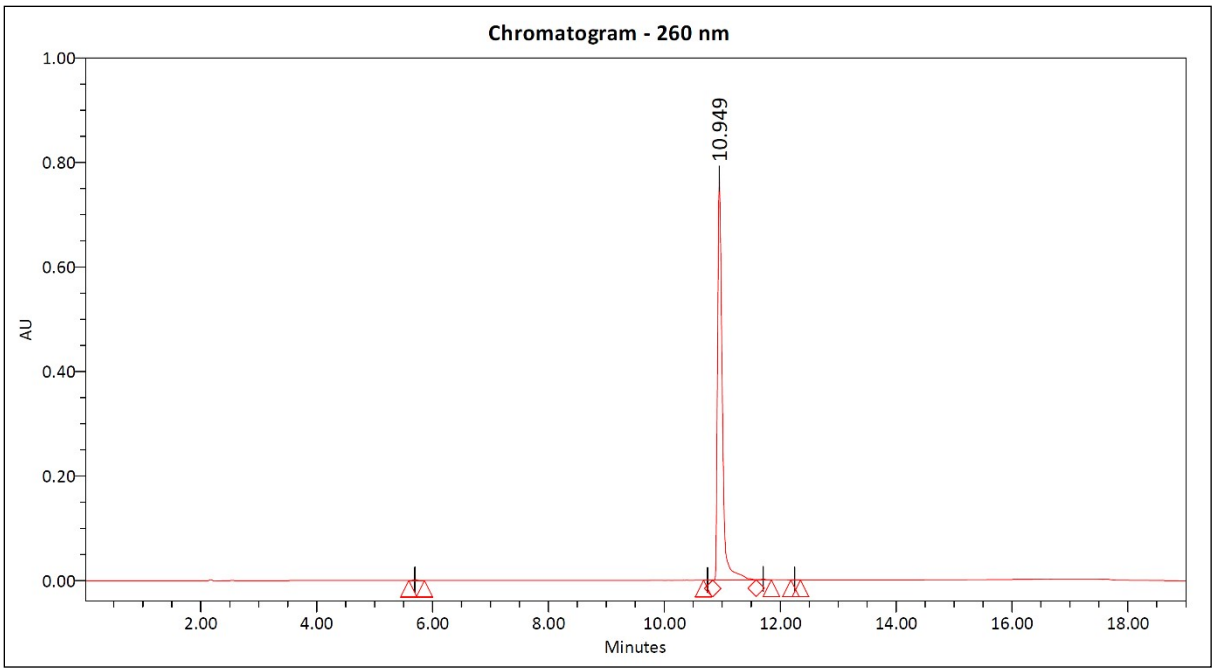

Figure S012. Analytical HPLC chromatogram (260 nm) of compound **4**.

2,2'-(6-(4-Carboxybenzyl)-3,6,9-triaza-1(2,6)-pyridinacyclodecaphane-3,9-diyl)diacetic acid (L^1)

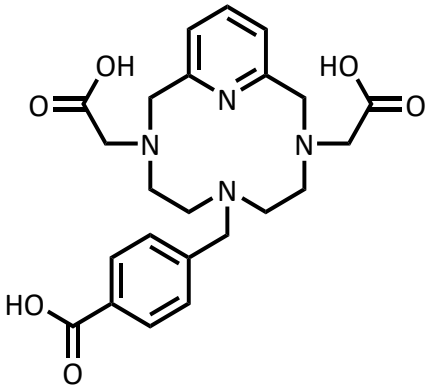

80 mg (2.00 mmol) sodium hydroxide was added to the solution of 160 mg (0.281 mmol) of diethyl 2,2'-(6-(4-(*tert*-butoxycarbonyl)benzyl)-3,6,9-triaza-1(2,6)-pyridinacyclodecaphane-3,9-diyl)diacetate (**4**) dissolved in 3.0 mL ethanol at room temperature. The reaction was then heated up to 60 °C and kept at the given temperature for an additional 3 h, cooled and the solvent was evaporated under reduced pressure using rotary evaporator. The crude product was purified by preparative HPLC. Lyophilization of the pure fractions afforded the pure ligand $\mathbf{L^1}$ as a white solid (110 mg, yield 86%).

Preparative HPLC: UV-Vis detection: 210 and 260 nm; retention time: 4.45 min; gradient: 0.00→10.00 min 5→35% B; eluent: mixture of 5 mM TFA in MQ-water (A) and acetonitrile (B); flow: 25.00 mL/min; injection volume: 250.00 µL; sample: 128 mg/mL H_2O; column: Phenomenex Luna Prep C18(2) 100 Å, 5 µm, 250 × 21.20 mm; column ID: H18-268346.

^{1}H NMR (400.13 MHz, D_2O) δ 2.94 (m, 4H), 3.52 (t, *J* = 5.4 Hz, 4H), 3.75 (m, 4H), 3.95 (s, 2H), 4.70 (s, 4H), 7.52 (d, *J* = 7.9 Hz, 2H), 7.62 (d, *J* = 8.2 Hz, 2H), 8.02 (d, *J* = 8.2 Hz, 2H), 8.04 (t, *J* = 7.7 Hz, 1H) ppm; **^{13}C-JMOD NMR** (100.62 MHz, D_2O) δ 49.57, 52.68, 56.83, 57.94, 59.07, 123.14, 129.82, 130.37, 130.43, 140.87, 141.07, 150.14, 163.14, 170.07 ppm; **UHRMS** (ESI+) *m/z* calculated for $C_{23}H_{28}N_4O_6$ $[M+H]^+$ 457.2082; found 457.2080. **HPLC** purity (260 nm): 99.50%; retention time: 4.597 min; gradient: 0.00→15.00 min 5→95% B; eluent: mixture of 5 mM TFA in MQ-water (A) and acetonitrile (B); flow: 1.00 mL/min; injection volume: 5.00 µL; sample: 2.24 mM in H_2O; column: Phenomenex Luna C18(2) 100 Å, 5 µm, 150 × 4.60 mm; column ID: H21-212012.

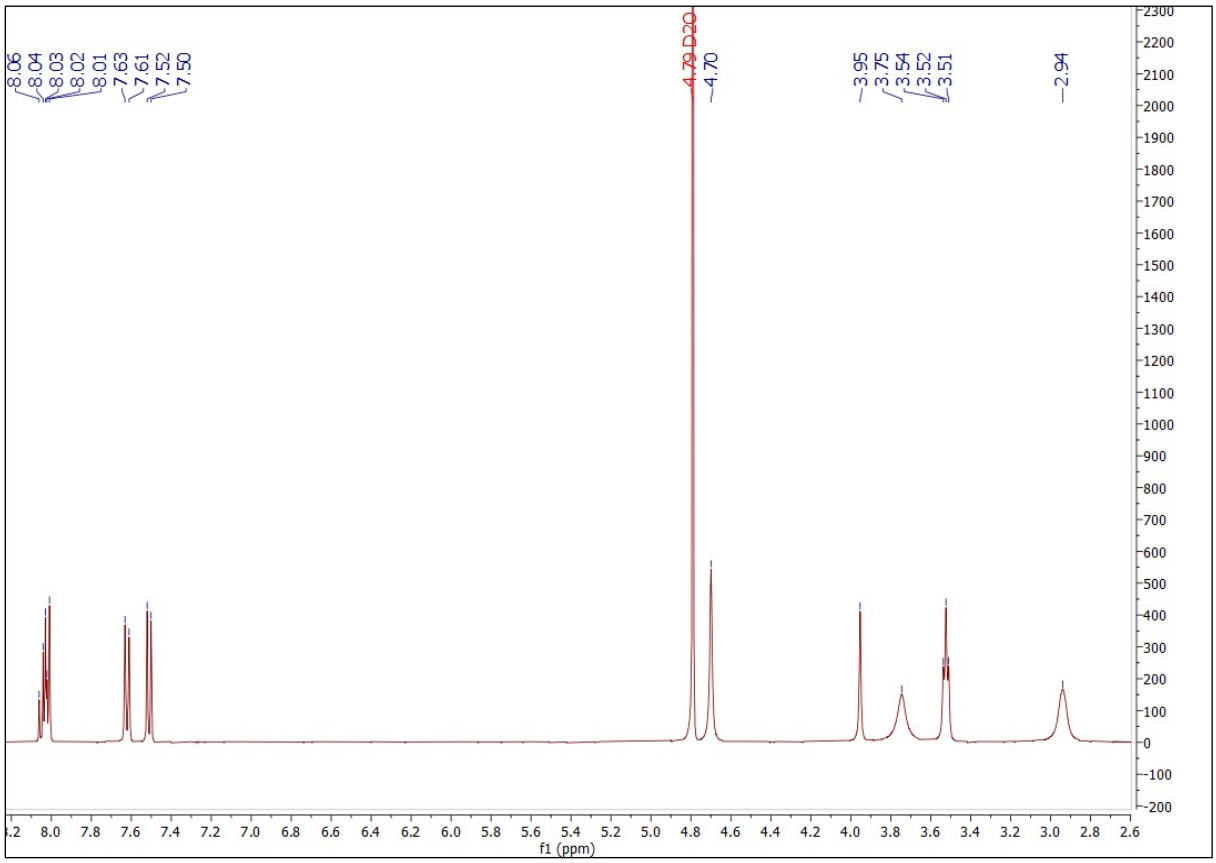

Figure S013. ^{1}H NMR (400.13 MHz, 298.0 K, D_2O) spectra of ligand **L^{1}**.

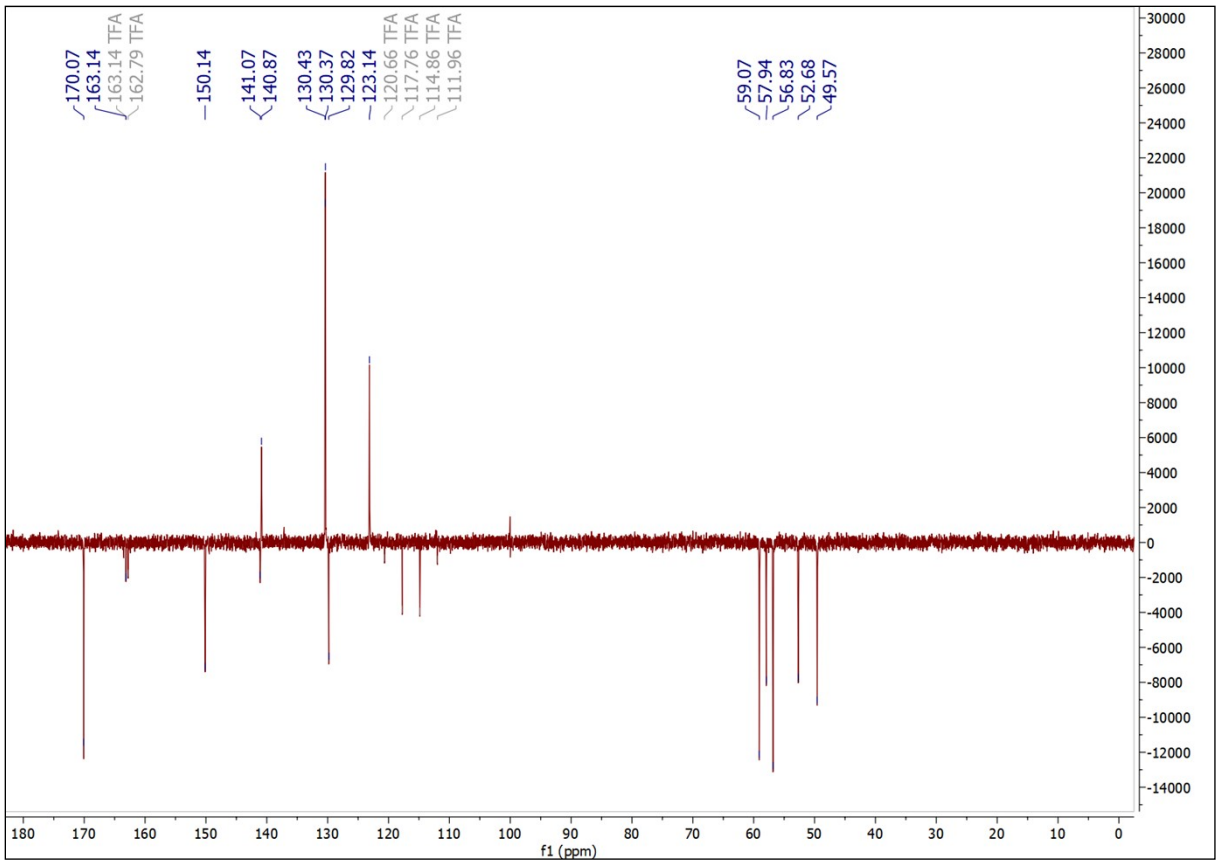

Figure S014. ^{13}C-JMOD NMR (100.62 MHz, 298.0 K, D_2O) spectra of ligand **L^1**.

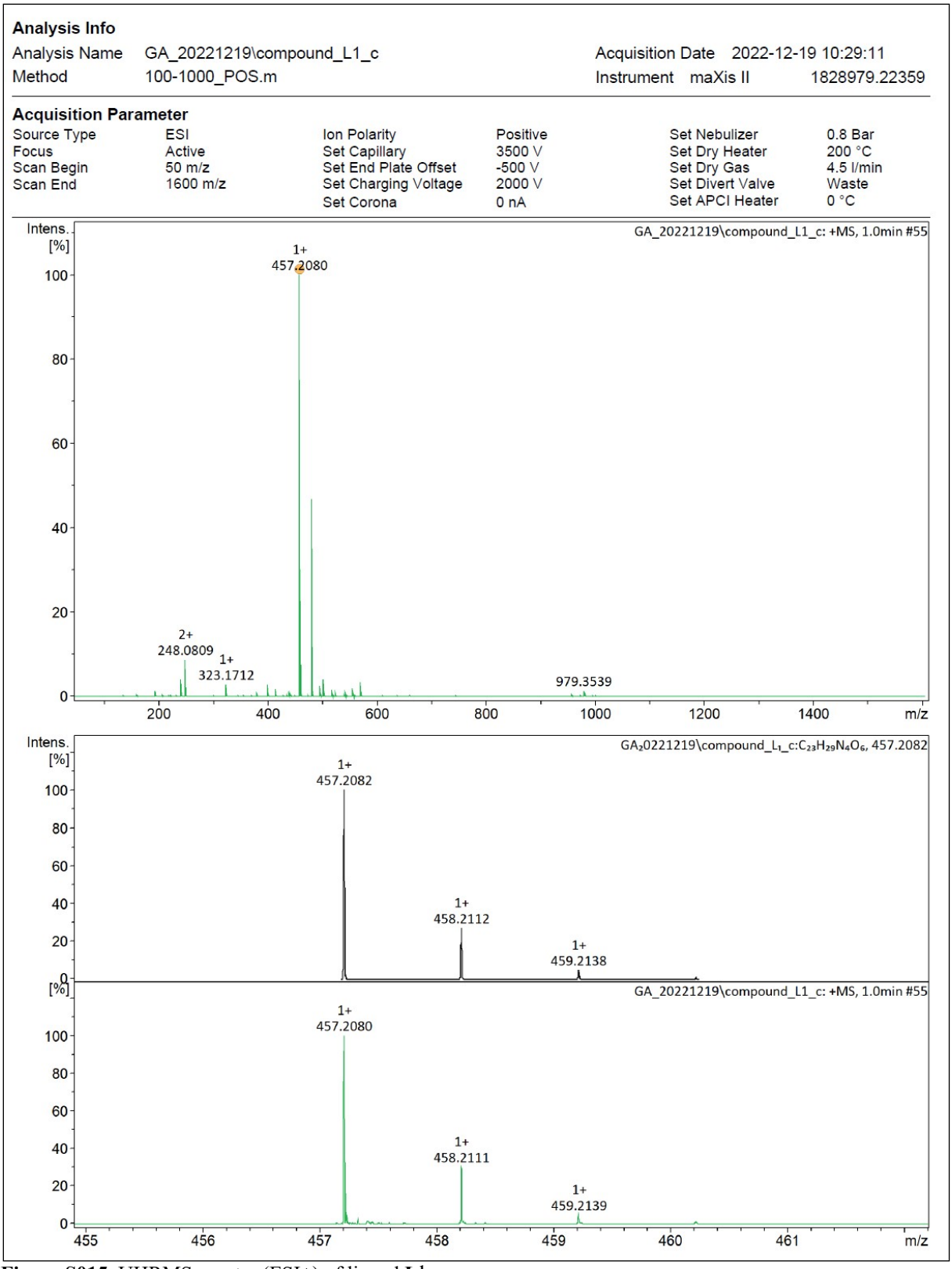

Figure S015. UHRMS spectra (ESI+) of ligand **L**[1].

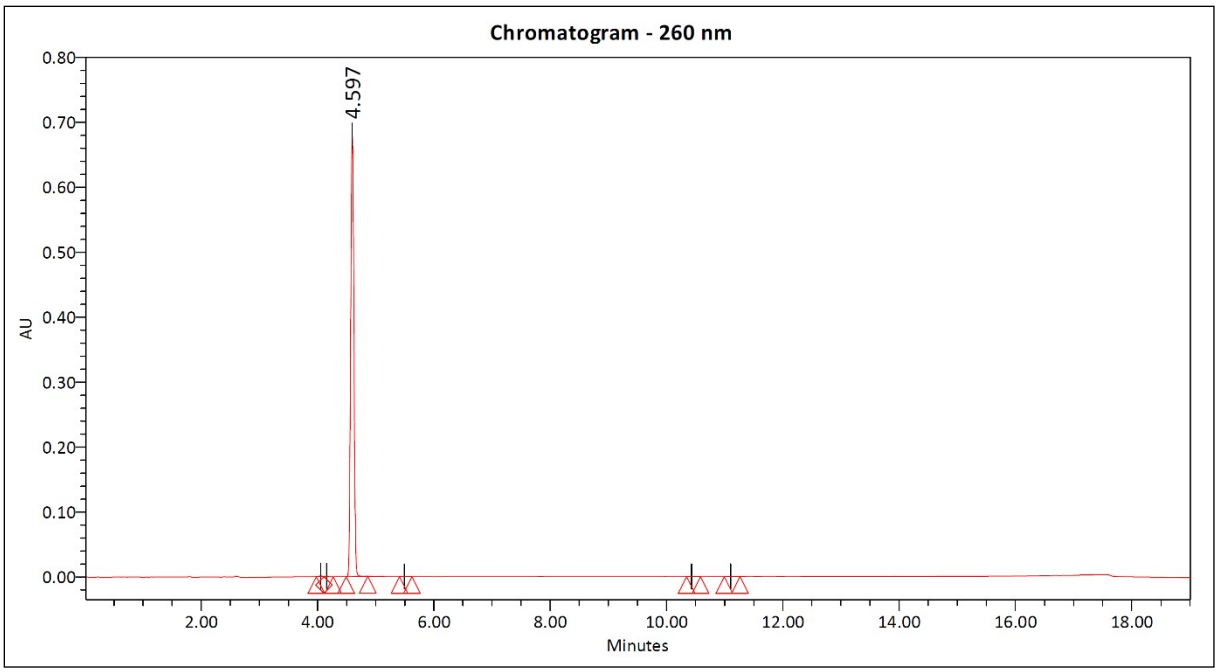

Figure S016. Analytical HPLC chromatogram (260 nm) of ligand **L**[1].

Diethyl 2,2'-(6-(*tert*-butoxycarbonyl)-3,6,9-triaza-1(2,6)-pyridinacyclodecaphane-3,9-diyl)(2R,2'R)-dipropionate (5)

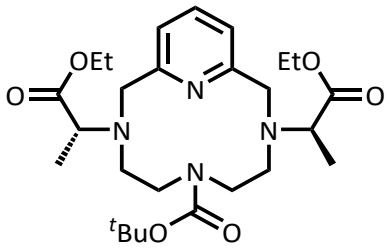

1.80 g (13.0 mmol) potassium carbonate was suspended in the solution of 1.00 g (3.26 mmol) of 6-Boc-Pyclen (**1**) (*tert*-butyl 3,6,9-triaza-1(2,6)-pyridinacyclodecaphane-6-carboxylate) dissolved in 40 mL CH_2Cl_2 (40 mL) under an argon atmosphere. The suspension then cooled in an ice-bath and 1.51 g (6.04 mmol) ethyl (S)-2-(trifluoromethylsulfonyloxy)propionate dissolved in 80 mL CH_2Cl_2 was added dropwise over the course of 30 min under h vigorous stirring. The suspension was stirred at room temperature for an additional 72 h, filtered and the solvent of the filtrate was evaporated off. The oily residue obtained was redissolved 50% ACN in H_2O and subjected to preparative HPLC chromatography. The substance was collected following the lyophilization of the fractions containing the pure product **5** as a white solid (1.30 g, yield 79%).

Preparative HPLC: UV-Vis detection: 210 and 260 nm; retention time: 5.74 min; gradient: 0.00→7.50 min 30→60% B; eluent: mixture of 5 mM TFA in MQ-water (A) and acetonitrile (B); flow: 25.00 mL/min; injection volume: 200.00 µL; sample: 700 mg / 7.00 mL 50% ACN in H_2O; column: Phenomenex Luna Prep C18(2) 100 Å, 5 µm, 250 × 21.20 mm; column ID: H18-268346.

^{1}H NMR (400.13 MHz, CD_3CN-d_3) δ 1.25 (t, J = 7.1 Hz, 6H), 1.31 (m, 9H), 1.47 (d, J = 7.2 Hz, 6H), 3.27 (m, 8H), 3.75 (m, 4H) 4.15 (q, J = 7.2 Hz, 2H), 4.19 (q, J = 7.1 Hz, 4H), 4.41 (s,

4H), 7.64 (d, *J* = 7.9 Hz, 2H), 8.23 (t, *J* = 7.9 Hz, 1H) ppm; **^{13}C-JMOD NMR** (100.62 MHz, CD_3CN-d_3) δ 14.48, 28.34, 51.44, 54.71, 55.39, 60.95, 62.52, 81.96, 124.80, 145.17, 153.71, 158.66, 172.90 ppm; **UHRMS** (ESI+) *m/z* calculated for $C_{26}H_{42}N_4O_6$ $[M+H]^+$ 507.3177; found 507.3177. **HPLC** purity (260 nm): 100.00%; retention time: 8.996 min; gradient: 0.00→15.00 min 30→90% B; eluent: mixture of 5 mM TFA in MQ-water (A) and acetonitrile (B); flow: 1.00 mL/min; injection volume: 20.00 µL; column: Phenomenex Luna C18(2) 100 Å, 5 µm, 150 × 4.60 mm; column ID: 345362.

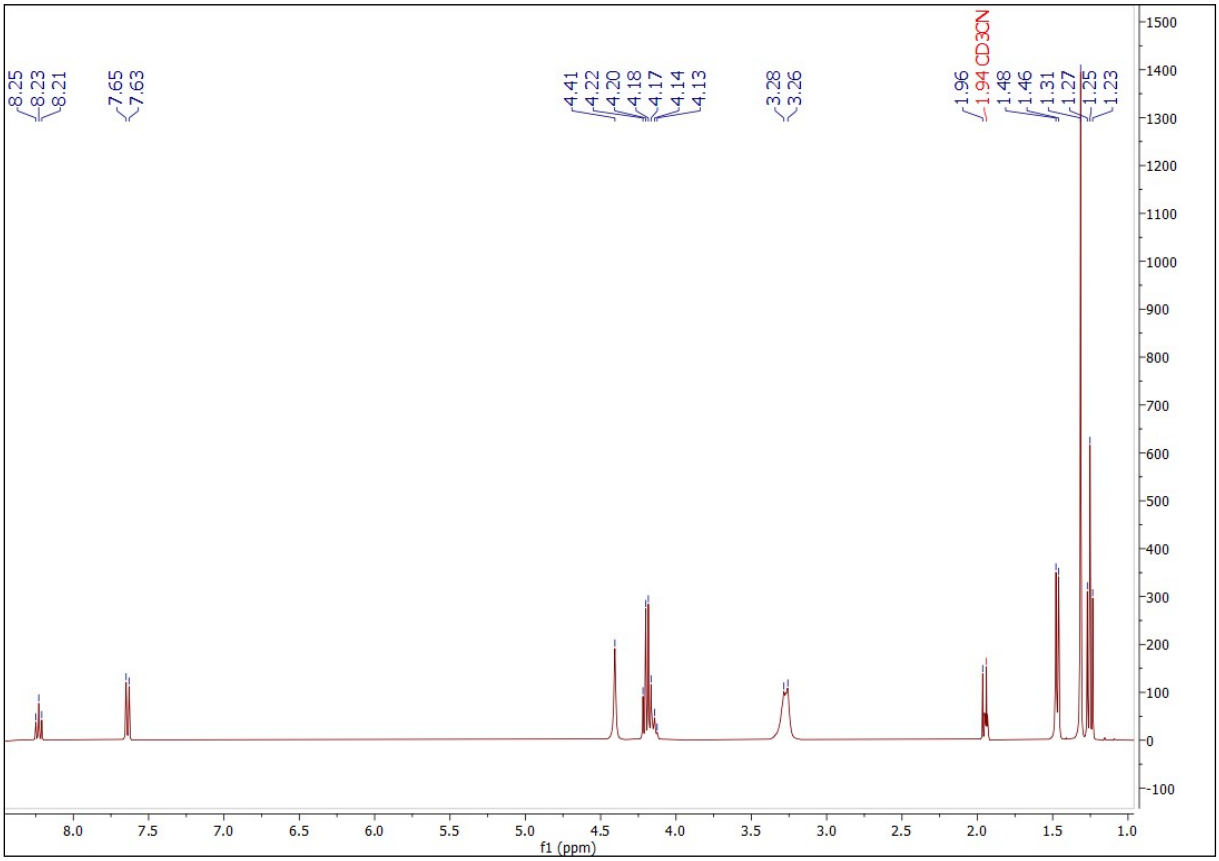

Figure S017. ^{1}H NMR (400.13 MHz, 298.0 K, CD_3CN-*d3*) spectra of compound **5**.

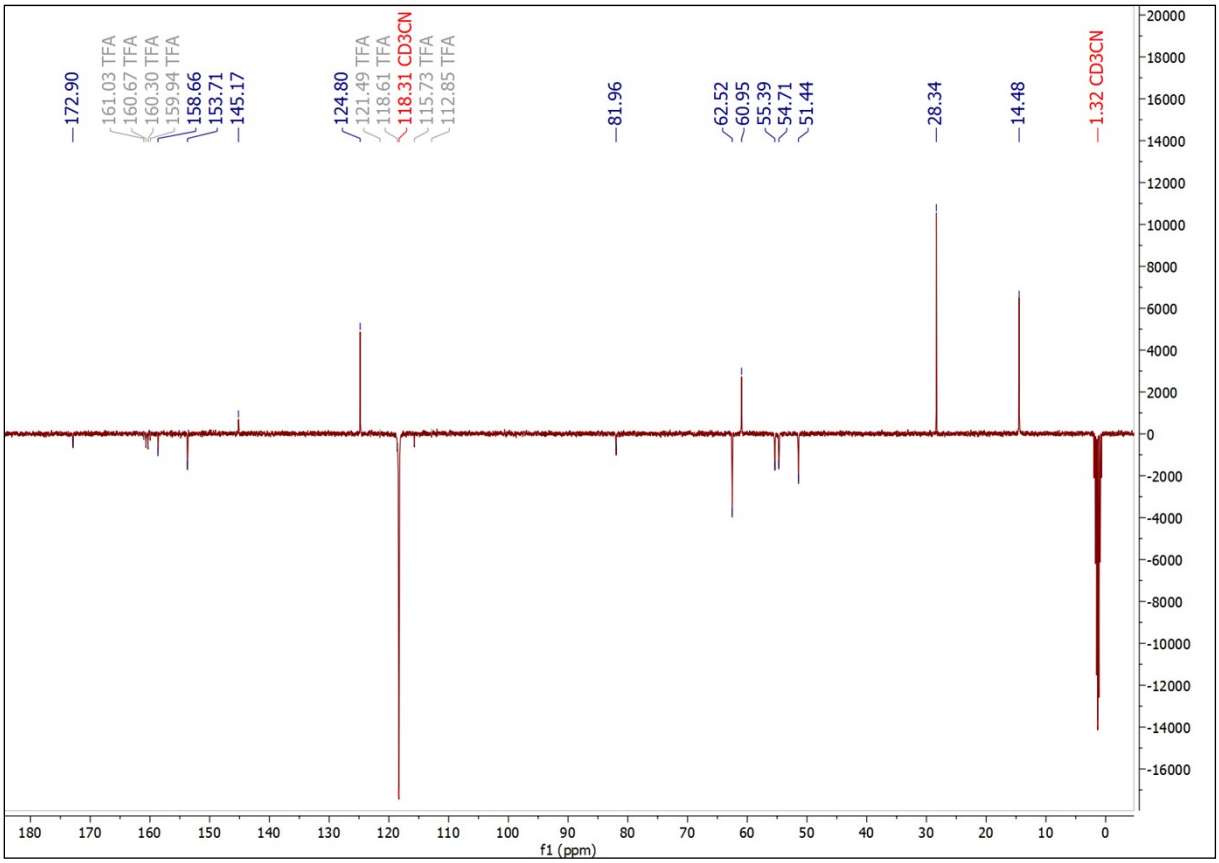

Figure S018. ^{13}C-JMOD NMR (100.62 MHz, 298.0 K, CD_3CN-*d3*) spectra of compound **5**.

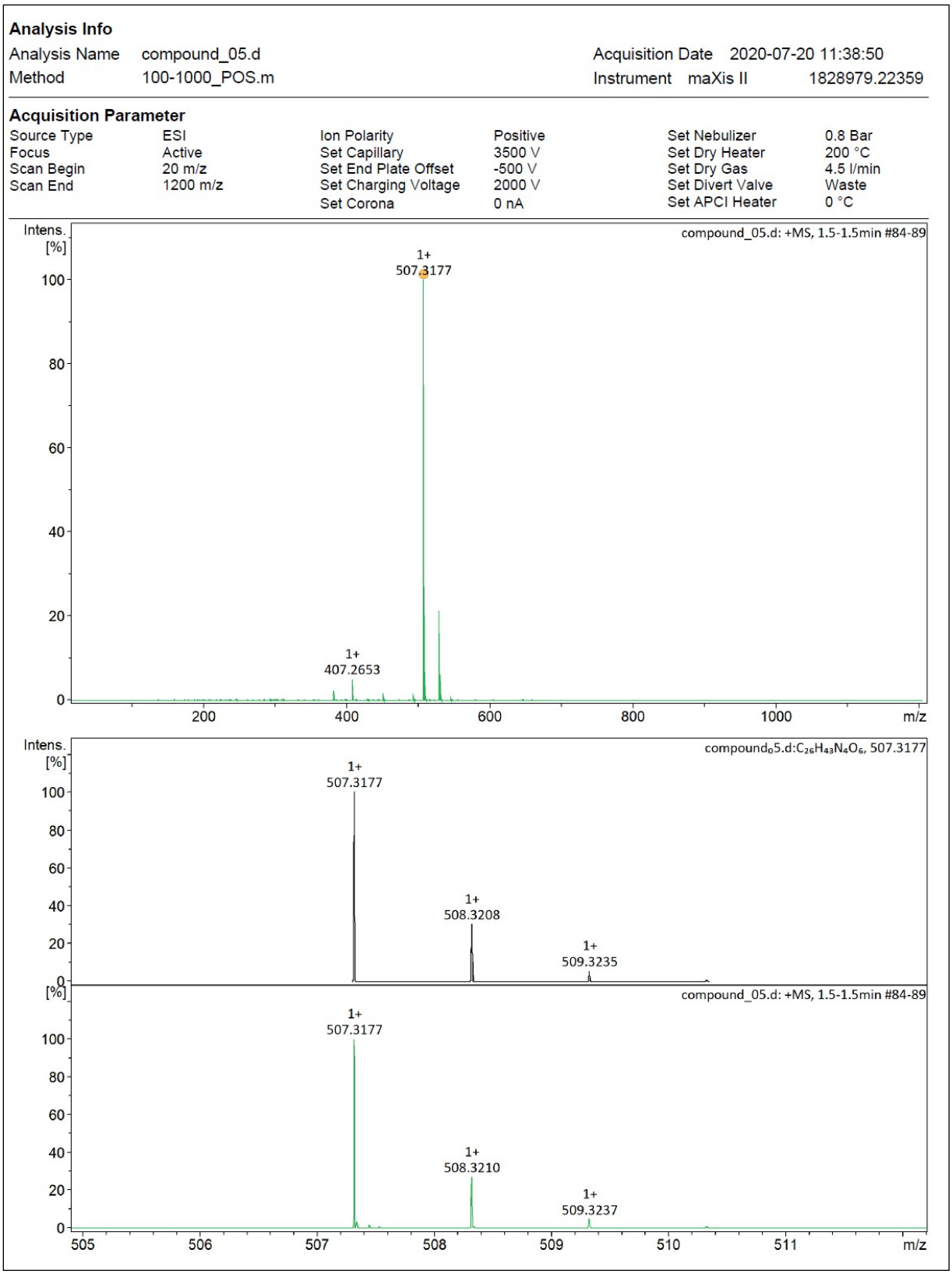

Figure S019. UHRMS spectra (ESI+) of compound **5**.

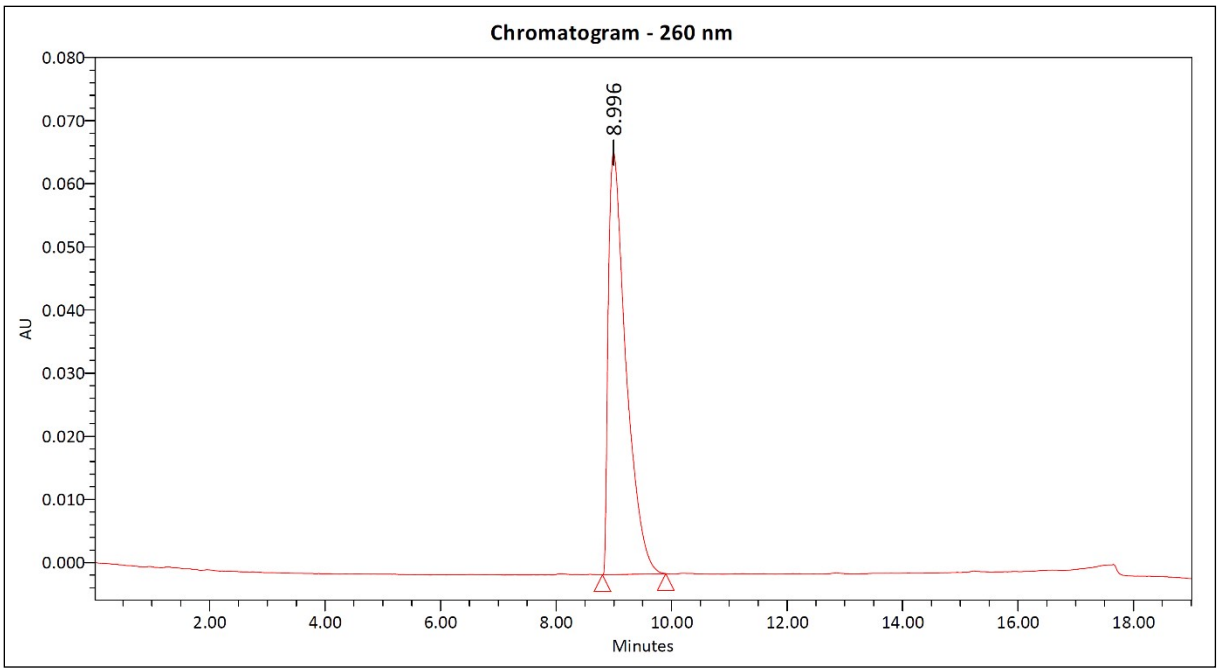

Figure S020. Analytical HPLC chromatogram (260 nm) of compound **5**.

Diethyl 2,2'-(3,6,9-triaza-1(2,6)-pyridinacyclodecaphane-3,9-diyl)(2R,2'R)-dipropionate (6)

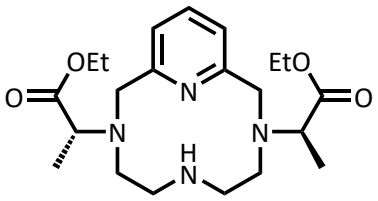

Trifluoroacetic acid (7 mL) was added dropwise to a solution of 651 mg (1.28 mmol) diethyl 2,2'-(6-(*tert*-butoxycarbonyl)-3,6,9-triaza-1(2,6)-pyridinacyclodecaphane-3,9-diyl)(2R,2'R)-dipropionate (**5**) dissolved in 15 mL CH_2Cl_2. The reaction at 0 °C. The reaction mixture was further stirred for an additional 24 hours at room temperature and the solvent was removed under reduced pressure to afford the product **6** as a white solid (505 mg, yield 96%).

^{1}H NMR (400.13 MHz, D_2O) δ 1.20 (t, *J* = 7.1 Hz, 6H), 1.52 (d, *J* = 7.2 Hz, 6H), 2.97 (m, 4H), 3.17 (m, 4H), 3.75 (m, 4H), 4.07 (q, *J* = 7.2 Hz, 2H), 4.15 (q, *J* = 7.1 Hz, 4H), 4.45 (bs, 4H), 7.81 (d, *J* = 7.9 Hz, 2H), 8.42 (t, *J* = 7.9 Hz, 1H) ppm; **^{13}C-JMOD NMR** (100.62 MHz, D_2O) δ 13.14, 45.38, 49.95, 61.82, 62.82, 123.96, 146.62, 153.15, 175.35 ppm; **UHRMS** (ESI+) *m/z* calculated for $C_{21}H_{34}N_4O_4$ $[M+H]^+$ 407.2653; found 407.2655. **HPLC** purity (260 nm): 97.27%; retention time: 5.354 min; gradient: 0.00→15.00 min 5→95%B; eluent: mixture of 5 mM TFA in MQ-water (A) and acetonitrile (B); flow: 1.00 mL/min; injection volume: 10.00 µL; sample: 0.30 mg/mL 50% ACN in H_2O; column: Phenomenex Luna C18(2) 100 Å, 3 µm, 150 × 4.60 mm; column ID: H20-260762.

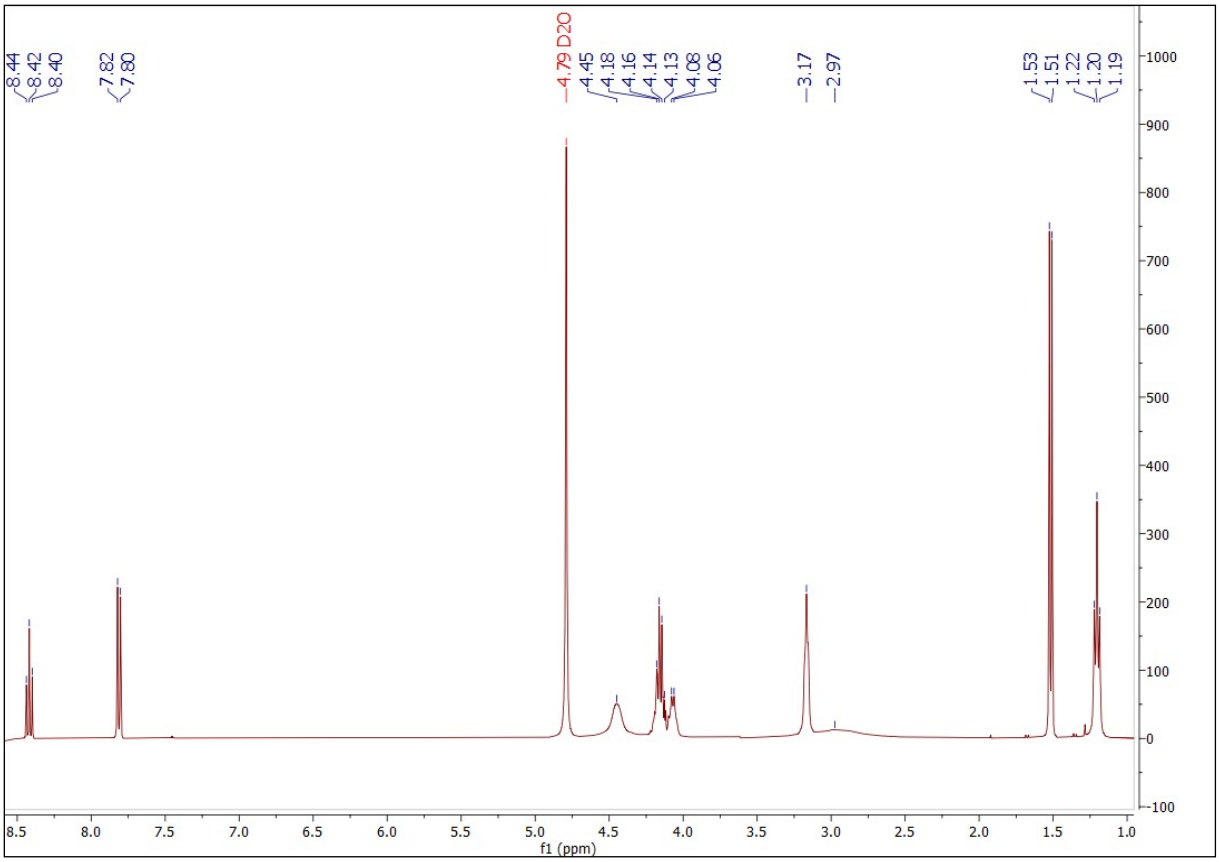

Figure S021. ^{1}H NMR (400.13 MHz, 298.0 K, D_2O) spectra of compound **6**.

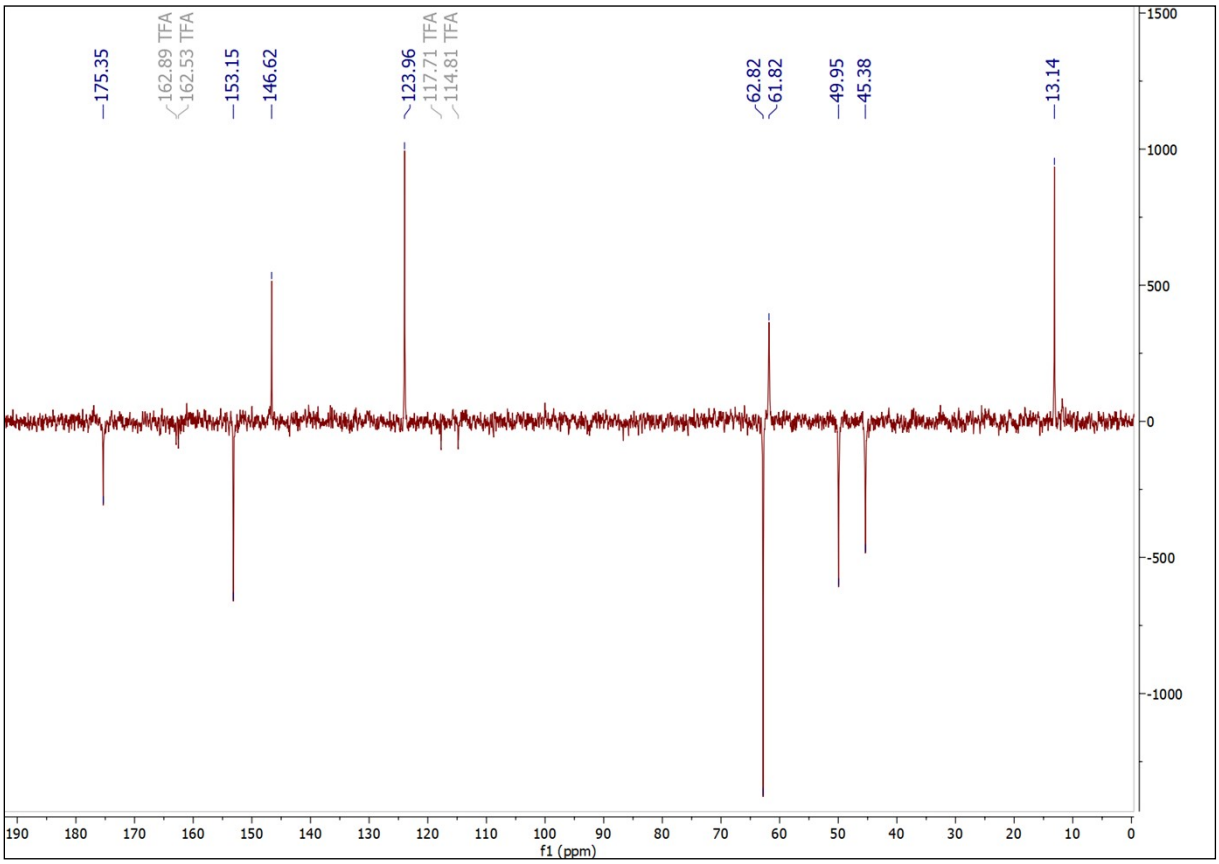

Figure S022. ^{13}C-JMOD NMR (100.62 MHz, 298.0 K, D_2O) spectra of compound **6**.

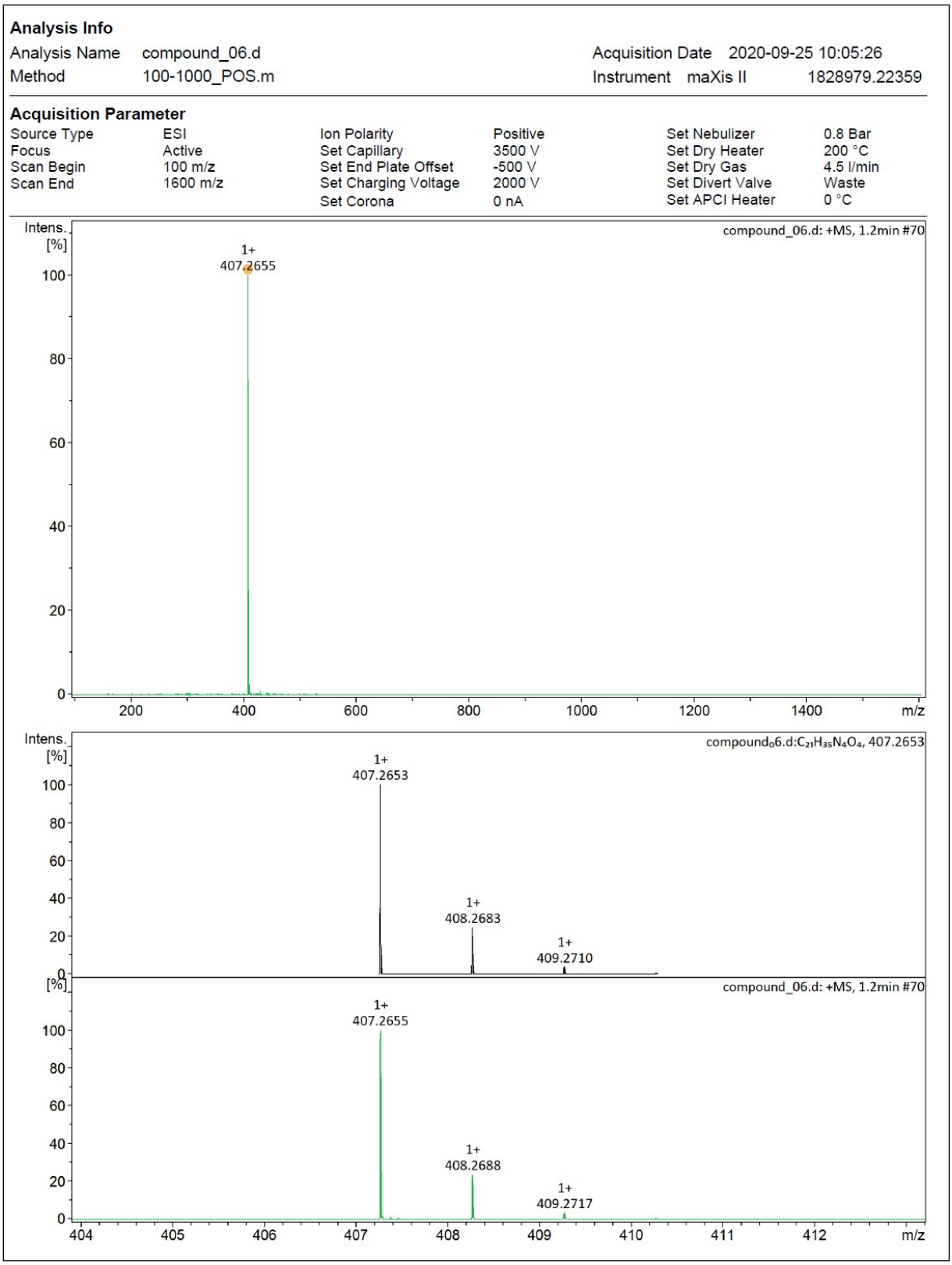

Figure S023. UHRMS spectra (ESI+) of compound **6**.

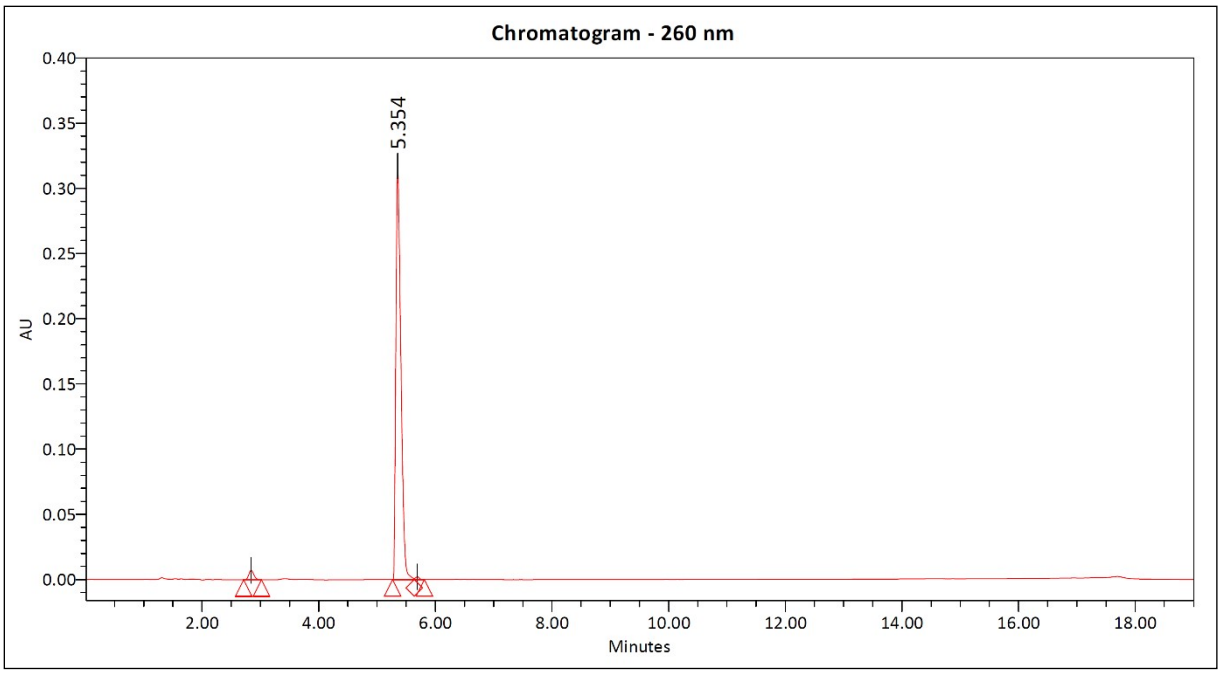

Figure S024. Analytical HPLC chromatogram (260 nm) of compound **6**.

Diethyl 2,2'-(6-(4-(*tert*-butoxycarbonyl)benzyl)-3,6,9-triaza-1(2,6)-pyridinacyclodecaphane-3,9-diyl)(2R,2'R)-dipropionate (7)

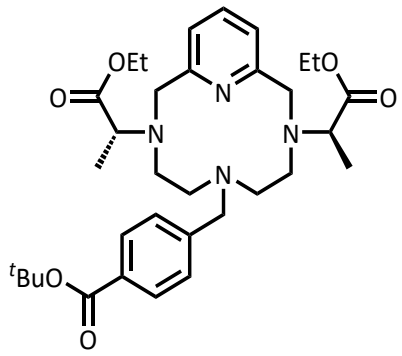

Potassium carbonate (102 mg, 0.738 mmol) and sodium iodide (11.0 mg, 0.0611 mmol) was added to a solution of 200 mg (0.492 mmol) diethyl 2,2'-(3,6,9-triaza-1(2,6)-pyridinacyclodecaphane-3,9-diyl)(2R,2'R)-dipropionate (**6**) in 100 mL acetonitrile under argon protected atmosphere at room temperature. The reaction mixture was then heated up to 65 °C and the solution of 140 mg (0.516 mmol) *tert*-butyl 4-(bromomethyl)benzoate dissolved in 20 mL of acetonitrile was added dropwise over the course of 30 min. The temperature of the reaction mixture was increased to 80 °C and stirred for an additional 72 h at the given temperature. The solvent was then removed under reduced pressure and the crude product obtained was purified by preparative HPLC. The fractions containing the pure product were combined and lyophilized. The target compound **7** was obtained as a white solid (152 mg, yield 52%).

Preparative HPLC: UV-Vis detection: 210 and 260 nm; retention time: 9.35 min; gradient: 0.00→13.00 min 30→60% B; eluent: mixture of 5 mM TFA in MQ-water (A) and acetonitrile (B); flow: 25.00 mL/min; injection volume: 300.00 µL; sample: 150 mg/mL 50% ACN in H_2O;

column: Phenomenex Luna Prep C18(2) 100 Å, 5 µm, 150 × 21.20 mm; column ID: 589811-5.

^{1}H NMR (400.13 MHz, CD_3CN-*d3*) δ 1.04 (m, 6H), 1.25 (m, 3H), 1.33 (m, 3H), 1.56 (s, 9H), 3.04 - 3.31 (m, 9H), 3.61 - 4.23 (m, 9H), 4.46 (m, 2H), 7.13 (m, 2H), 7.67 (d, *J* = 8.0 Hz, 2H), 7.69 (t, *J* = 7.7 Hz, 1H), 7.97 (d, *J* = 8.0 Hz, 2H) ppm; **^{13}C NMR-JMOD** (100.62 MHz, CD_3CN-*d3*) δ 12.93, 14.39, 14.66, 17.75, 28.32, 50.50, 52.65, 54.51, 54.52, 55.20, 55.68, 61.46, 61.57, 63.16, 63.37, 82.38, 120.71, 121.22, 130.74, 131.61, 133.86, 135.68, 139.26, 161.72, 162.31, 165.74, 173.48, 174.06 ppm; **UHRMS** (ESI+) *m/z* calculated for $C_{33}H_{48}N_4O_6$ $[M+H]^+$ 597.3647; found 597.3644. **HPLC** purity (260 nm): 98.93%; retention time: 11.687 min; gradient: 0.00→15.00 min 5→95% B; eluent: mixture of 5 mM TFA in MQ-water (A) and acetonitrile (B); flow: 1.00 mL/min; injection volume: 10.00 µL; sample: 0.50 mg/1.00 mL 50% ACN in H_2O; column: Phenomenex Luna C18(2) 100 Å, 3 µm, 150 × 4.60 mm; column ID: H20-260762.

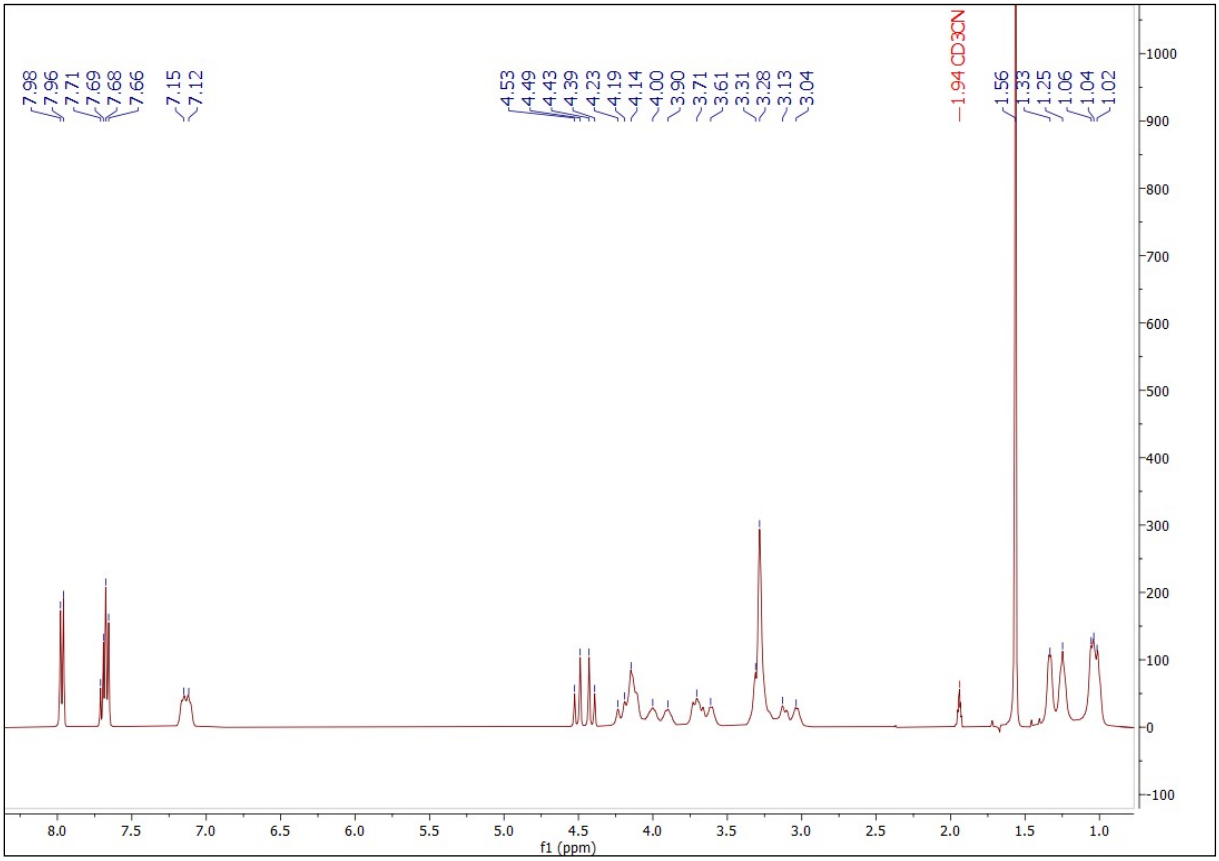

Figure S025. ^{1}H NMR (400.13 MHz, 298.0 K, CD_3CN-*d3*) spectra of compound **7**.

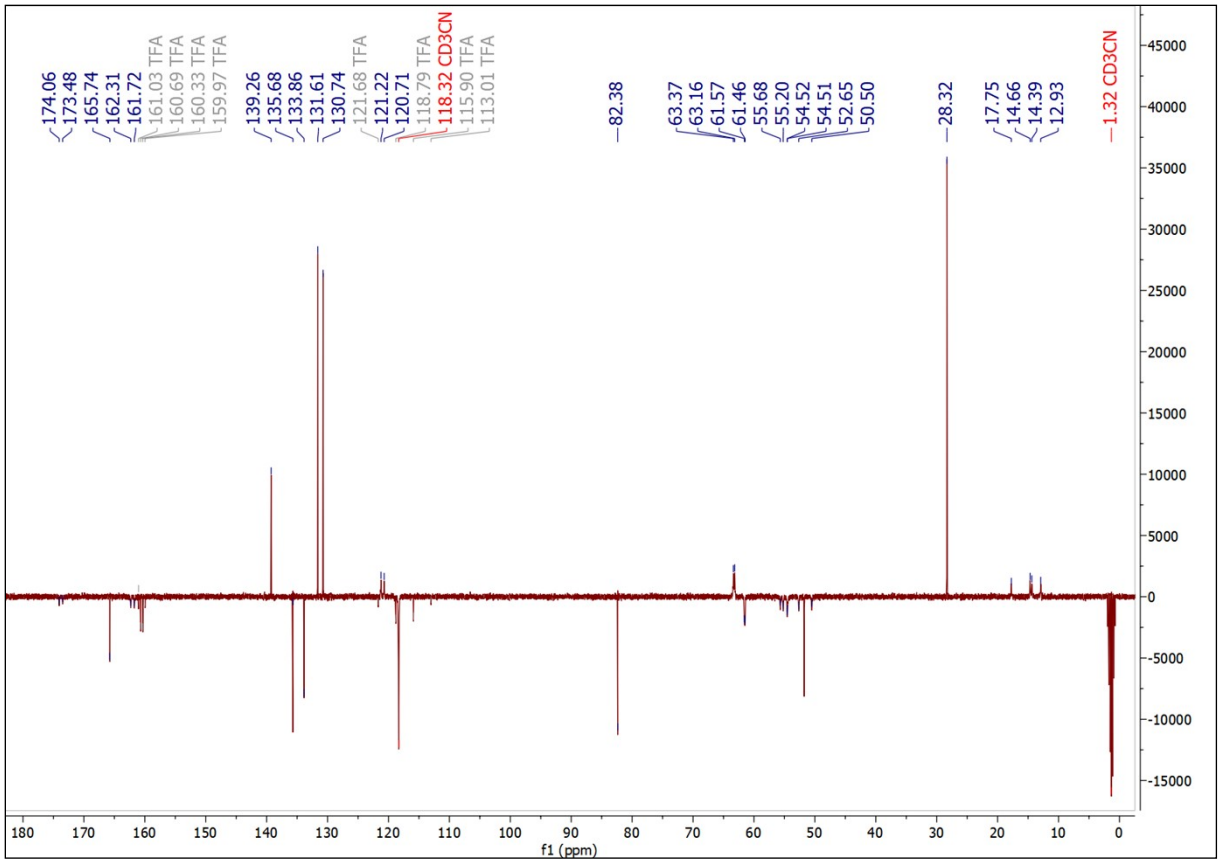

Figure S026. ^{13}C-JMOD NMR (100.62 MHz, 298.0 K, CD_3CN-*d3*) spectra of compound **7**.

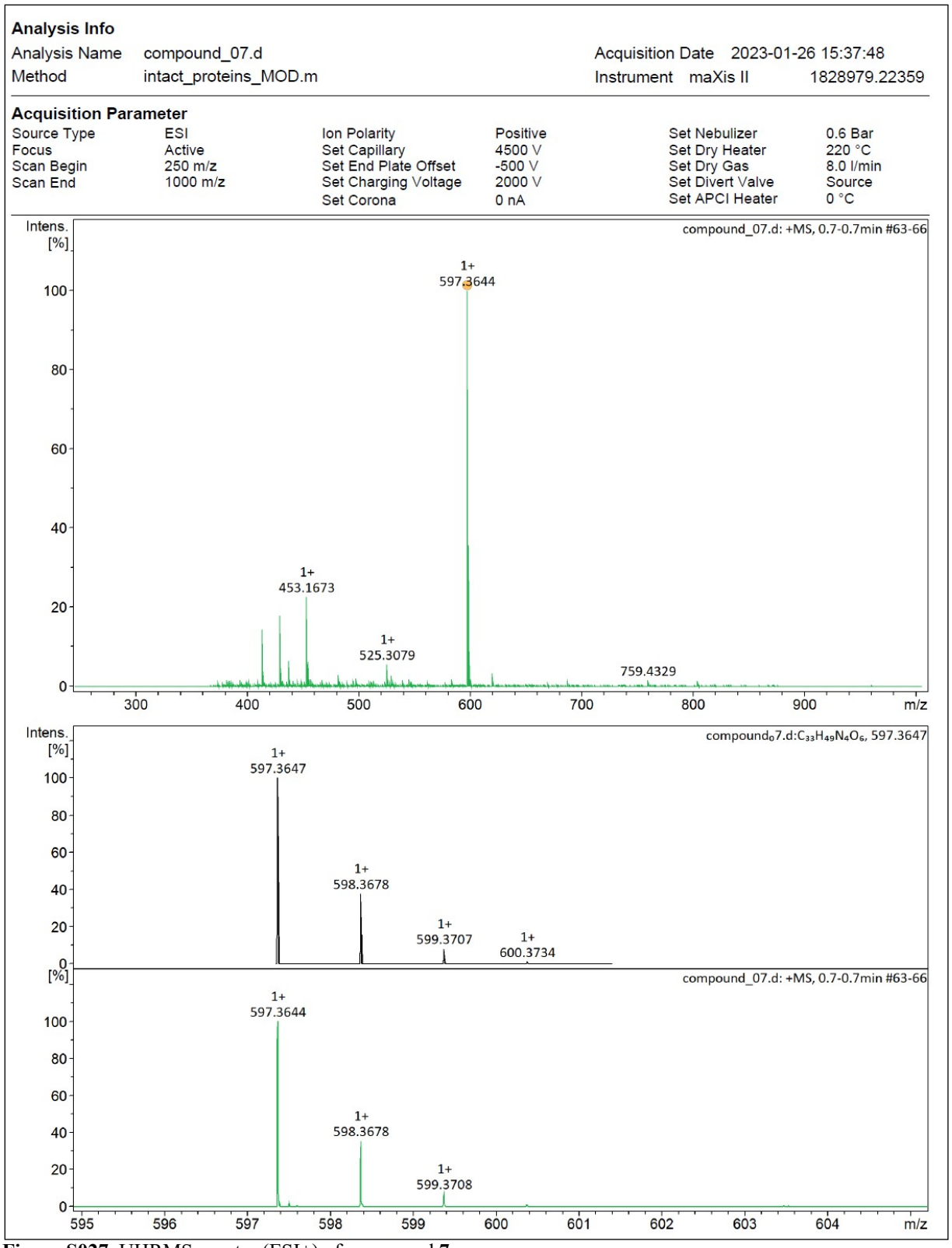

Figure S027. UHRMS spectra (ESI+) of compound **7**.

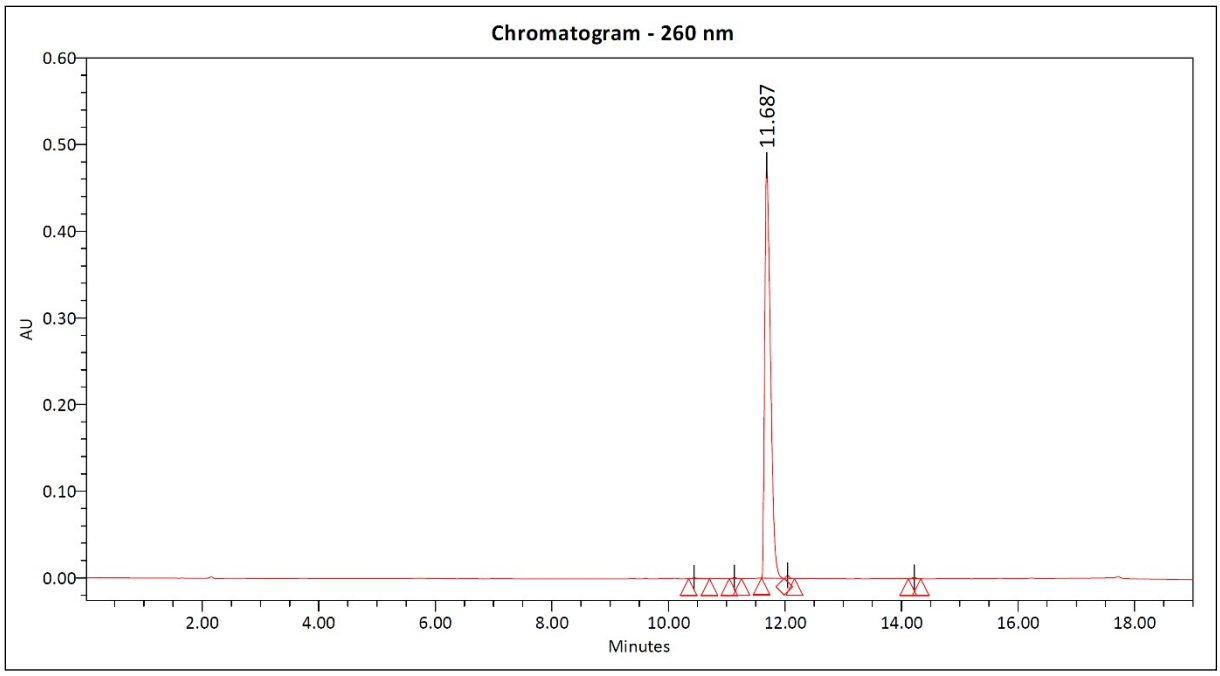

Figure S028. Analytical HPLC chromatogram (260 nm) of compound **7**.

(2R,2'R)-2,2'-(6-(4-carboxybenzyl)-3,6,9-triaza-1(2,6)-pyridinacyclodecaphane-3,9-diyl)dipropionic acid (L^2)

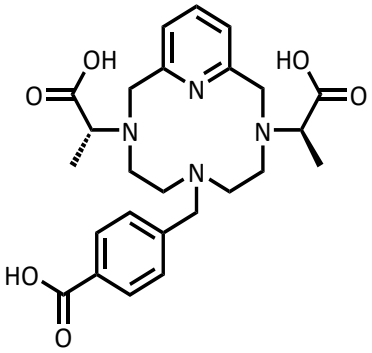

118 mg (2.95 mmol) sodium hydroxide was added to a solution of diethyl 2,2'-(6-(4-(*tert*-butoxycarbonyl)benzyl)-3,6,9-triaza-1(2,6)-pyridinacyclodecaphane-3,9-diyl)(2R,2'R)-dipropionate (**7**) prepared by dissolving 120 mg (0.201 mmol) of **7** in 25 mL ethanol, at room temperature. The reaction mixture was then heated up to 60 °C and kept at the given temperature for 3 h. The solvent was then removed using rotary evaporator to afford the crude product, which was purified by preparative HPLC. Lyophilization of the fractions with pure product returned the ligand $\mathbf{L^2}$ as a white solid (85 mg, yield 87%).

Preparative HPLC: UV-Vis detection: 210 and 260 nm; retention time: 9.02 min; gradient: 0.00→11.00 min 0→22% B; eluent: mixture of 5 mM TFA in MQ-water (A) and acetonitrile (B); flow: 25.00 mL/min; injection volume: 100.00 µL; sample: 97 mg/mL H_2O; column: Phenomenex Luna Prep C18(2) 100 Å, 5 µm, 150 × 21.20 mm; column ID: 589811-5.

^{1}H NMR (360.13 MHz, D_2O) δ 1.54 (s, 3H), 1.56 (s, 3H), 2.70 (m, 2H), 2.89 (m, 2H), 3.45 - 3.56 (m, 4H), 3.76 (m, 9H), 4.46 (m, 4H), 4.65 (m, 4H), 7.59 (d, 2H), 7.52 (d, 2H), 7.94 (d, J = 7.7 Hz, 2H), 8.01 (t, 1H) ppm; **^{13}C-JMOD NMR** (90.56 MHz, D_2O) δ 9.95, 49.25, 51.14,

55.42, 57.75, 57.80, 62.75, 123.35, 129.60, 129.95, 130.38, 133.32, 140.62, 149.43, 162.64, 169.91 ppm; **UHRMS** (ESI+) *m/z* calculated for $C_{25}H_{32}N_4O_6$ $[M+Na]^+$ 507.2214; found 507.2210. **HPLC** purity (260 nm): 99.08%; retention time: 5.294 min; gradient: 0.00→6.00 min 5→41% B; eluent: mixture of 5 mM TFA in MQ-water (A) and acetonitrile (B); flow: 1.00 mL/min; injection volume: 10.00 µL; sample: 0.30 mg/mL H_2O; column: Phenomenex Luna C18(2) 100 Å, 3 µm, 150 × 4.60 mm; column ID: H20-260762.

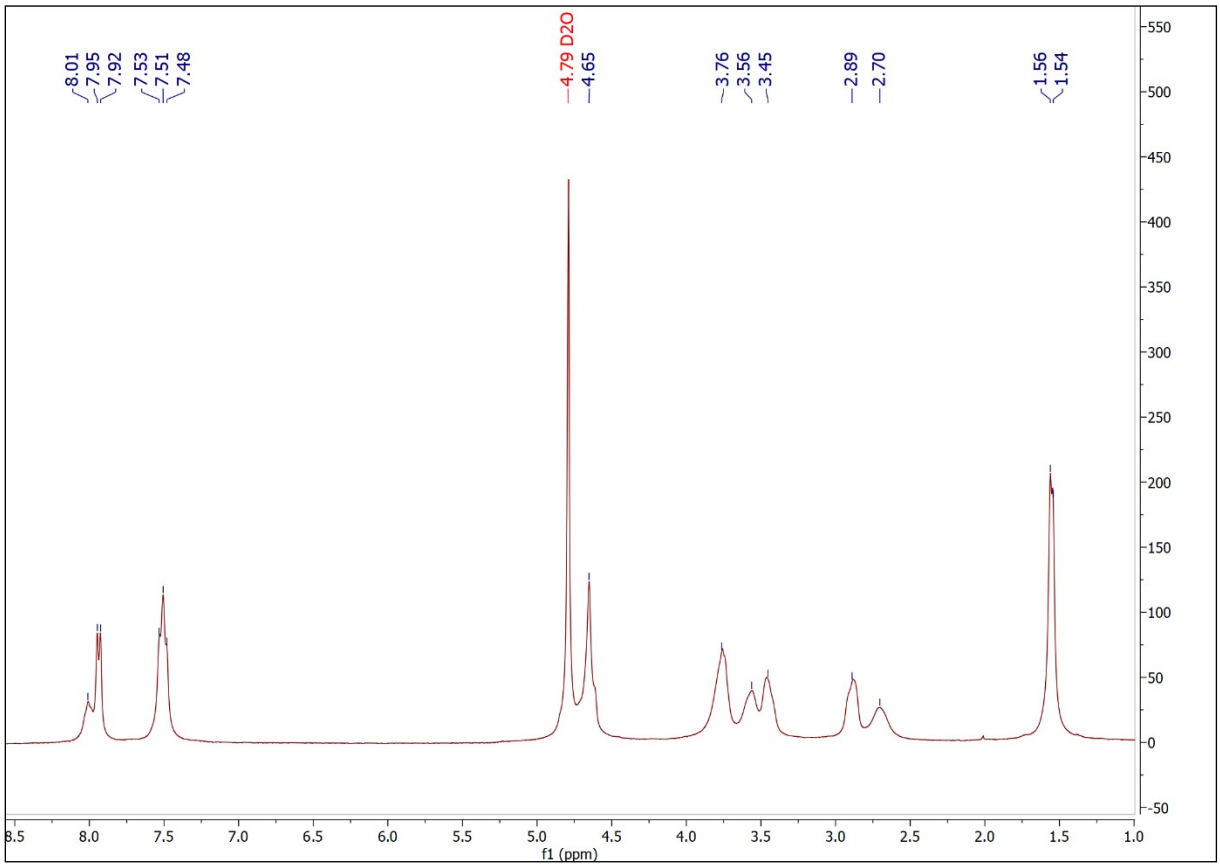

Figure S029. ^{1}H NMR (360.13 MHz, 298.0 K, D_2O) spectra of ligand **L²**.

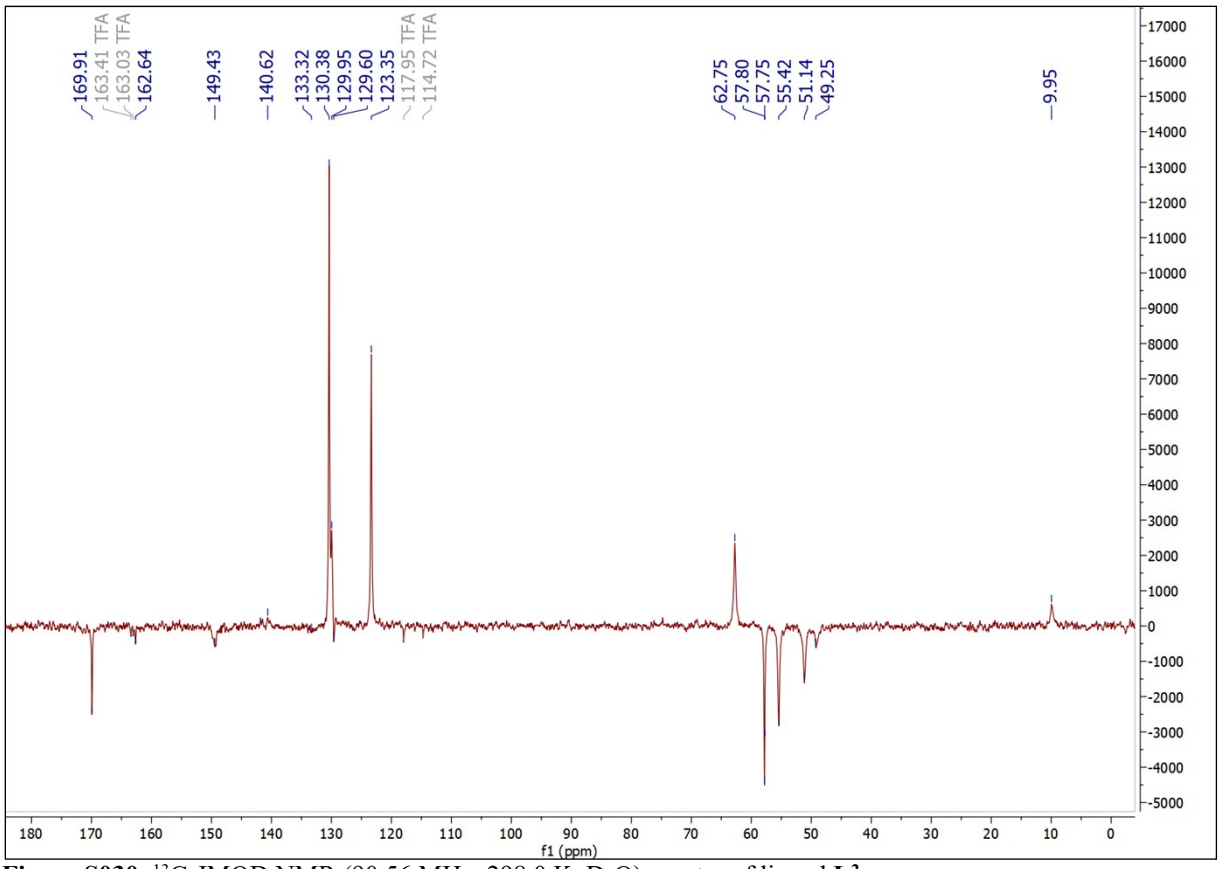

Figure S030. ^{13}C-JMOD NMR (90.56 MHz, 298.0 K, D_2O) spectra of ligand **L²**.

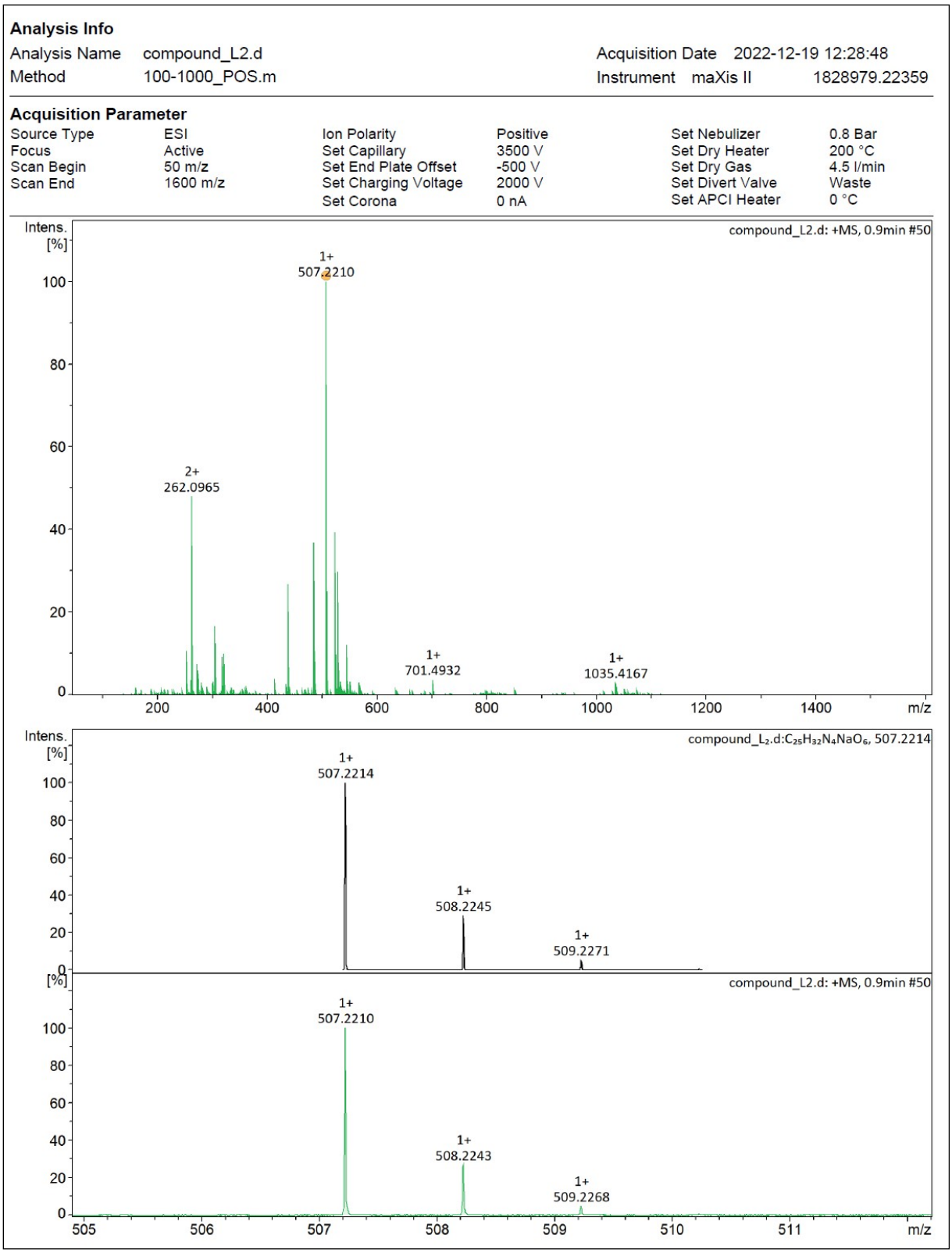

Figure S031. UHRMS spectra (ESI+) of ligand **L²**.

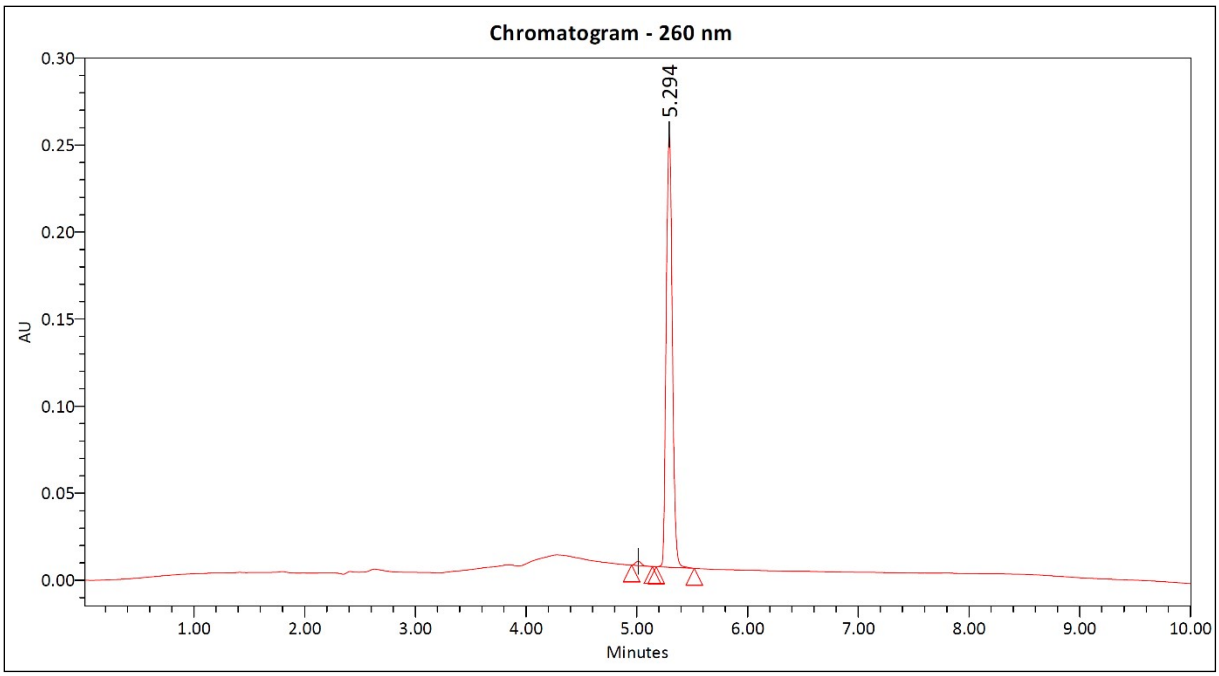

Figure S032. Analytical HPLC chromatogram (260 nm) of ligand $\mathbf{L^2}$.

2,2'-(3,6,9-triaza-1(2,6)-pyridinacyclodecaphane-3,9-diyl)bis(1-(piperidin-1-yl)ethan-1-one) (8)

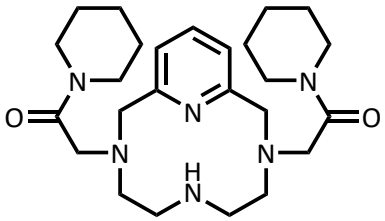

To a solution of Pyclen (3,6,9-triaza-1(2,6)-pyridinacyclodecaphane) (250 mg, 1.21 mmol) in acetonitrile (200 mL), under an argon atmosphere, was added sodium acetate trihydrate (660 mg, 4.85 mmol). The reaction was then heated to 60 °C and, with vigorous stirring, solution of 2-bromo-1-(piperidin-1-yl)ethan-1-one (624 mg, 3.02 mmol) in acetonitrile (60 mL) was added dropwise over the course of 9 h. The reaction mixture was stirred at 60 °C for 48 h. The solvent was then removed in vacuum to afford the crude product, which was purified by preparative HPLC to furnish the product **2** as a white solid (220 mg, yield 40%).

Preparative HPLC: UV-Vis detection: 210 and 260 nm; retention time: 16.09 min; gradient: 0.00→20.00 min 8→28% B; eluent: mixture of 5 mM TFA in MQ-water (A) and acetonitrile (B); flow: 25.00 mL/min; injection volume: 600.00 µL; sample: 550 mg / 5.00 mL 50% ACN in H_2O; column: Phenomenex Luna Prep C18(2) 100 Å, 10 µm, 250 × 21.20 mm; part number: 00G-4324-P0.

^{1}H NMR (360.13 MHz, D_2O) δ 1.45 (m, 4H), 1.54 (m, 8H), 2.95 (m, 4H), 3.22 (m, 4H), 3.31 (m, 4H), 3.39 (m, 4H), 4.09 (s, 4H), 4.43 (s, 4H), 7.60 (d, J = 8.0 Hz, 2H), 8.18 (t, J = 8.0 Hz, 1H) ppm; **^{13}C-JMOD NMR** (90.56 MHz, D_2O) δ 23.43, 25.03, 25.48, 43.50, 44.77, 45.72, 52.82, 57.26, 58.30, 123.30, 144.24, 153.09, 167.89 ppm; **UHRMS** (ESI+) *m/z* calculated for $C_{25}H_{40}N_6O_2$ $[M+H]^+$ 457.3286; found 457.3284. **HPLC** purity (260 nm): 95.90%; retention

time: 8.111 min; gradient: 0.00→15.00 min 0→90% B; eluent: mixture of 5 mM TFA in MQ-water (A) and acetonitrile (B); flow: 1,00 mL/min; injection volume: 1.00 µL; sample: 1.00 mg / 100 µL 50% ACN in H_2O; column: Phenomenex Luna C18(2) 100 Å, 5 µm, 150 × 4.60 mm; column ID: 345362.

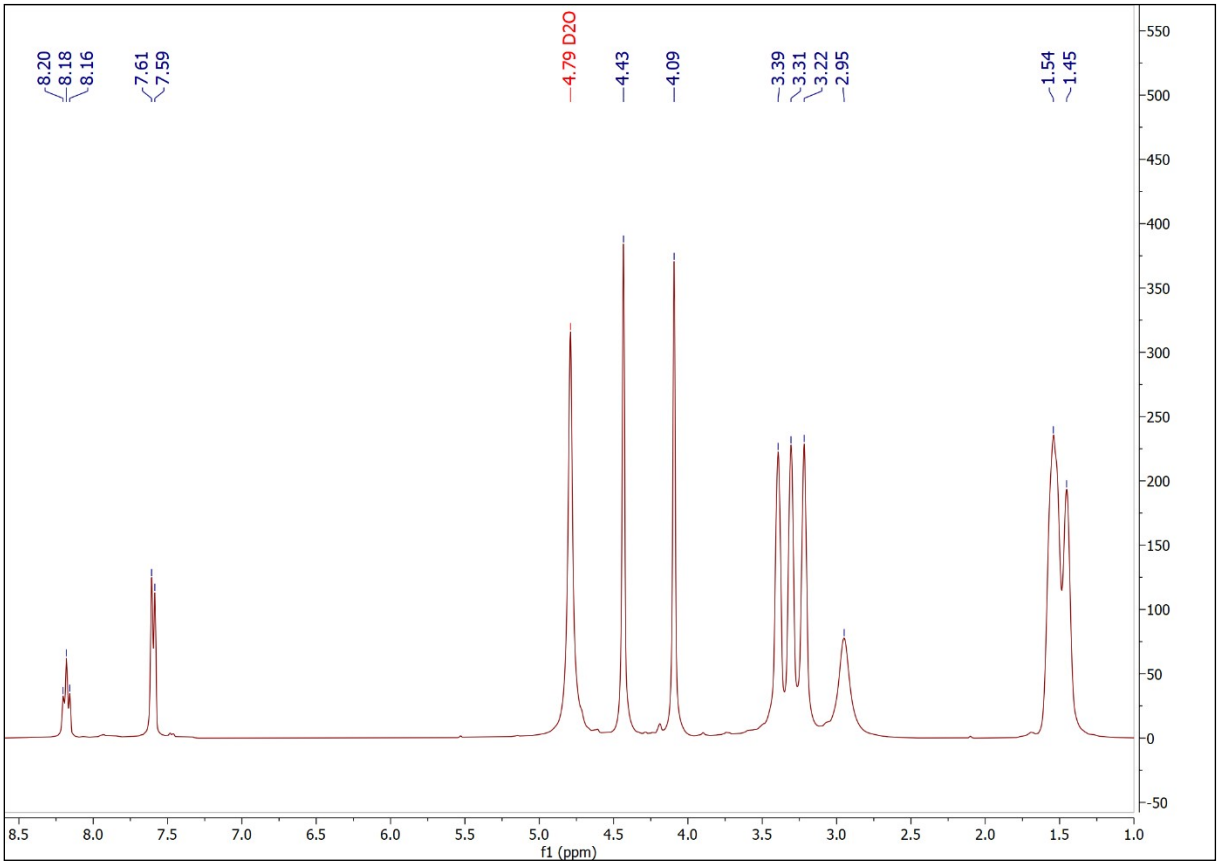

Figure S033. ^{1}H NMR (360.13 MHz, 298.0 K, D_2O) spectra of compound **8**.

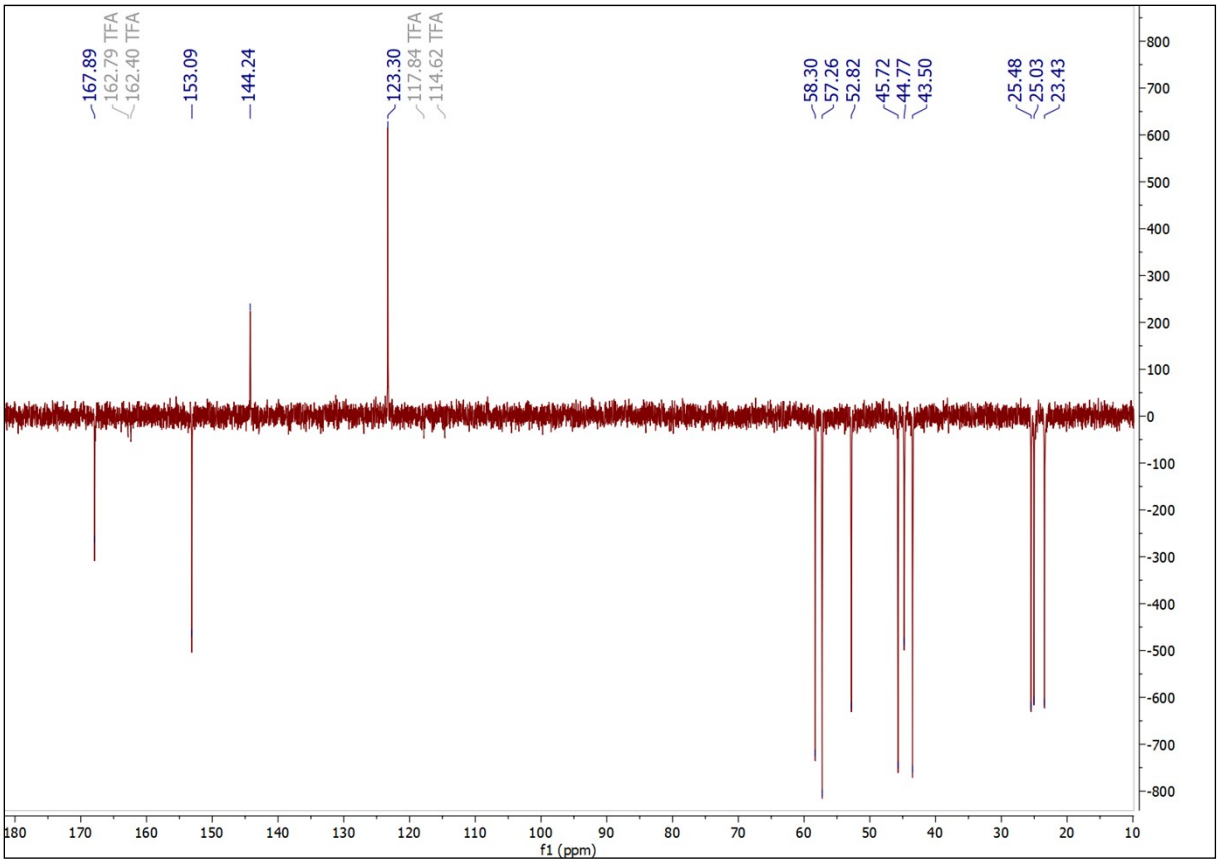

Figure S034. ^{13}C-JMOD NMR (90.56 MHz, 298.0 K, D_2O) spectra of compound **8**.

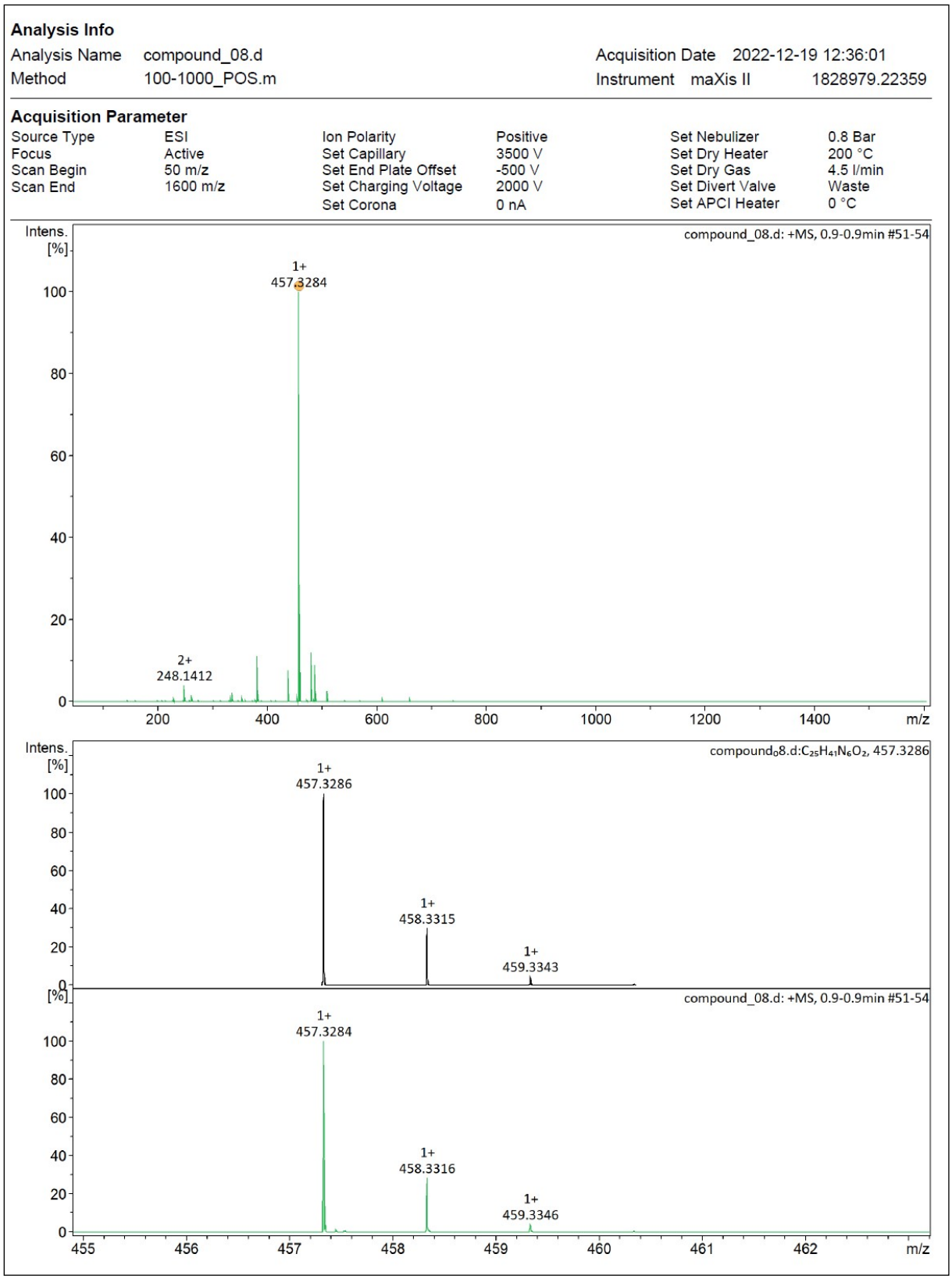

Figure S035. UHRMS spectra (ESI+) of compound **8**.

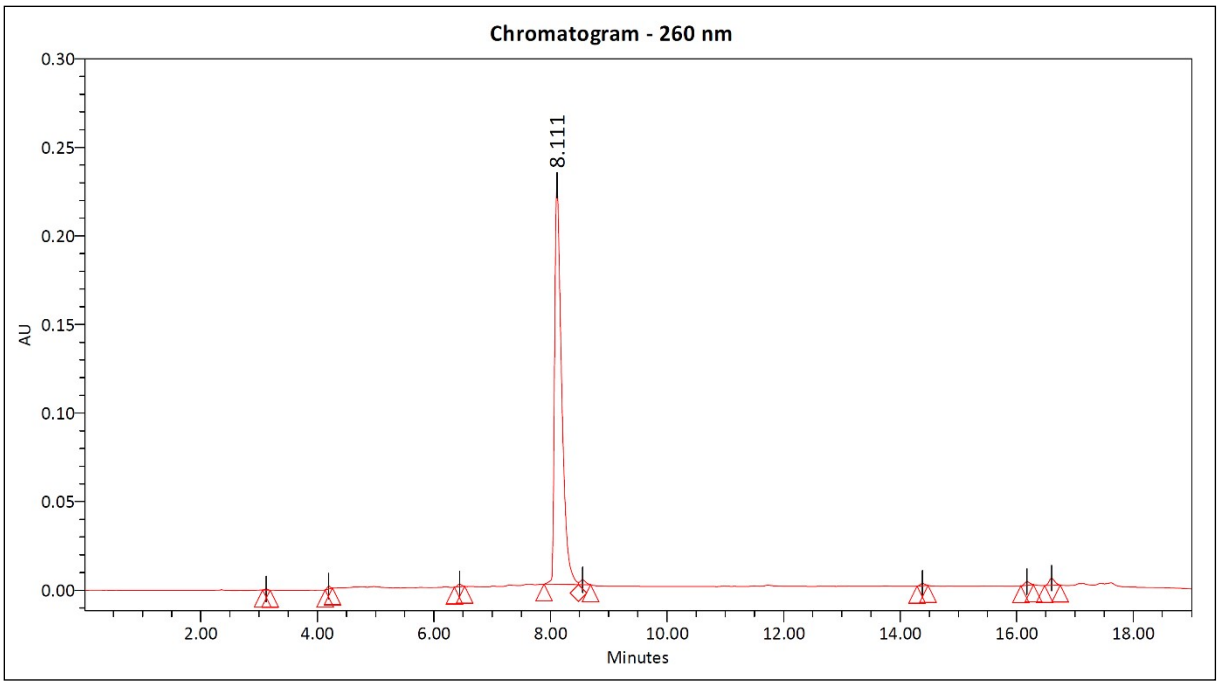

Figure S036. Analytical HPLC chromatogram (260 nm) of compound **8**.

Tert-butyl 4-((3,9-bis(2-oxo-2-(piperidin-1-yl)ethyl)-3,6,9-triaza-1(2,6)-pyridinacyclodecaphane-6-yl)methyl)benzoate (9)

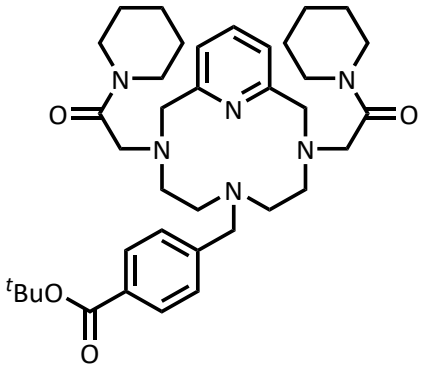

Potassium carbonate (76 mg, 0.55 mmol) and sodium iodide (17.4 mg, 0.116 mmol) was added to the solution of 2,2'-(3,6,9-triaza-1(2,6)-pyridinacyclodecaphane-3,9-diyl)bis(1-(piperidin-1-yl)ethan-1-one) (**8**) (100 mg, 0.219 mmol) in 50 mL acetonitrile, under argon protected atmosphere at room temperature. The reaction mixture was then heated up to 60 °C and the solution of *tert*-butyl 4-(bromomethyl)benzoate (60.2 mg (0.222 mmol) dissolved in 20 mL acetonitrile) was added dropwise over the course of 30 min. The reaction mixture was stirred at 60 °C for an additional 48 h, cooled and the solvent evaporated under reduced pressure. The crude product obtained was purified by preparative HPLC. The combined fractions were lyophilized after freezing to give the product **7** as a white solid (120 mg, yield 84%).

Preparative HPLC: UV-Vis detection: 210 and 260 nm; retention time: 6.02 min; gradient: 0.00→10.00 min 20→70% B; eluent: mixture of 5 mM TFA in MQ-water (A) and acetonitrile (B); flow: 25.00 mL/min; injection volume: 500.00 µL; sample: 142 mg/mL 50% ACN in H_2O;

column: Phenomenex Luna Prep C18(2) 100 Å, 5 µm, 250 × 21.20 mm; column ID: H18-268346.

^{1}H NMR (360.13 MHz, CD_3CN-*d_3*) δ 1.52 (m, 8H), 1.58 (s, 9H), 1.60 (m, 4H), 2.95 (m, 4H), 3.09 (m, 4H), 3.46 (m, 4H), 3.50 (m, 4H), 3.80 (s, 4H), 3.94 (s, 2H), 4.51 (s, 4H), 7.37 (d, *J* = 7.8 Hz, 2H), 7.62 (d, *J* = 8.5 Hz, 2H), 7.92 (t, *J* = 7.8 Hz, 1H), 7.92 (d, *J* = 8.5 Hz, 2H) ppm; **^{13}C-JMOD NMR** (90.56 MHz, CD_3CN-*d_3*) δ 24.85, 26.13, 26.63, 28.41, 43.72, 46.32, 51.86, 53.51, 56.95, 57.82, 60.12, 82.28, 123.27, 130.52, 131.71, 133.00, 140.62, 140.72, 154.15, 164.91, 166.09 ppm; **UHRMS** (ESI+) *m/z* calculated for $C_{37}H_{54}N_6O_4$ $[M+H]^+$ 647.4279; found 647.4278. **HPLC** purity (260 nm): 98.99 %; retention time: 10.326 min; gradient: 0.00→15.00 min 0→90 % B; eluent: mixture of 5 mM TFA in MQ-water (A) and acetonitrile (B); flow: 1.00 mL/min; injection volume: 10.00 µL; sample: 0.25 mg/mL 50% ACN in H_2O; column: Phenomenex Luna C18(2) 100 Å, 5 µm, 150 × 4.60 mm; column ID: 345362.

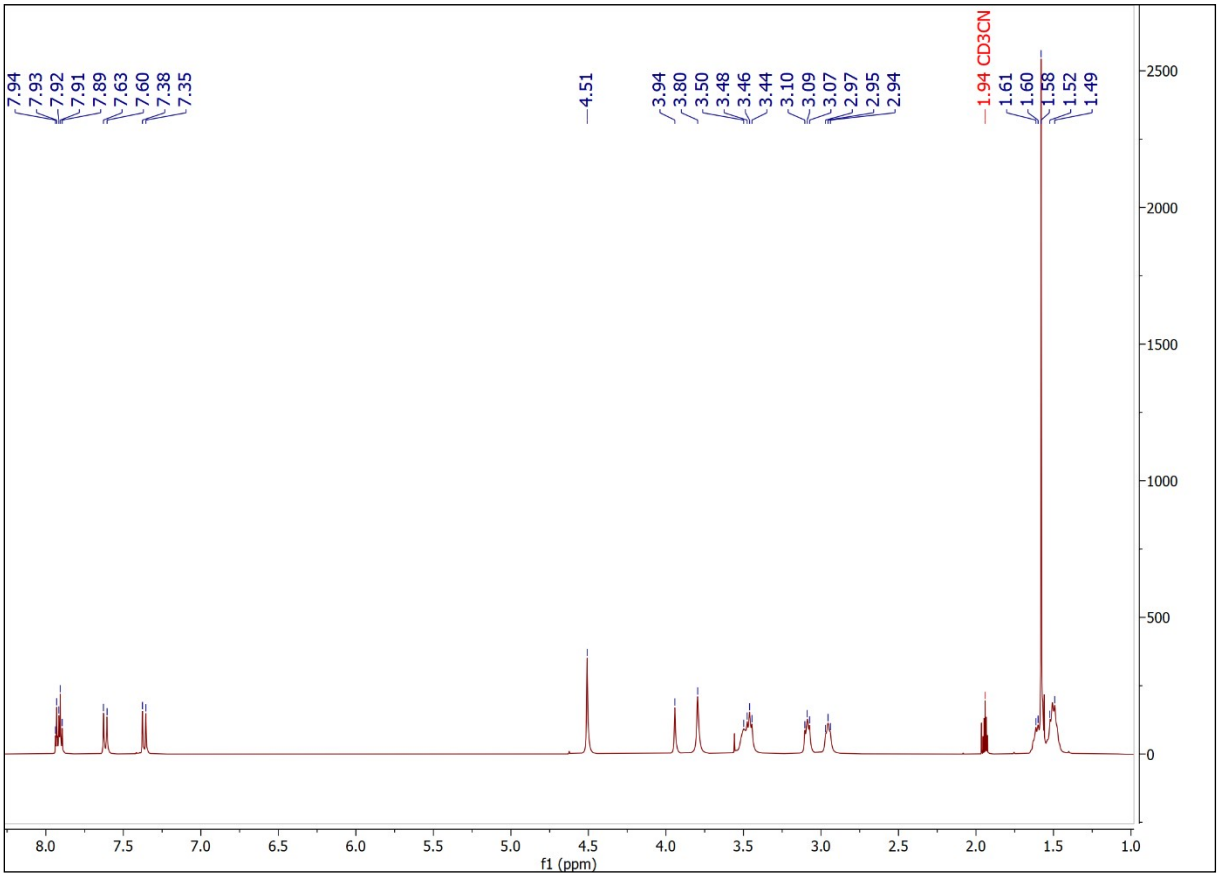

Figure S037. ^{1}H NMR (360.13 MHz, 298.0 K, CD_3CN-*d3*) spectra of compound **9**.

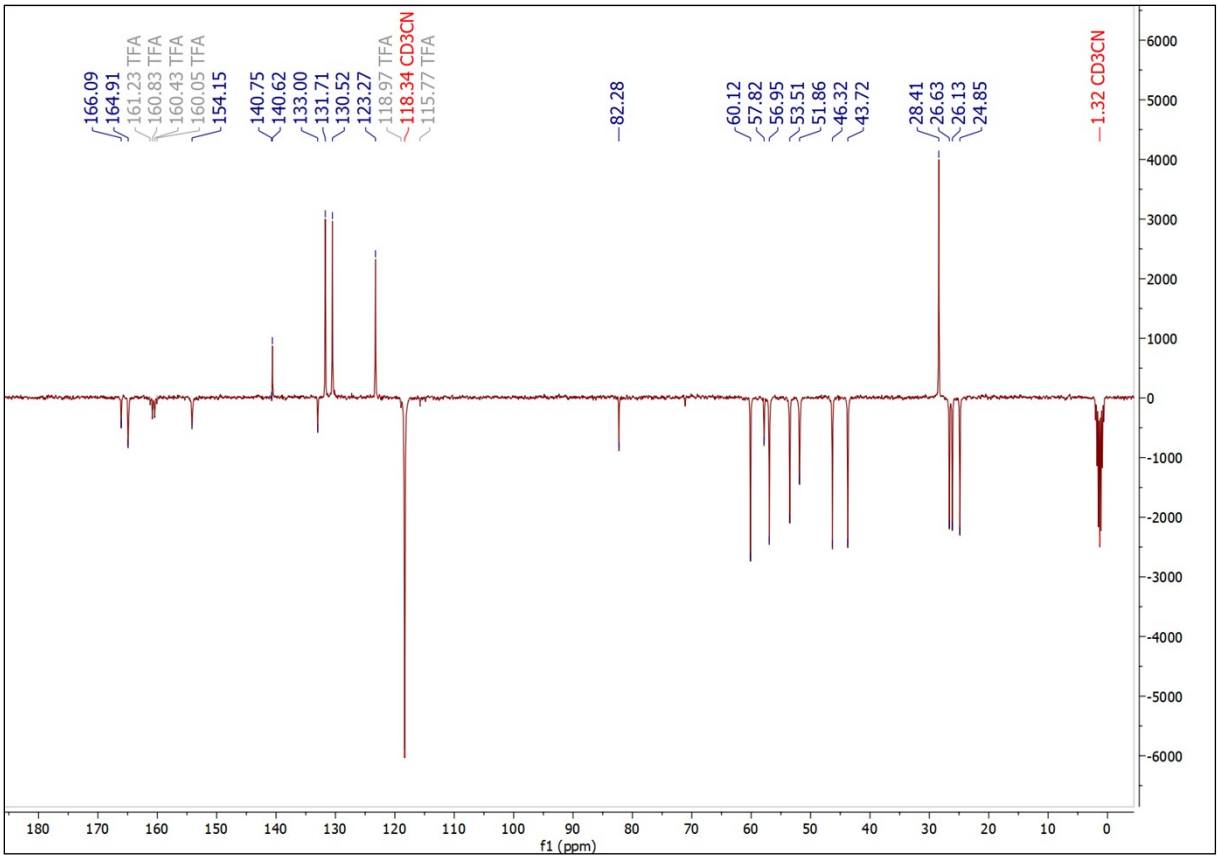

Figure S038. ^{13}C-JMOD NMR (90.56 MHz, 298.0 K, CD_3CN-*d3*) spectra of compound **9**.

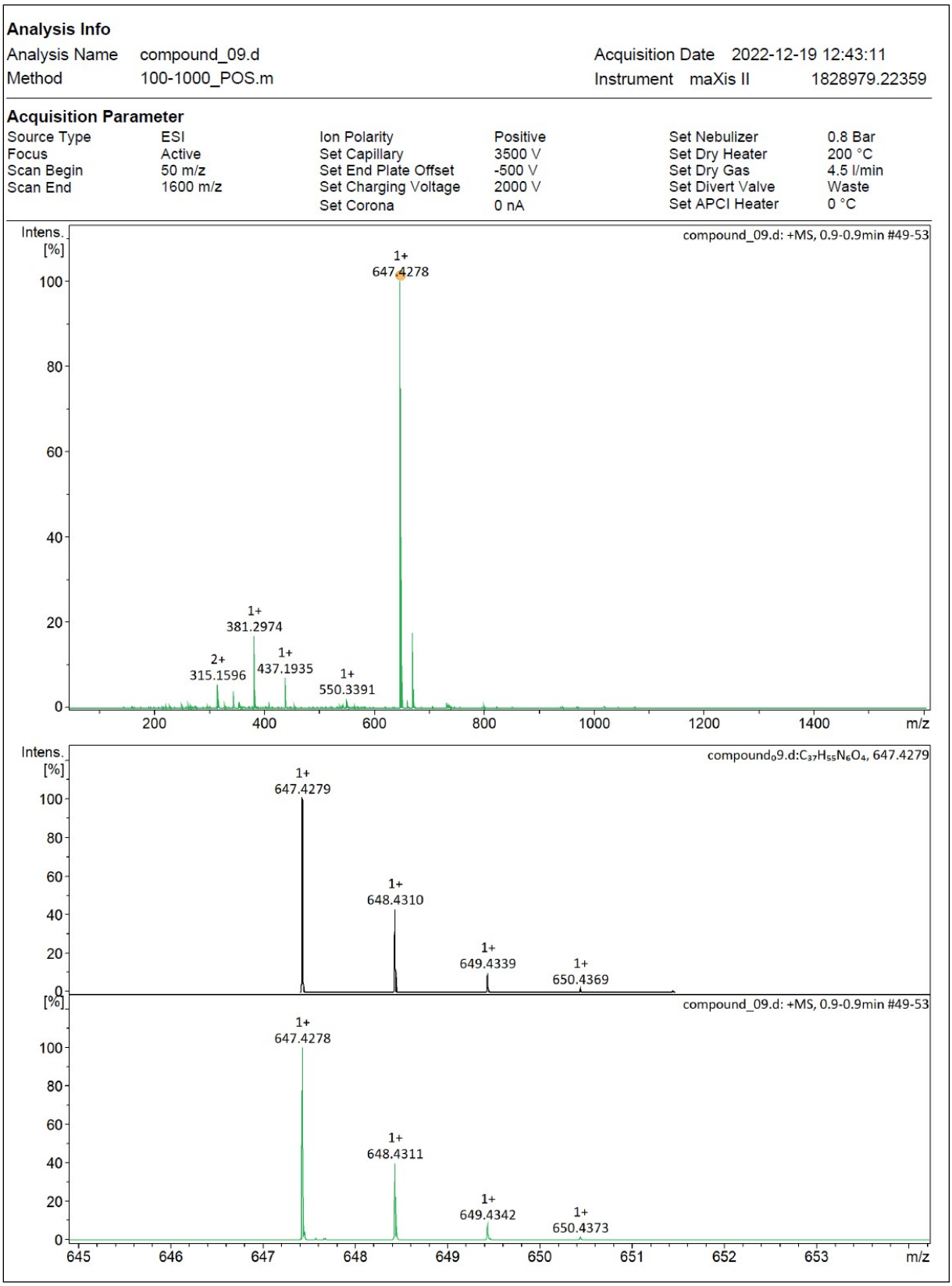

Figure S039. UHRMS spectra (ESI+) of compound **9**.

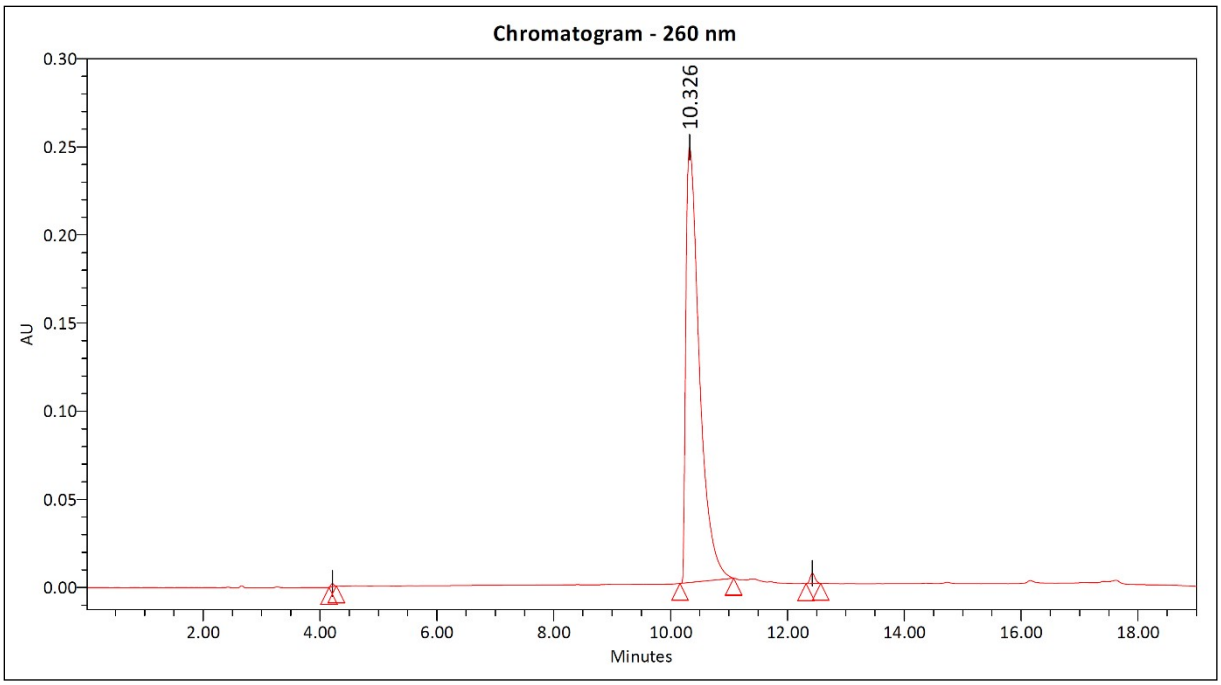

Figure S040. Analytical HPLC chromatogram (260 nm) of compound **9**.

4-((3,9-bis(2-oxo-2-(piperidin-1-yl)ethyl)-3,6,9-triaza-1(2,6)-pyridinacyclodecaphane-6-yl)methyl)benzoic acid (L^3)

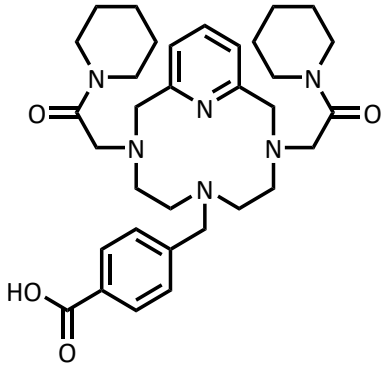

110 mg (0.170 mmol) of *tert*-butyl 4-((3,9-bis(2-oxo-2-(piperidin-1-yl)ethyl)-3,6,9-triaza-1(2,6)-pyridinacyclodecaphane-6-yl)methyl)benzoate (**9**) was dissolved in 15 mL dichloromethane and trifluoroacetic acid (7 mL) was added dropwise to this solution while cooling it with ice/water bath (0 °C). The reaction mixture was stirred for 12 hours at room temperature and the solvent was removed under reduced pressure to afford crude product, which was purified then by preparative HPLC. The fractions containing the pure substance were combined, lyophilized to give the $\mathbf{L^3}$ ligand as a white solid (96 mg, yield 96%).

Preparative HPLC: UV-Vis detection: 210 and 260 nm; retention time: 8.06 min; gradient: 0.00→10.00 min 0→40% B; eluent: mixture of 5 mM TFA in MQ-water (A) and acetonitrile (B); flow: 25.00 mL/min; injection volume: 500.00 µL; sample: 137 mg / 800 µL 40% ACN in H_2O; column: Phenomenex Luna Prep C18(2) 100 Å, 5 µm, 250 × 21.20 mm; column ID: H18-268346.

^{1}H NMR (400.13 MHz, CD_3CN-d_3) δ 1.49 (m, 8H), 1.60 (m, 4H), 3.01 (m, 4H), 3.10 (m, 4H), 3.41 (m, 4H), 3.49 (m, 4H), 3.68 (s, 4H), 4.05 (s, 2H), 4.40 (s, 4H), 7.31 (d, J = 7.8 Hz, 2H), 7.61 (d, J = 8.1 Hz, 2H), 7.87 (t, J = 7.8 Hz, 1H), 7.96 (d, J = 8.5 Hz, 2H) ppm; **^{13}C-JMOD NMR** (100.62 MHz, CD_3CN-d_3) 24.85, 26.16, 26.64, 43.59, 46.30, 51.51, 52.42, 53.09, 56.99, 59.94, 122.91, 130.92, 131.72, 132.37, 139.87, 140.26, 155.42, 165.64, 167.86 ppm; **UHRMS** (ESI+) *m/z* calculated for $C_{33}H_{46}N_6O_4$ $[M+H]^+$ 591.3653; found 591.3653. **HPLC** purity (260 nm): 98.95%; retention time: 7.741 min; gradient: 0.00→15.00 min 0→90% B; eluent: mixture of 5 mM TFA in MQ-water (A) and acetonitrile (B); flow: 1.00 mL/min; injection volume: 10.00 µL; sample: 0.60 mg/mL 50% ACN in H_2O; column: Phenomenex Luna C18(2) 100 Å, 5 µm, 150 × 4.60 mm; column ID: 345362.

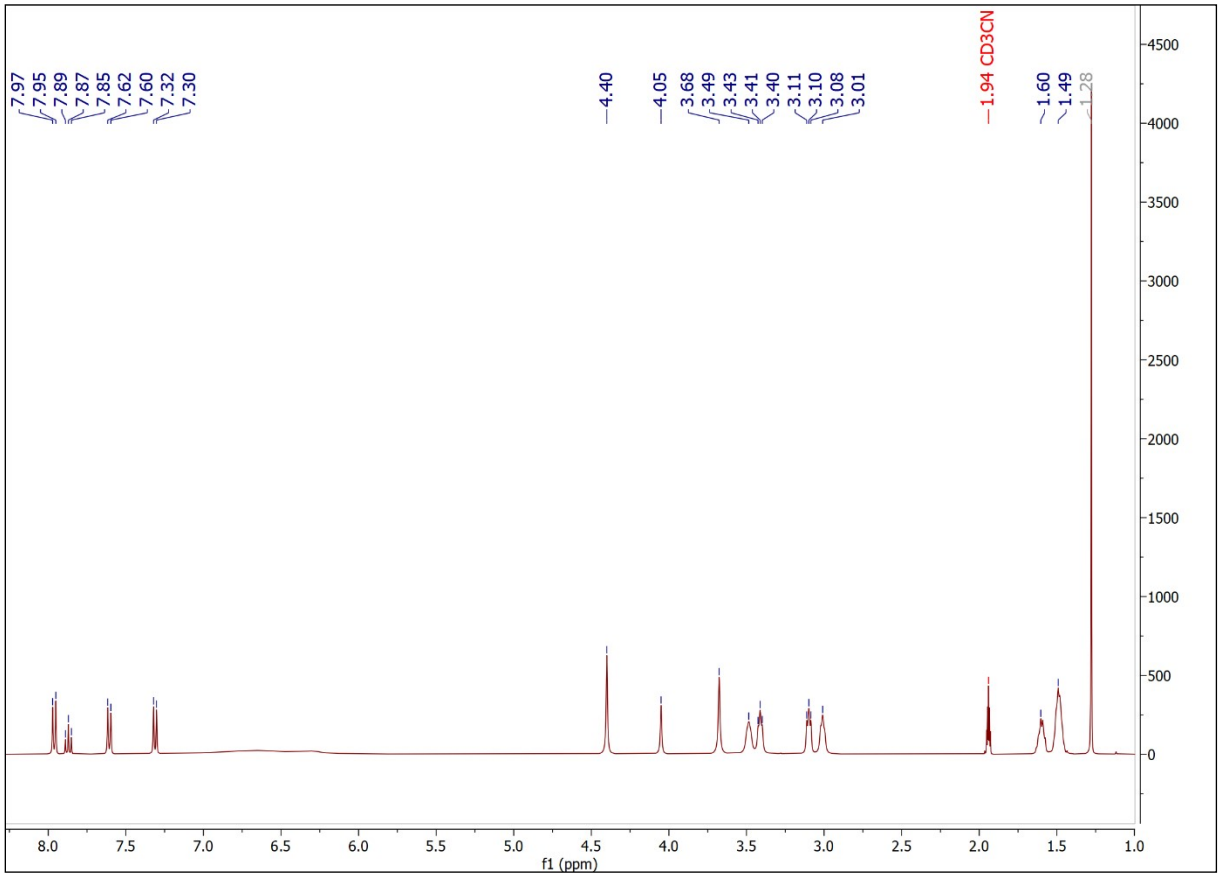

Figure S041. ^{1}H NMR (400.13 MHz, 298.0 K, CD_3CN-*d3*) spectra of ligand **L^{3}**.

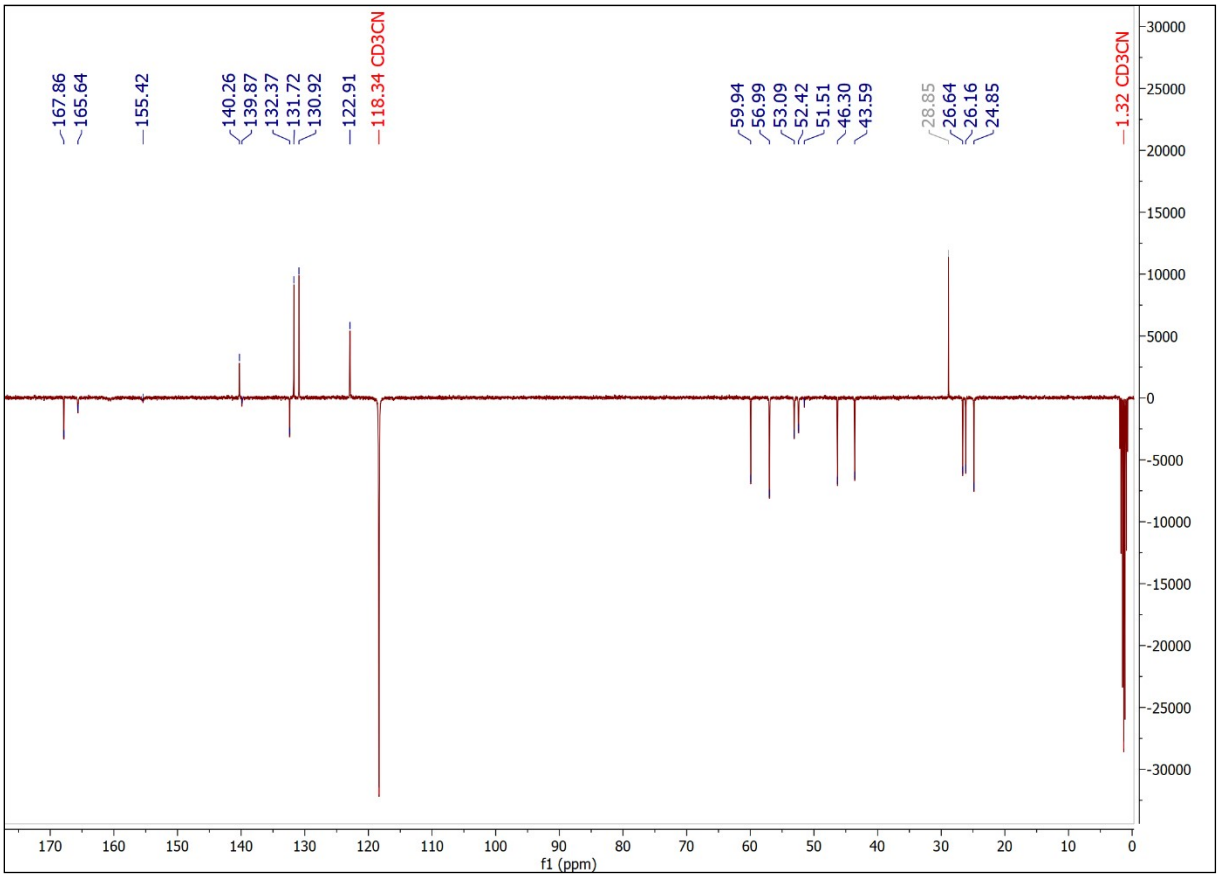

Figure S042. ^{13}C-JMOD NMR (100.62 MHz, 298.0 K, CD_3CN-*d3*) spectra of ligand **L^3**.

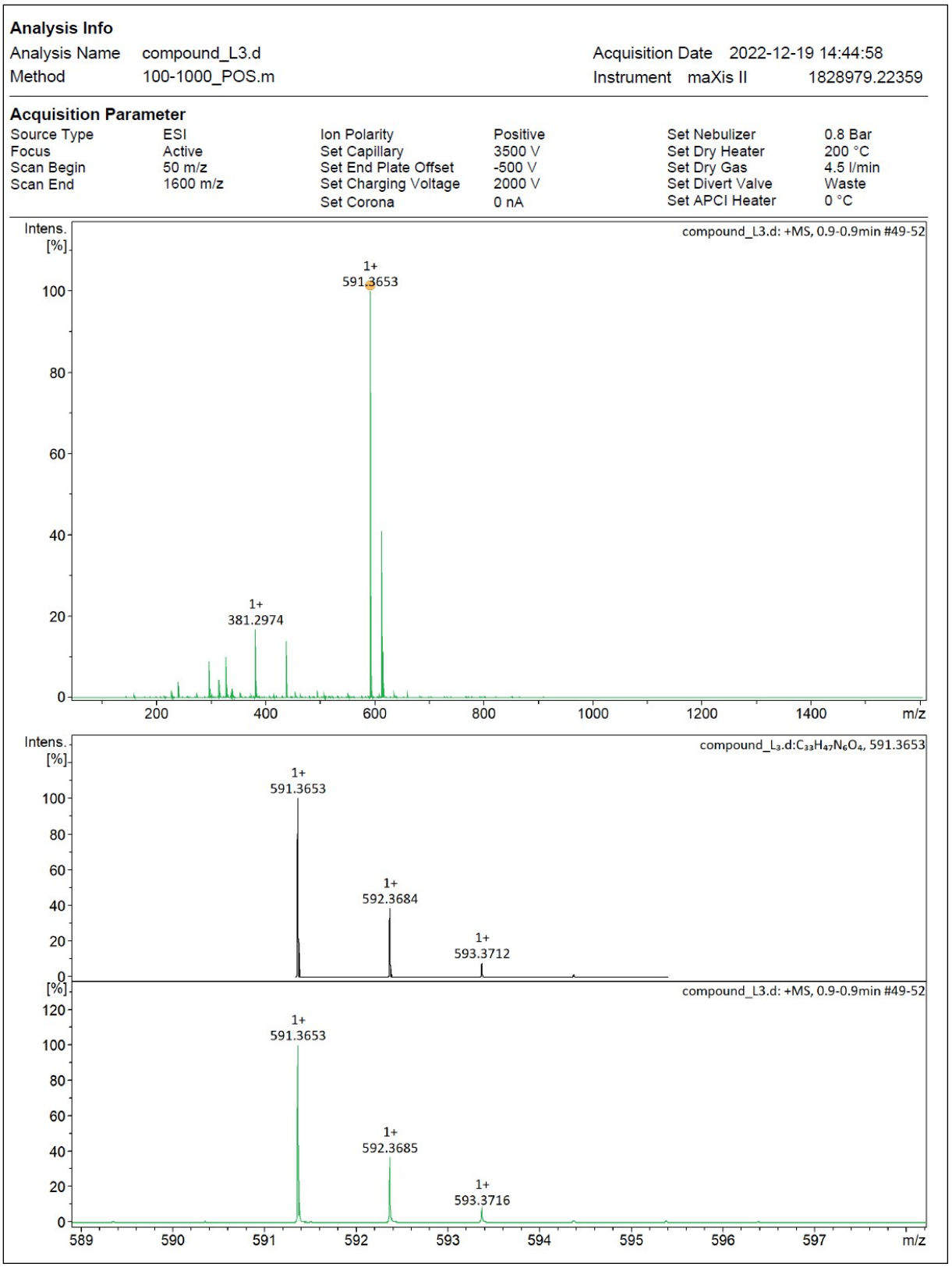

Figure S043. UHRMS spectra (ESI+) of ligand **L**[3].

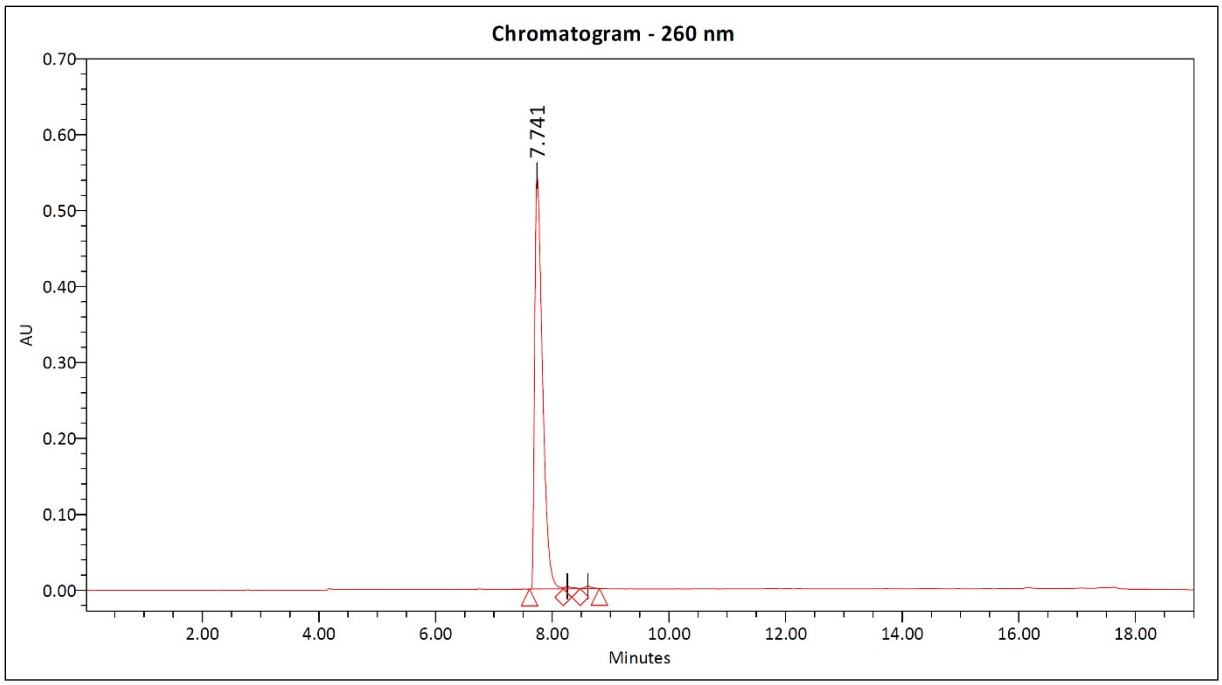

Figure S044. Analytical HPLC chromatogram (260 nm) of ligand $\mathbf{L^3}$.

2. Physicochemical characterization of the Mn(II) complexes formed by the BFCs: stability and speciation, dissociation and relaxivity

Metal stock solutions were prepared from the highest analytical grade chemicals, and their concentrations were determined by complexometric titration with standardized Na_2H_2EDTA and eriochrome black T indicator in the presence of ascorbic acid and potassium hydrogen tartrate. Equilibrium studies were performed by pH-potentiometry or ^{1}H-relaxometry (in the case of PC2AM^{pip}Bn^{p}CO2H ligand owing to the slow formation of its Mn(II) chelate). The details of experimental setup (calibration procedure, correction applied in order to correct for the difference caused by the diffusion potential etc.) was published elsewhere.[3] Protonation constants of the ligands and stability constants of their Mn(II) complexes were determined by titrating of 2.5 mM ligand solution in the absence and presence of Mn(II) using standardized NaOH solution in the pH range of 1.75-11.80. The protonation constants of the ligand (log K_i^H) are defined as follows:

$$K_i^H = \frac{[H_iL]}{[H_{i-1}L][H^+]}$$

where $i = 1, 2, \ldots, 5$ and $[H_{i-1}L]$ and $[H^+]$ are the equilibrium concentrations of the ligand ($i = 1$), its protonated forms ($i = 2, \ldots, 4$) and hydrogen ion, respectively. The stability constants are defined as follows (where $i = 0$ for the hydroxido complex and $i = 1$ for the protonated complex):

$$K_{ML} = \frac{[ML]}{[M][L]} \text{ and } K_{MH_iL} = \frac{[MH_iL]}{[MH_{i-1}L][H^+]}$$

As mentioned above, for the bis(amide) derivative ligand (3,9-PC2AM^{pip}Bn^{p}CO$_2$H) batch method was applied owing to the slow formation of its Mn(II) complex. Ten samples containing the ligand and the Mn(II) ion (at a concentration of 2.0 mM) and constant ionic strength (0.15 M NaCl) were prepared in the pH range of 1.66-4.73 and equilibrated for two weeks, followed by the measurement of their T_1 and T_2 relaxation times (25 °C and 1.41 T). The measurement was repeated after an additional two weeks in order to ensure that the equilibrium in the samples was attained followed by the measurement of their pH. The equilibrium data obtained were fitted by using the PSEQUAD computer program.[4] Relaxivity (r_{1p} and r_{2p}) of the complexes were determined by using accepted literature protocols in samples of 0.3-0.4 mL volume by using Bruker Minispec MQ-20 and MQ-60 NMR analysers. The temperature of the sample holder was set 25.0 (±0.2) °C and controlled with a circulating water bath thermostat. The r_{1p} values for the investigated complexes were determined by means of inversion recovery method (180°–τ–90°), averaging 3-6 data readouts obtained at 14 different τ delay times, while r_{2p} data were collected by using Carl-Purcell-Meiboom-Gill (CPMG) spin-echo pulse sequence. The pH values were either set by using a 0.05 M 4-(2-hydroxyethyl)-1-piperazine-ethanesulfonic acid (HEPES) buffer (pH = 7.4) or monitored (stability determination) using a Metrohm 827 pH lab pH-meter and a Metrohm 6.0234.100 combined electrode in the pH range of 1.66-4.73 calibrated by two-point calibration routine. The transmetallation reaction propagated by Zn(II) ions was monitored by measuring the T_2 relaxation times as a function of time at pH = 6.0 set by 2-(*N*-morpholino)ethanesulphonic acid (MES) buffer at 50 mM concentration in the presence of 25 equivalents of Zn(II) ions at 37 °C. These conditions were used recently by P.

Caravan et al. and employed here to obtain data being comparable directly with those evidenced for $[Mn(PyC3A)]^-$ and parent [Mn(PC2A)] complexes.[5]

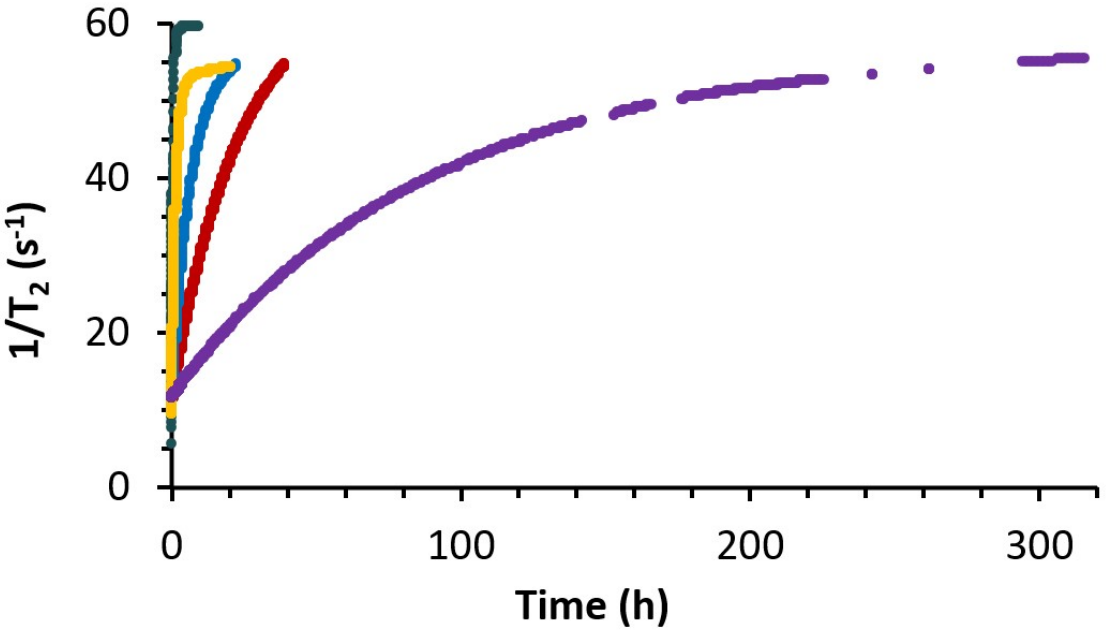

Figure S045. Dissociation of the $[Mn(PC2A)(H_2O)]^-$, $[Mn(3,9\text{-}PC2ABn^{pNO_2})(H_2O)]$, $[Mn(3,9\text{-}PC2ABn^{pCO_2H})(H_2O)]^-$, $[Mn(3,9\text{-}PC2MABn^{pCO_2H})(H_2O)]^-$, and $[Mn(3,9\text{-}PC2AM^{pip}Bn^{pCO_2H})(H_2O)]^-$ complexes in the presence of 25 equiv. of Zn(II) at pH=6.0 as determined by T_2 realxometry at 1,41 T and 37 °C.

Table S001. The relaxivities ($mM^{-1}s^{-1}$) of the Mn(II) complexes formed with PyC3A, 3,9-PC2A, 3,9-PC2ABn^{pNO_2}, 3,9-PC2MABn^{pCO_2H}, and 3,9-PC2AM^{pip}Bn^{pCO_2H} ligands at 25 °C / 37 °C and pH = 7.4.

		PyC3A[a]	3,9-PC2A [b]	**3,9-PC2A Bn^{pNO_2}**	**3,9-PC2A Bn^{pCO_2H}**	**3,9-PC2MA Bn^{pCO_2H}**	**3,9-PC2AM^{pip} Bn^{pCO_2H}**
0,49 T	r_{1p}	3.3 / 2.1	2.91 / -	4.19 / -	5.13 / 5.03	4.05 / 3.05	5.78 / 4.32
	r_{2p}	- / -	3.96 / -	- / -	7.89 / 11.42	5.95 / 4.44	8.98 / 6.78
1,41 T	r_{1p}	2.8 / 2.5	2.40 / -	- / -	4.95 / 3.69	3.92 / 2.76	5.83 / 4.17
	r_{2p}	- / 4.9	4.82 / -	- / -	11.29 / 8.22	9.44 / 7.15	13.57/10.12

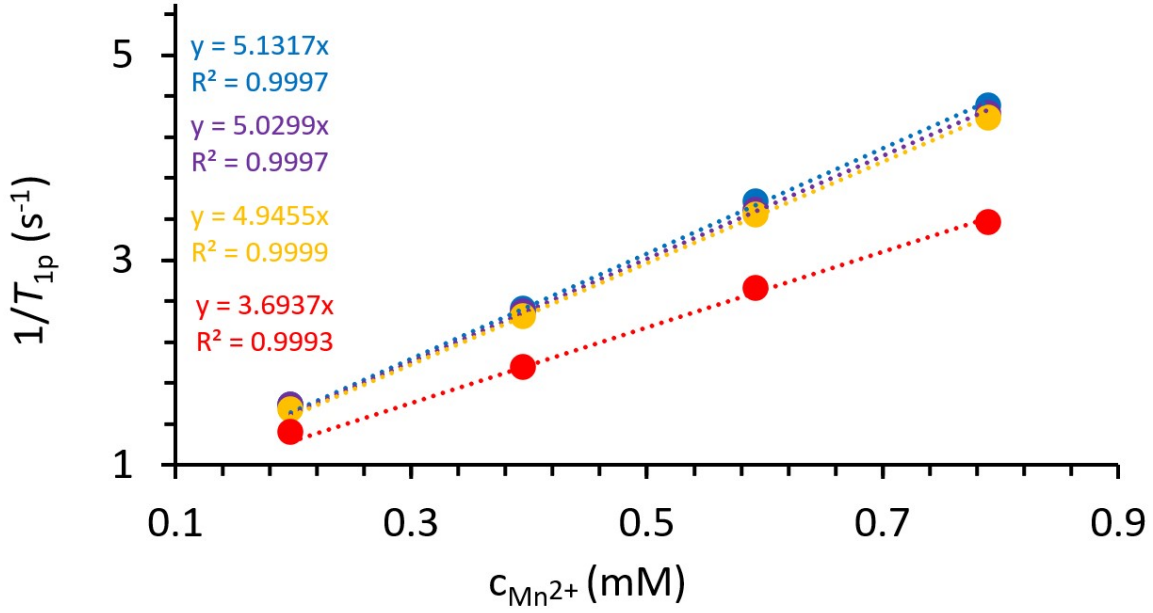

Figure S046. Determination of r_{1p} relaxivity for [Mn(3,9-PC2ABn^{pCO2H})(H_2O)]$^-$ at 0.49 T (25 °C / 37 °C) and 1.41 T (25 °C / 37 °C) field strength.

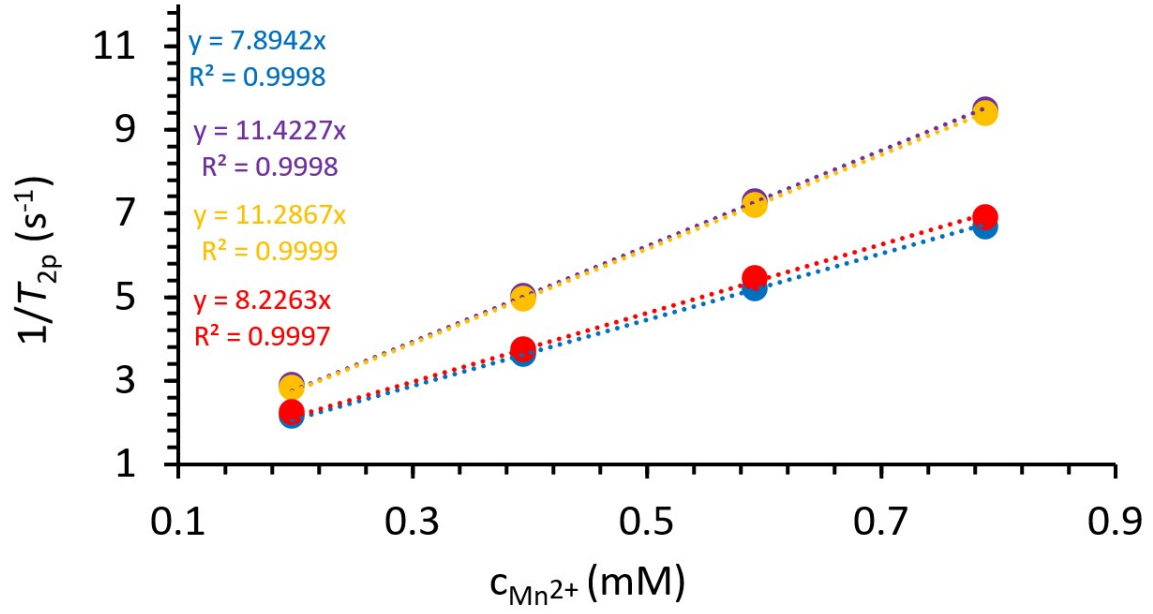

Figure S047. Determination of r_{2p} relaxivity for [Mn(3,9-PC2ABn^{pCO2H})(H_2O)]$^-$ at 0.49 T (25 °C / 37 °C) and 1.41 T (25 °C / 37 °C) field strength.

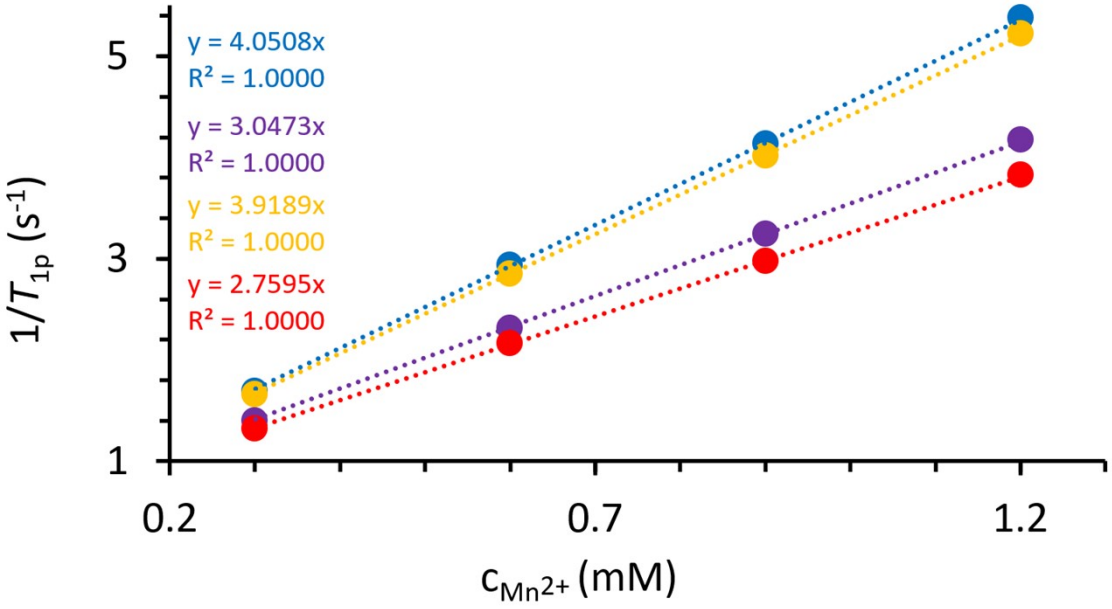

Figure S048. Determination of r_{1p} relaxivity for [Mn(3,9-PC2MABn^{pCO_2H})(H_2O)]$^-$ at 0.49 T (25 °C / 37 °C) and 1.41 T (25 °C / 37 °C) field strength.

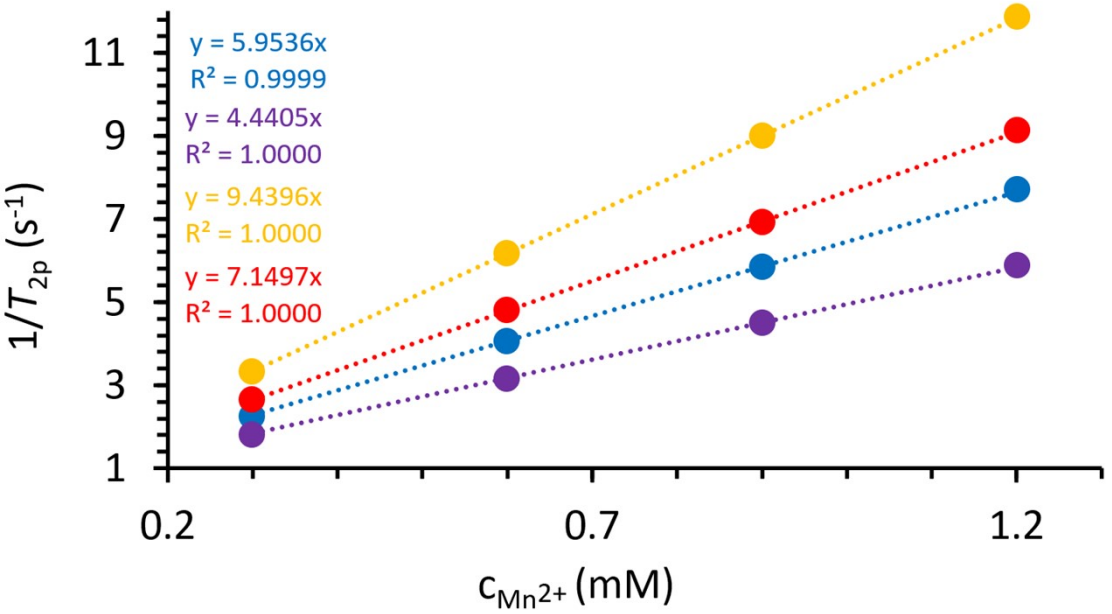

Figure S049. Determination of r_{2p} relaxivity for [Mn(3,9-PC2MABn^{pCO_2H})(H_2O)]$^-$ at 0.49 T (25 °C / 37 °C) and 1.41 T (25 °C / 37 °C) field strength.

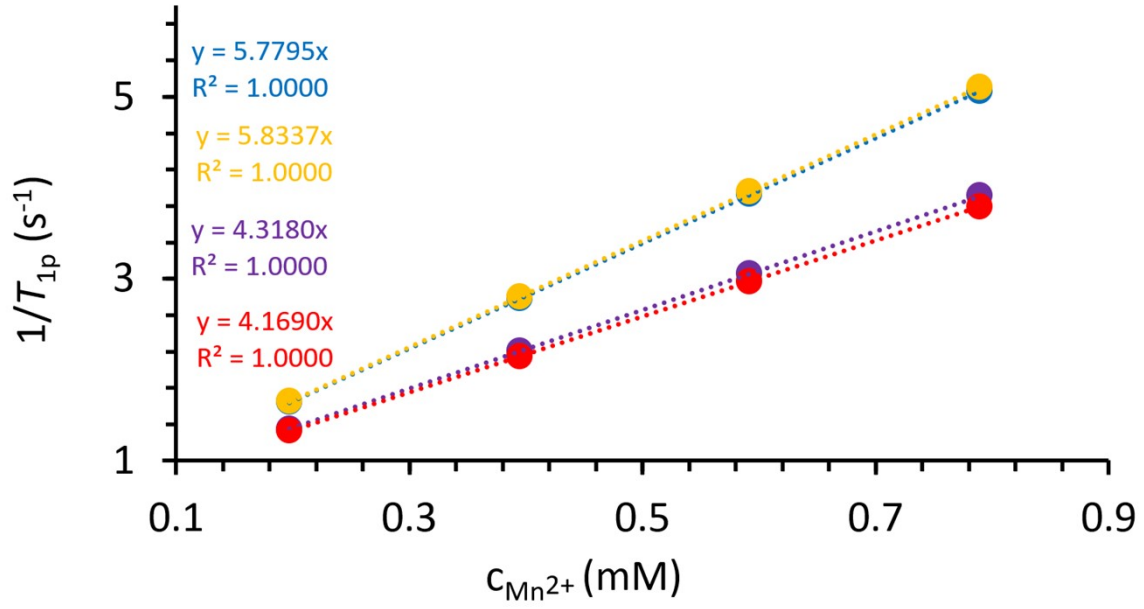

Figure S050. Determination of r_{1p} relaxivity for [Mn(3,9-PC2AM^{pip}Bn^{pCO2H})(H_2O)]$^-$ at 0.49 T 25 °C / 37 °C) and 1.41 T (25 °C / 37 °C) field strength.

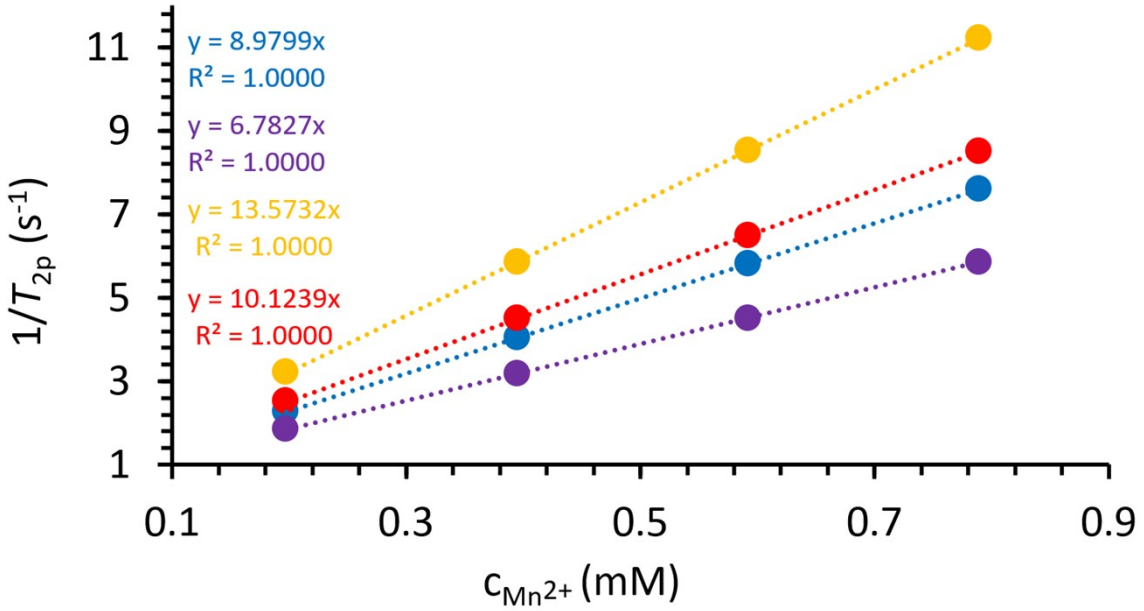

Figure S051. Determination of r_{2p} relaxivity for [Mn(3,9-PC2AM^{pip}Bn^{pCO2H})(H_2O)]$^-$ at 0.49 T 25 °C / 37 °C) and 1.41 T (25 °C / 37 °C) field strength.

3. [^{52}Mn]Mn labelling of the ligands

Radiochemistry experiments

General

To avoid metallic contaminations, all solvents that were used for the radiochemical experiments possessed high purity. HCl for trace analysis was purchased from VWR. The ^{52}Mn radioisotope was produced by an MGC-20 cyclotron at the Institute for Nuclear Research, Hungary. Activity measurements were carried out with AtomLab 500 dose calibrator. AG® 1-X8 resin (200-400 mesh, chloride form) was purchased from Bio-Rad.

Production and purification of ^{52}Mn radioisotope in the laboratory of Institute for Nuclear Research

The ^{52}Mn isotope was produced by proton irradiation with an 18 MeV beam on a natural Cr target via a ^{52}Cr(p,n)^{52}Mn reaction. The purification of the radionuclide was based on a previously published method,[6] which used anion-exchange resin and concentrated HCl for the separation. Overnight after the irradiation, the target was dissolved in 6 ml 6M HCl to transform chromium and manganese into chloride form. The solutions were gently evaporated to dryness and redissolved in 4 ml concentrated HCl. The sample was loaded onto an AG® 1-X8 anion exchange column (115×15 mm), which was preconditioned with 3-column volume concentrated HCl. The column was washed with approximately 25 ml concentrated HCl (until the green colour of the $CrCl_3$ was ceased), and the ^{52}Mn radioisotope was eluted with about 15 ml 6M HCl solution. The radiomanganese-containing solution was evaporated to dryness and redissolved in Milli-Q water.

The typical activity of the 52Mn at the end of the separation step was 50 MBq, while its volume (containing the radioactivity) was 200 µL.

^{52}Mn labelling of 3,9-PC2ABn$^{p\mathrm{CO_2H}}$, 3,9-PC2MABn$^{p\mathrm{CO_2H}}$, 3,9-PC2AM$^{\mathrm{pip}}$Bn$^{p\mathrm{CO_2H}}$

The investigation of ^{52}Mn labelling efficiency of 3,9-PC2ABn$^{p\mathrm{CO2H}}$, 3,9-PC2MABn$^{p\mathrm{CO2H}}$, 3,9-PC2AM$^{\mathrm{pip}}$Bn$^{\mathrm{pCO2H}}$ chelators using different ligand concentrations (3,9-PC2ABn$^{p\mathrm{CO2H}}$: 2.19, 21.9, 219 µM, and 2.19 mM; 3,9-PC2MABn$^{p\mathrm{CO2H}}$: 2.07, 20.7, 207 µM, and 2.07 mM; 3,9-PC2AM$^{\mathrm{pip}}$Bn$^{\mathrm{pCO2H}}$: 1.69, 16.9, 169 µM, and 1.69 mM) at room temperature. 1 µL ^{52}Mn in Milli-Q water (~70 kBq) was added to 300 µL chelator solution with different concentrations in 5 mM HEPES buffer (pH = 7). The reaction mixtures were held at room temperature, 37 °C, 50 °C, and 85 °C in the case of 3,9-PC2AM$^{\mathrm{pip}}$Bn$^{p\mathrm{CO2H}}$. The mixtures were analysed with a HPLC system (Knauer Smartline, Berlin, Germany) equipped with Gabi Star Radio Activity Detector (250µL loop, Raytest, Straubenhardt, Germany) equipped with YMC-Pack ODS-AQ column (150.0 mm × 4.6 mm, 120 Å, 3 µm, YMC Co.,Ltd., Kyoto, Japan) with a flow rate of 1.00 mL/min (gradient elution (A): Phosphate buffer 20 mM (pH = 6), (B): ACN) at different time points of 5 min (following the mixing), 0.5, 1.0, 1.5, 2.0 hours in case of 3,9-PC2ABn$^{p\mathrm{CO2H}}$, 3,9-PC2MABn$^{p\mathrm{CO2H}}$ chelates and 5 min (following the mixing), 0.5, 1.0, 1.5, 2.0, 4.0, 5.0, 6.0 hours in case of 3,9-PC2AM$^{\mathrm{pip}}$Bn$^{p\mathrm{CO2H}}$.

trans-CDTA challenge of [^{52}Mn][Mn(3,9-PC2ABn^{pCO_2H})], [^{52}Mn][Mn(3,9-PC2MABn^{pCO_2H})], [^{52}Mn][Mn](3,9-PC2AM^{pip}Bn^{pCO_2H})]

300 µL of the ligand solutions at 20 µM concentration (3,9-PC2ABn^{pCO_2H}: 21.9 µM; 3,9-PC2MABn^{pCO_2H}: 20.7 µM; 3,9-PC2AM^{pip}Bn^{pCO_2H}: 16.9 µM) in 5 mM HEPES (pH = 7) and 1.0 µL ^{52}Mn in Milli-Q water (~70 kBq) were mixed and incubated for 1 hour at room temperature. After the incubation time, 6.6 µL 100 mM *t*-CDTA solution was added to the mixture and analysed with the above-mentioned HPLC method at 1-, 4-, 8-, 12-, 24-, 48-, and 96-hours' time points.

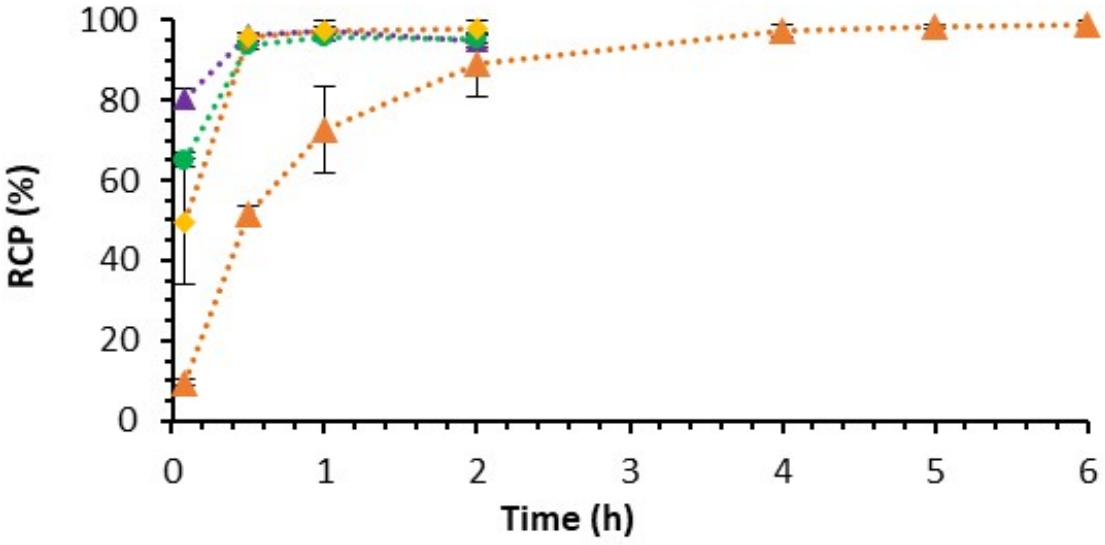

Figure S052. The effect of the ligand concentration (▲1.69 mM, ● 169 µM, ◆ 16.9 µM, ▲ 1.69 µM) on the radiolabelling yields (mean ± standard deviation, n = 3) of 3,9-PC2AM^{pip}Bn^{pCO_2H} by [^{52}Mn]Mn(II) studied at room temperature (buffered by HEPES with pH=7.0).

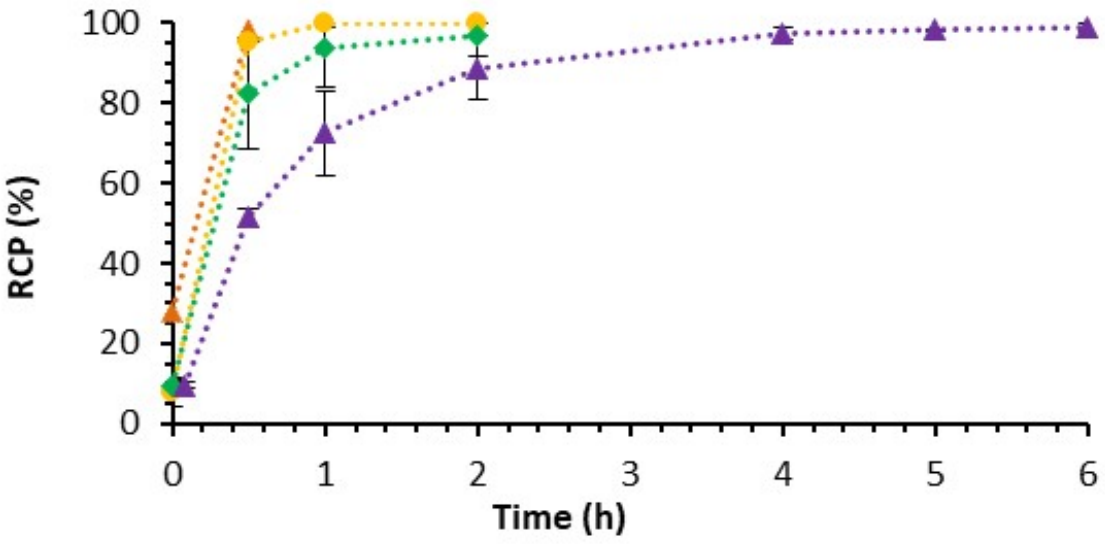

Figure S053. The effect of temperature (▲ 27°C, ◆ 37°C, ● 50°C, ▲ 85°C) on the radiolabelling yields (mean ± standard deviation, n = 3) of 3,9-PC2AM^{pip}Bn^{pCO_2H} by [^{52}Mn]Mn(II) studied with the use of 1.69 µM chelator concentration (buffered by HEPES with pH=7.0).

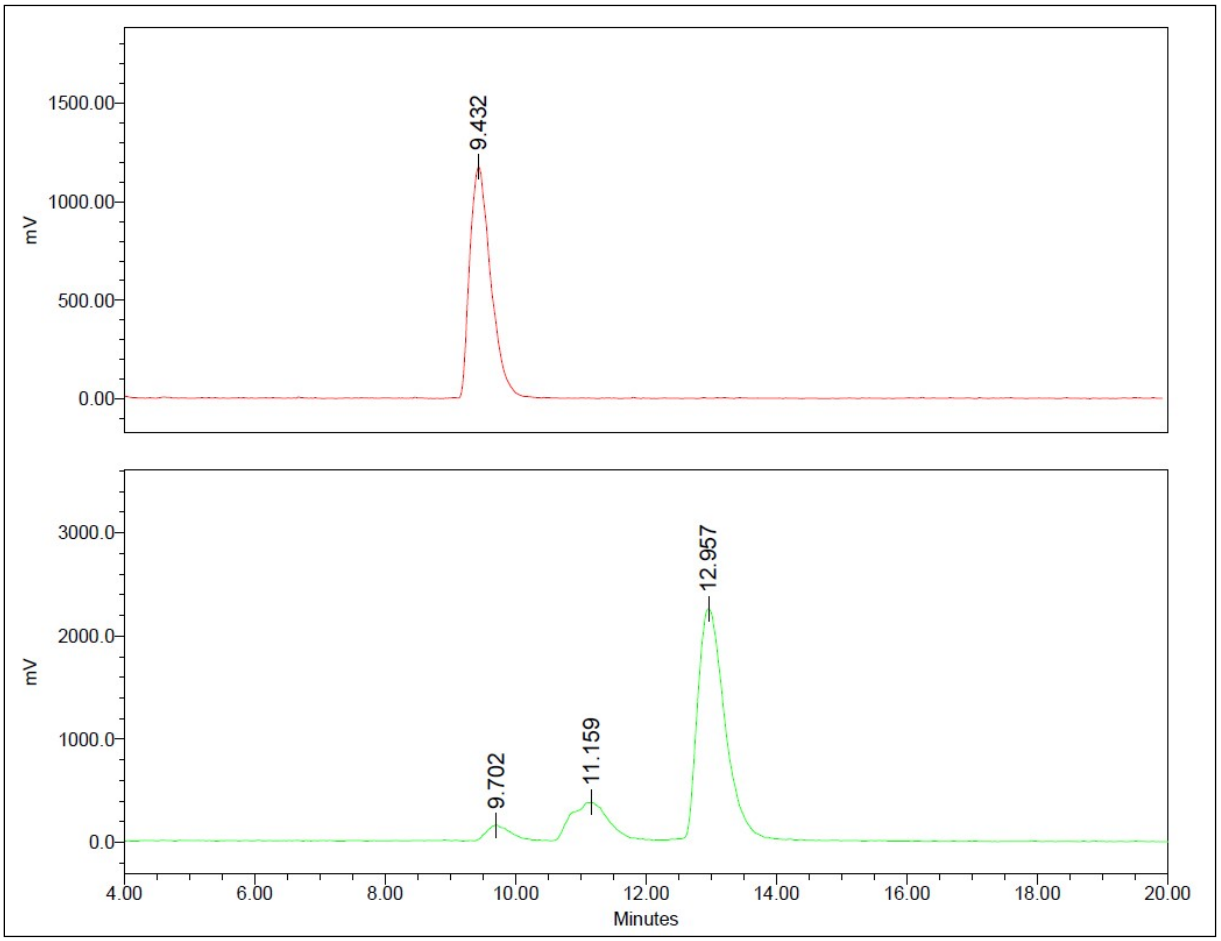

Figure S054. Radio-HPLC chromatograms of radiolabelled 3,9-PC2AM^{pip}Bn^{pCO_2H} (**L^3**) (prepared from a stock solution of several days) (green) and 3,9-PC2ABn^{pCO_2H} (**L^1**) (red).
Gradient: 0.00→5.00 min 5% B, 5.00→15.00 min 5→55% B; eluent: mixture of 20 mM Phosphate buffer (pH = 6) (A) and acetonitrile (B).

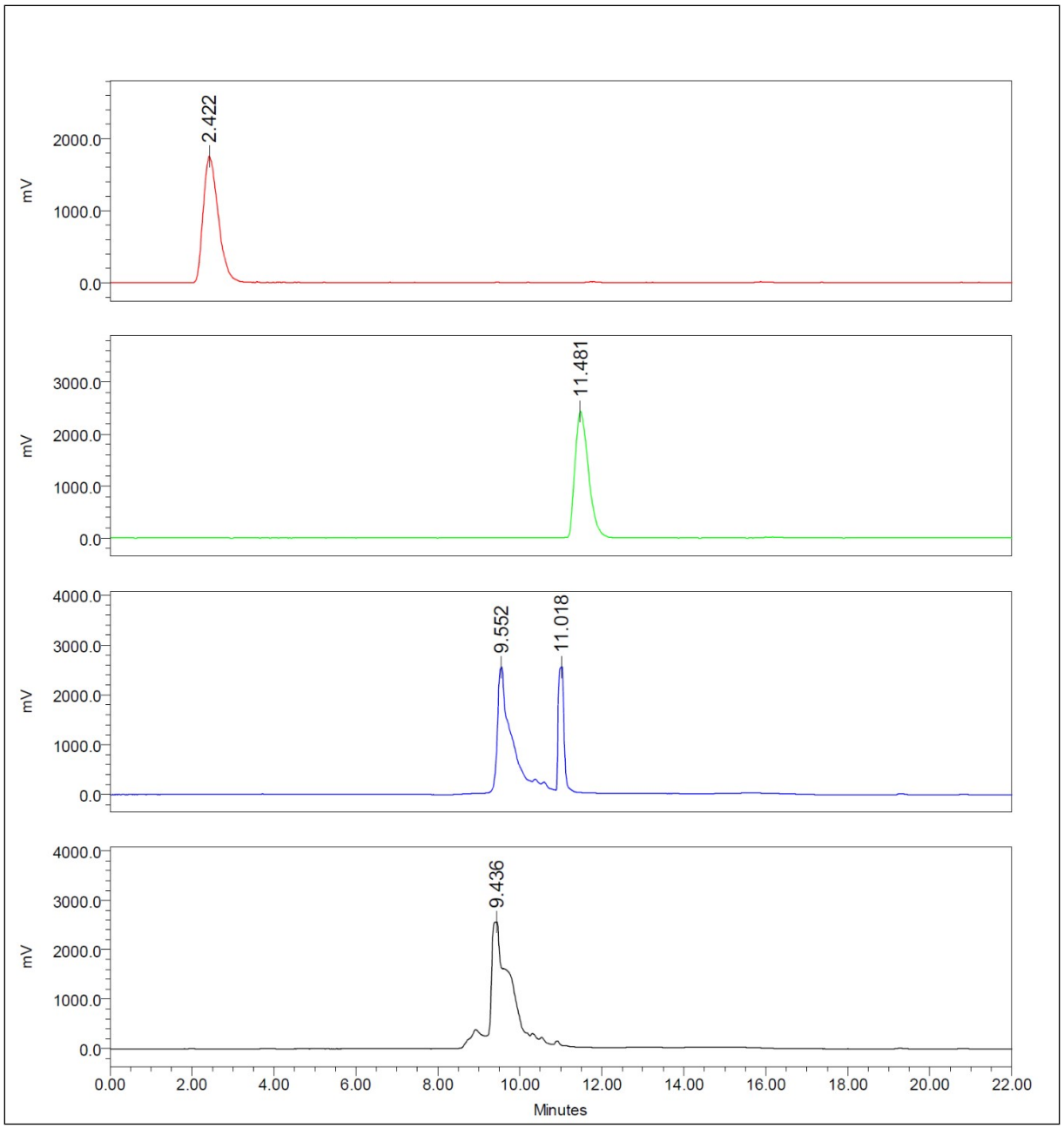

Figure S055. HPLC identification of [[^{52}Mn]Mn(**L^{1}**)] for labelling: *radio-chromatograms of [^{52}Mn]MnCl$_2$ (red) and [[$^{52/55}$Mn]Mn(3,9-PC2ABn^{pCO2H})] (green); UV-Vis chromatogram (254 nm) of [[$^{52/55}$Mn]Mn(3,9-PC2ABn^{pCO2H})] (blue) and 3,9-PC2ABn^{pCO2H} (**L^{1}**) (black).* Gradient: 0.00→5.00 min 0% B, 5.00→20.00 min 0→55% B; eluent: mixture of 20 mM Phosphate buffer (pH = 6) (A) and acetonitrile (B).

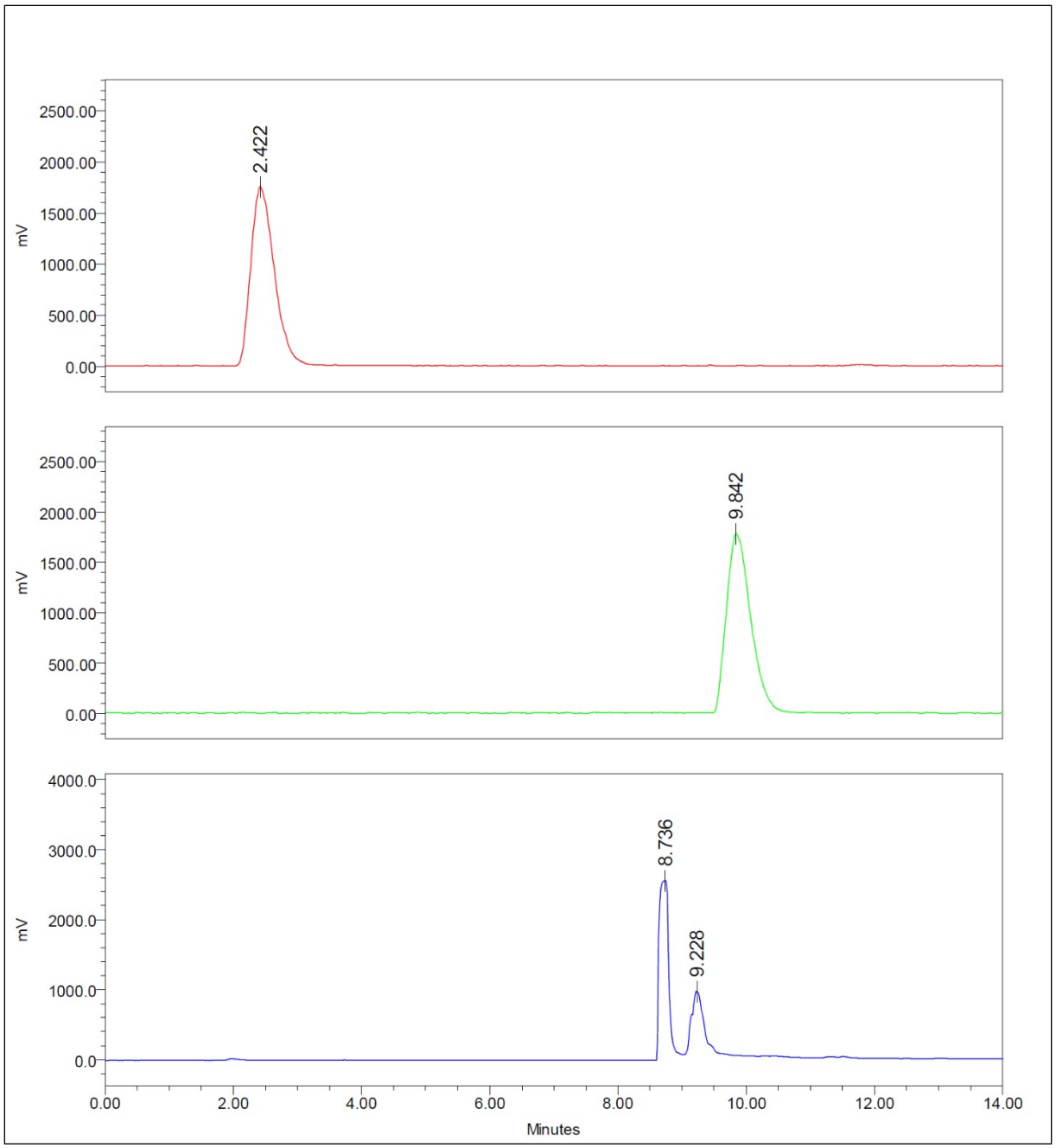

Figure S056. HPLC identification of [[^{52}Mn]Mn(**L**^{2})] for labelling: *radio-chromatograms of [^{52}Mn]MnCl$_2$ (red) and [[$^{52/55}$Mn]Mn(3,9-PC2MABn^{pCO2H})] (green); UV-Vis chromatogram (254 nm) of [[$^{52/55}$Mn]Mn(3,9-PC2MABn^{pCO2H})] (blue).* Gradient: 0.00→5.00 min 0% B, 5.00→16.00 min 0→22% B; eluent: mixture of 20 mM Phosphate buffer (pH = 6) (A) and acetonitrile (B).

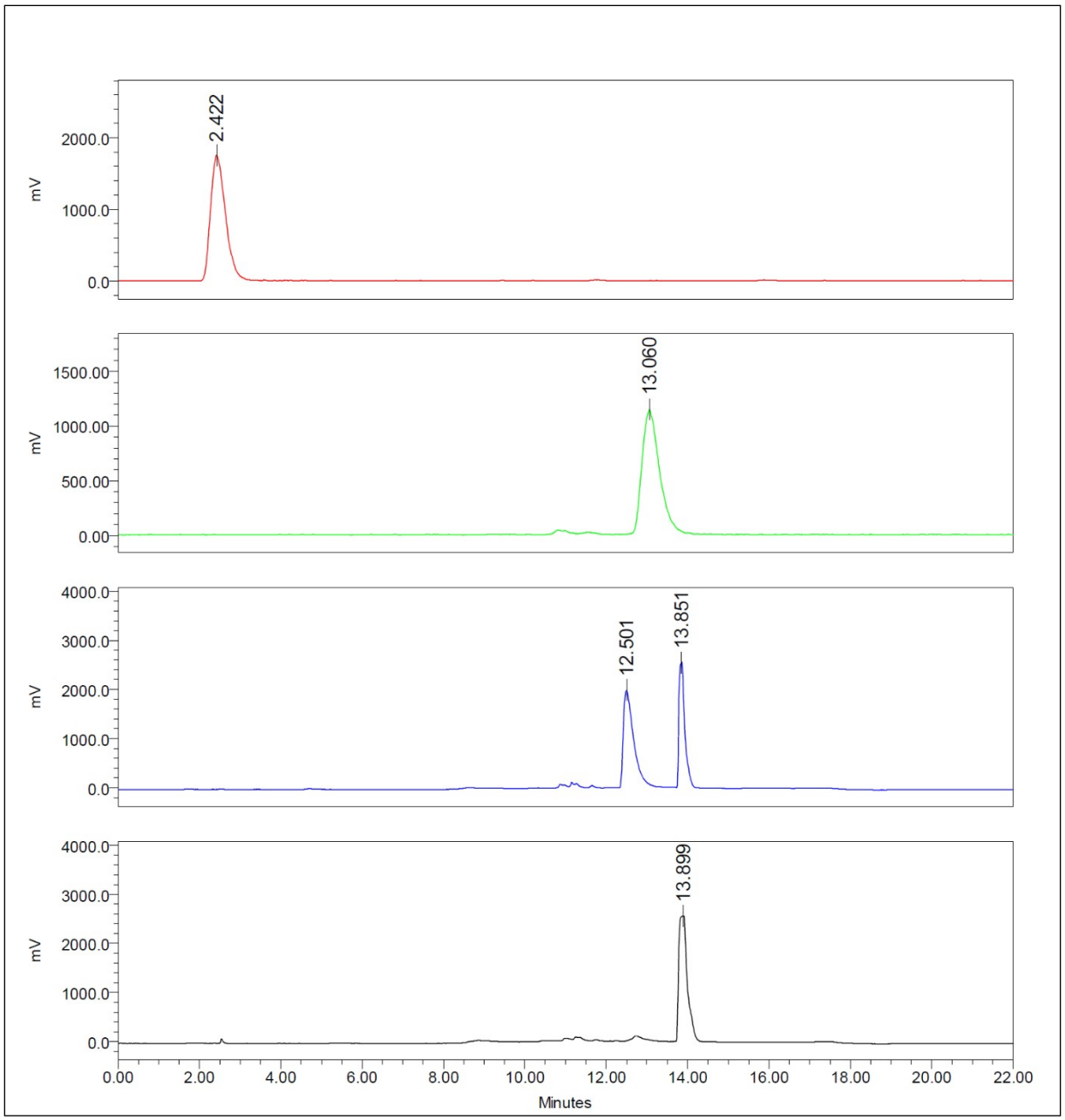

Figure S057. HPLC identification of [[^{52}Mn]Mn(**L^{3}**)] for labelling: *radio-chromatograms of [^{52}Mn]MnCl$_2$ (red) and [[$^{52/55}$Mn]Mn(3,9-PC2AM^{pip}Bn^{pCO_2H})] (green); UV-Vis chromatograms (254 nm) of [[$^{52/55}$Mn]Mn(3,9-PC2AM^{pip}Bn^{pCO_2H})] (blue) and 3,9-PC2AM^{pip}Bn^{pCO_2H} (**L^{3}**) (black).* Gradient: 0.00→5.00 min 5% B, 5.00→15.00 min 5→55% B; eluent: mixture of 20 mM Phosphate buffer (pH = 6) (A) and acetonitrile (B).

Production of ^{52}Mn in the laboratory of Scanomed Ltd.

^{52}Mn was produced in cyclotron by bombarding natural chromium powder in magnesium matrix with 14 MeV protons. After irradiation the magnesium content of the target was dissolved in 10% (m/m) HNO_3. Chromium was separated from the solution and was washed with 3 ml water twice to remove HNO_3 remnant. Residual chromium powder was dissolved in 2 ml of cc. HCl at 95°C for 1.5 hours. The solution was diluted with absolute ethanol, setting the final concentration of cc. HCl to 3% (V/V) 10.82 M HCl in absolute ethanol. This was led through an AG 1-X8 anion exchanger column (350 mg), equilibrated by washing with 5 mL of 0.1 M u.p. HCl, 10 mL of u.p. water and 10 mL of 3% (V/V) 10.82 M HCl in absolute ethanol,

^{52}Mn retains on the column. The loaded column was washed with 10 mL of 3% (V/V) 10.82 M HCl in absolute ethanol, ^{52}Mn was eluted in 0.5 mL of 0.1 M up. HCl and evaporated to dryness. This entire procedure was then repeated twice. In the second and third purification steps, the dry [^{52}Mn]$MnCl_2$ was dissolved in 300 µL 10.82 M up. HCl and mixed with 9.7 mL of absolute ethanol. The amount of resin in the second and third column was reduced to 300 mg and 250 mg, respectively. A short purification was implemented for removal of the unwanted metal ions (iron, zinc, copper). For this, after the third separation the sample of ^{52}Mn (in 0.1 M HCl) was evaporated to dryness and then dissolved in 200 µL of 3 M HCl. This was led through a DGA resin (100 mg, pre-equilibrated in 3 M HCl) and the effluent containing the ^{52}Mn isotope, along with a wash volume of an additional 2 x 150 µL of 3 M HCl were collected and concentrated to dryness and was dissolved in 0.1 M up. HCl. The activity of the solution was measured by ISOMED 2010 Dose calibrator at ^{52}Mn channel calibrated by gamma measurements.

Labelling optimization of 3,9-PC2ABn$^{p\mathrm{CO_2H}}$

The effect of pH, temperature and ligand concentration on the labelling of 3,9-PC2ABn$^{p\mathrm{CO_2H}}$ with ^{52}Mn has been examined in detail. The effect of pH and concentration of 3,9-PC2ABn$^{p\mathrm{CO_2H}}$ on the radiochemical purity (RCP) was examined in the presence of 1, 3, 10 and 30 µM ligand, in the pH range of 3-7. A 10 µL [^{52}Mn]$MnCl_2$ solution (~200 kBq), 80 µL buffer solution and 10 µl of 10, 30, 100 or 300 µM ligand solutions were mixed in order to reach the required concentration of ligands. Sodium acetate (0.5 M; u.p.) was applied as buffer in the pH range of 4-6, and 0.5 M cellpure HEPES was used at pH = 7 and 8. Reactions were carried out in Eppendorf tubes with 5 min reaction time at 25°C, and 95°C in a dry bath. Labelling of 3,9-PC2ABn$^{p\mathrm{CO_2H}}$ with ^{52}Mn was followed by Raytest miniGita Star thin layer chromatography scanner. 3 µl of the reaction mixture was dropped to a glass macrofiber chromatography paper impregnated with silica gel (iTLC-SG) strip and developed in 0.5 M sodium citrate eluent (pH = 5.5). $^{52}Mn^{II}$ in the form of citrate complex was eluted with the solvent front (R_f = 0.8-1.0), whereas the retention factor of [^{52}Mn[Mn(3,9-PC2ABn$^{p\mathrm{CO_2H}}$)] were found to be 0.1-0.2.

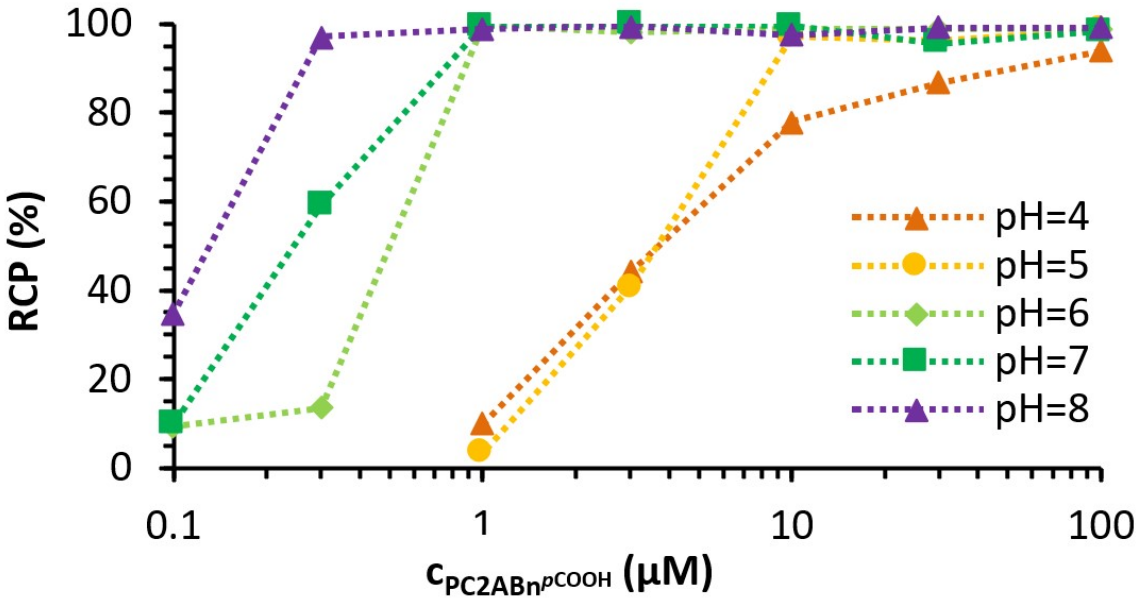

Figure S058. Radiolabelling optimization of 3,9-PC2ABn$^{p\mathrm{CO_2H}}$ with [^{52}Mn]Mn(II) at 95°C with 5 min reaction time in the pH range of 4 – 8 (n = 1).

4. Synthesis of the bifunctional chelator (BFC)

3,9-bis((4-nitrophenyl)sulfonyl)-3,6,9-triaza-1(2,6)-pyridinacyclodecaphane (11)

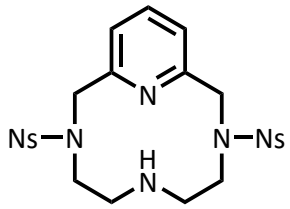

Tert-butyl 3,9-bis((4-nitrophenyl)sulfonyl)-3,6,9-triaza-1(2,6)-pyridinacyclodecaphane-6-carboxylate (**10**) (20.0 g, 29.6 mmol) was dissolved in CH_2Cl_2 (45 mL) and trifluoroacetic acid (21 mL) was added dropwise to this solution. The reaction mixture was stirred at room temperature for 12 hours and concentrated under reduced pressure. The oily residue was redissolved in a mixture of water and acetonitrile (1:1 by volume) and lyophilized which afforded the desired product **11** as a beige solid (15.7 mg, yield 92%).

^{1}H NMR (360.13 MHz, DMSO-d_6) δ 3.30 (t, 4H), 3.64 (t, 4H), 4.57 (s, 4H), 7.43 (d, J = 7.7, 2H), 7.88 (t, J = 7.7, 1H), 8.19 (d, J = 8.9, 4H), 8.45 (d, J = 8.9, 4H), 10.20 (bs, 1H) ppm; **^{13}C-JMOD NMR** (90.55 MHz, DMSO-d_6) δ 44.72, 47.27, 51.62, 121.11, 124.99, 129.06, 139.02, 142.73, 150.28, 157.69 ppm; **UHRMS** (ESI+) *m/z* calculated for $C_{23}H_{24}N_6O_8S_2$ $[M+H]^+$ 577.1170; found 577.1168; **HPLC** purity (260 nm): 98.33%; retention time: 10.103 min; gradient: 0.00→15.00 min 5→95% B; eluent: mixture of 5 mM TFA in MQ-water (A) and acetonitrile (B); flow: 1.00 mL/min; injection volume: 10.00 µL; sample: 1.00 mg/mL 100% ACN; column: Phenomenex Luna C18(2) 100 Å, 3 µm, 150 × 4.60 mm; column ID: 181147-3.

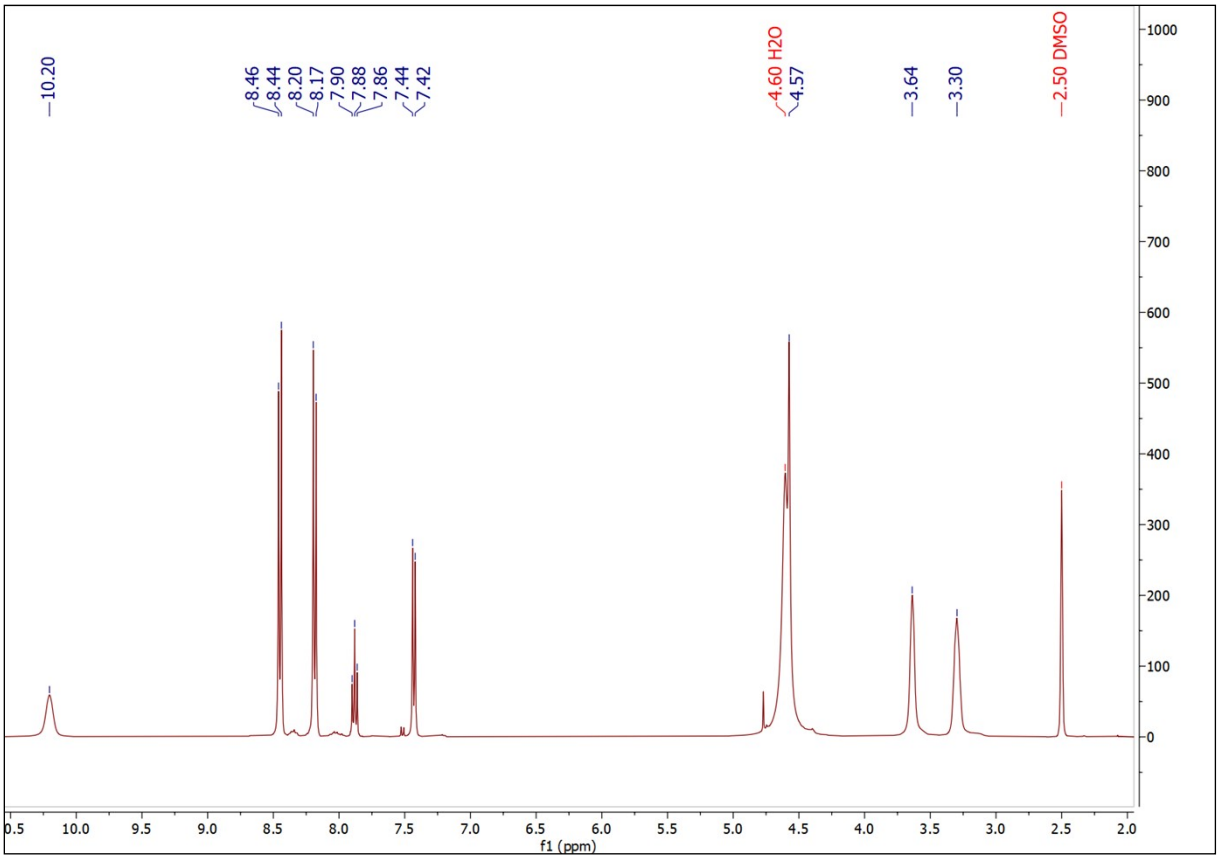

Figure S059. [1]H NMR (360.13 MHz, 298.0 K, DMSO-*d6*) spectra of compound **11**.

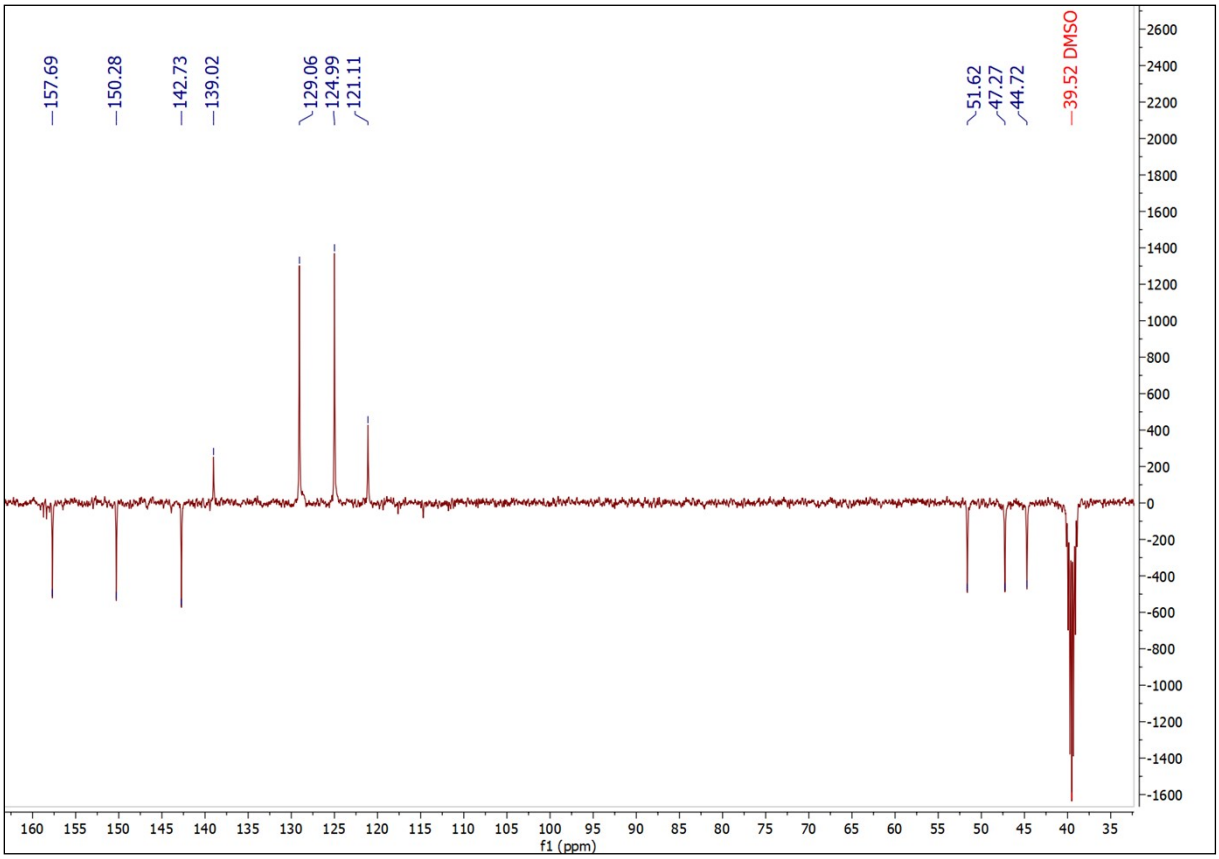

Figure S060. [13]C-JMOD (90.55 MHz, 298.0 K, DMSO-*d6*) NMR spectra of compound **11**.

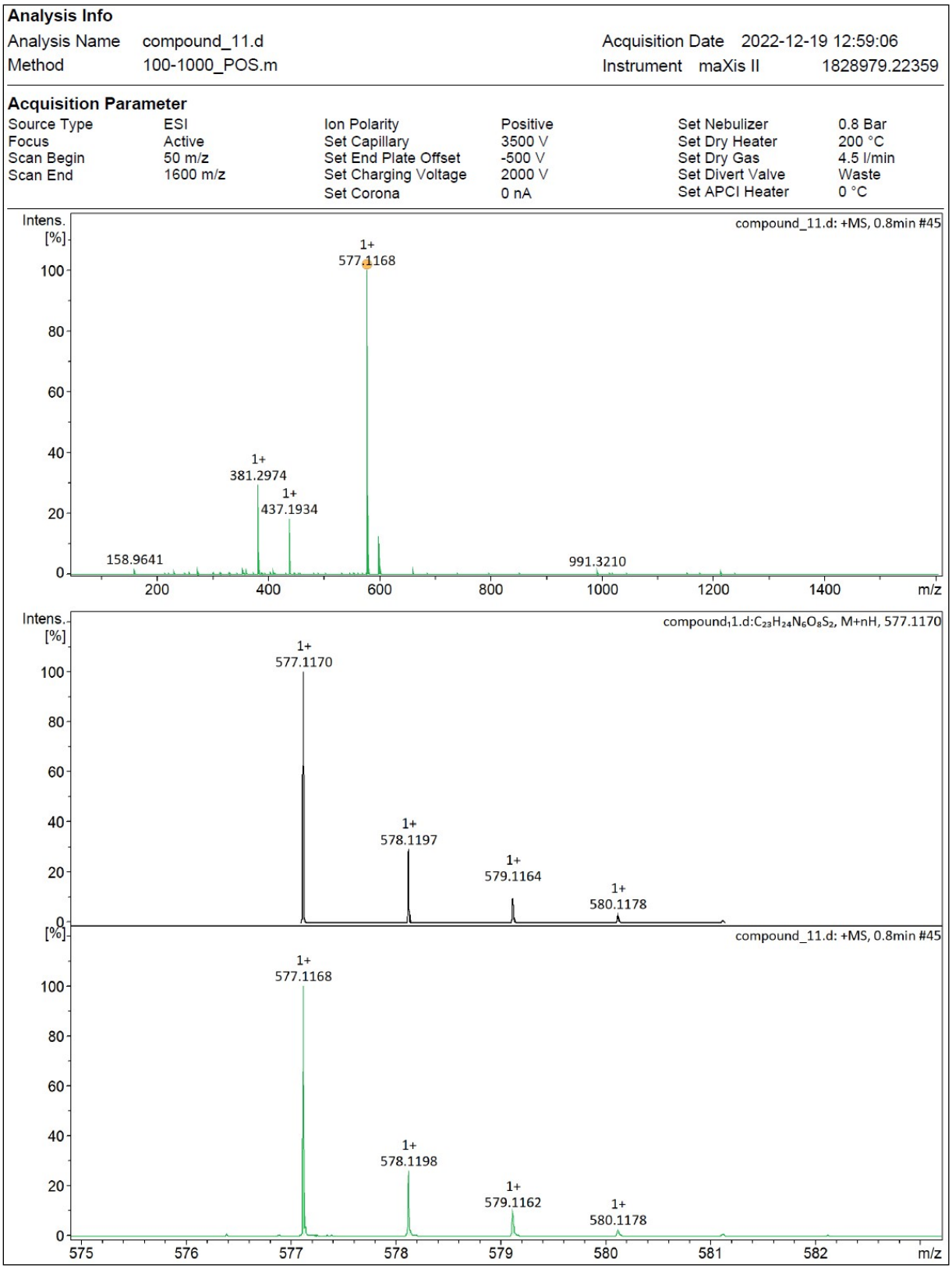

Figure S061. UHRMS spectra (ESI+) of compound **11**.

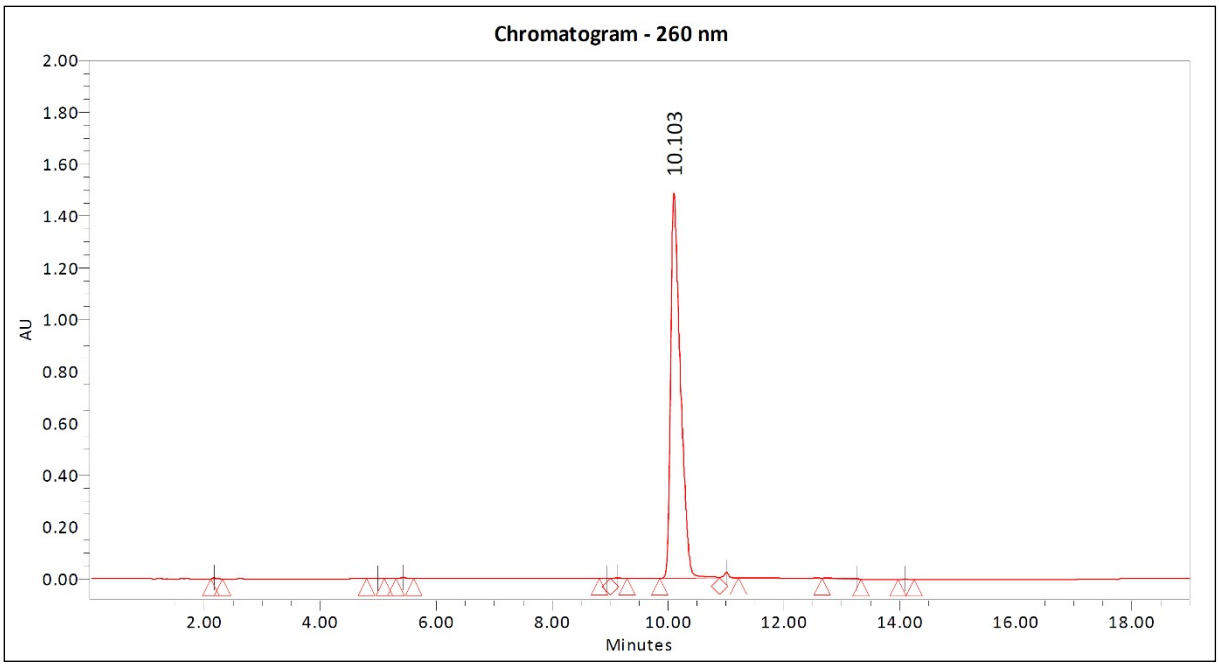

Figure S062. Analytical HPLC chromatogram (260 nm) of compound **11**.

Tert-butyl 4-((3,9-bis((4-nitrophenyl)sulfonyl)-3,6,9-triaza-1(2,6)-pyridinacyclodecaphane-6-yl)methyl)benzoate (12)

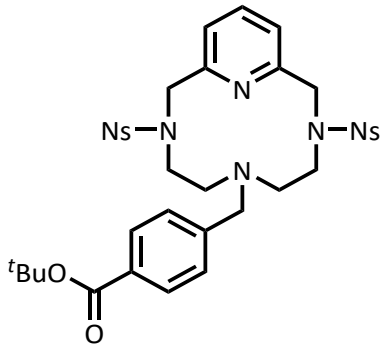

5.02 g (8.67 mmol) of 3,9-bis((4-nitrophenyl)sulfonyl)-3,6,9-triaza-1(2,6)-pyridinacyclodecaphane (**11**) was dissolved in in 700 mL of CH_3CN and 358 mg (2.39 mmol) sodium iodide as well as 6.10 µL (34.67 mmol) *N,N*-diisopropylethylamine was added to the solution. The temperature of the reaction mixture was brought up to 80 °C and stirred for 15 min. The solution of 2.35 g (8.67 mmol) alkylating agent (*tert*-butyl 4-(bromomethyl)benzoate) dissolved in 50 mL acetonitrile was added to the reaction mixture dropwise. The reaction mixture was stirred at 80 °C for 48 h, cooled down to room temperature and the solvent was then removed under reduced pressure vacuum to afford the crude product. Recrystallization from acetone returned the product **12** as a white solid (6.18 g, yield 93%).

^{1}H NMR (400.13 MHz, DMSO-d_6) δ 1.57 (s, 9H), 3.31 (m, 2H), 3.53 (m, 4H), 4.35 (m, 4H), 4.51 - 4.71 (m, 4H), 4.88 (s, 4H), 7.56 (d, J = 7.7, 2H), 7.82 (d, J = 7.9, 2H), 7.99 (t, J = 7.8, 1H), 8.04 (d, J = 7.7, 2H), 8.37 (d, J = 8.4 Hz, 4H), 8.49 (d, J = 8.4 Hz, 2H) ppm; **^{13}C-JMOD NMR** (100.62 MHz, DMSO-d_6) δ; 27.75, 41.74, 45.91, 46.78, 52.41, 81.33, 122.06, 124.87, 129.42, 129.81, 131.59, 132.38, 132.71, 139.65, 141.78, 150.44, 157.55, 164.36 ppm; **UHRMS** (ESI+) *m/z* calculated for $C_{35}H_{38}N_6O_{10}S_2$ $[M+H]^+$ 767.2164; found

767.2164; **HPLC** purity (260 nm): 95.39%; retention time: 12.182 min; gradient: 0.00→15.00 min 5→95% B; eluent: mixture of 5 mM TFA in MQ-water (A) and acetonitrile (B); flow: 1.00 mL/min; injection volume: 1.00 µL; sample: 0.26 mg / 100 µL ACN + 2% DMF; column: Phenomenex Luna C18(2) 100 Å, 5 µm, 150 × 4.60 mm; column ID: H21-212012.

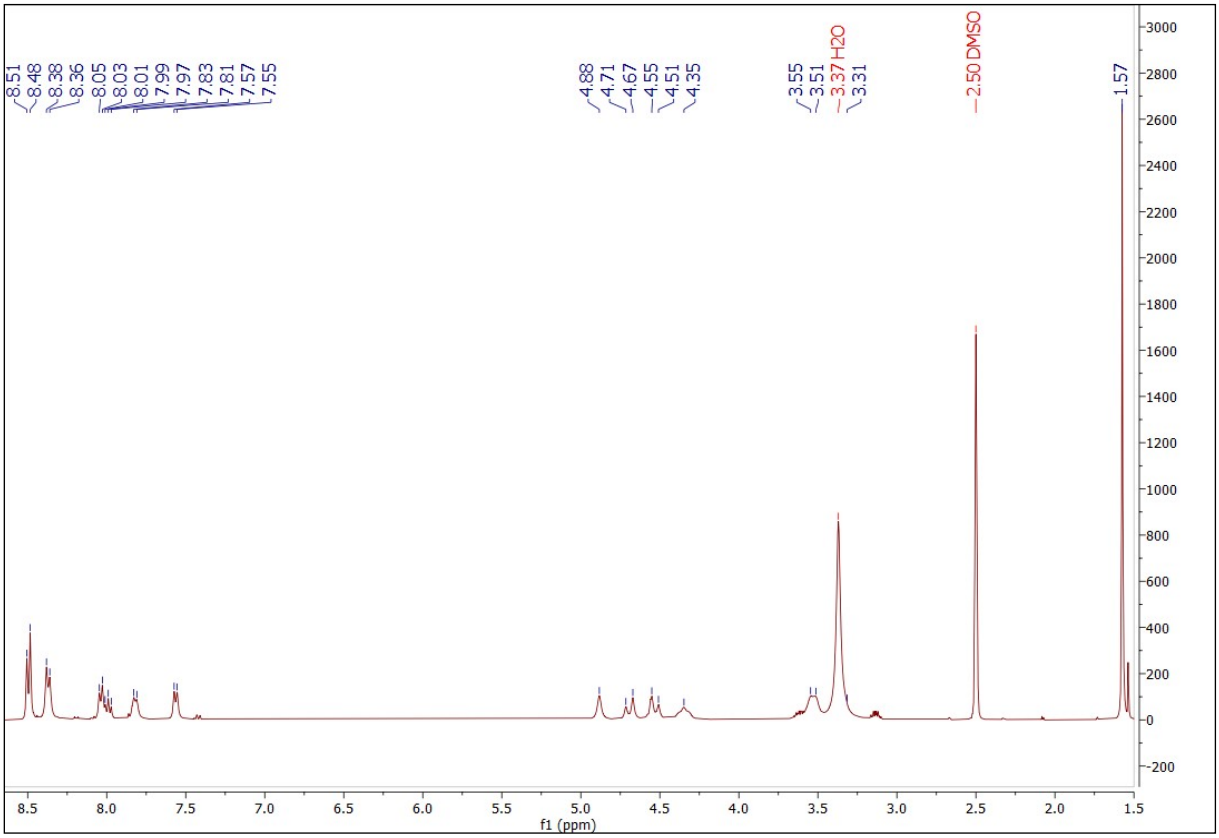

Figure S063. ^{1}H NMR (400.13 MHz, 298.0 K, DMSO-*d6*) spectra of compound **12**.

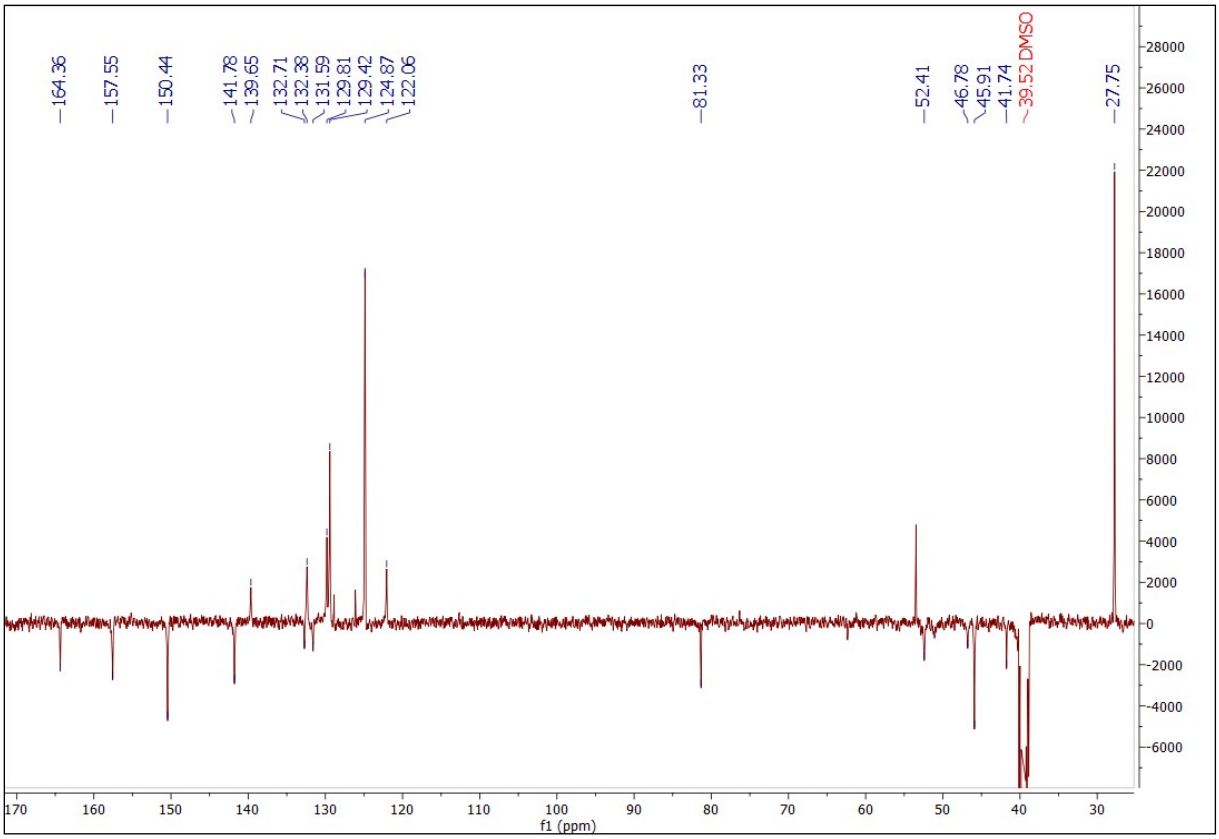

Figure S064. ^{13}C-JMOD NMR (100.62 MHz, 298.0 K, DMSO-*d6*) spectra of compound **12**.

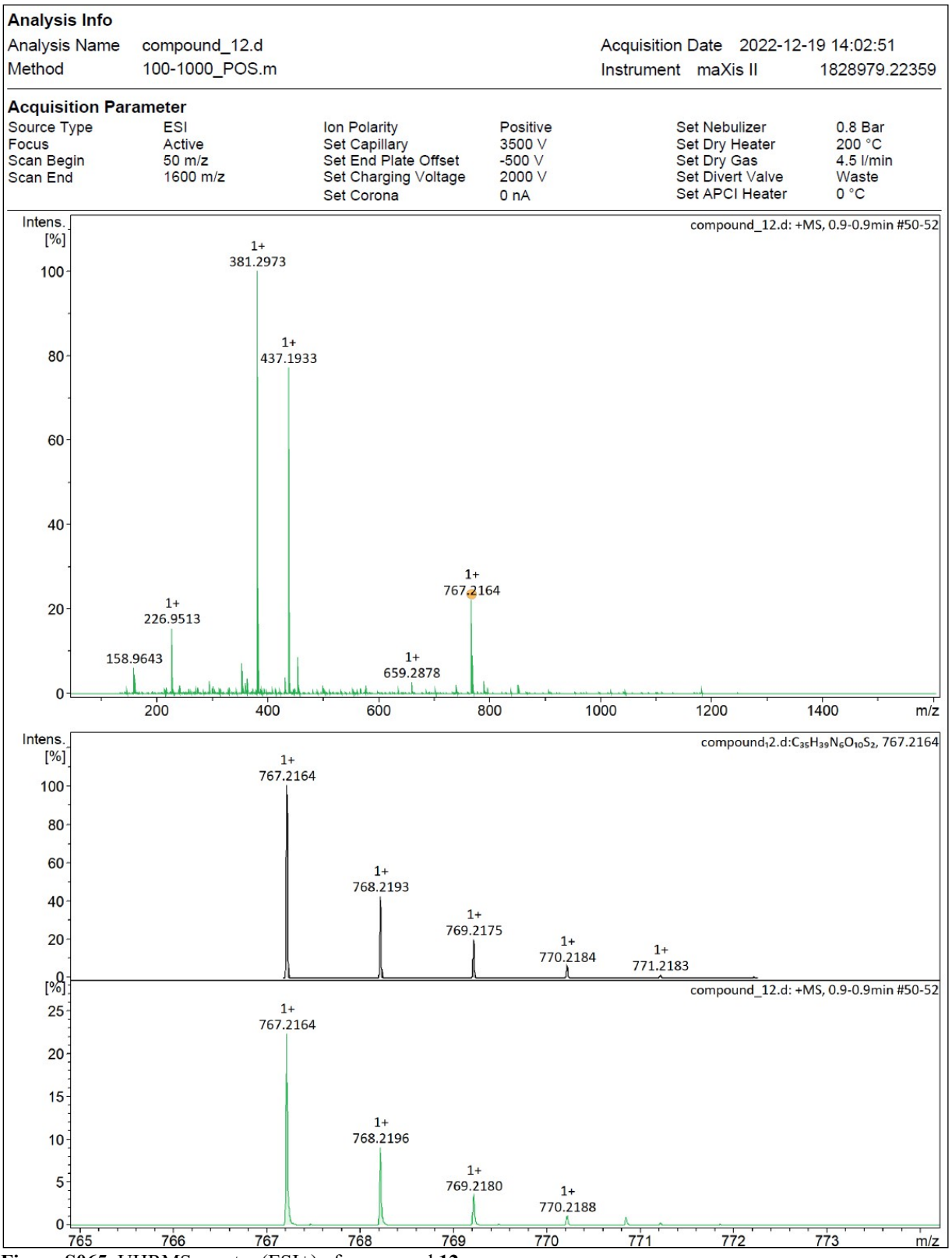

Figure S065. UHRMS spectra (ESI+) of compound **12**.

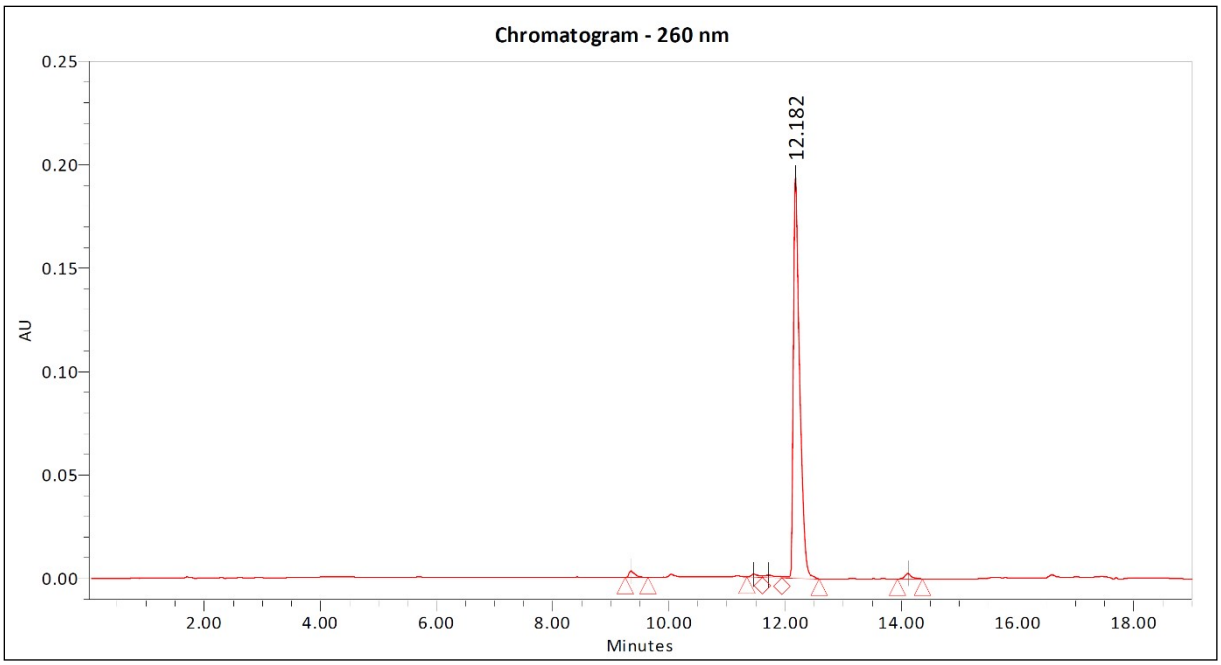

Figure S066. Analytical HPLC chromatogram (260 nm) of compound **12**.

***Tert*-butyl 4-(3,6,9-triaza-1(2,6)-pyridinacyclodecaphane-6-ylmethyl)benzoate (13)**

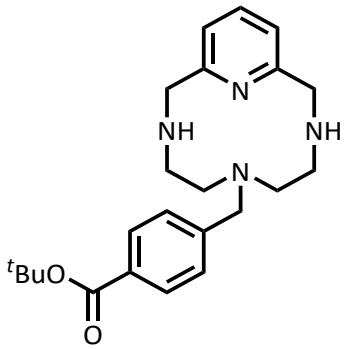

3.33 g (4.34 mmol) of *tert*-butyl 4-((3,9-bis((4-nitrophenyl)sulfonyl)-3,6,9-triaza-1(2,6)-pyridinacyclodecaphane-6-yl)methyl)benzoate (**12**) was dissolved in 30 mL of *N,N*-dimethylformamide and 5.70 g (41.24 mmol) of anhydrous potassium carbonate was added to the stirred solution. 1.50 mL of thiophenol (14.61 mmol) was added and the flask under argon atmosphere. The resulting suspension was further stirred at room temperature for 24 hours and the solvent was removed under vacuum. The crude product was purified by flash chromatography on Teledyne ISCO Redi*SepR*f® Gold silica gel 40-gram column, using ethyl acetate (A) and 10% ammonia (25%) in methanol (B) as an eluent (gradient: 0.00→7.00 min: 0% (B), 7.00→22.00 min 0→90% (B), flow: 40 mL/min, retention time: 18 min). Fractions containing the pure product were combined, evaporated, and the residue redissolved in a mixture of water and acetonitrile (1:1 by the volume). Lyophilization of the given solution returned the product (**13**) as a white solid (1.00 g, yield 58%).

^{1}H NMR (360.13 MHz, MeOD-d_4) δ 1.59 (s, 9H), 2.84 (m, 4H), 3.29 (m, 4H), 3.98 (s, 2H), 4.65 (s, 4H), 7.50 (d, J = 7.8, 2H), 7.55 (d, J = 8.2, 2H), 7.98 (d, J = 8.2, 2H), 7.99 (t, J = 7.8 Hz, 1H) ppm; **^{13}C-JMOD NMR** (90.55 MHz, MeOD-d_4) δ; 28.39, 47.36, 49.00, 50.96, 51.62, 60.03, 82.40, 123.21, 130.76, 130.79, 132.70, 140.78, 142.43, 151.08, 167.07 ppm; **UHRMS**

(ESI+) *m/z* calculated for $C_{23}H_{32}N_4O_2$ $[M+H]^+$ 397.2598; found 397.2594; **HPLC** purity (260 nm): 99.57%; retention time: 6.956 min; gradient: 0.00→15.00 min 5→95% B; eluent: mixture of 5 mM TFA in MQ-water (A) and acetonitrile (B); flow: 1.00 mL/min; injection volume: 10.00 µL; sample: 0.60 mg / 200 µL H_2O; column: Phenomenex Luna C18(2) 100 Å, 5 µm, 150 × 4.60 mm; column ID: H21-212012.

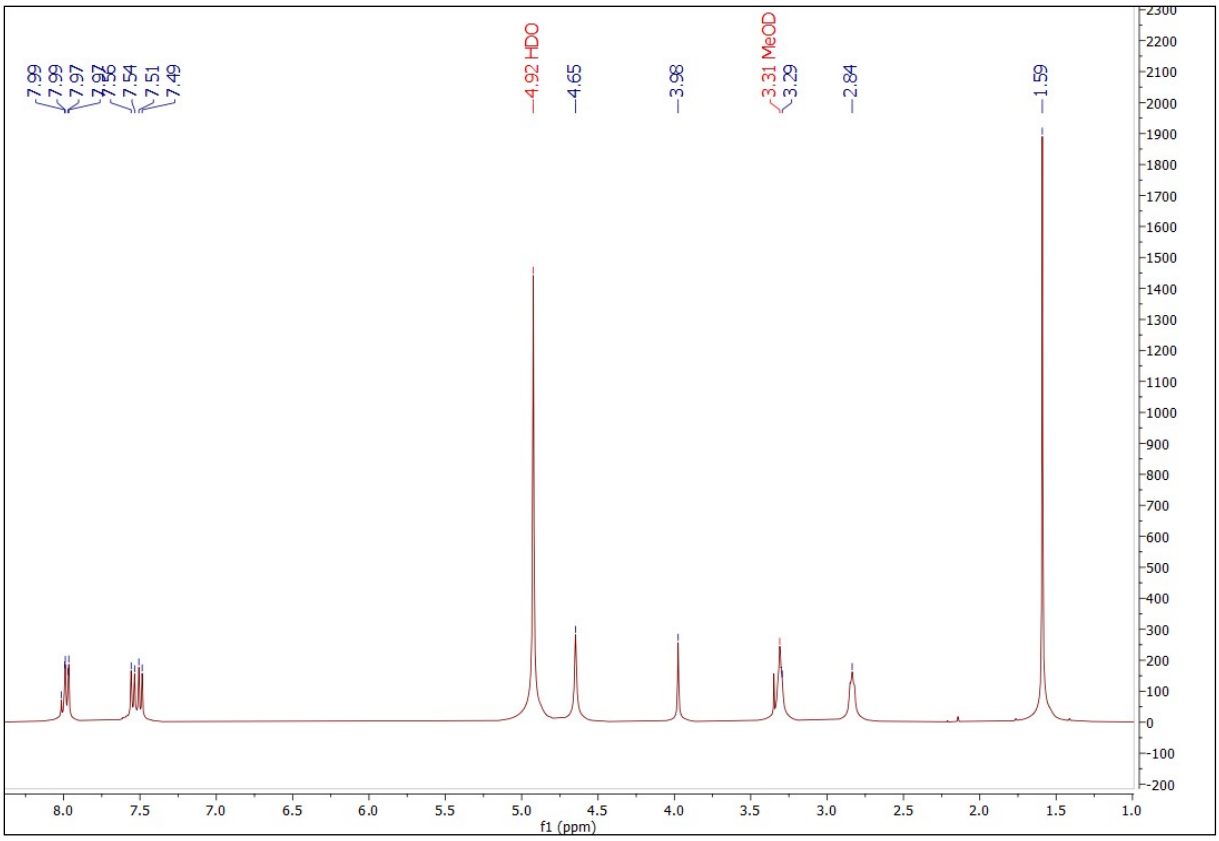

Figure S067. ^{1}H NMR (360.13 MHz, 298.0 K, MeOD-*d4*) spectra of compound **13**.

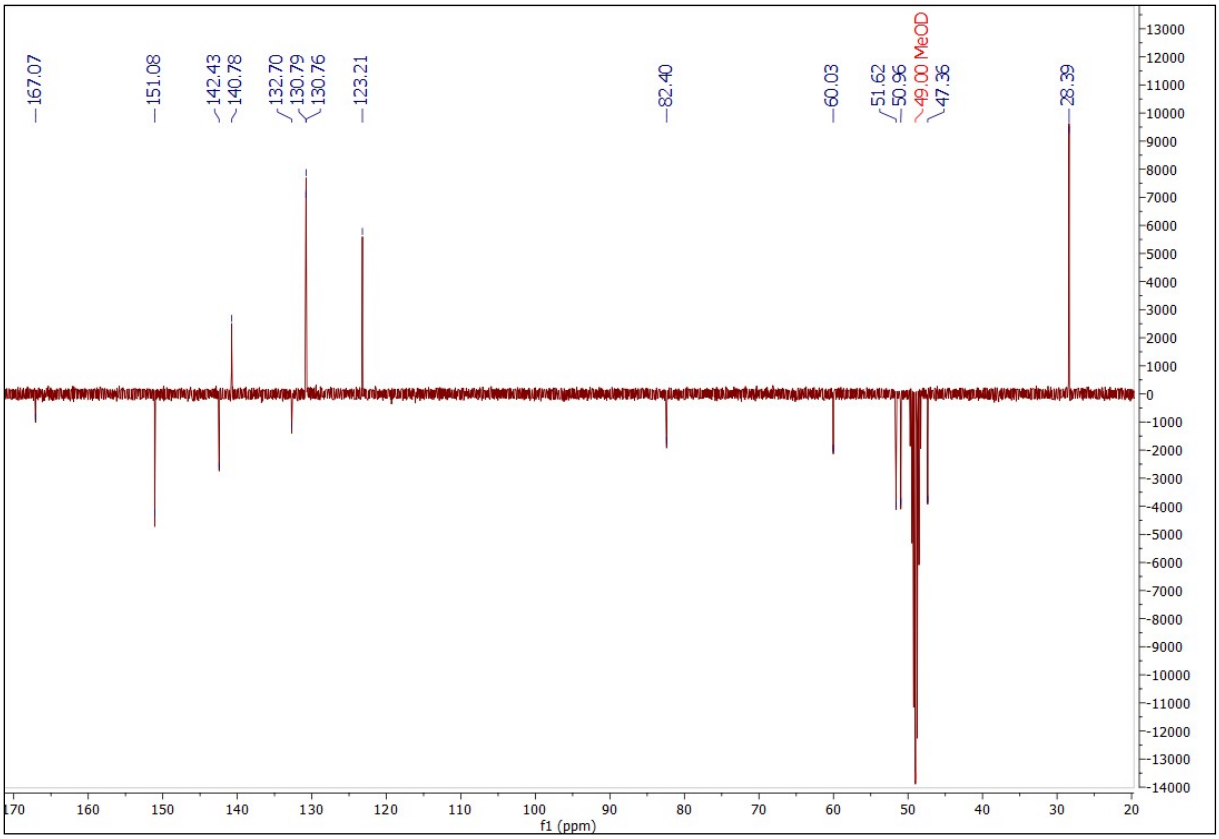

Figure S068. ^{13}C-JMOD NMR (90.55 MHz, 298.0 K, MeOD-*d4*) spectra of compound **13**.

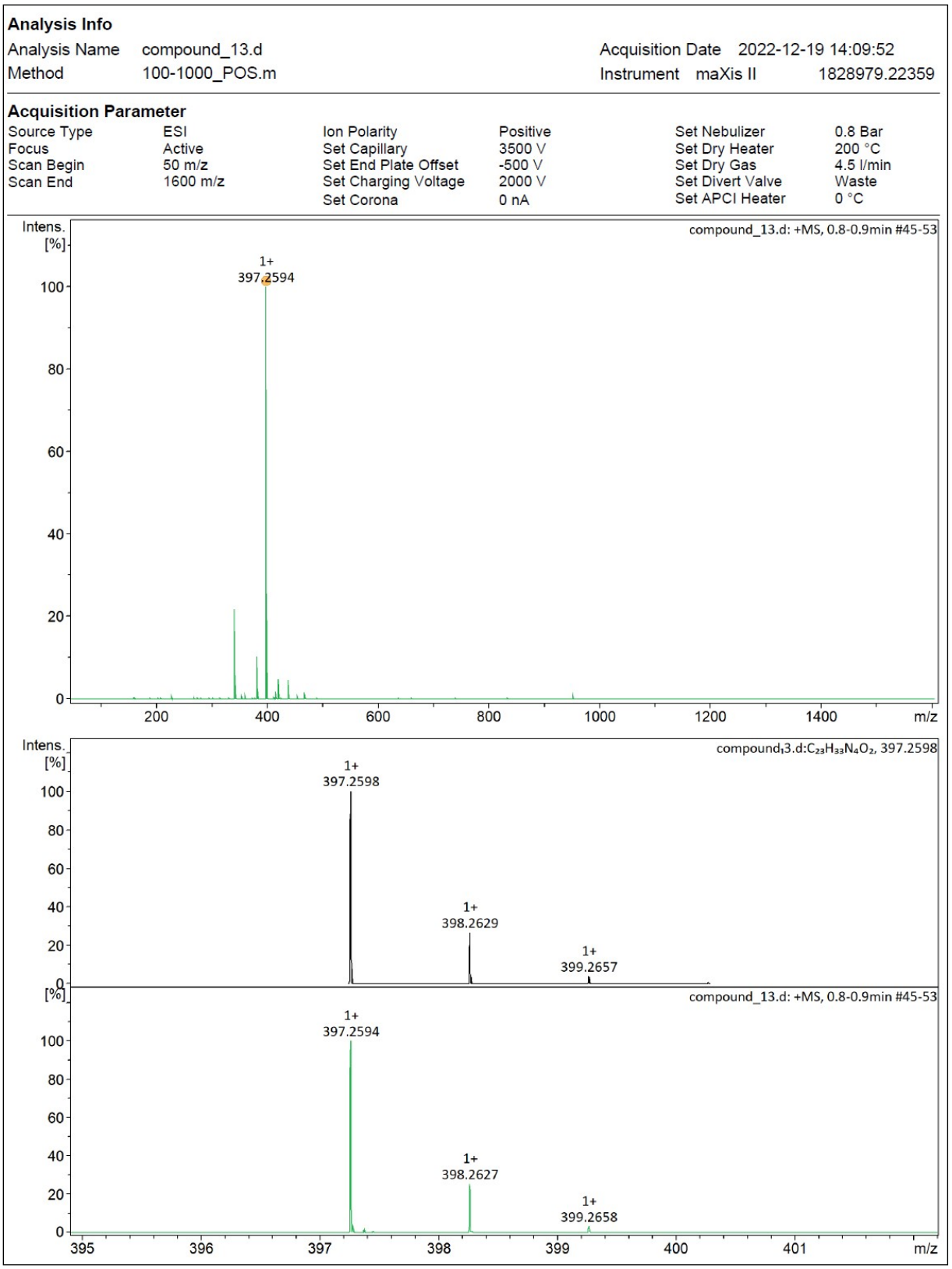

Figure S069. UHRMS spectra (ESI+) of compound **13**.

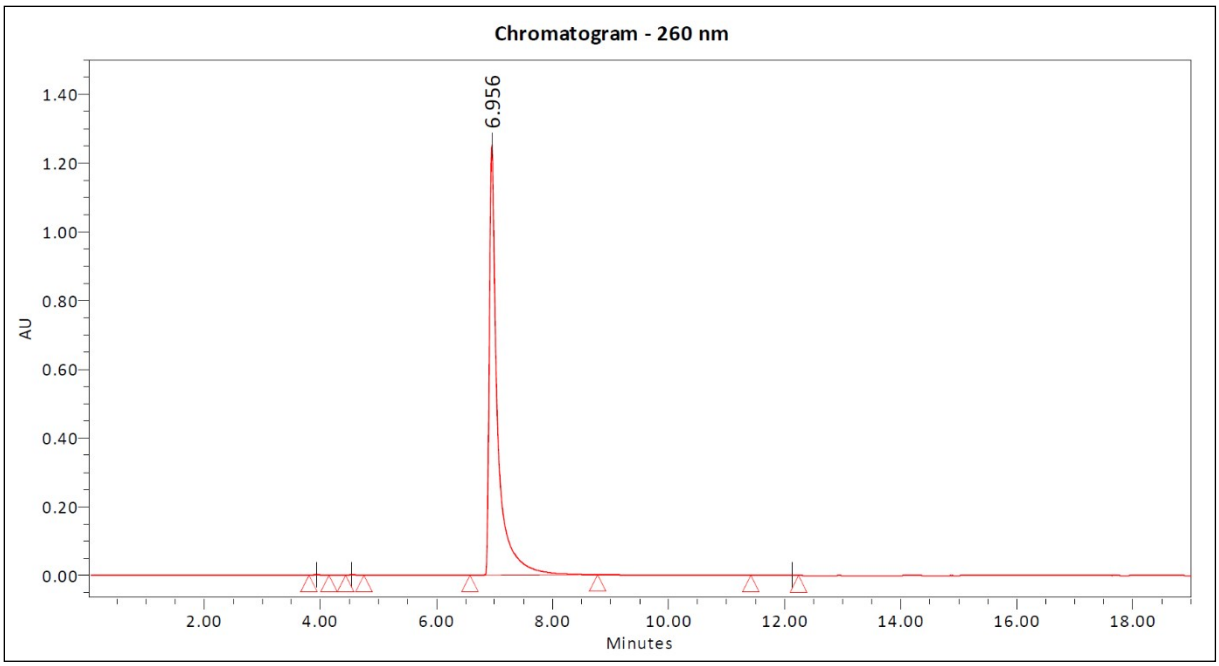

Figure S070. Analytical HPLC chromatogram (260 nm) of compound **13**.

4-(3,6,9-Triaza-1(2,6)-pyridinacyclodecaphane-6-ylmethyl)benzoic acid (14)

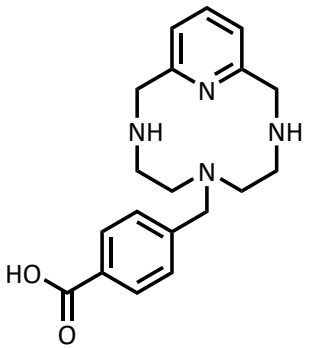

Tert-butyl 4-(3,6,9-triaza-1(2,6)-pyridinacyclodecaphane-6-ylmethyl)benzoate (**13**) (500 mg, 1.26 mmol) was dissolved in 15.0 mL of CH_2Cl_2 and 7.0 mL trifluoroacetic acid was added dropwise to this solution at room temperature. The reaction mixture was stirred at room temperature for 12 hours and concentrated under vacuum to afford **14** as a white solid (400 mg, yield 93%).

^{1}H NMR (400.13 MHz, MeOD-d_4) δ 2.84 (t, J = 5.4 Hz, 4H), 3.32 (m, 4H), 3.98 (s, 2H), 4.64 (s, 4H), 7.49 (d, J = 7.8 Hz, 2H, 7.55 (d, J = 8.1, 2H), 7.99 (t, J = 7.8, 1H), 8.05 (d, J = 8.2 Hz, 2H) ppm; **^{13}C-JMOD NMR** (100.62 MHz, MeOD-d_4) δ 47.36, 49.00, 50.97, 51.59, 60.00, 123.22, 130.84, 131.19, 131.55, 140.80, 142.68, 151.12, 169.49 ppm; **UHRMS** (ESI+) *m/z* calculated for $C_{19}H_{24}N_4O_2$ $[M+H]^+$ 341.1972; found 341.1970; **HPLC** purity (260 nm): 99.12%; retention time: 4.347 min; gradient: 0.00→15.00 min 5→95 %B; eluent: mixture of 5 mM TFA in MQ-water (A) and acetonitrile (B); flow: 1.00 mL/min; injection volume: 1.00 µL; sample: 0.62 mg / 100 µL H_2O; column: Phenomenex Luna C18(2) 100 Å, 5 µm, 150 × 4.60 mm; column ID: H21-212012.

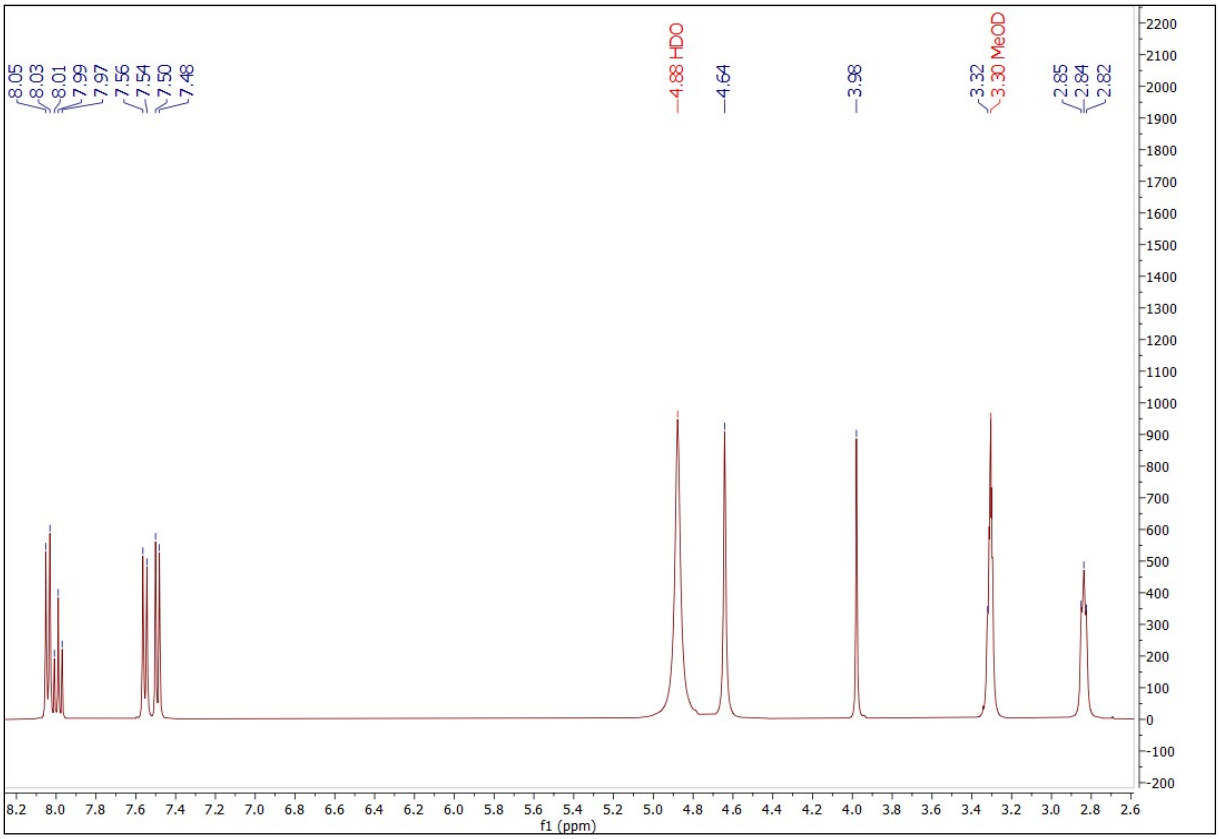

Figure S071. [1]H NMR (400.13 MHz, 298.0 K, MeOD-*d4*) spectra of compound **14**.

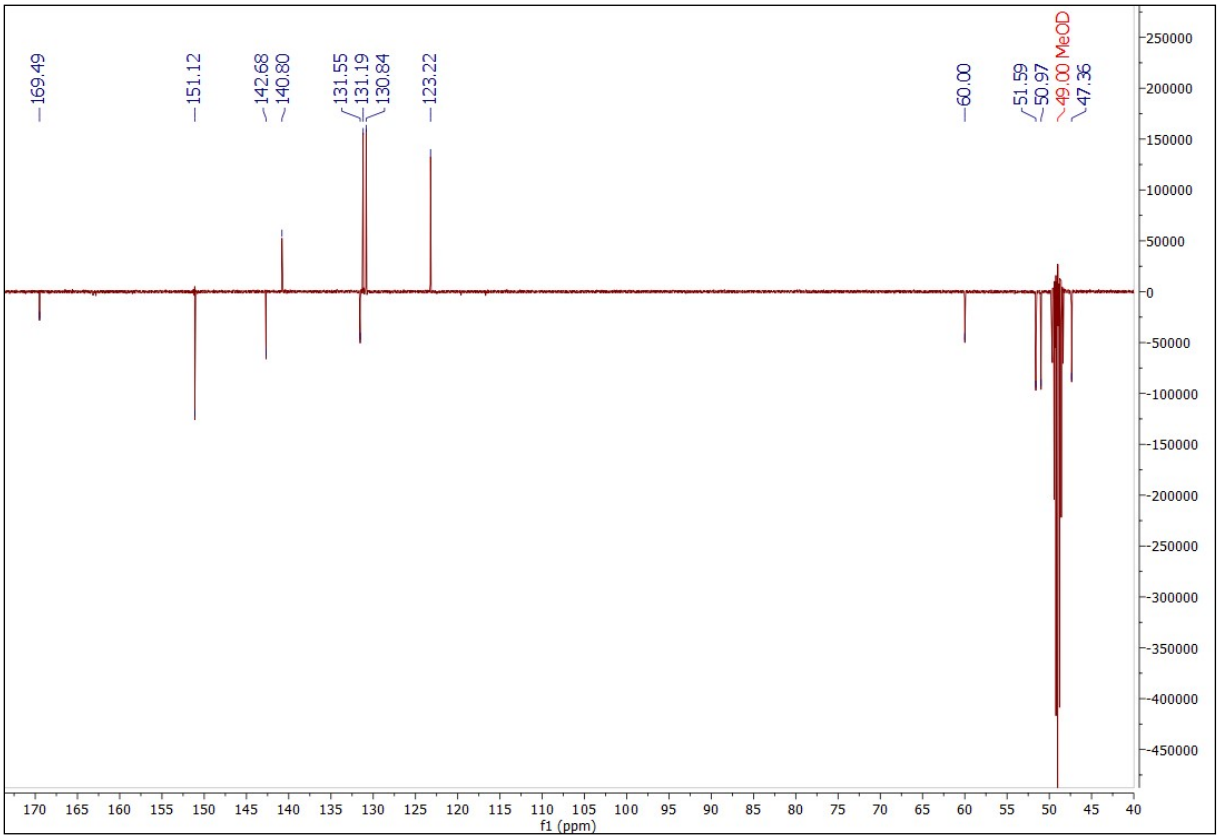

Figure S072. [13]C-JMOD NMR (100.62 MHz, 298.0 K, MeOD-*d4*) spectra of compound **14**.

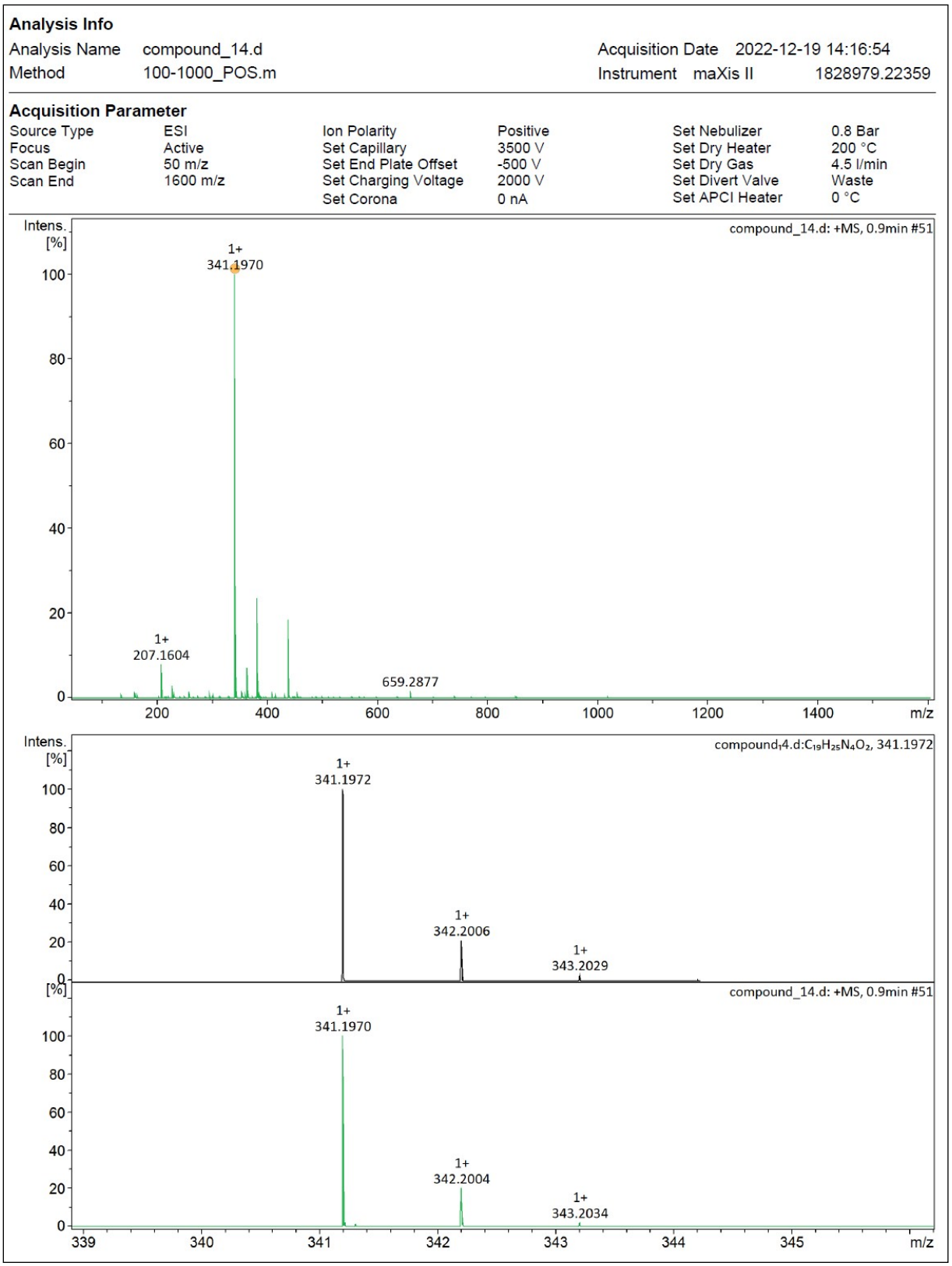

Figure S073. UHRMS spectra (ESI+) of compound **14**.

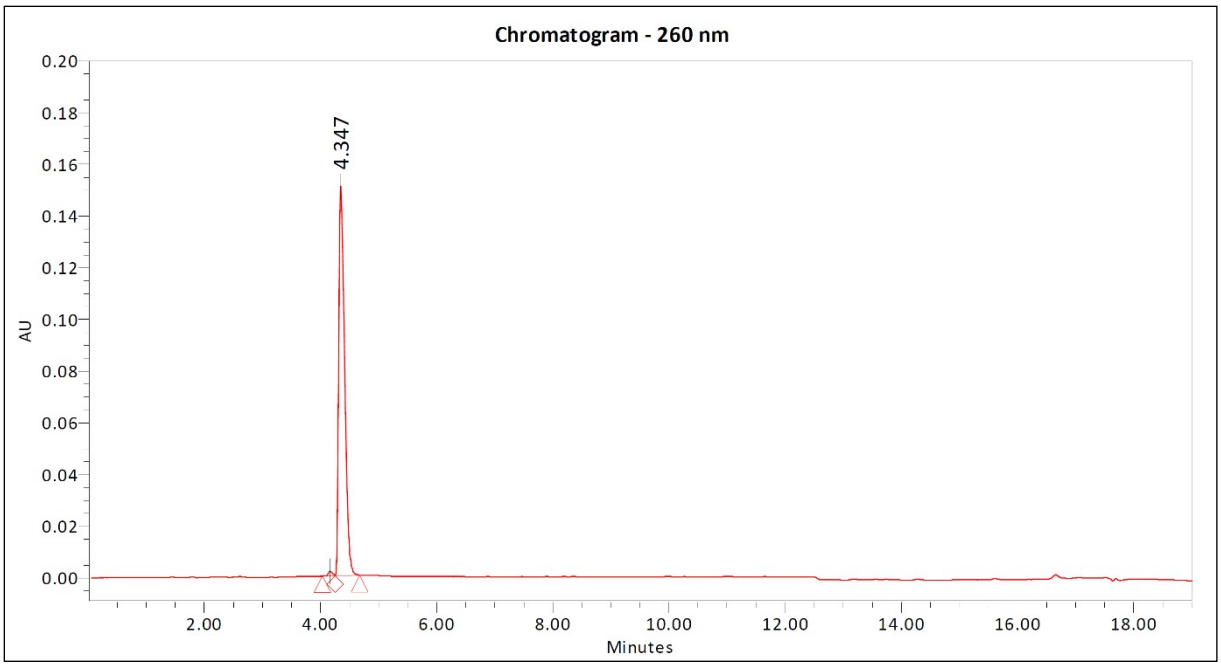

Figure S074. Analytical HPLC chromatogram (260 nm) of compound **14**.

4-((3,9-Bis(2-(*tert*-butoxy)-2-oxoethyl)-3,6,9-triaza-1(2,6)-pyridinacyclodecaphane-6-yl)methyl)benzoic acid (15)

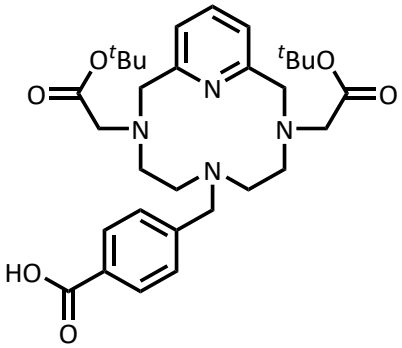

To a solution of 4-(3,6,9-triaza-1(2,6)-pyridinacyclodecaphane-6-ylmethyl)benzoic acid (**14**) (250 mg, 0.734 mmol) in anhydrous *N,N*-dimethylformamide (50 mL) placed under an argon atmosphere 600 µL (3.44 mmol) of *N,N*-diisopropylethylamine was added at room temperature. The reaction mixture was heated up to 60 °C and the solution of *tert*-butyl bromoacetate (0.228 mL, 1.36 mmol) in anhydrous *N,N*-dimethylformamide (20 mL) was added dropwise over the course of 30 min. The reaction mixture was stirred at 60 °C for an additional 48 h. The solvent was then removed under reduced pressure to afford the crude product, which was purified by preparative HPLC. The fractions containing the pure substance were combined and freezer dried. **15** was obtained as a white solid (174 mg, yield 42%).

Preparative HPLC: UV-Vis detection: 210 and 260 nm; retention time: 9.10 min; gradient: 0.00→12.00 min 25→85% B; eluent: mixture of 5 mM TFA in MQ-water (A) and acetonitrile (B); flow: 25.00 mL/min; injection volume: 300.00 µL; sample: 418 mg/1 mL 50% ACN in H_2O; column: Phenomenex Luna Prep C18(2) 100 Å, 5 µm, 250 × 21.20 mm; column ID: H18-268346.

^{1}H NMR (400.13 MHz, $CDCl_3$) δ 1.41 (s, 18H), 3.23 (m, 4H), 3.30 (m, 8H), 4.11 (s, 4H), 4.47 (s, 2H), 7.17 (d, *J* = 7.7 Hz, 2H), 7.52 (d, *J* = 8.1, 2H), 7.75 (t, *J* = 7.7, 1H), 7.97 (d, *J* = 8.2 Hz, 2H) ppm; **^{13}C-JMOD NMR** (100.62 MHz, $CDCl_3$) δ 28.10, 50.14, 54.62, 57.46, 58.36, 82.78, 121.86, 130.75, 130.89, 131.53, 135.27, 139.52, 157.35, 168.55, 169.32 ppm; **UHRMS** (ESI+) *m/z* calculated for $C_{31}H_{44}N_4O_6$ $[M+H]^+$ 569.3334; found 569.3330; **HPLC** purity (260 nm): 95.62%; retention time: 9.420 min; gradient: 0.00→15.00 min 30→60% B; eluent: mixture of 5 mM TFA in MQ-water (A) and acetonitrile (B); flow: 1.00 mL/min; injection volume: 10.00 µL; sample: 0.60 mg / 1.00 mL 50% ACN in H_2O; column: Phenomenex Luna C18(2) 100 Å, 3 µm, 150 × 4.60 mm; column ID: H20-261386.

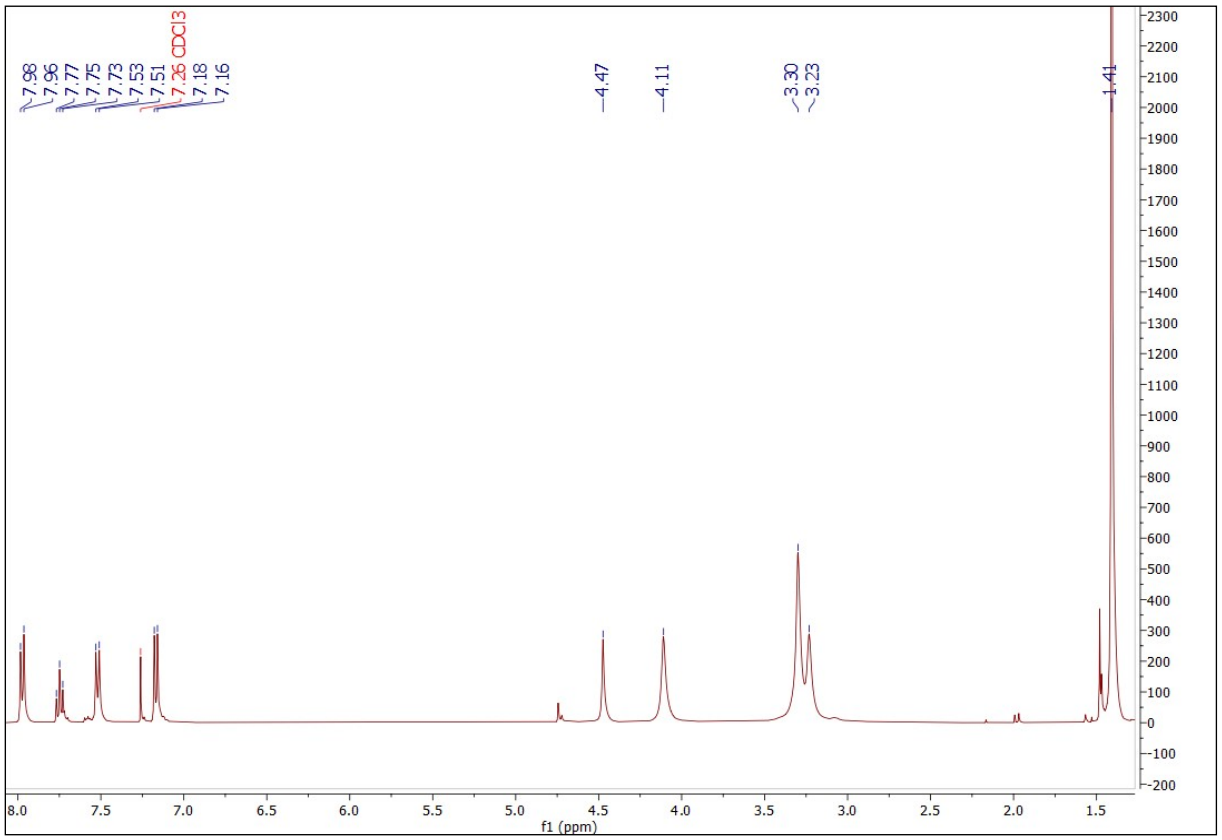

Figure S075. ^{1}H NMR (400.13 MHz, 298.0 K, $CDCl_3$) spectra of compound **15**.

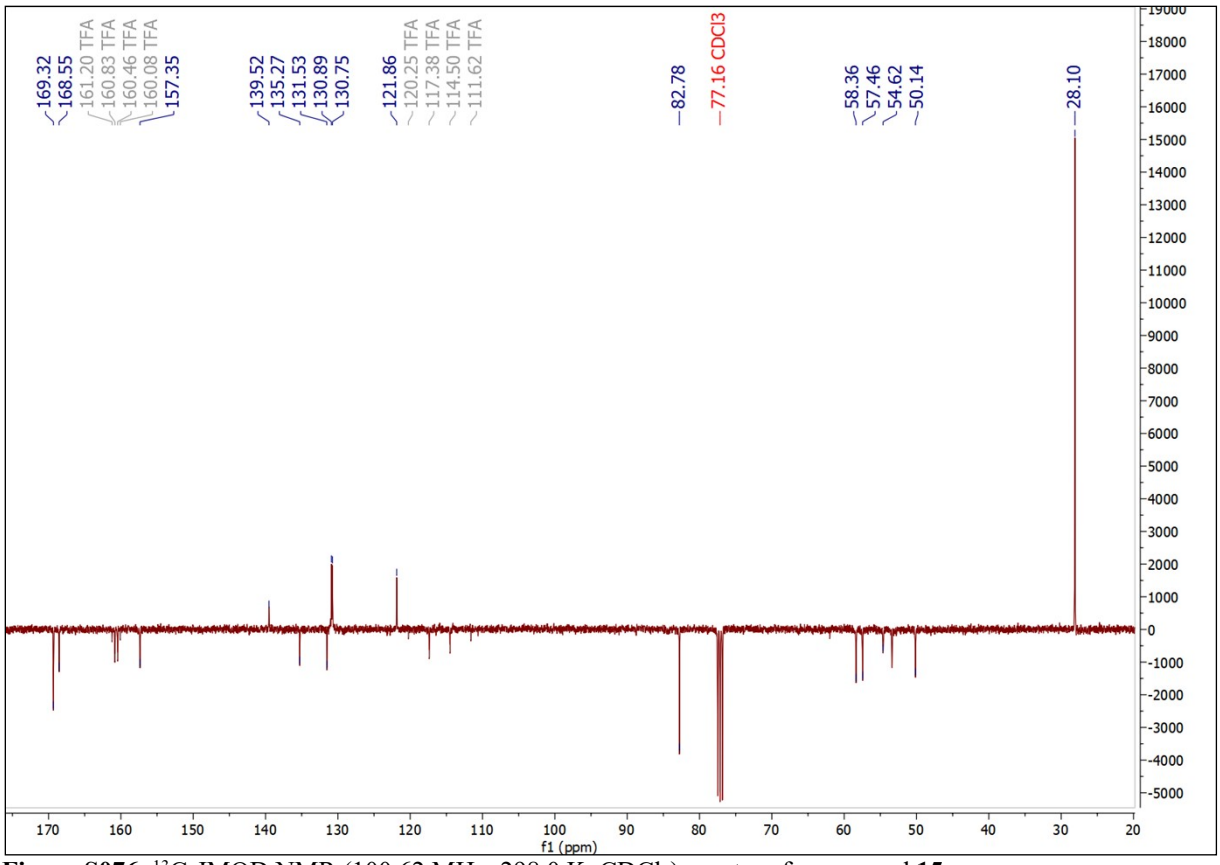

Figure S076. ^{13}C-JMOD NMR (100.62 MHz, 298.0 K, $CDCl_3$) spectra of compound **15**.

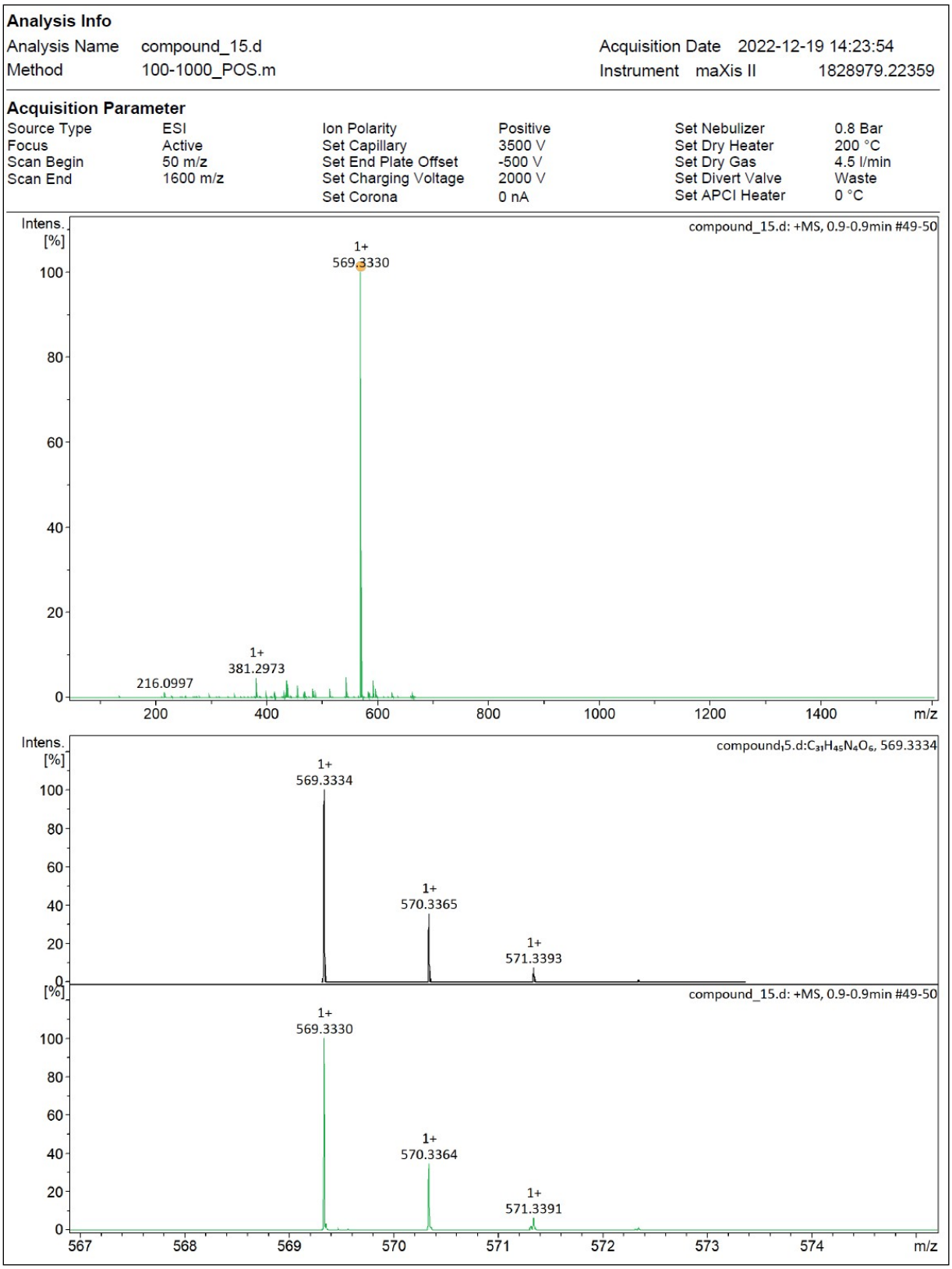

Figure S077. UHRMS spectra (ESI+) of compound **15**.

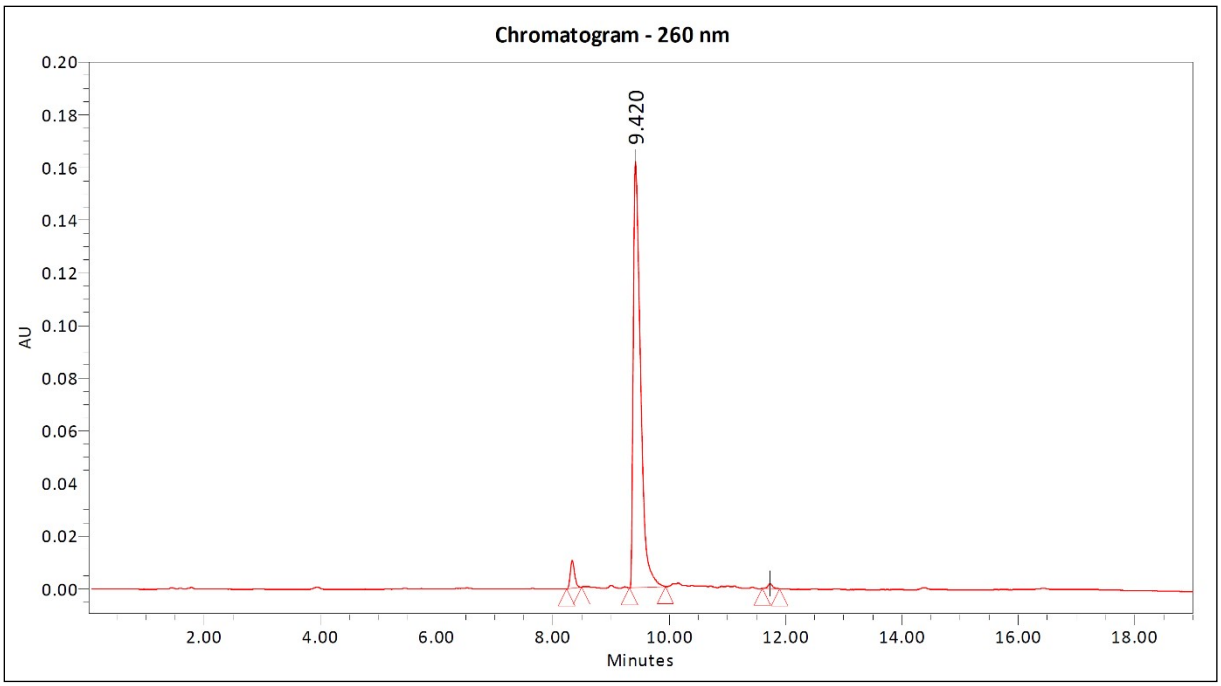

Figure S078. Analytical HPLC chromatogram (260 nm) of compound **15**.

Di-*tert*-butyl 2,2'-(6-(4-((2-(2,5-dioxo-2,5-dihydro-1H-pyrrol-1-yl)ethyl)carbamoyl)benzyl)-3,6,9-triaza-1(2,6)-pyridinacyclodecaphane-3,9-diyl)diacetate (16)

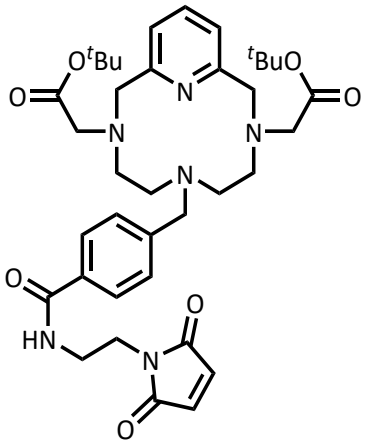

27.1 mg (0.200 mmol) HOBt, 59.2 mg (15.6 mmol), HBTU and 150 µL (0.861 mmol) DIPEA was added to the solution of 4-((3,9-Bis(2-(*tert*-butoxy)-2-oxoethyl)-3,6,9-triaza-1(2,6)-pyridinacyclodecaphane-6-yl)methyl)benzoic acid (**15**) prepared by dissolving 80.0 mg (0.141 mmol) of 15 in 20 mL of dichloromethane. The reaction mixture was stirred at room temperature for 30 min, and 27.4 mg (0.155 mmol) 1-(2-aminoethyl)-1H-pyrrole-2,5-dione hydrochloride was added to the reaction mixture under argon protected atmosphere. The mixture was stirred for an additional 48 hours at room temperature and the solvent was removed in vacuum to afford the crude product, which was purified by preparative HPLC. The combined pure fractions were lyophilized after freezing to furnish the product **16** as a white solid (55 mg, yield 56%).

Preparative HPLC: UV-Vis detection: 210 and 260 nm; retention time: 9.13 min; gradient: 0.00→15.00 min 30→60% B; eluent: mixture of 5 mM TFA in MQ-water (A) and acetonitrile (B); flow: 25.00 mL/min; injection volume: 250.00 µL; sample: 18 mg / 500 µL 50% ACN in H_2O; column: Phenomenex Luna Prep C18(2) 100 Å, 5 µm, 250 × 21.20 mm; column ID: H18-268346.

^{1}H NMR (400.13 MHz, CD_3CN-*d3*) δ 1.43 (s, 18H), 3.06 - 3.36 (m, 12H), 3.50 (q, *J* = 6.0 Hz, 2H), 3.66 (t, *J* = 5.7 Hz, 2H), 4.00 (s, 4H), 4.37 (s, 2H), 6.75 (s, 2H), 7.17 (d, *J* = 7.7 Hz, 2H), 7.22 (t, *J* = 5.7 Hz, 1H), 7.55 (d, *J* = 8.1, 2H), 7.73 (d, *J* = 8.2, 2H), 7.75 (t, *J* = 7.7 Hz, 1H) ppm; **UHRMS** (ESI+) *m/z* calculated for $C_{37}H_{50}N_6O_7$ $[M+H]^+$ 691.3814; found 691.3814; **HPLC** purity (260 nm): 99.77%; retention time: 10.726 min; gradient: 0.00→15.00 min 5→95% B; eluent: mixture of 5 mM TFA in MQ-water (A) and acetonitrile (B); flow: 1.00 mL/min; injection volume: 5.00 µL; sample: 0.53 mg / 300 µL 50% ACN in H_2O; column: Phenomenex Luna C18(2) 100 Å, 3 µm, 150 × 4.60 mm; column ID: H20-261386.

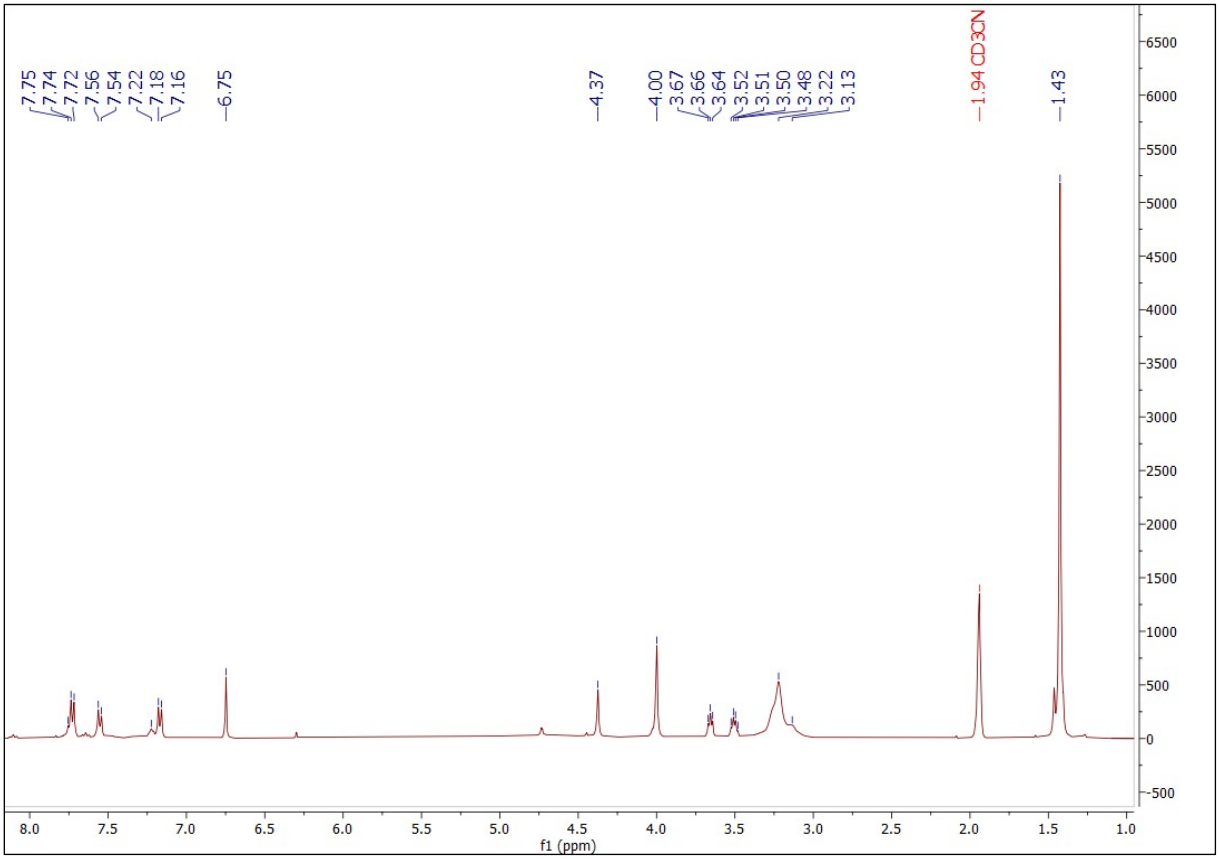

Figure S079. ^{1}H NMR (400.13 MHz, 298.0 K, CD3CN-*d3*) spectra of compound **16**.

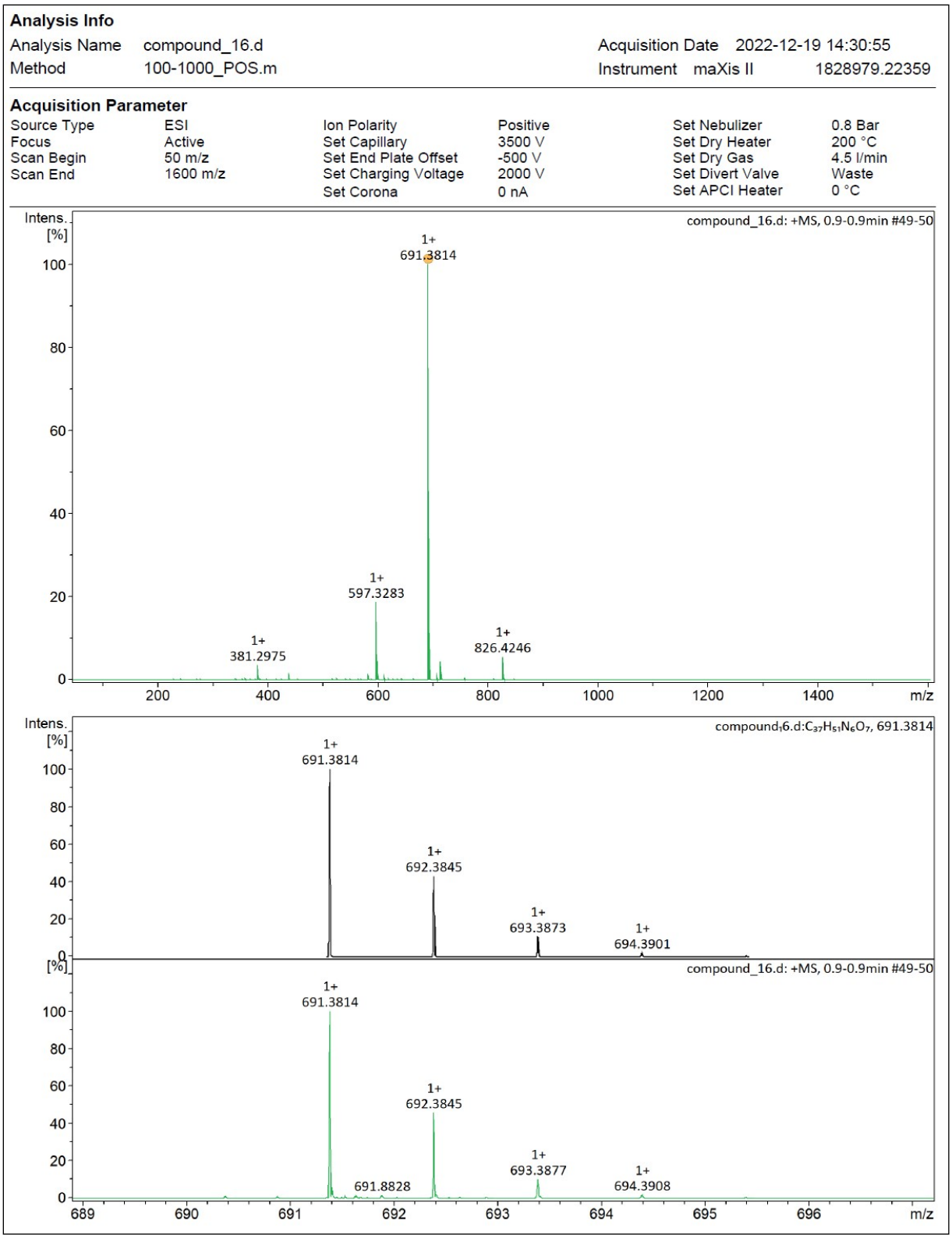

Figure S080. UHRMS spectra (ESI+) of compound **16**.

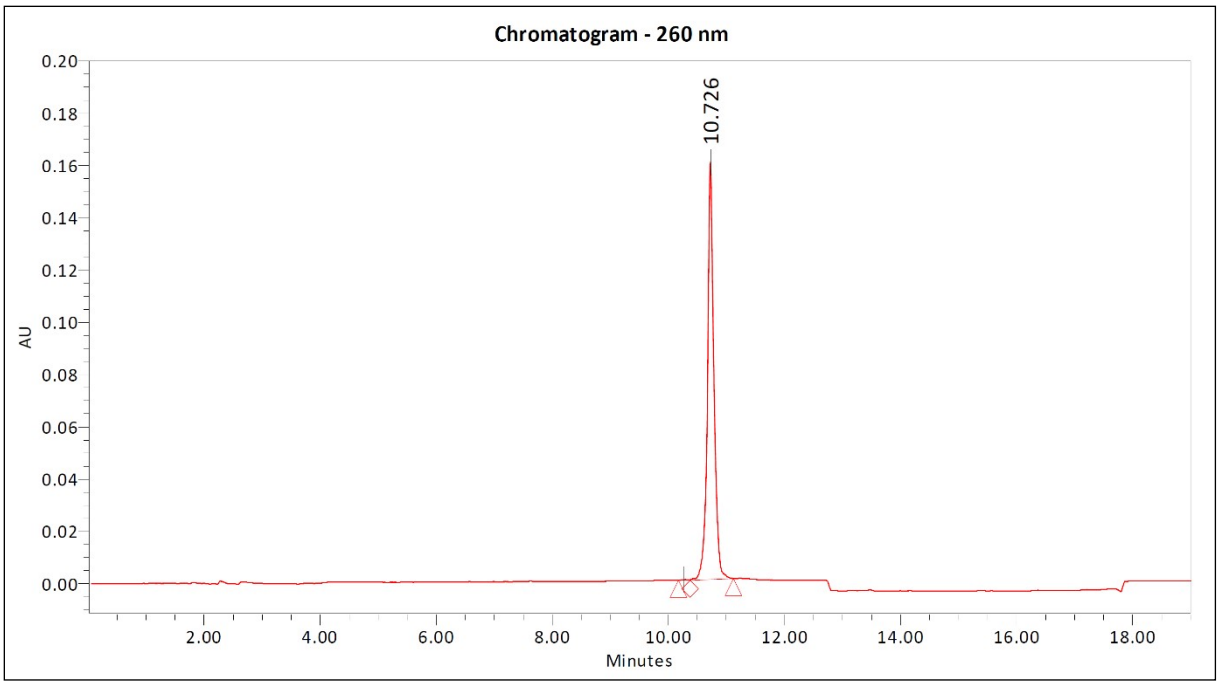

Figure S081. Analytical HPLC chromatogram (260 nm) of compound **16**.

2,2'-(6-(4-((2-(2,5-dioxo-2,5-dihydro-1H-pyrrol-1-yl)ethyl)carbamoyl)benzyl)-3,6,9-triaza-1(2,6)-pyridinacyclodecaphane-3,9-diyl)diacetic acid (17)

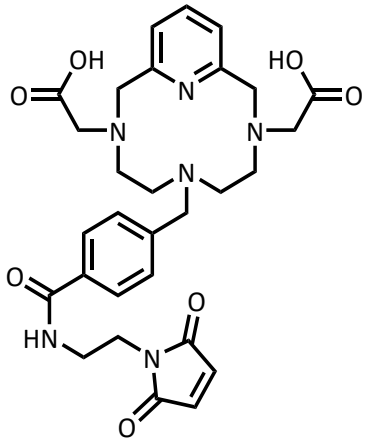

11.1 mg (0.0161 mmol) di-*tert*-butyl 2,2'-(6-(4-((2-(2,5-dioxo-2,5-dihydro-1H-pyrrol-1-yl)ethyl)carbamoyl)benzyl)-3,6,9-triaza-1(2,6)-pyridinacyclodecaphane-3,9-diyl)diacetate (**16**) was dissolved in the mixture of 1.50 mL CH_2Cl_2 and 0.70 mL trifluoroacetic acid was added dropwise to this solution while cooling and keeping it at 0 °C. The reaction mixture was stirred for an additional 24 hours at room temperature and the solvent was removed under reduced pressure to afford the crude product, which was then purified by preparative HPLC. Combing the fractions containing the pure product and lyophilization returned the bifunctional ligand **17** as a white solid (8.4 mg, yield 90%).

Preparative HPLC: UV-Vis detection: 210 and 260 nm; retention time: 6.85 min; gradient: 0.00→15.00 min 5→35% B; eluent: mixture of 5 mM TFA in MQ-water (A) and acetonitrile (B); flow: 25.00 mL/min; injection volume: 600.00 µL; sample: 9 mg / 200 µL 40% ACN in

H_2O; column: Phenomenex Luna Prep C18(2) 100 Å, 5 µm, 250 × 21.20 mm; column ID: H18-268346.

^{1}H NMR (400.13 MHz, CD_3CN-*d_3*) δ 3.22 (m, 8H), 3.52 (m, 4H), 3.58 (m, 2H), 3.62 (m, 2H), 4.28 (s, 4H), 4.37 (s, 2H), 6.75 (s, 2H), 7.34 (m, 1H), 7.48 (d, *J* = 7.7 Hz, 2H), 7.59 (d, *J* = 7.9, 2H), 7.76 (d, *J* = 7.9, 2H), 8.09 (t, *J* = 7.7 Hz, 1H) ppm; **UHRMS** (ESI+) *m/z* calculated for $C_{29}H_{34}N_6O_7$ $[M+H]^+$ 579.2562; found 579.2563; **HPLC** purity (260 nm): 98.72%; retention time: 5.295 min; gradient: 0.00→15.00 min 5→95% B; eluent: mixture of 5 mM TFA in MQ-water (A) and acetonitrile (B); flow: 1.00 mL/min; injection volume: 5.00 µL; sample: 0.20 mg / 300 µL 30% ACN in H_2O; column: Phenomenex Luna C18(2) 100 Å, 3 µm, 150 × 4.60 mm; column ID: 181147-3.

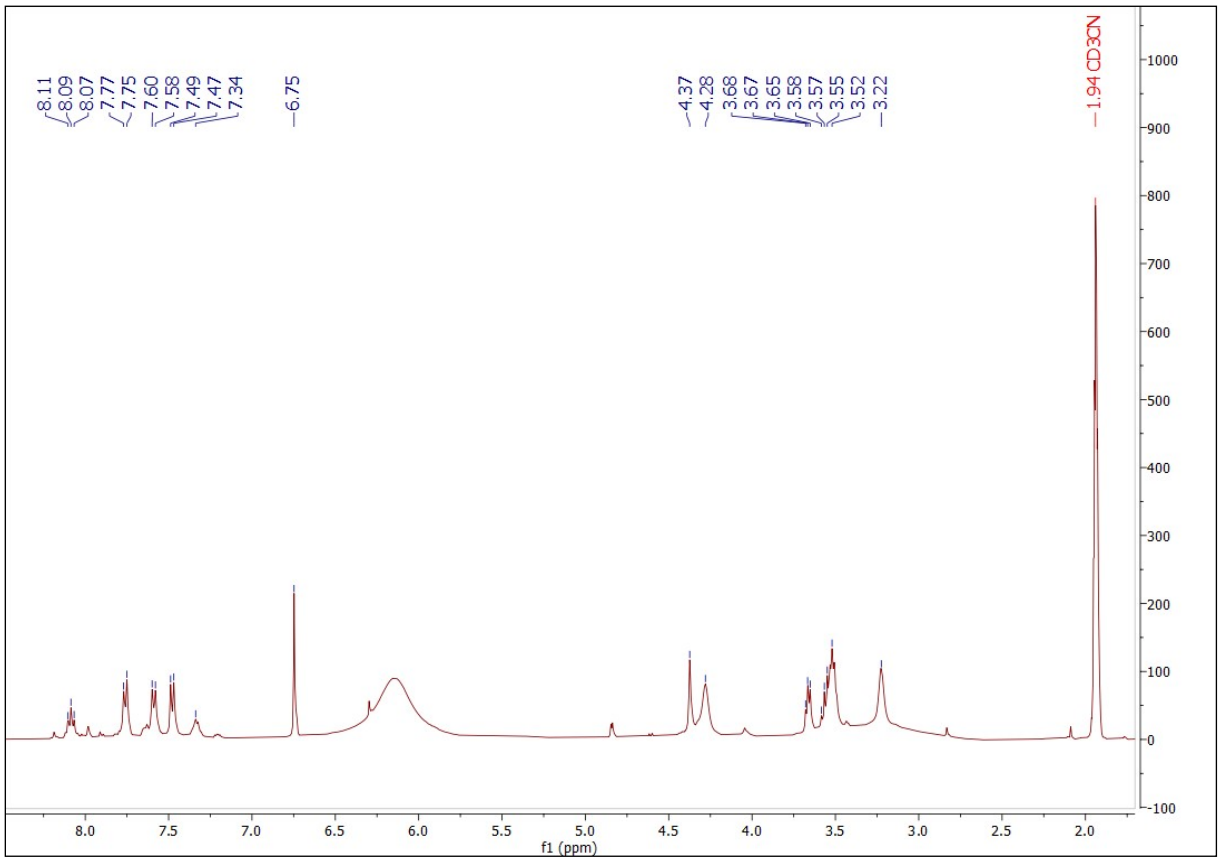

Figure S082. ^{1}H NMR (400.13 MHz, 298.0 K, CD3CN-*d3*) spectra of compound **17**.

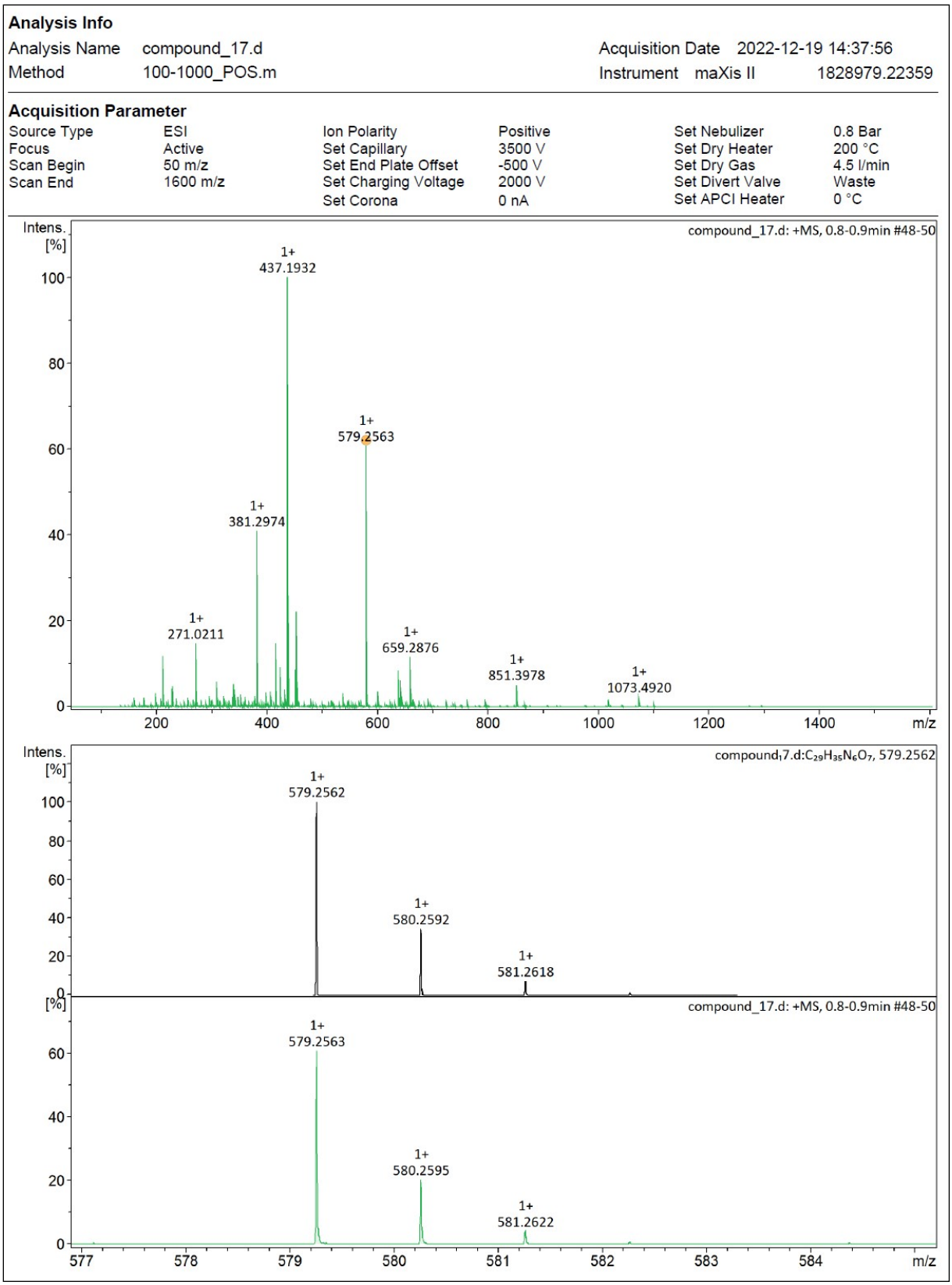

Figure S083. UHRMS spectra (ESI+) of compound **17**.

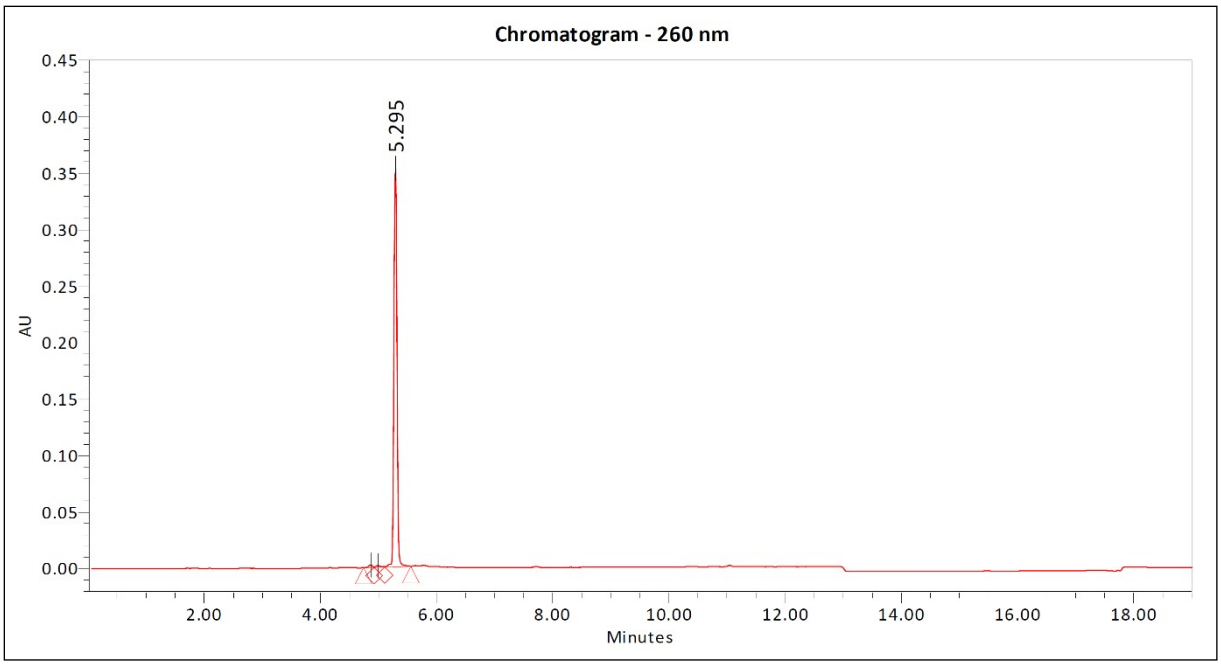

Figure S084. Analytical HPLC chromatogram (260 nm) of compound **17**.

2,2'-(6-(4-nitrobenzyl)-3,6,9-triaza-1(2,6)-pyridinacyclodecaphane-3,9-diyl)diacetic acid (L^0)

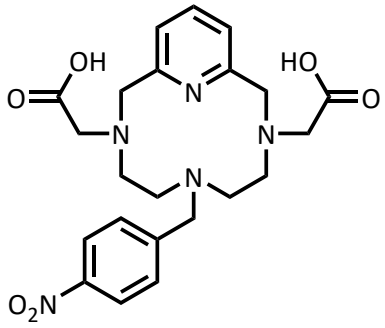

To a solution of 150 mg (0.528 mmol) 2,2'-(3,6,9-triaza-1(2,6)-pyridinacyclodecaphane-3,9-diyl)diacetonitrile (**20**) in 150 mL acetonitrile, 185 µL (1.06 mmol) of *N,N*-diisopropylethylamine and 45.0 mg (0.271 mmol) sodium iodide was added at room temperature under an argon atmosphere. The reaction mixture was then heated up to 60 °C and the solution of 125 mg (0.589 mmol) 1-(bromomethyl)-4-nitrobenzene dissolved in 5 mL acetonitrile was added dropwise over the course of 5 min. The reaction mixture was stirred at 60 °C for an additional 72 h, cooled to room temperature and the solvent was then evaporated off under reduced pressure and the residue was dissolved in 10 mL of cold distilled water. The pH of the solution was adjusted to 13.0 by using solid NaOH, and the product was extracted 3 times using cold chloroform (3 × 10 mL). The combined organic phase was dried over Na_2SO_4 and evaporated under vacuum. The crude product (**21**) was dissolved in 10 mL of 12 M HCl solution. The reaction mixture was stirred at 110 °C for an additional 3 h. After the completion of the reaction the solvent was removed under reduced pressure. The crude product obtained was purified by preparative HPLC. The combined fractions containing the pure substance were lyophilized. Freezer-drying returned the ligand $\mathbf{L^0}$ as a white solid (160 mg, yield 66%).

Preparative HPLC: UV-Vis detection: 210 and 260 nm; retention time: 3.54 min; gradient: 0.00→7.50 min 15→40% B; eluent: mixture of 5 mM TFA in MQ-water (A) and acetonitrile (B); flow: 25.00 mL/min; injection volume: 300.00 µL; sample: 350 mg / 4 mL 50% ACN in H_2O; column: Phenomenex Luna Prep C18(2) 100 Å, 10 µm, 250 × 21.20 mm; column ID: 429545-1.

^{1}H NMR (360.13 MHz, D_2O) δ 3.02 (m, 4H), 3.46 (m, 4H), 3.87 (m, 4H) 4.18 (s, 2H), 4.65 (s, 4H), 7.57 (d, J = 7.9 Hz, 2H), 7.71 (d, J = 8.5 Hz, 2H), 8.12 (t, J = 7.9 Hz, 1H), 8.22 (d, J = 8.5 Hz, 2H) ppm; **^{13}C-JMOD NMR** (90.56 MHz, D_2O) δ 50.67, 52.30, 56.07, 57.17, 58.69, 123.56, 124.08, 132.08, 140.36, 142.36, 148.01, 150.47, 171.30 ppm; **UHRMS** (ESI+) *m/z* calculated for $C_{22}H_{27}N_5O_6$ $[M+H]^+$ 458.2034; found 458.2034. **HPLC** purity (260 nm): 95.65%; retention time: 2.522 min; gradient: 0.00→25.00 min 15% B; eluent: mixture of 20 mM PBS in MQ-water (pH = 7.00) (A) and acetonitrile (B); flow: 1.00 mL/min; injection volume: 30.00 µL; column: Phenomenex Luna C18(2) 100 Å, 5 µm, 150 × 4.60 mm; column ID: 345362.

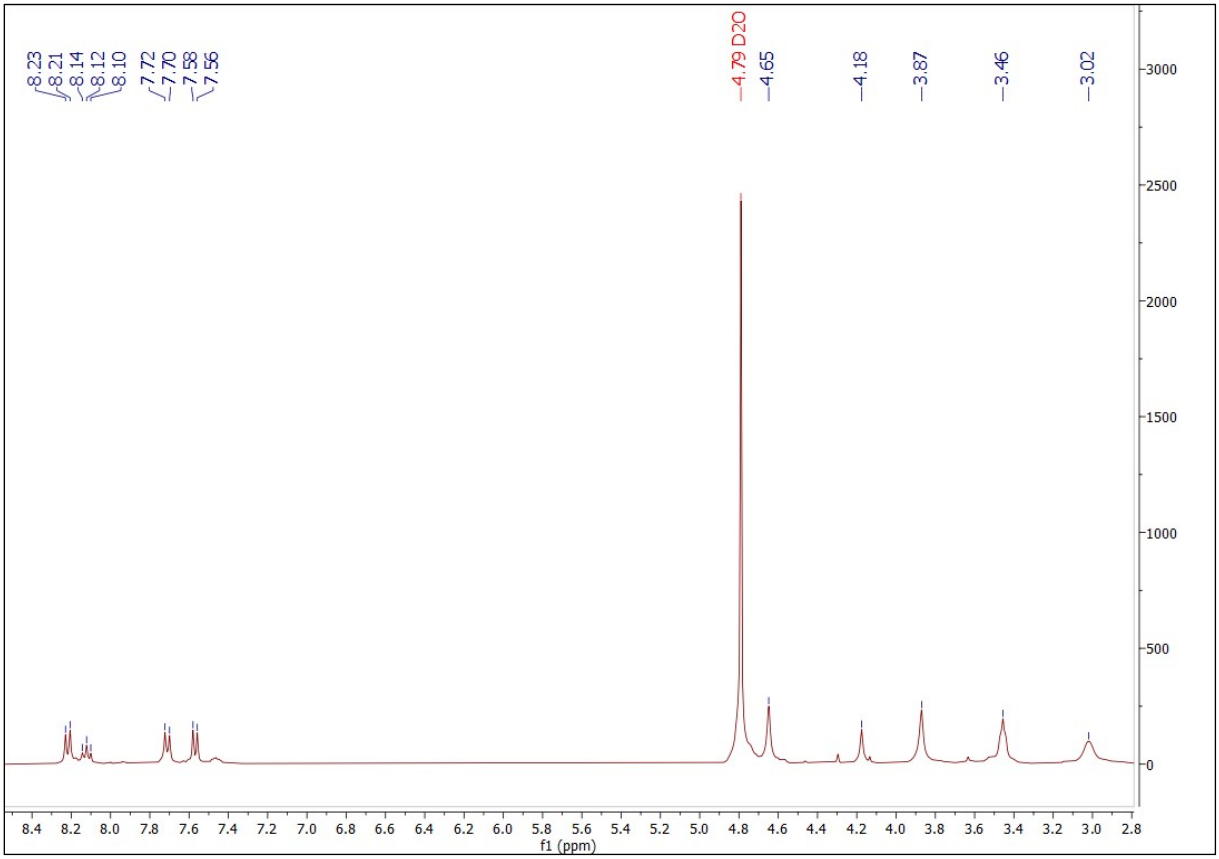

Figure S085. ^{1}H NMR (360.13 MHz, 298.0 K, D_2O) spectra of ligand **L^0**.

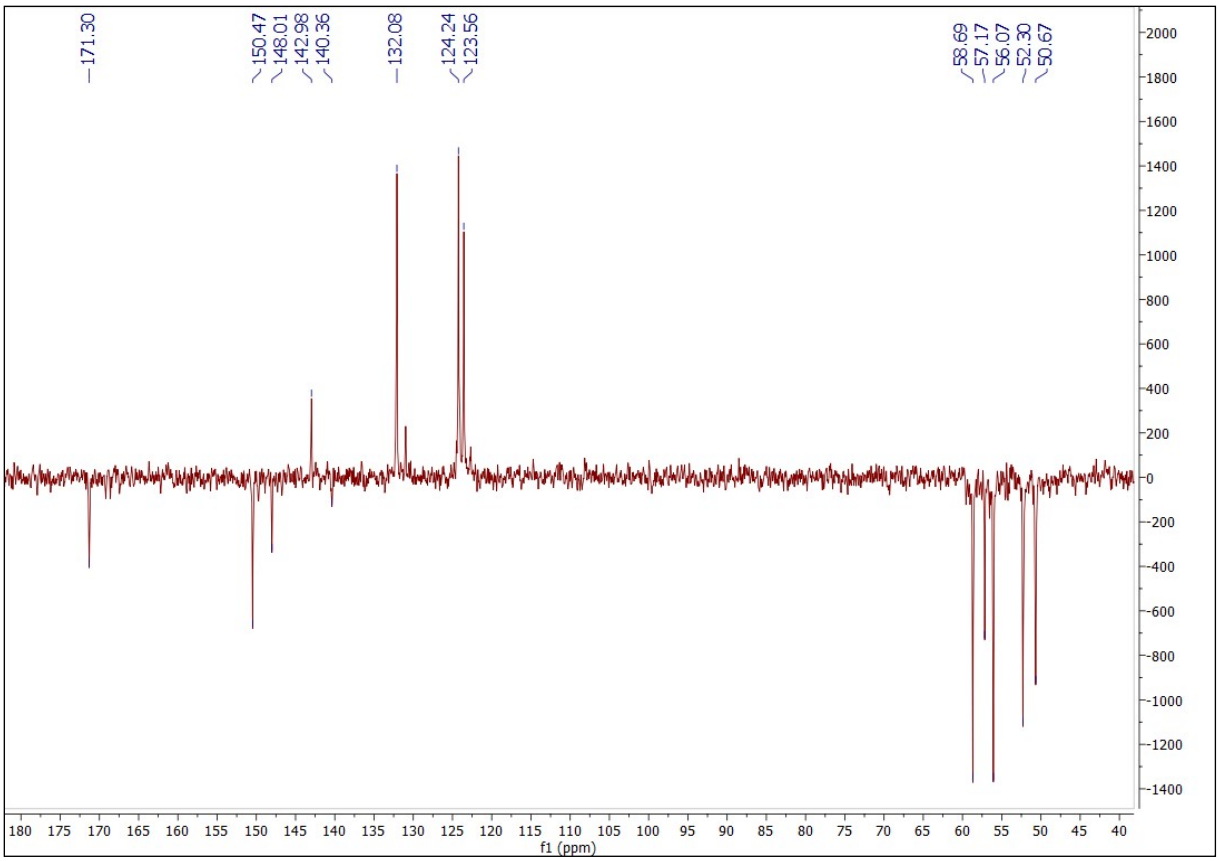

Figure S086. ^{13}C-JMOD NMR (90.56 MHz, 298.0 K, D_2O) spectra of ligand $\mathbf{L^0}$.

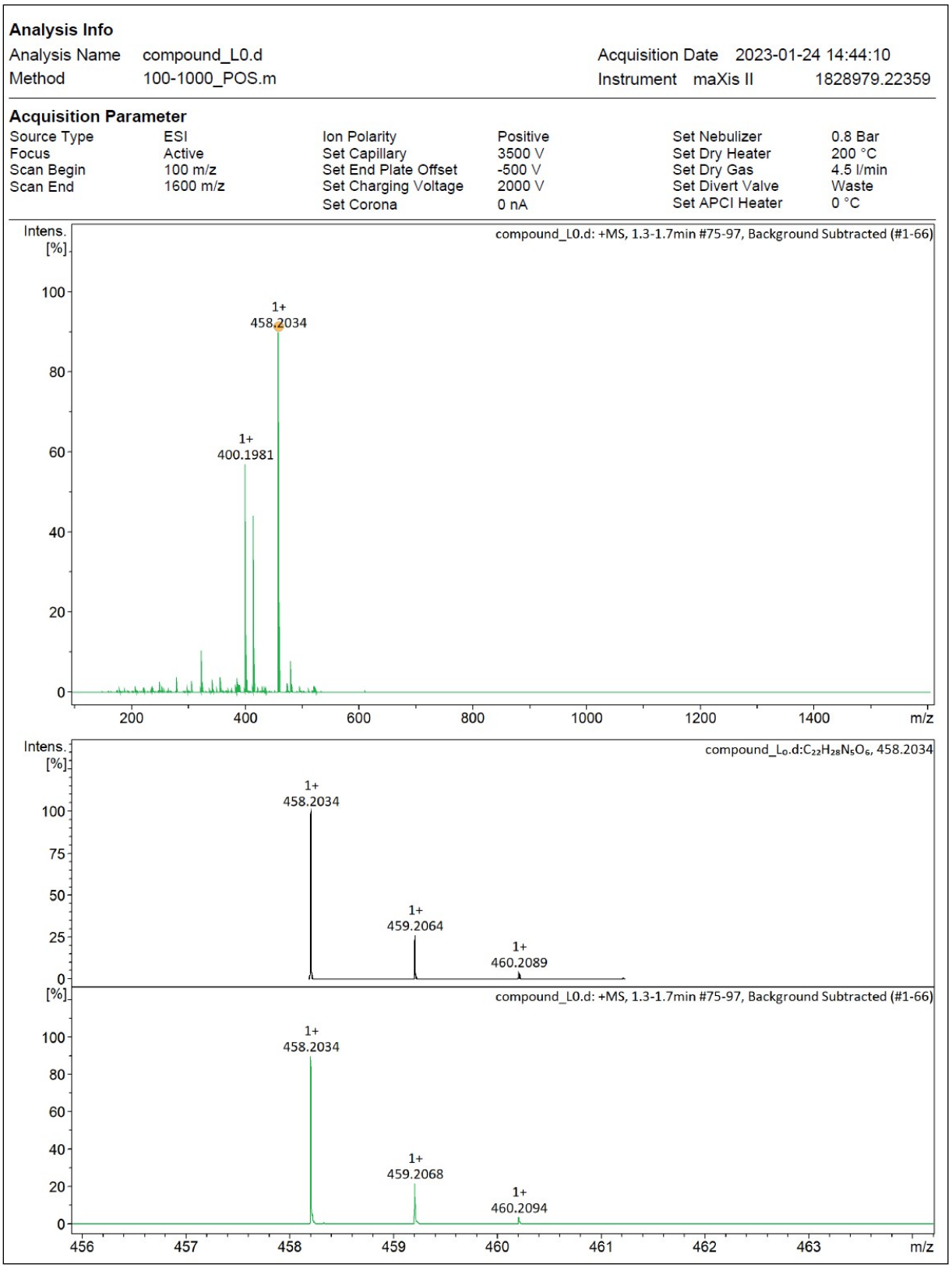

Figure S087. UHRMS spectra (ESI+) of ligand $\mathbf{L^0}$.

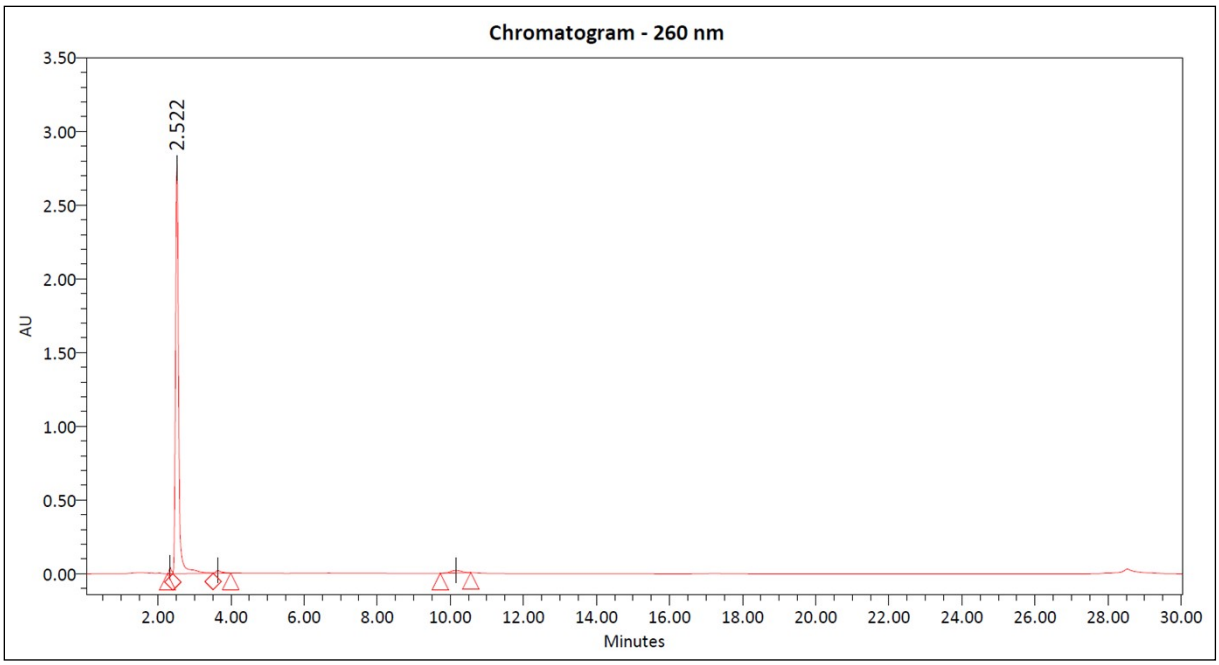

Figure S088. Analytical HPLC chromatogram (260 nm) of ligand $\mathbf{L^0}$.

5. Expression and purification of the anti-HER2 affibody

Materials and Methods

pET19b_6×His-SUMO-Affibody anti-HER2 prokaryotic expression plasmid (ordered from GenScript) was designed to include DNA encoding for $Z_{HER2:2891}$ Affibody N-terminally fused with six residues of histidine followed by SUMO protein, with a SUMO protease cleavage site present between the tags and the anti-HER2 affibody. The plasmid was used to transform *E. coli* BL21(DE3) bacterial strain. *E. coli* were grown in LB medium supplemented with 100 µg/ml ampicillin until the optical density (OD_{600nm}) reached 1.0. The affibody expression was induced by adding 1 mM IPTG and the culture was incubated overnight (16 h) at 37 ºC with 150 rpm shaking. Second day, bacterial cells were centrifuged 10 min at 7000×*g* and 4 ºC and the pellet was stored at -80 ºC until further processing. For protein purification, bacterial cells were resuspended in lysis buffer (20 mM Tris, 500 mM NaCl, 20 mM imidazole, 2 mM DTT, 0.1% Triton X-100, protease inhibitors cocktail (UltraCruz), 1 mM PMSF, pH = 8.0) and homogenized using a potter. Then, the slurry was processed by French Press (Thermo) and the resulted lysate was clarified by centrifugation 30 min at 40000×*g* and 4 ºC. The supernatant was collected, filtered through a 0.45 µm syringe filter unit (Millex, Millipore) and purified by Ni-based affinity chromatography on a HisTrap HP 5ml column (GE Healthcare) using an ÄKTA Basic FPLC system (GE Healthcare). The elution of protein was performed using a 0-100% gradient of 500 mM imidazole in 30 min, 1 ml/min flow. The collected fractions were analysed by 15% SDS-PAGE and the fractions containing the protein of interest were pooled together and submitted to an overnight dialysis against a buffer containing 50 mM Tris, 350 mM NaCl, 2 mM DTT, 0,1% NP-40, pH = 8.0, at 4 ºC. The purified fusion protein, 6×His-SUMO - anti-HER2 affibody was submitted to digestion with SUMO protease (expressed and purified in-house) in a 1:20 protease: affibody ratio, overnight at 30 ºC followed by re-purification using Ni-Sepharose resin (Cytiva). The untagged anti-HER2 affibody remained in solution, while 6×His-SUMO tag and SUMO protease were bound to Ni-Sepharose beads and removed by centrifugation at 1000×*g*, at 4 °C. The concentration of the affibody in solution was determined by absorbance measurements at 280 nm using the FLUOstar Omega spectrophotometer (BMG Labtech). Finally, the purified anti-HER2 affibody was analysed by 15% SDS-PAGE under reducing conditions and by nano-liquid chromatography-tandem mass spectrometry (nLC-MS/MS).

Analysis of anti-HER2 affibody dimerization state

For the dimerization test, a solution of simple anti-HER2 affibody without tags with a concentration of 0.47 µg/µl was used. An initial sample of affibody was first incubated with SDS-PAGE loading buffer (LB) without any reducing agent, for 5 min at 80 ºC and then centrifuged for 1 min, 13000 x g, at room temperature (RT). Then, the sample was split into four separate conditions: a negative control without reducing agents, incubation with only dithiothreitol (DTT), working concentration 50 mM, for 5 min at 80 º C, incubation with only *N*-ethyl-maleimide (NEM), working concentration 91 mM, RT and lastly, treatment with both DTT and NEM. All the samples were run in a non-reducing SDS-PAGE.

Mass spectrometry analyses

Materials

For the mass spectrometry experiments, we used: LC-MS CHROMASOLV™ water and acetonitrile, LC-MS grade, ammonium bicarbonate, iodoacetamide (I6125) and dithiothreitol (DTT, 43815) from Sigma-Aldrich; LC-MS grade formic acid (56302) from

Fluka; trypsin (sequencing grade) from Promega. For desalting, we used GL-Tip SDB (7820-11200) and GL-Tip GC (7820-11201), both from GL Sciences. The Invitrogen NuPAGE™ 4-12%, Bis-Tris protein gels (NP0321BOX) were used for protein separation before in-gel digestion.

Methods

In the bottom-up approach for protein identification, proteins extracted from a sample are converted to peptides using a protease or chemical reagents. In our current approach, we used trypsin to obtain peptides amenable for LC-MS/MS analysis. The obtained tryptic peptides were injected and subject to reversed-phase liquid chromatography before mass spectrometry (MS) analysis. The peptides can be detected by their specific m/z ion current (ions) which depends on their molecular weight and thus their sequence. To obtain further sequence-specific information once detected, these ions are isolated in the instrument and subject to gas-phase fractionation in which specific m/z fragment ions are detected, which can be used further for sequence assignment (*b* and *y* ions – see Figure S089 below and references[7-9]). *b* ions result from the peptide backbone C-N bond cleavage and retain the charge towards the N-terminal fragment, while *y* ions retain the charge towards the C-terminal fragments.

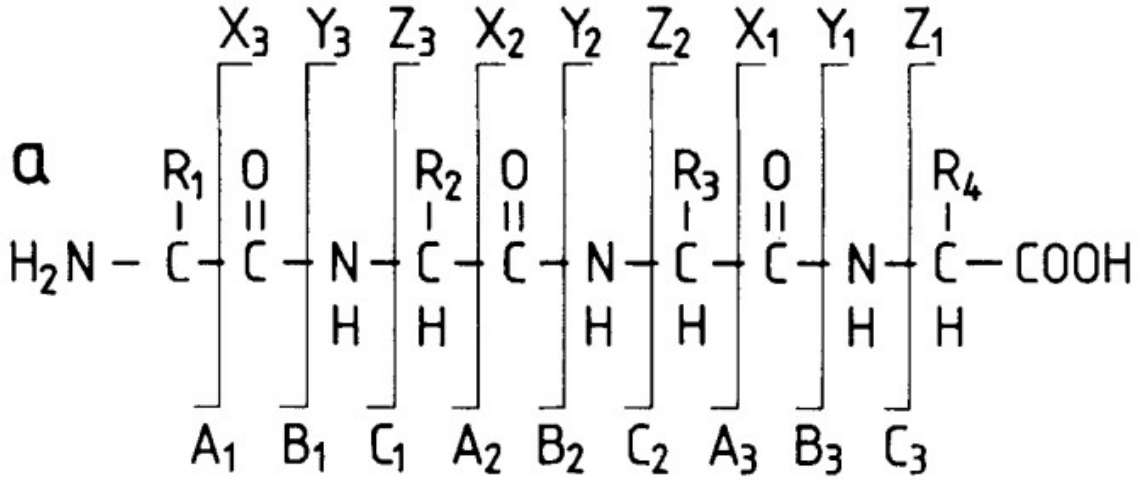

Figure S089. Peptide *b* and *y* ions (Source: Reference[7]).

Since proteins can give rise to multiple peptides considering also potential missed cleavages, the MS obtained data can became quite complex for manual analysis and usually fragment-centric algorithms are employed to obtain sequence-specific information. In this approach all the protein sequences from the source organism are *in silico* digested and *b* and *y* ions are generated for each peptide (see references[10, 11] as examples of algorithms matching). The software looks for potential matches between the instrument obtained spectra and the ones generated, scoring accordingly each match which is usually defined as a PSM (Peptide Spectrum Match). Since multiple matches are possible, most of the software use the target-decoy approach (see references[12, 13]) to maintain under control the false matches (the so-called False Discovery Rate - FDR). In the target-decoy approach, randomized protein (or reversed C- to N-terminus) sequences which are biologically irrelevant are subject to the same process of *in silico* protease digestion and the instrument-specific MS/MS spectra are further matched against these non-relevant sequences. Since in the second case all matches are random, the assigned scores of the matches for the second search are lower than the first one (which contains the true matches) and a cut-off score is chosen in order to keep the highest number of true matches and the lowest number from false matches. Thus, the cut-off PSM score usually reflects how many potential false matches are included in the reported table of PSM sequences (Figure

S090). FDR is considered an estimation of false positive matches among all identifications reported.

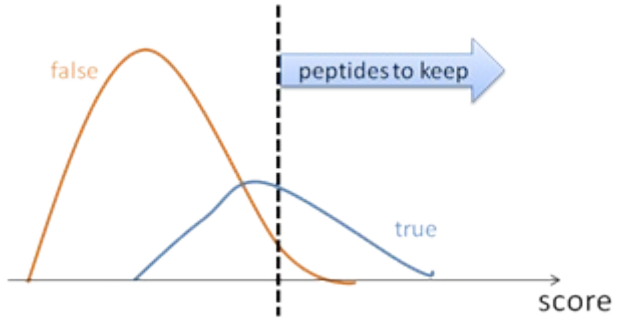

Figure S090. PSMs score distribution from the decoy and target database. (Source: reference[14] - https://www.bioinfor.com/)

Since the bottom-up MS protein analysis is peptide-centric, it is always difficult to translate peptide identifications to protein identifications, usually because of the redundancy problem, as many proteins can share the same peptides (see reference[15]). For this approach, most algorithms obtain an initial protein list based on all of the identified peptides. The proteins which share peptides are grouped, thus actually reporting protein groups. However, unlike the full list of proteins, protein groups are defined by their unique peptides, which are distinct peptides, not shared with other protein groups.

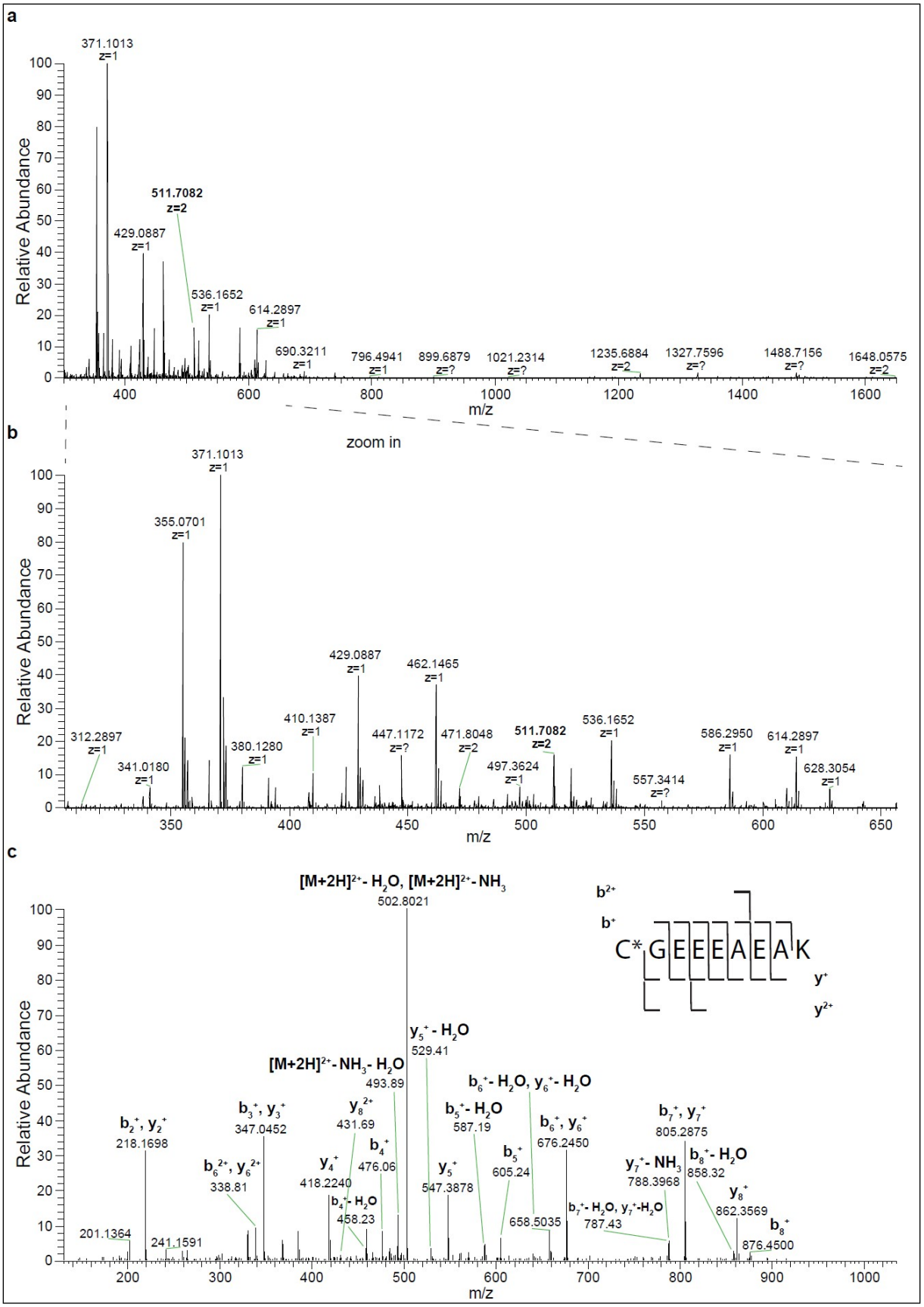
a
371.1013
z=1
511.7082
z=2
429.0887
z=1
536.1652
z=1
614.2897
z=1
690.3211
z=1
796.4941
z=1
899.6879
z=?
1021.2314
z=?
1235.6884
z=2
1327.7596
z=?
1488.7156
z=?
1648.0575
z=2
Relative Abundance
m/z
zoom in
b
371.1013
z=1
355.0701
z=1
429.0887
z=1
462.1465
z=1
410.1387
z=1
312.2897
z=1
380.1280
z=1
447.1172
z=?
471.8048
z=2
511.7082
z=2
536.1652
z=1
586.2950
z=1
614.2897
z=1
341.0180
z=1
497.3624
z=1
557.3414
z=?
628.3054
z=1
Relative Abundance
m/z
c
[M+2H]2+- H2O, [M+2H]2+- NH3
502.8021
b2+
b+
C*GEEEAEAK
y+
y2+
y5+ - H2O
529.41
[M+2H]2+- NH3- H2O
493.89
b6+- H2O, y6+- H2O
b5+- H2O
587.19
b6+, y6+
676.2450
b7+, y7+
805.2875
b3+, y3+
347.0452
y82+
431.69
b2+, y2+
218.1698
b4+
476.06
b5+
605.24
b8+- H2O
858.32
y7+- NH3
788.3968
b62+, y62+
338.81
y4+
418.2240
y5+
547.3878
y8+
862.3569
b4+- H2O
458.23
b7+- H2O, y7+-H2O
787.43
658.5035
b8+
876.4500
201.1364
241.1591
Relative Abundance
m/z

Figure S091. Identification of peptide "CGEEEAEAK", the first peptide from the sequence of the anti-HER2 affibody molecule. a) Mass spectrum of an MS1 scan in which peptide "CGEEEAEAK" (carbamidomethylated at Cysteine; depicted in bold) was detected as +2 charge, at m/z of 511.7082 Da (MH^+ 1022.40917 Da, ΔM of -0.2 mmu/-0.4 ppm); b) Zoom in between m/z of approximately 310 and 650 of the scan depicted in a), where the first peptide from anti-HER2 affibody is depicted in bold; c) Product ion spectrum of the peptide "CGEEEAEAK", obtained by collision-induced dissociation. Several *b* and *y* ions as well as unfragmented ions of the peptide, with neutral losses of water and/or ammonia are shown. The carbamidomethylated Cysteine residue is depicted as "C*" in the sequence "C*GEEEAEAK".

Mass spectrometry identification of proteins using the bottom-up approach

In-gel digestion

Bacterially expressed and purified 6xHis-SUMO-anti-HER2 affibody protein as well as the products of reaction obtained from the in-solution cleavage of 6xHis-SUMO-anti-HER2 affibody by Sumo protease (6xHis-SUMO tag and anti-HER2 affibody) were subjected to an in-gel digestion protocol, as previously described[16, 17]. The samples were first migrated in NuPAGE™ 4-12%, Bis-Tris protein gels, then Coomassie-stained. Sequencing grade modified trypsin (10 ng/μL) was used for protein digestion. The resulted peptides were kept at -20 °C until nano-liquid chromatography-tandem mass spectrometry (nLC-MS/MS) analysis.

LC-MS/MS analysis

The peptides were resuspended in mobile phase A (0.1% formic acid and 2% acetonitrile) and transferred into nLC vials. The peptides were injected using an EASY nLC II liquid chromatograph (2 cm × 100 μm C18 trap column, followed by 10 cm × 75 μm C18 analytical column), which was online coupled to an LTQ™ - Orbitrap Velos Pro™ mass spectrometer (all from Thermo Fisher Scientific). A 40 min gradient of 2% to 30% mobile phase B (0.1% formic acid in 98% acetonitrile) with a flow rate of 300 nL/min was set up for the elution of the peptides. The acquisition method was constituted of an initial scan (between 300 and 1650 m/z, at 60,000 resolution at the m/z of 400), which was followed by a data-dependent analysis of the five most intense peaks (with charges +2, +3 or higher) from that precursor ion scan, using collision-induced dissociation (CID) as fragmentation method. Two technical replicates (runs) were performed for each sample.

Protein identification

For each sample, all the spectrum files acquired in the two technical replicates were searched using the Sequest HT algorithm of Proteome Discoverer v1.4 (Thermo Fisher Scientific). The searches were performed with the following settings: a modified version of the UniProtKB/Swiss-Prot database, trypsin (full) as enzyme, with a maximum of two missed cleavages; precursor mass tolerance of 10 ppm; fragment mass tolerance of 0.6 Da; methionine oxidation (+15.995 Da) as dynamic modification and carbamidomethylation (+57.021 Da) on cysteine as static modification. The new database was generated by adding the following five sequences to the UniProtKB/Swiss-Prot database (downloaded in May 2016, with 463712 sequences): Affibody_HER2, 6xHis-SUMO-Affibody_HER2 (with and without the first methionine) and 6xHis-SUMO tag (with and without the first methionine). A decoy database search (reversed protein sequences) was also enabled. A protein was considered present in a sample, if at least two unique peptides were identified, at 5% FDR, PSM level.

Mass spectrometry analysis of purified anti-HER2 affibody

Sample preparation

Purified anti-HER2 affibody was desalted using pipette-tip columns containing C18 resin (Pierce™ C18 Tips, Thermo Fisher Scientific) according to the protocol described by the manufacturer. The resulted anti-HER2 affibody molecules were dried in a vacuum concentrator (Thermo Fisher Scientific), then stored at -20 °C until the nLC-MS/MS analysis.

nLC-MS/MS analysis of anti-HER2 affibody

The purified and desalted Affibody sample was thawed on ice and resuspended in mobile phase A, then transferred into nLC vials. The anti-HER2 affibody molecules were analysed by nLC-MS/MS, using the same instruments as in the bottom-up approach described above. Also, the C18 columns and the acquisition method were the same as the ones described earlier. Xcalibur™ (Thermo Fisher Scientific) software was used for data acquisition. One run was performed.

Data analysis

The spectra (total and extracted ion chromatograms) were visualized and anti-HER2 affibody ions were manually searched using Xcalibur™ (Thermo Fisher Scientific) software. To detect the anti-HER2 affibody ions, calculations were made based on the theoretical monoisotopic molecular weight of anti-HER2 affibody protein, 7255.63 Da. The existence of oxidized molecules of anti-HER2 affibody was also taken into consideration.

The mass spectrometry proteomics data have been deposited to the ProteomeXchange Consortium via the PRIDE partner repository with the dataset PXD039821.[18]

Results

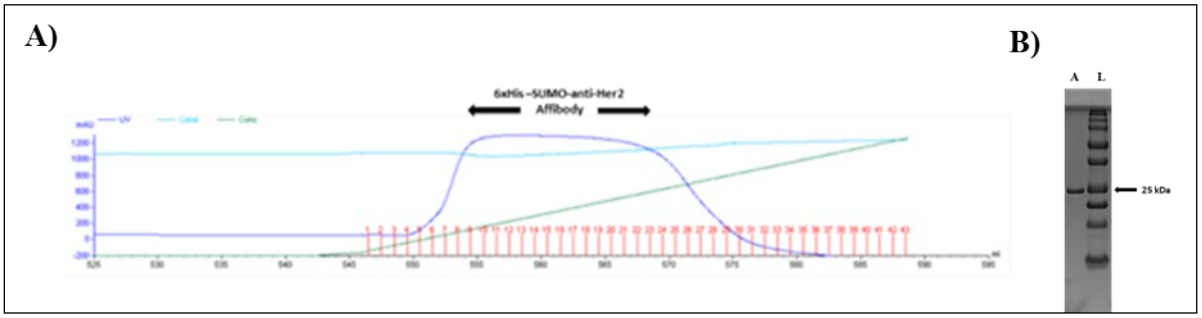

Figure S092 Purification of 6xHis–SUMO-anti-HER2 affibody construct. A) Chromatogram of SUMO-affibody construct purified by affinity chromatography using ÄKTA Basic FPLC system; B) SDS-PAGE gel of 6xHis-SUMO-HER2-Affibody purified by affinity chromatography: A - Affibody construct; L - molecular mass marker.

Table S002 Peptides corresponding to 6xHis-SUMO-anti-HER2 affibody protein, identified at 5% FDR (Table extracted from Proteome Discoverer v1.4)

Confidence	Sequence	# PSMs	Modifications	XCorr	Charge	MH+ [Da]	ΔM [ppm]	m/z [Da]	RT [min]	# Missed Cleavages
High	IQADQTPEDLDmEDNDIIEAHR	372	M12(Oxidation)	6.448483	3	2584.141	-2.46086	862.0517	31.66089	0
High	KLNDSQAPK	4		3.56925	2	1000.542	-0.49642	500.7745	0.647148	1

High	GSSHHHHHHGSGLVPR	14		4.20 6615	4	1738 .838	- 0.22 546	435. 4649	6.05 7888	0
High	EQIGGcGEEEAEAK	112	C6(Carbami domethyl)	4.57 607	2	1506 .638	- 0.09 588	753. 8224	23.3 3145	0
High	GSASmSDSEVNQEAKPEVKPEV KPETHINLK	35	M5(Oxidati on)	5.90 4352	4	3394 .679	- 0.16 451	849. 4252	52.8 7125	0
High	KLYDDPSQSSELLSEAKK	6		5.78 6386	3	2038 .035	0.71 7967	680. 0167	24.7 8328	2
High	LYDDPSQSSELLSEAKK	2		4.06 0386	2	1909 .94	0.45 3226	955. 4736	26.5 9	1
High	KLYDDPSQSSELLSEAK	164		5.70 5522	2	1909 .932	- 3.82 897	955. 4695	27.6 2394	1
High	VSDGSSEIFFK	93		3.98 134	2	1215 .589	- 0.17 641	608. 2982	33.4 1157	0
High	GSASMSDSEVNQEAKPEVKPEV KPETHINLKVSDGSSEIFFK	5		5.22 3331	4	4575 .257	0.18 0845	1144 .57	29.4 627	1
High	LYDDPSQSSELLSEAK	98		6.05 0234	3	1781 .841	- 1.88 566	594. 6184	30.8 1131	0
High	VSDGSSEIFFKIK	2		3.89 4797	2	1456 .769	0.38 1067	728. 8881	30.0 6527	1
High	FLYDGIRIQADQTPEDLDMEDND IIEAHR	1		4.33 0655	4	3432 .612	3.14 6881	858. 9085	39.3 4811	1
High	NAYWEIALLPNLTNQQKR	5		4.42 836	2	2172 .155	- 0.69 179	1086 .581	41.5 8604	1
High	EMRNAYWEIALLPNLTNQQK	2		4.56 4835	3	2432 .242	0.96 9873	811. 4187	42.5 3386	1
High	NAYWEIALLPNLTNQQK	75		5.60 5001	2	2016 .053	- 1.20 705	1008 .53	40.5 8728	0
High	AFIRKLYDDPSQSSELLSEAK	1		4.07 4962	3	2397 .229	- 0.28 918	799. 7479	30.2 4469	2
High	YAKEMRNAYWEIALLPNLTNQQ K	1		4.26 6846	4	2794 .428	- 2.40 627	699. 3624	39.4 1436	2
Medi um	RLMEAFAK	1		2.84 0959	2	965. 523	- 0.79 178	483. 2651	19.0 8151	1

Table S003: Peptides corresponding to anti-HER2 affibody protein, identified at 5% FDR (Table extracted from Proteome Discoverer v1.4)

Confidence	Sequence	# PSMs	XCorr	Charge	MH+ [Da]	ΔM [ppm]	m/z [Da]	RT [min]	# Missed Cleavages
High	KLYDDPSQSSELLSEAKK	13	6.021504	3	2038.033	-0.53985	680.0158	26.76647	2
High	KLYDDPSQSSELLSEAK	76	5.577745	2	1909.94	0.261487	955.4734	29.31923	1
High	LYDDPSQSSELLSEAK	67	5.527565	2	1781.844	-0.13116	891.4255	32.83487	0
High	NAYWEIALLPNLTNQQK	10	4.945772	2	2016.056	0.367233	1008.531	46.1906	0
High	LYDDPSQSSELLSEAKK	4	4.572146	2	1909.939	-0.18591	955.473	27.74761	1
High	AFIRKLYDDPSQSSELLSEAK	2	4.143363	3	2397.23	0.016344	799.7481	31.59845	2
High	NAYWEIALLPNLTNQQKR	4	3.630459	2	2172.157	0.432161	1086.582	42.57532	1
High	KLNDSQAPK	7	3.324273	2	1000.542	-0.49642	500.7745	5.54554	1

Table S004 Peptides corresponding to 6xHis-SUMO tag protein, identified at 5% FDR (Table extracted from Proteome Discoverer v1.4)

Confidence	Sequence	# PSMs	Modifications	XCorr	Charge	MH+ [Da]	ΔM [ppm]	m/z [Da]	RT [min]	# Missed Cleavages
High	IQADQTPEDLDMEDNDIIEAHR	533		5.727445	3	2568.153	0.273262	856.7224	43.53008	0
High	IQADQTPEDLDmEDNDIIEAHREQIGG	22	M12(Oxidation)	5.170602	3	3068.375	-0.07667	1023.463	31.50726	1
High	GSASmSDSEVNQEAKPEVKPEVKPETHINLK	21	M5(Oxidation)	4.894579	3	3394.671	-2.44397	1132.229	20.09778	0
High	GSSHHHHHHGSGLVPR	61		4.799834	4	1738.841	1.389189	435.4656	6.09446	0
High	VSDGSSEIFFKIK	6		4.250444	2	1456.767	-0.87586	728.8871	31.29409	1
High	VSDGSSEIFFK	109		3.95687	2	1215.589	-0.37725	608.298	47.73157	0
High	RLMEAFAKR	2		3.638168	3	1121.625	0.489986	374.5467	17.1584	2
Medium	LMEAFAKRQGK	2		2.859824	2	1278.698	-0.38439	639.8528	16.22449	2
Medium	FLYDGIR	6		2.718746	2	883.4672	-0.05729	442.2372	53.3527	0

Medium	VSDGSSEIFFKIKK	1		2.695405	2	1584.864	0.196666	792.9354	25.75284	2
Medium	RLMEAFAK	2		2.606688	2	965.5245	0.788583	483.2659	38.14174	1

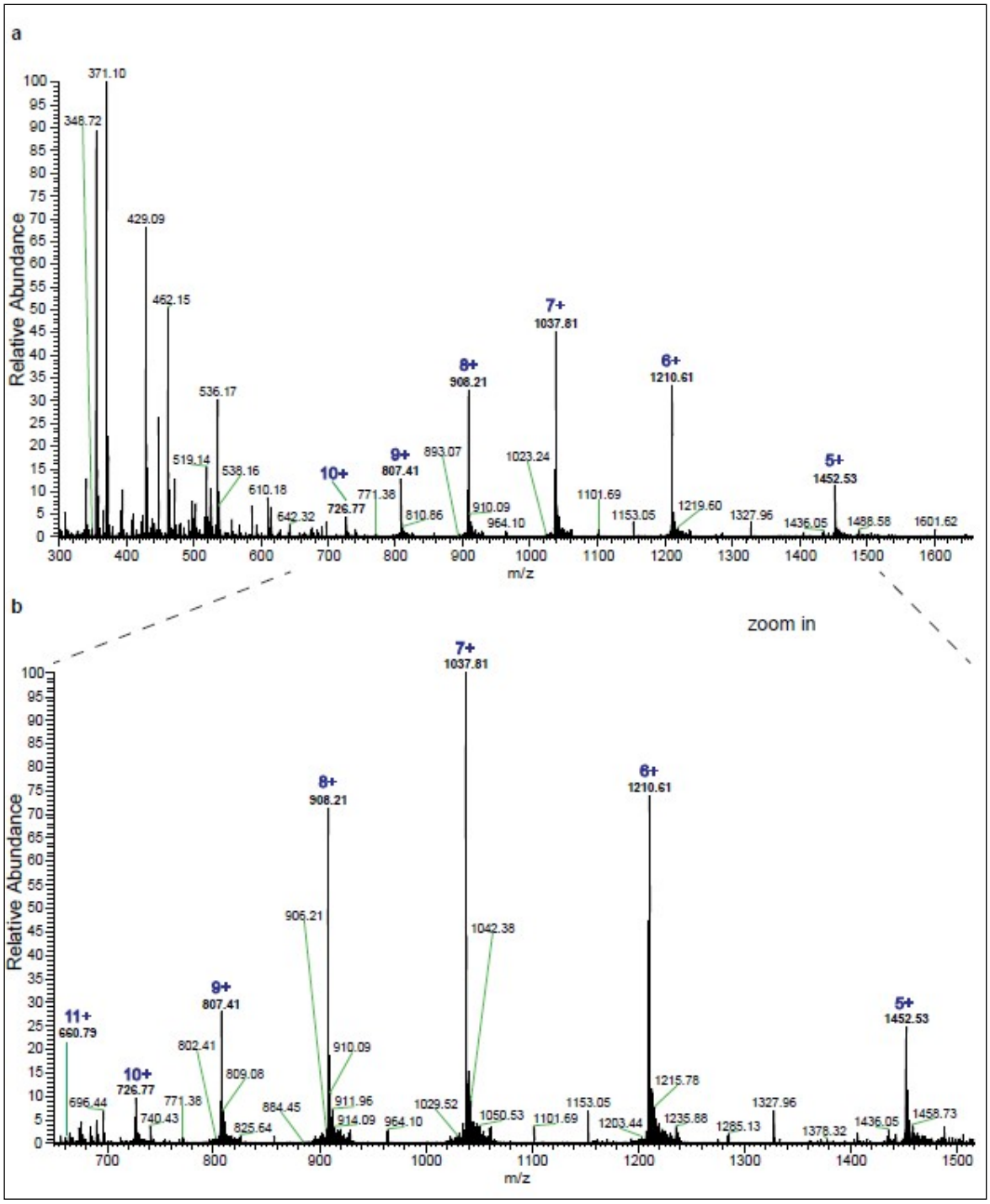

Figure S093. Nano-LC-MS/MS analysis of purified anti-HER2 affibody. a) Mass spectrum (extracted ion chromatogram, XIC) of anti-HER2 affibody, with most of its ions from the charge state envelope (the charges are written above each ion, in blue). b) Zoom in on the XIC, evidencing the complete charge state envelope of anti-HER2 affibody detected (the charges written above each ion, in blue).

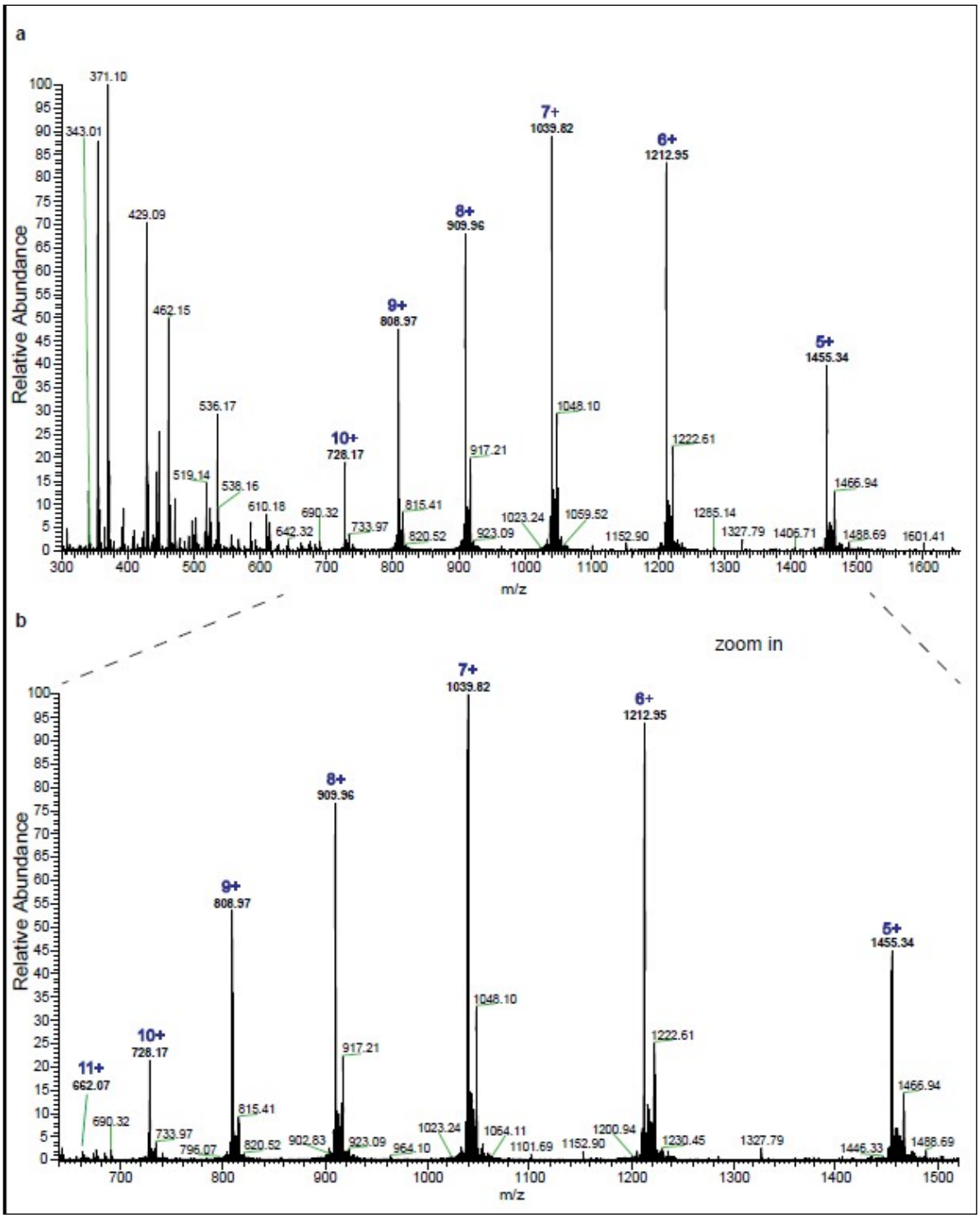

Figure S094. Nano-LC-MS/MS analysis of purified anti-HER2 affibody. a) Mass spectrum (XIC) of the mono-oxidated form of anti-HER2 affibody, with most of its ions from the charge state envelope (charges written above each ion, in blue). b) Zoom in on the XIC, evidencing all detected ions from the charge state envelope of the mono-oxidated anti-HER2 affibody (charges written above each ion, in blue).

6. Coupling and labelling of the BFC with anti-HER2 affibody

Conjugation of 3,9-PC2ABn^{pMA}-Cys-HER2-affibody (18)

To a solution of 2 mg affibody in 1 mL MQ water, 60 µL of Dithiothreitol (DTT) (1 M solution in MQ water prepared freshly) was added at room temperature under an argon atmosphere and the reaction mixture was incubated at 37 °C for 12 h. The mixture was then purified by preparative HPLC. Lyophilization of the pure fractions afforded the protein $Z_{HER2:2891}$-Cys.

2 mg of reduced $Z_{HER2:2891}$-Cys affibody redissolved in 1 mL of MQ water, 333 µL of 1 M ammonium acetate (pH = 5.5) and 60 µL solution of 3,9-PC2ABn^{pMA} (**17**) chelator (20 mg/mL in ACN) was added. The vial was filled with argon gas and incubated at 37 °C for 5 days. The progress of the coupling reaction was monitored by ESI-MS and upon reaching near complete conversion, the product was purified by preparative HPLC. Lyophilization of the pure fractions afforded the 3,9-PC2ABn^{pMA}-Cys-HER2-affibody (**18**) conjugate.

Preparative HPLC: UV-Vis detection: 220 and 280 nm; retention time: 6.00 min; gradient: 0.00→15.00 min 10→100% B; eluent: mixture of 0.1 TFA in MQ-water (A) and 0.1% TFA in acetonitrile (B); flow: 6.60 mL/min; column: Waters 300 Å, 5 µm XBridge Peptide BEH C18 OBD Prep (150 mm × 10.0 mm, 300 Å, 5 µm, Waters Inc., Milford, MA, USA).

UHRMS (ESI+) *m/z* calculated for $C_{346}H_{538}N_{94}O_{110}S_2$ $[M+9H]^{9+}$ 871.4388; found 871.4389; *m/z* calculated for $C_{346}H_{538}N_{94}O_{110}S_2$ [M] 7833.8836; found deconvoluted 7833.8836. **HPLC** purity (220 nm): 100%; retention time: 5.939 min; gradient: 0.00→15.00 min 10→100% B; eluent: mixture of 0.1% TFA in MQ-water (A) and 0.1% TFA in acetonitrile (B); flow: 1.00 mL / min; column: Waters 300 Å, 5 µm XBridge Peptide BEH C18 OBD Column (4.60 mm × 150 mm, Waters Inc., Milford, MA, USA), column ID: 01233824214601. **LCMS** (ESI+) *m/z* calculated for $C_{346}H_{538}N_{94}O_{110}S_2$ $[M+8H]^{8+}$ (100% Abundance) 980.7441; found 980.7512; *m/z* calculated for $C_{346}H_{538}N_{94}O_{110}S_2$ [M] 7837.8938; found deconvoluted 7838.7002.

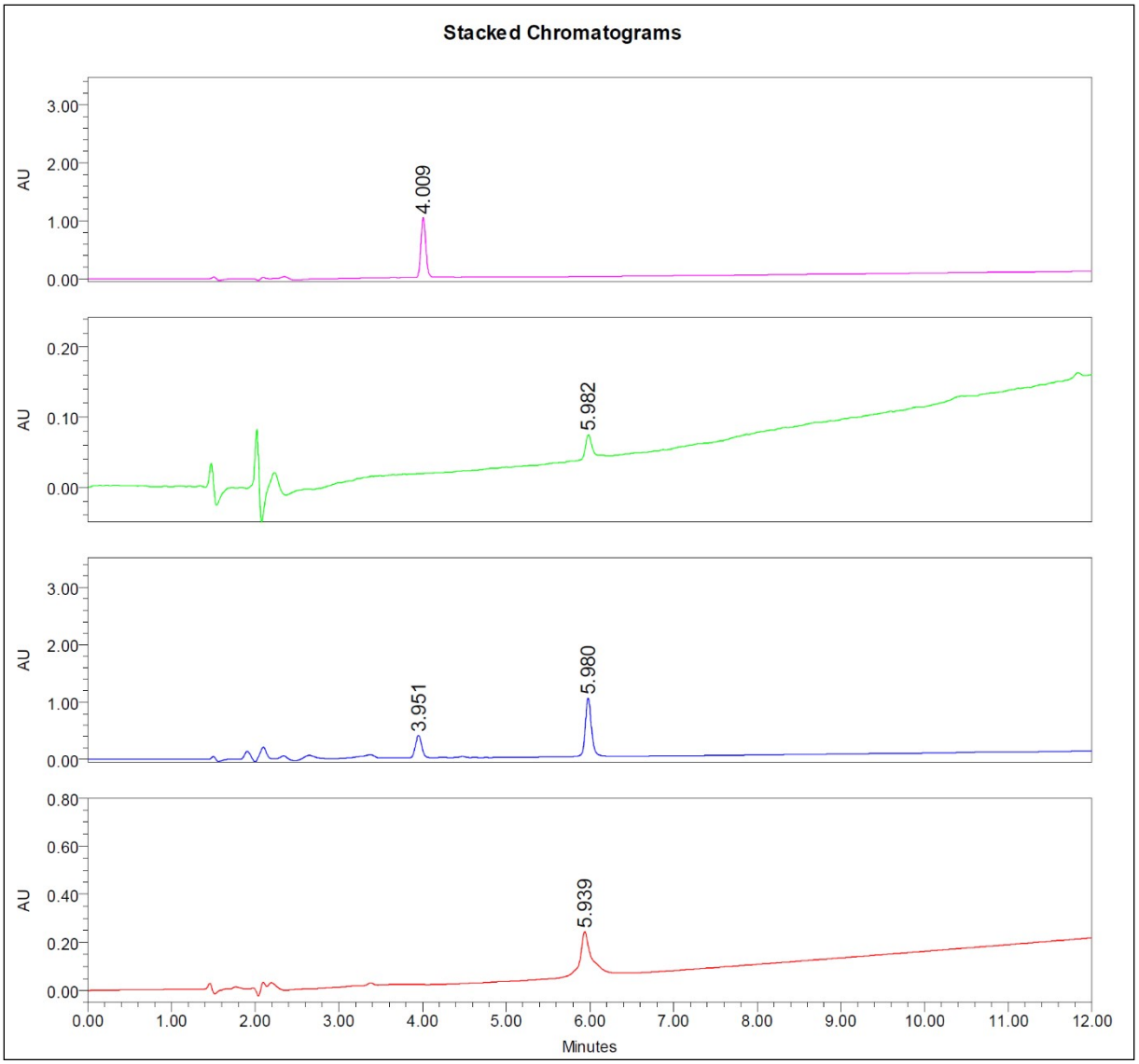

Figure S095. Stacked HPLC chromatograms of the UV-Vis (220 nm) trace of the 3,9-PC2ABn^{pMA} BFC (**17**) alone (pink), affibody alone (green), conjugation (blue) and the final 3,9-PC2ABn^{pMA}-Cys-HER2-affibody (**18**) bioconjugate alone (red).

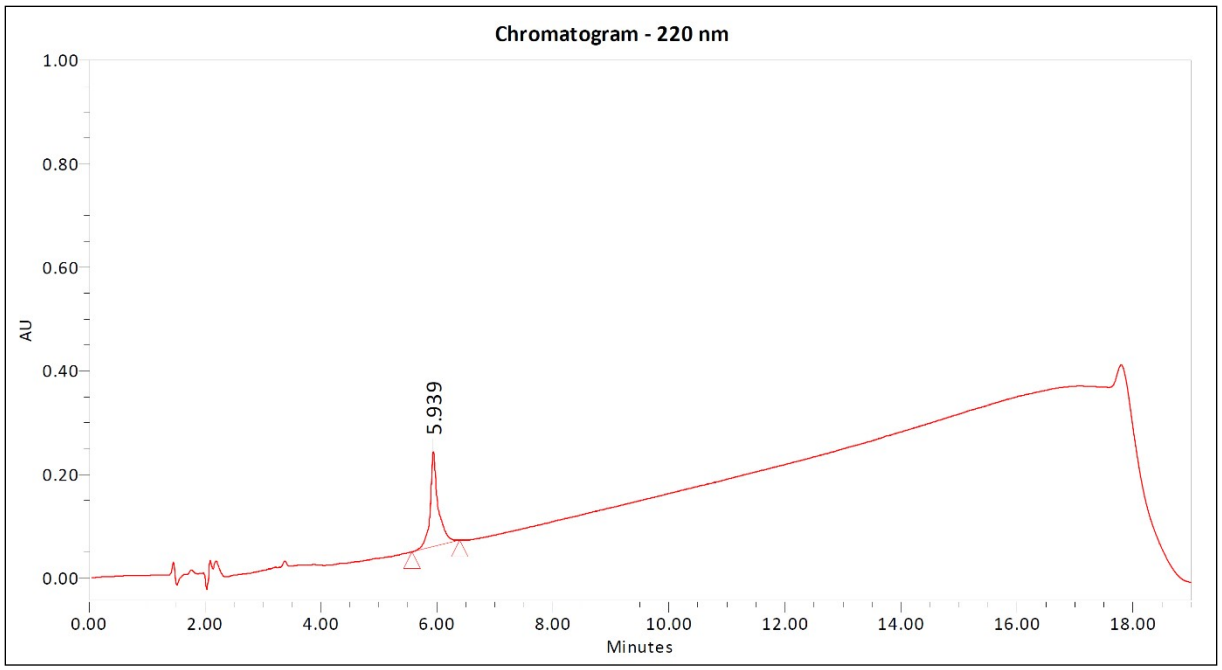

Figure S096. Analytical HPLC chromatogram (220 nm) of conjugate **18**.

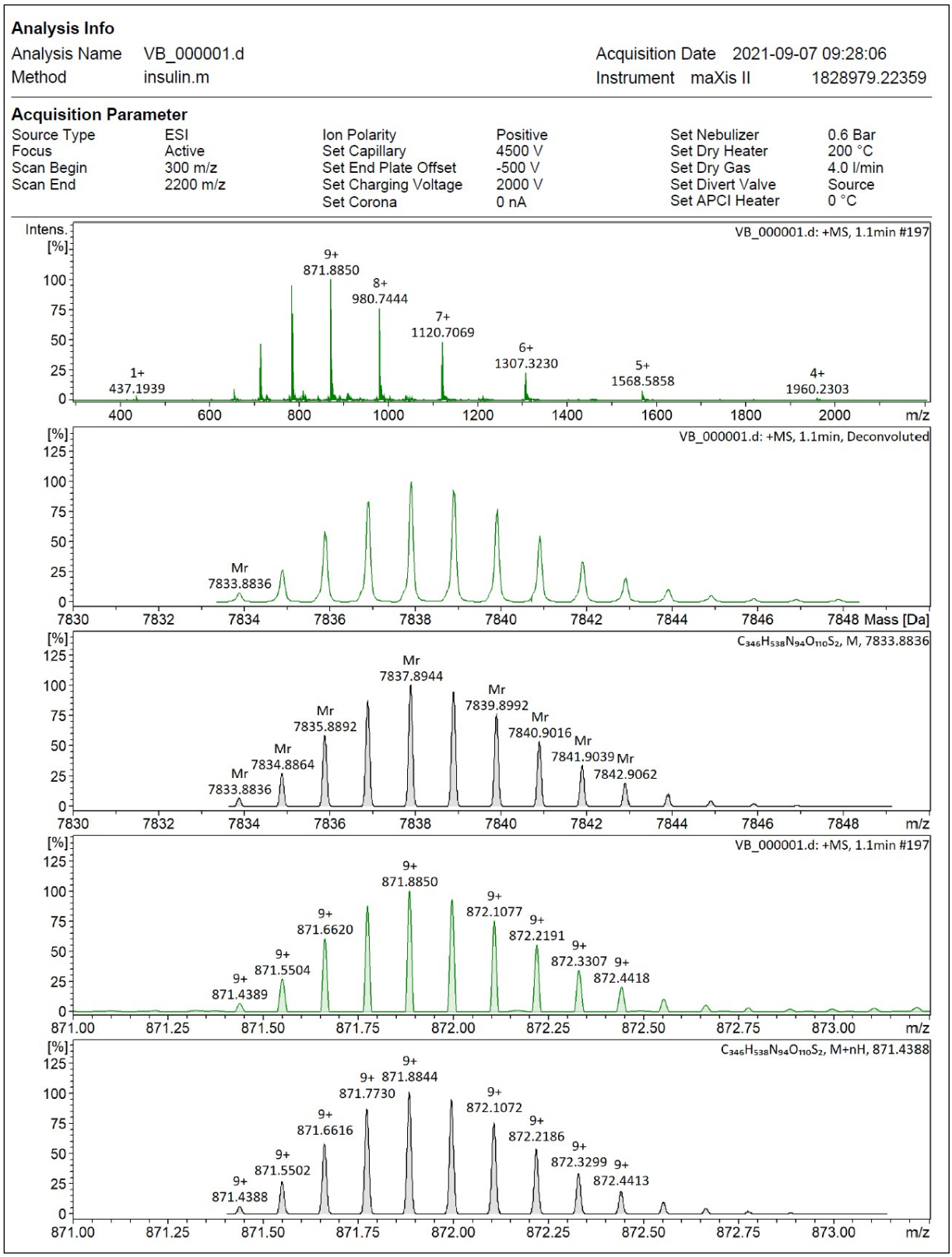

Figure S097. UHRMS spectra (ESI+) of conjugate **18**.

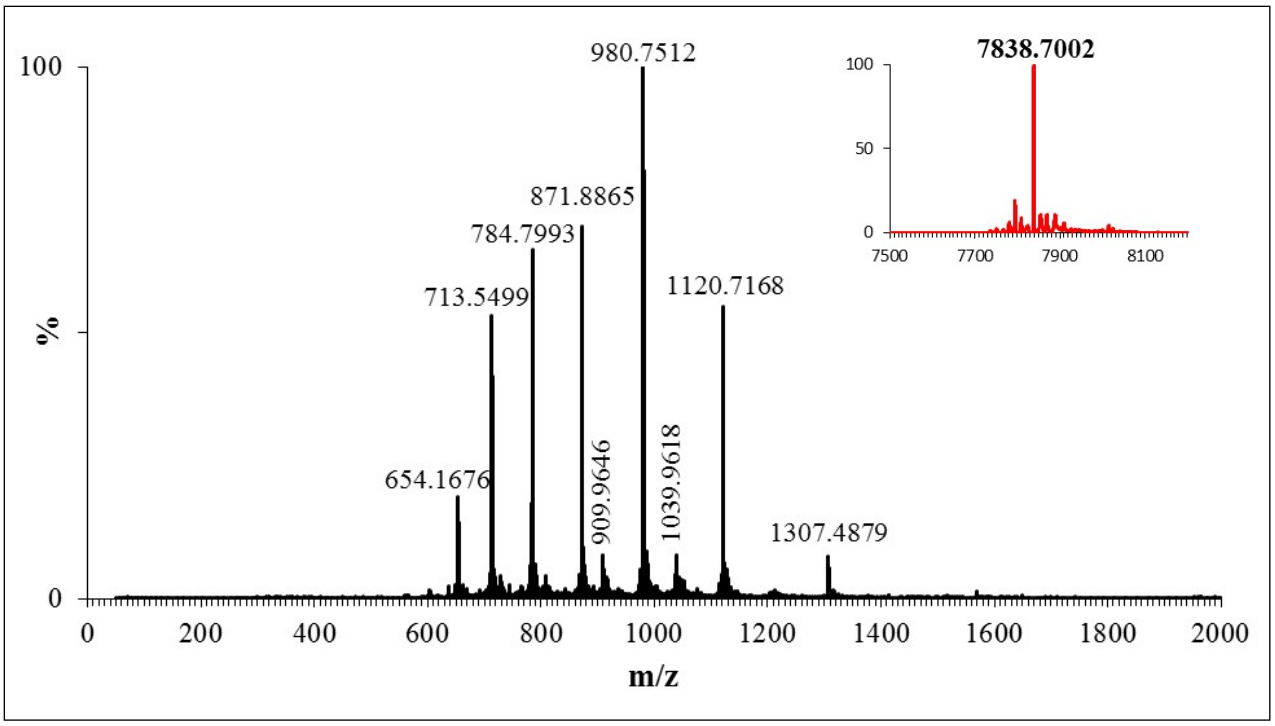

Figure S098. Measured (black) and deconvulated (red) LC-MS spectra of conjugate **18**.

Production of [[^{52}Mn]Mn(3,9-PC2ABn^{pMA})(H_2O)]-Cys-HER2-affibody (19)

For biodistribution studies HEPES (4.35 µmol, pH = 7.02) buffer and 3,9-PC2ABn^{pMA}-Cys-HER2-affibody (3.8-7.6 nmol) solution was added to [^{52}Mn]$MnCl_2$ (1.68 – 3.36 MBq). The radiolabelling experiments were performed at room temperature in closed 1.5 mL Eppendorf tubes for 15 min. The reaction mixture was diluted to the necessary volume with Saline and was used for PET examinations without further purification.

LCMS (ESI+) *m/z* calculated for $C_{346}H_{536}N_{94}O_{110}S_2Mn$ $[M+8H]^{8+}$ (100% Abundance) 987.3594; found 987.3646; **UV-Vis chromatogram** retention time: 3.73 min; **Radio-chromatogram** purity: 100%, retention time: 3.90 min; isocratic: 50% B; eluent: mixture of 0.1% HCOOH in MQ-water (A) and acetonitrile (B); flow: 0.60 mL / min; column: Waters 450 Å, 2.7 µm BioResolve™ RP mAb Polyphenyl Column (2.1 mm × 100 mmn Waters Inc., Milford, MA, USA, part No: 186008945).

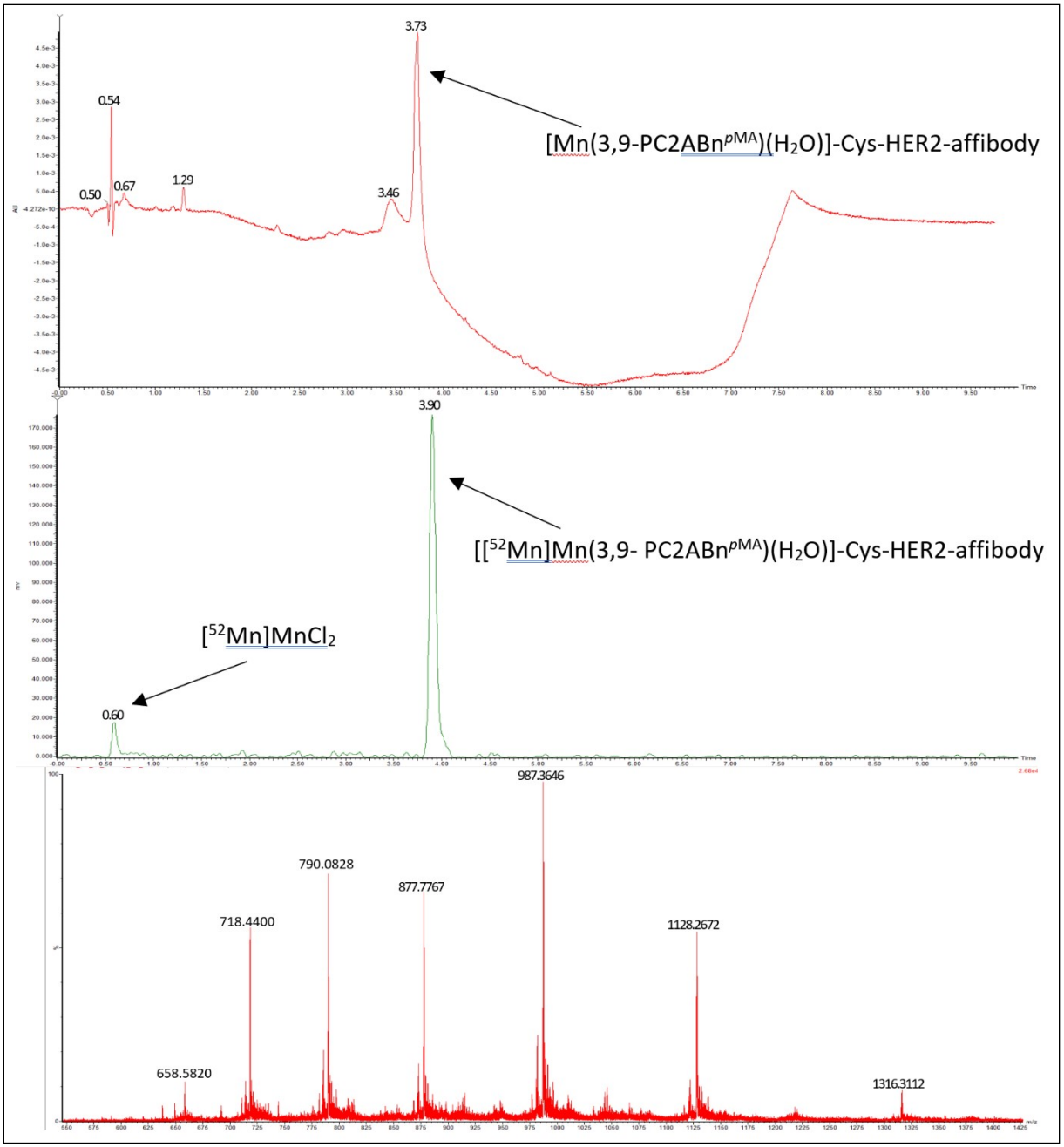

Figure S099. LC-MS identification of [[^{52}Mn]Mn(3,9-PC2ABn^{pMA})(H_2O)]-Cys-HER2-affibody **19** for labelling: *(upper) UV-Vis chromatogram (254 nm), (middle) radio-chromatogram, (lower) MS spectra (ESI+) of the 3.73 minute peak.*

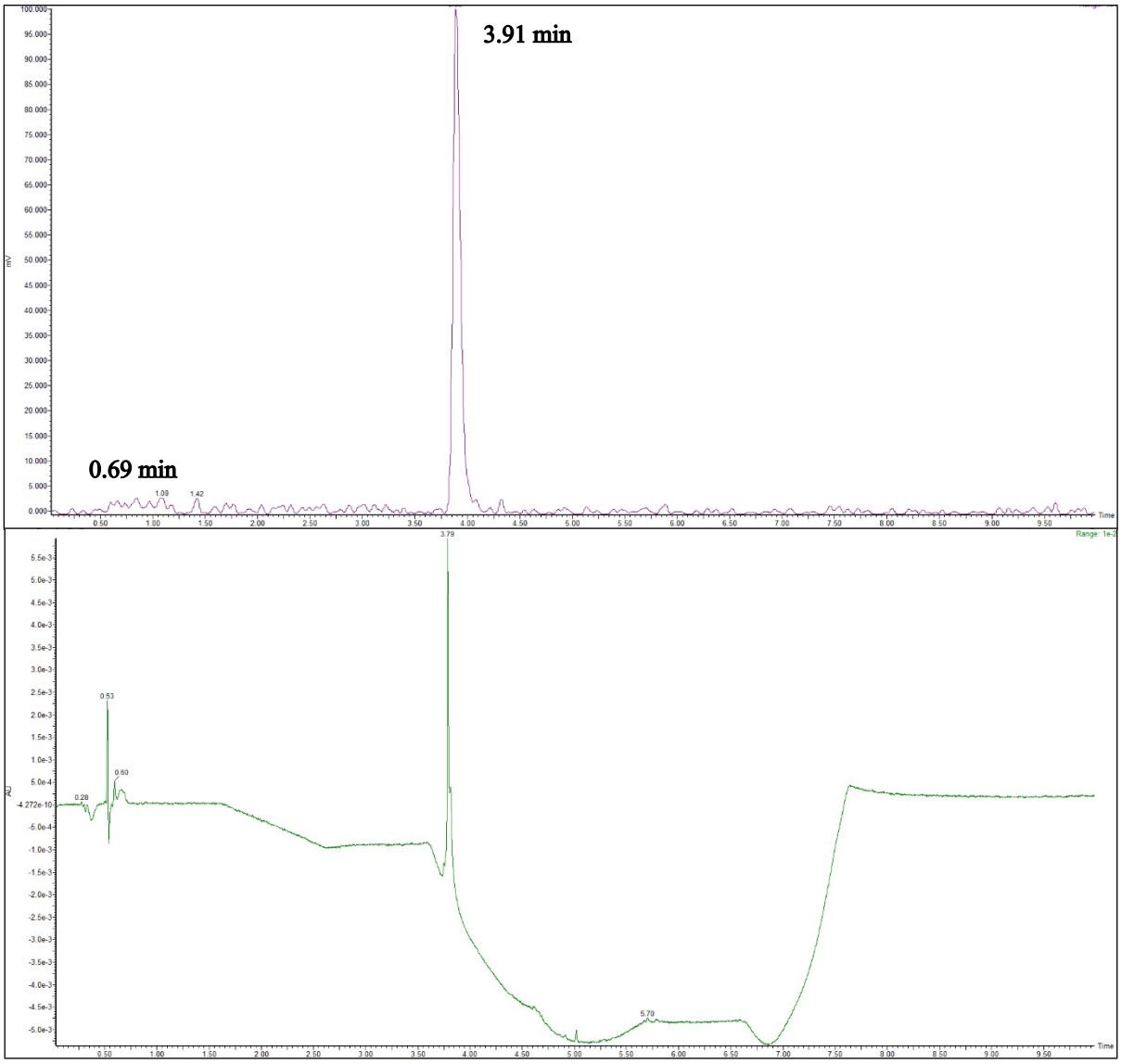

Figure S100. LC analysis of [[^{52}Mn]Mn(3,9-PC2ABn^{pMA})(H_2O)]-Cys-HER2-affibody **19**:
(upper) radio-chromatogram, (lower) UV chromatogram (274 nm).

7. HER2+ cells labelling with affibody-AlexaFluor 555 conjugate

Conjugation of AlexaFluor 555 to Anti-HER2-Affibody (23)

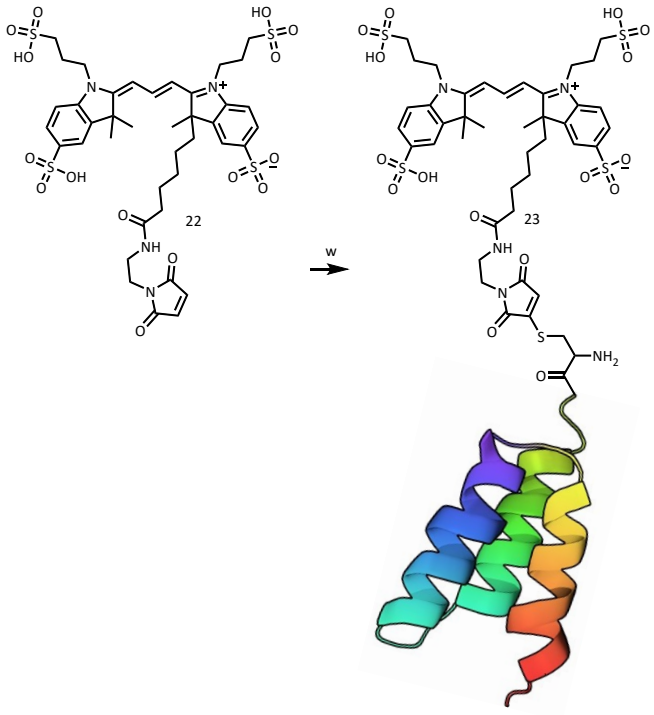

Scheme S002. Conjugation of the Alexa Fluor™ 555 C2 Maleimide[19] **22** to the affibody: (w) $Z_{HER2:2891}$-Cys affibody in 0.20 M ammonium-acetate (pH = 5.5), 37 °C, Ar-atm, 5 days.

To a solution of 2 mg affibody in 1 mL MQ water, 60 µL of Dithiothreitol (DTT) (1 M solution in MQ water prepared freshly) was added at room temperature under an argon atmosphere and the reaction mixture was incubated at 37 °C for 12 h. The mixture was then purified by preparative HPLC. Lyophilization of the pure fractions afforded the protein $Z_{HER2:2891}$-Cys.

200 µg of reduced $Z_{HER2:2891}$-Cys affibody redissolved in 200 µL of 200 mM ammonium acetate (pH = 5.5 in MQ water) and 8 µL (1 mg / 80 µL in high-quality anhydrous dimethyl sulfoxide) Alexa Fluor™ 555 C2 Maleimide dye (**22**) (Thermo Fisher Scientific Catalog number: A20346) was added. The vial was filled with argon gas and incubated at 37 °C for 5 days. The progress of the coupling reaction was monitored by HPLC and upon reaching approximately 70% conversion, the product was purified by preparative HPLC. Lyophilization of the pure fractions afforded the Alexa Fluor™-555-$C2^{MA}$-Cys-HER2-affibody (**23**) conjugate.

Preparative HPLC: UV-Vis detection: 220 and 555 nm; retention time: 16.20 min; gradient: 0.00→20.00 min 6→36% B; eluent: mixture of 0.1 TFA in MQ-water (A) and 0.1% TFA in acetonitrile (B); flow: 6.60 mL/min; column: Waters 300 Å, 5 µm XBridge Peptide BEH C18 OBD Prep (150 mm × 10.0 mm, 300 Å, 5 µm, Waters Inc., Milford, MA, USA).

UHRMS (ESI+) *m/z* calculated for $C_{357}H_{554}N_{92}O_{118}S_6$ $[M+6H]^{6+}$ 1369.3156; found 1369.3126; *m/z* calculated for $C_{357}H_{554}N_{92}O_{118}S_6$ [M] 8209.8497; found deconvoluted 8209.8370. **HPLC** purity (220 nm): 100%; retention time: 16.172 min; gradient: 0.00→20.00 min 6→36% B; eluent: mixture of 0.1% TFA in MQ-water (A) and 0.1% TFA in acetonitrile (B); flow:

1.00 mL / min; column: Waters 300 Å, 5 µm XBridge Peptide BEH C18 OBD Column (4.60 mm × 150 mm, Waters Inc., Milford, MA, USA), column ID: 01233824214601.

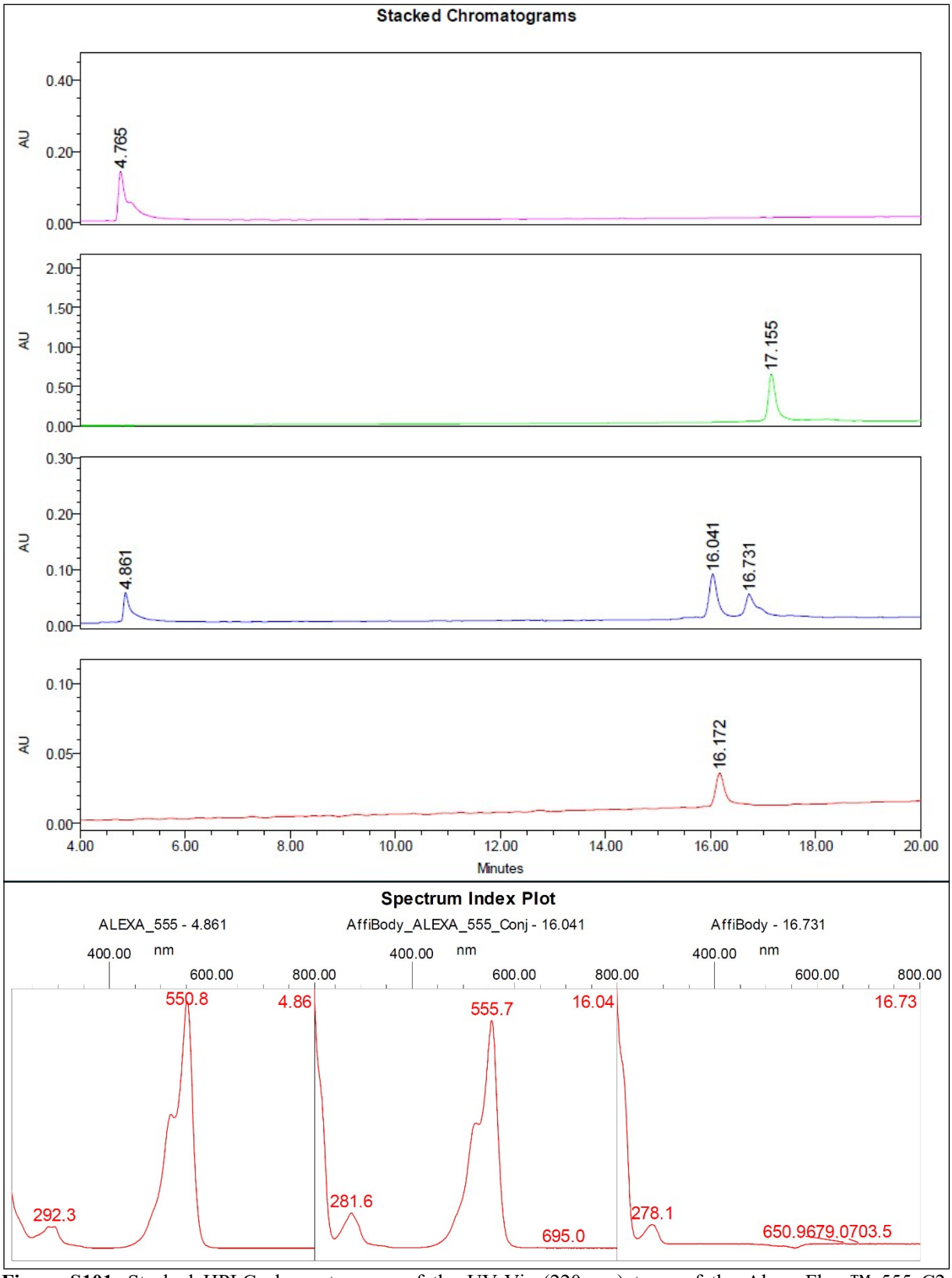

Figure S101. Stacked HPLC chromatograms of the UV-Vis (220 nm) trace of the Alexa Fluor™ 555 C2 Maleimide alone (**22**) (pink), affibody alone (green), conjugation (blue) and the final affibody-Alexa Fluor 555 conjugate (**23**) alone (red). UV-Vis spectra (200-800 nm) of the peaks (4.861 min: Alexa Fluor™ 555 C2 Maleimide (**22**); 16.041 min: affibody-Alexa Fluor 555 conjugate (23); 16.731 min: affibody) from the chromatogram of the conjugation (blue).

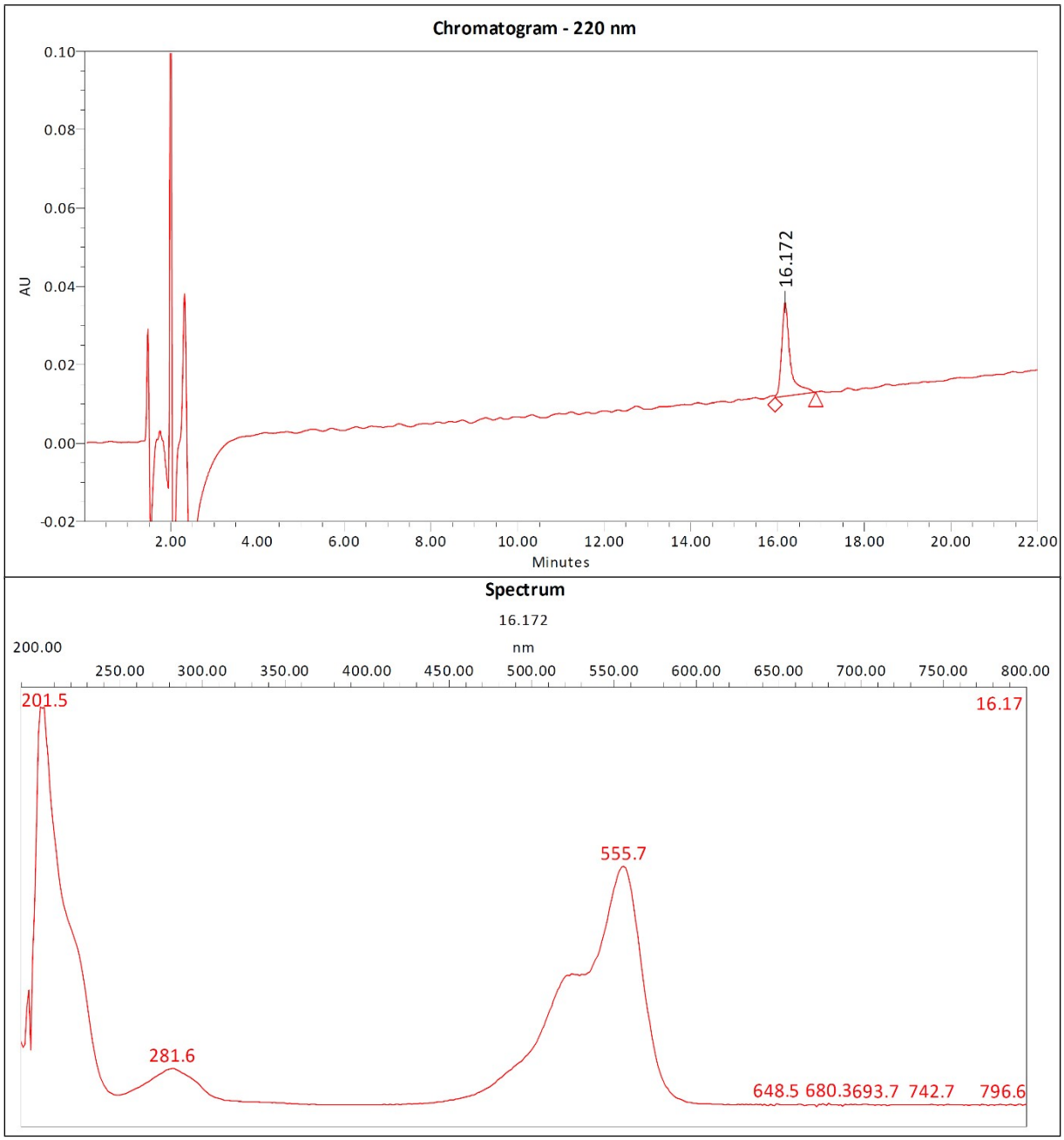

Figure S102. Analytical HPLC chromatogram (220 nm) of conjugate **23**. And UV-Vis spectra (200-800 nm) of affibody-Alexa Fluor 555 conjugate (**23**) (16.172 min).

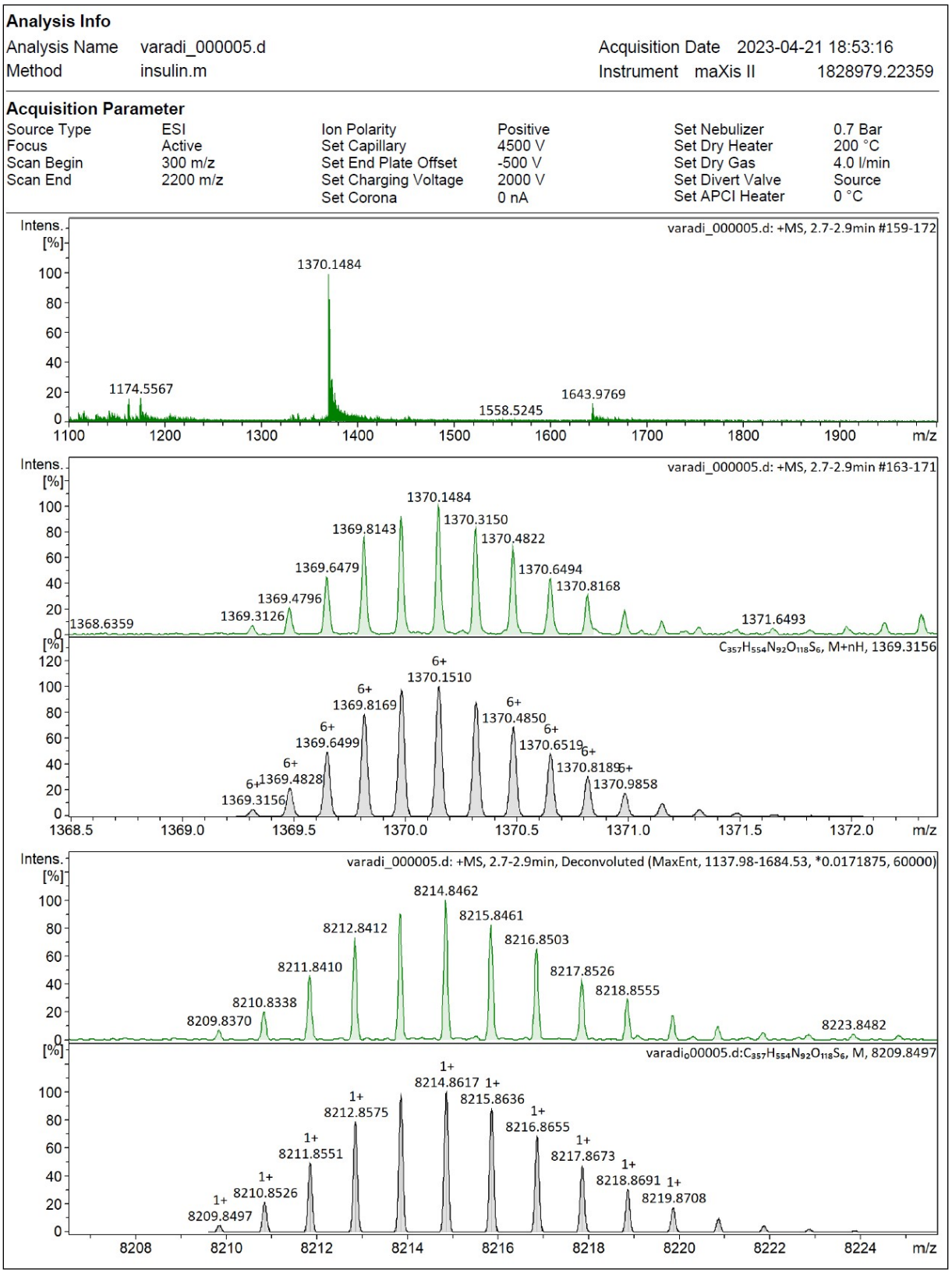

Figure S103. UHRMS spectra (ESI+) of conjugate **23**.

Cell lines

The human ovarian cancer SKOV3 cell line (kindly provided by Dr. Ioana Berindan-Neagoe from the Research Center for Functional Genomics, Biomedicine and Translational Medicine UMF Cluj, Romania) was cultured in RPMI1640 medium supplemented with 10% FBS and non-essential amino acids. The human breast cancer (luminal A subtype) MCF-7 cell line, and the human embryonic kidney HEK293T cell line, were cultured in Dulbecco's modified Eagle's medium (DMEM) with 10% FBS and non-essential amino acids. RPMI medium, FBS and non-essential amino acids were purchased from Gibco while DMEM was purchased from PAN Biotech.

Flow cytometry analysis

Binding specificity of AlexaFluor 555-labelled anti-HER2 affibody was tested on HER2-positive SKOV3 cells. MCF-7 was used as HER2-low/negative control cell line, while HEK293T cells, which don't express HER2 on their cell surface, were used as negative control cell lines.[20] Cells were first detached from the dishes with StemPro Accutase (Gibco), resuspended in FACS buffer (PBS with 2% FBS) and counted with a hemocytometer counting chamber. Then, 1×10^6 or 0.5×10^6 cells of each cell line were washed with FACS buffer and incubated with either 400 nM of unlabelled affibody (named hereafter affiblocked) or with FACS buffer (named hereafter non-blocked) for 15 min in a water bath at 37 ºC. The unbound affibody was removed by washing the cells once with FACS buffer. Then, both the affiblocked and non-blocked cells were split into 100000 cells *per* tube and further incubated with different concentrations of AlexaFluor 555-labelled affibody for 1h on ice. Nine different serial dilutions of labelled affibody (0.04 nM, 0.08 nM, 0.16 nM, 0.32 nM, 0.64 nM, 1.25 nM, 2.5 nM, 5 nM, and 10 nM) were initially tested to set the optimal working range of concentrations for a good binding response signal. Only four of the dilutions (0.08 nM, 0.16 nM, 2.5 nM and 10 nM) were used in the subsequent experiments. For each cell line studied, a negative control consisting in cells untreated with labelled affibody was prepared. After incubation, the cells were washed with FACS buffer to remove the excess of unbound labelled affibody, resuspended in 100 µl FACS buffer and the mean fluorescence intensity was measured using a FACSAria III instrument (BD Biosciences) equipped with a 561 nm laser. The obtained flow cytometry data was analysed using Community Cytobank platform (https://community.cytobank.org, Beckman Coulter). The experiments were performed in triplicate for SKOV3 and HEK293T cells, and in dublicate for MCF-7 cells.

8. Small-Animal PET/MRI imaging with [^{52}Mn]Mn-labelled Anti-HER2-affibody

Materials and methods

The animal study was authorized by the Ethical Committee for Animal Research, University of Debrecen, Hungary (permission number: 16/2020/DEMÁB). Laboratory animals were kept and treated in compliance with all applicable sections of the Hungarian Laws and animal welfare directions and regulations of the European Union.

Cell line and animal models

For tumour induction 4T1 (triple negative mouse breast cancer) and MDA-MB (HER2+, HER2 overexpressed human breast cancer) cell lines were used. All cell lines were kindly gifted by the University of Debrecen. 14 weeks old female CB17 SCID mice ((n = 3); Animalab Ltd, Budapest, Hungary) were used in this study. Mice received sterile food and water ad libitum and housed under sterile conditions using IVC (individually ventilated cages). 1 mouse was injected with MDA-MB (HER2+) cell line, and 2 mice were injected with 4T1 cell line. The sample mice weighted 23-24 g; both groups received 2 injections of the respective cell line. The first injection was done subcutaneously at the shoulder area, the second injection was performed intramammarily at the orthotopic site, inguinal breast fat pad. Each injection contained $5x10^6$ cells in 100 µL saline solution. 9 – 22 days after tumour cell inoculation, when the xenograft had reached 6 – 7 mm in maximum diameter, the mice were injected with 2.7 ± 0.69 MBq of the radiopharmaceutical intravenously via the lateral tail vein.

PET imaging and in vivo measurements

PET/MRI scans were performed using a preclinical nanoScan PET/MRI 1T (Mediso LTD., Hungary). Inhalational anaesthesia using isoflurane 3% for induction and 2% for maintenance, combined with Oxygen (1.0-2.0 L/min) and N_2O (0.8-1.0 L/min) was used. Throughout the scanning process mice were put on special scanning bed (MultiCell Imaging Chamber, Mediso LTD., Hungary) to maintain the body temperature and to prevent movement of mice. For both groups PET scans were performed 4 h, 1 day and 3 days post injection, and the 4T1 bearing mouse received an additional 2-day post injection scan.

The PET acquisitions were 20 min static using 98.5 mm FOV, energy window was set to 400-600 keV. For anatomical references, the mice were scanned by MRI T1 gradient echo with 0.5 mm slice thickness, 50 slices, 20° flip angle. After the scans, MLEM reconstruction was completed by Nuclide software (Mediso LTD, Hungary) with attenuation correction, random correction, and scatter correction. From the reconstructed images, using InterView FUSION software (Mediso, Hungary), ROIs and VOIs were drawn with diameter of 3 mm over tumours and major organs which were blood pool, liver, kidney, and muscle as background reference. The uptakes of tumours and organs were measured in the unit of standardized uptake value (SUV).

MDA-MB HER2+

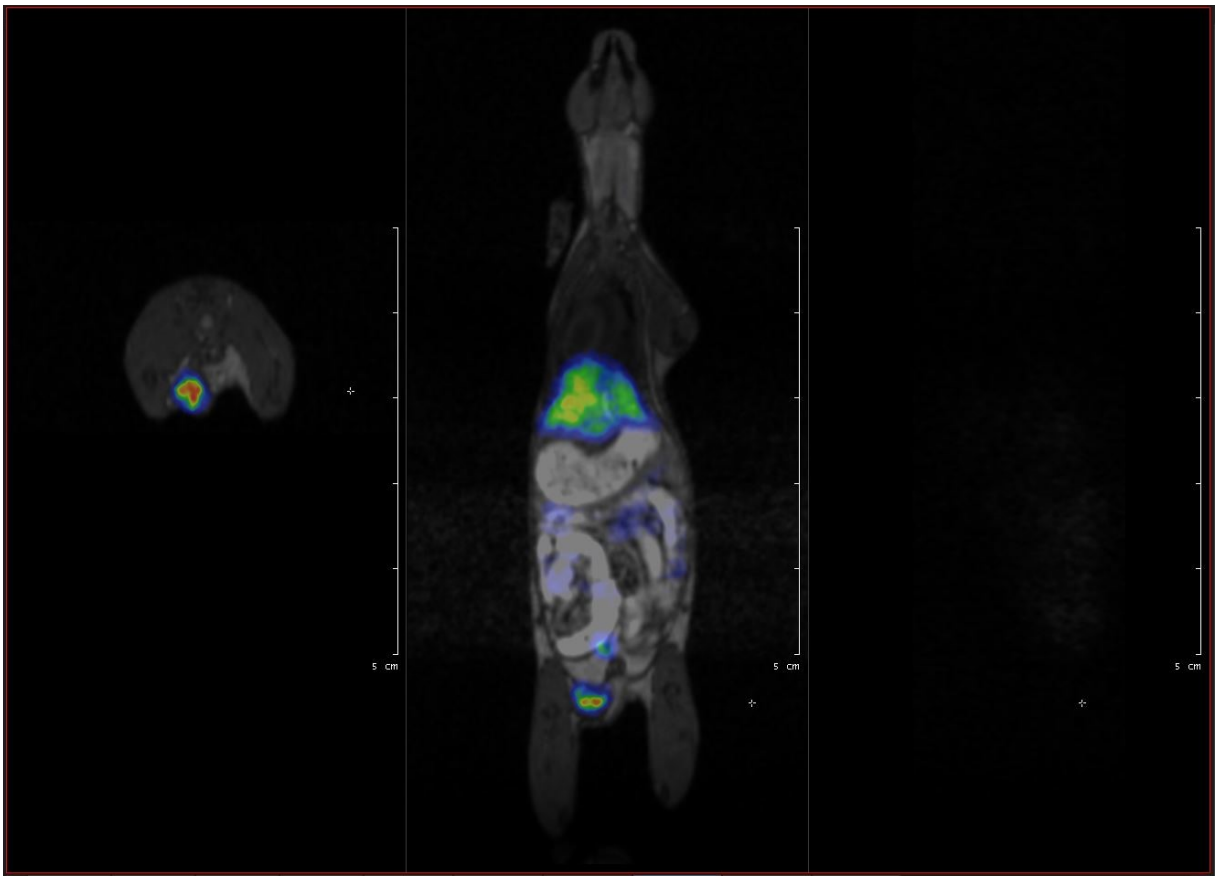

Figure S104. NanoPET/MR imaging of MDA-MB (HER2+) tumour-bearing SCID mouse (7FBJ). Representative decay-corrected coronal PET images showing slices without kidney (w/o k) (area of the breast fat pad (orthotopic)) and transaxial PET images at 4 hours after the intravenous injection of [[^{52}Mn]Mn(3,9-PC2ABn^{pMA})(H_2O)]-Cys-HER2-affibody.

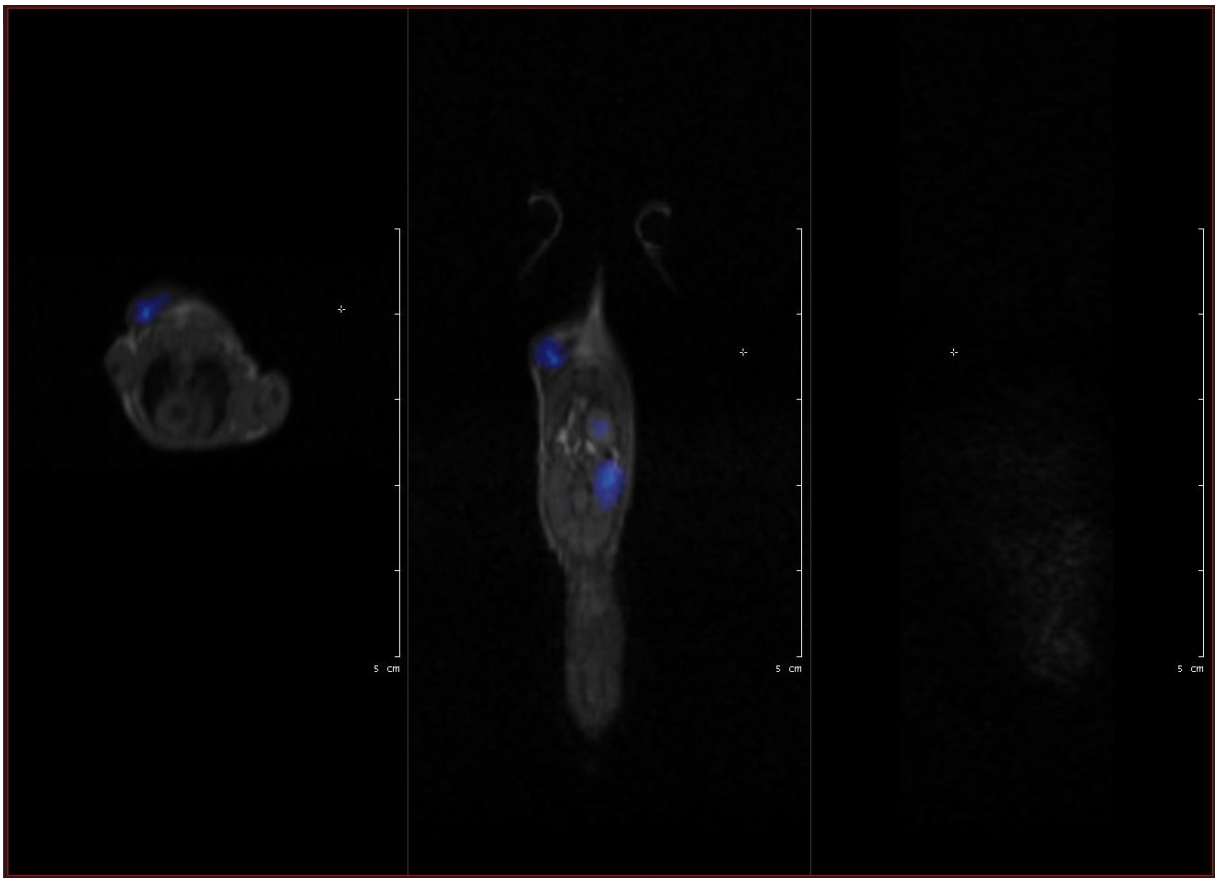

Figure S105. NanoPET/MR imaging of MDA-MB (HER2+) tumour-bearing SCID mouse (7FBJ). Representative decay-corrected coronal PET images showing slices without kidney (w/o k) (area of the shoulder (heterotopic)) and transaxial PET images at 4 hours after the intravenous injection of [[^{52}Mn]Mn(3,9-PC2ABn$^{p\text{MA}}$)(H_2O)]-Cys-HER2-affibody.

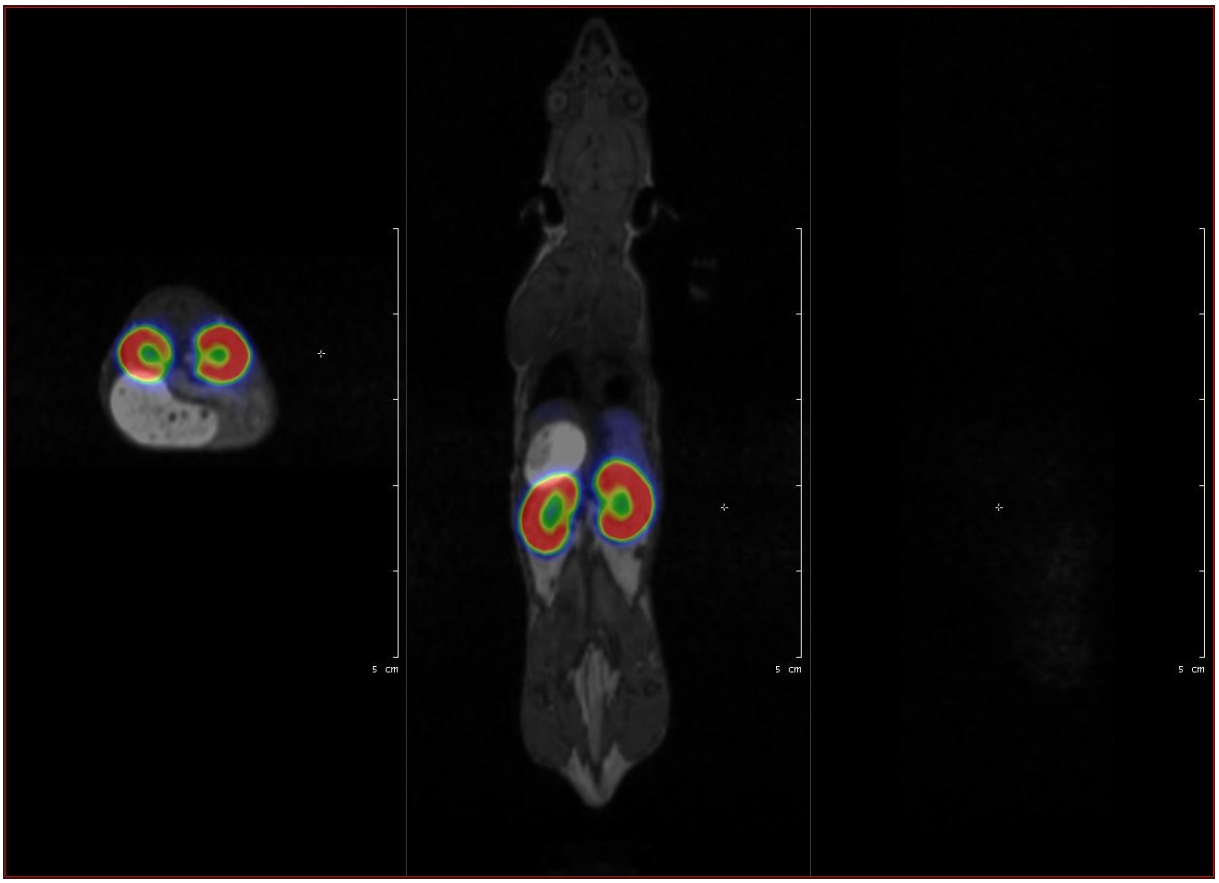

Figure S106. NanoPET/MR imaging of MDA-MB (HER2+) tumour-bearing SCID mouse (7FBJ). Representative decay-corrected coronal PET images showing slices with kidney (k) and transaxial PET images at 4 hours after the intravenous injection of [[^{52}Mn]Mn(3,9-PC2ABn^{pMA})(H_2O)]-Cys-HER2-affibody.

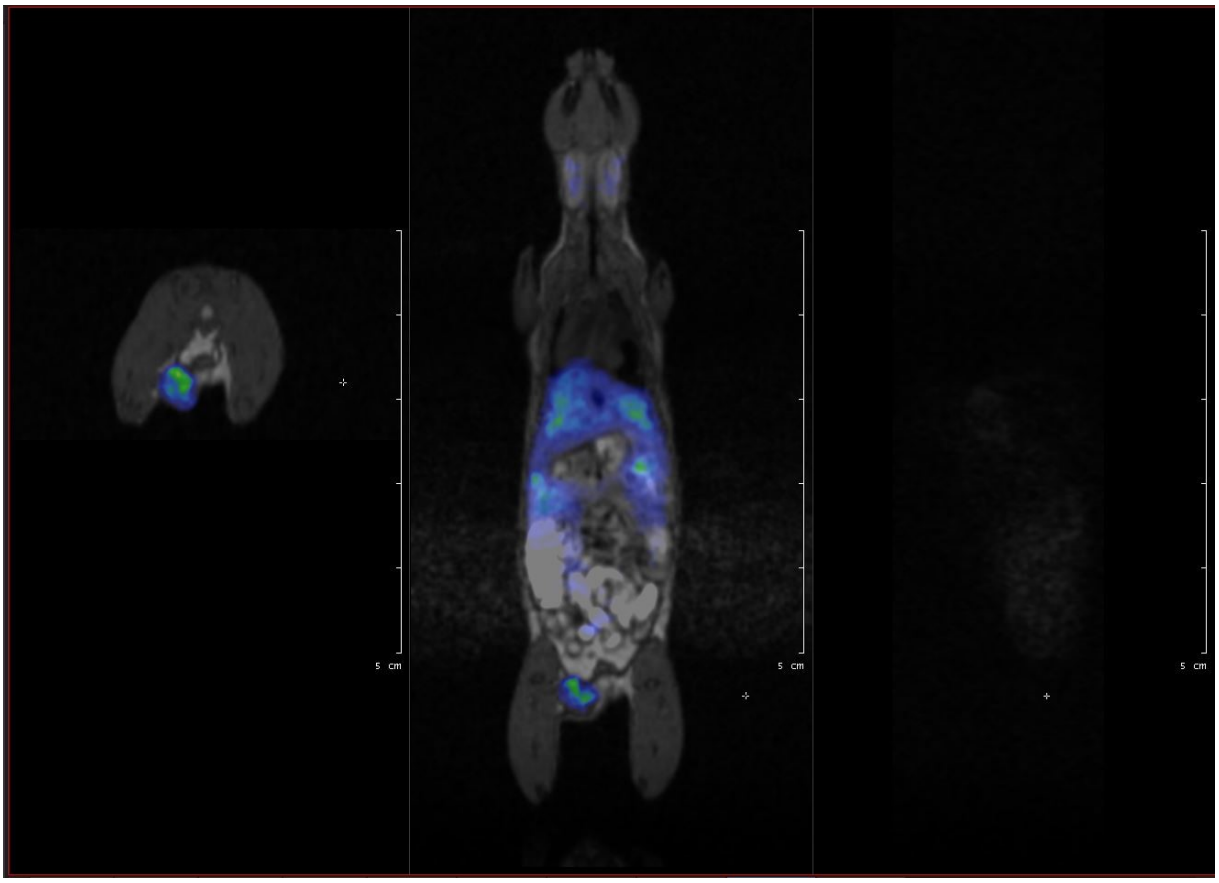

Figure S107. NanoPET/MR imaging of MDA-MB (HER2+) tumour-bearing SCID mouse (7FBJ). Representative decay-corrected coronal PET images showing slices without kidney (w/o k) (area of the breast fat pad (orthotopic)) and transaxial PET images at 24 hours after the intravenous injection of [[^{52}Mn]Mn(3,9-PC2ABn$^{p\text{MA}}$)(H_2O)]-Cys-HER2-affibody.

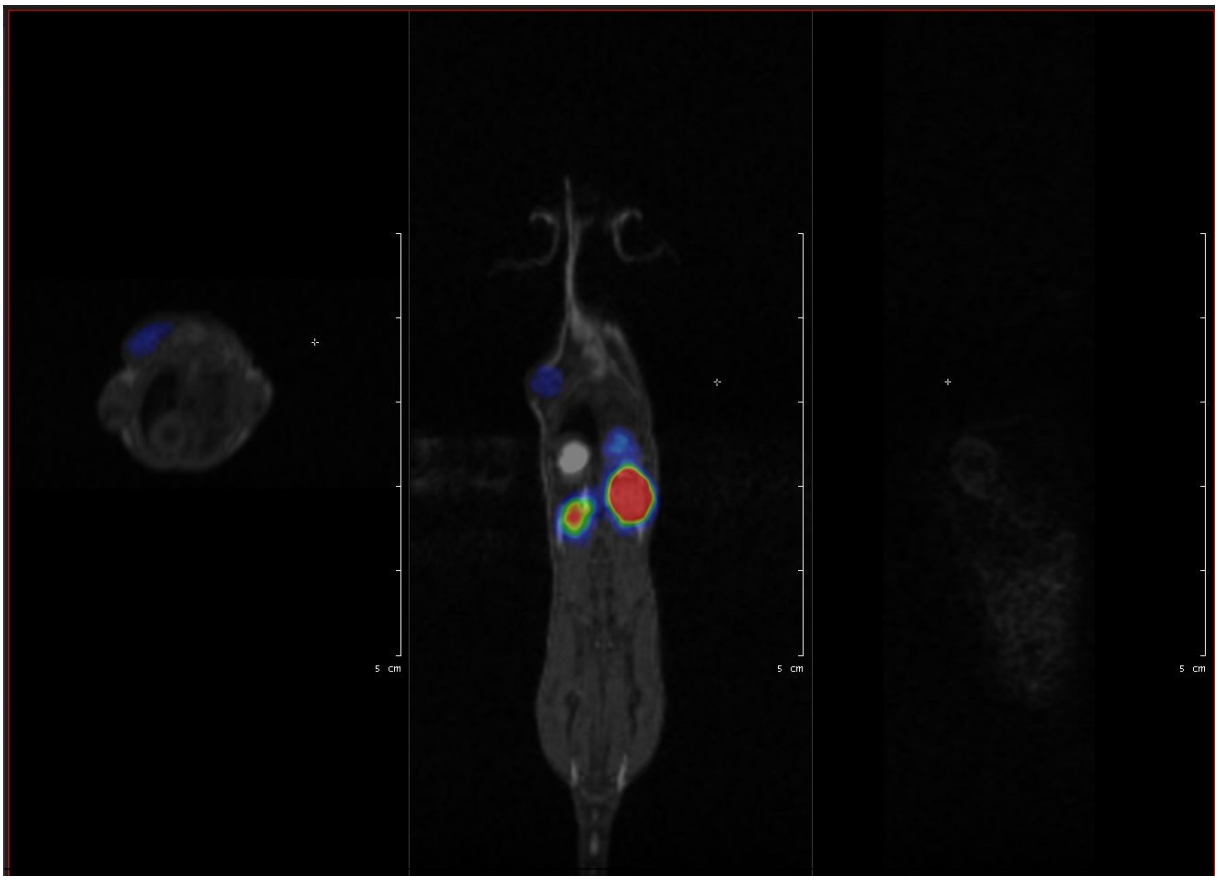

Figure S108. NanoPET/MR imaging of MDA-MB (HER2+) tumour-bearing SCID mouse (7FBJ). Representative decay-corrected coronal PET images showing slices without kidney (w/o k) (area of the shoulder (heterotopic)) and transaxial PET images at 24 hours after the intravenous injection of [[^{52}Mn]Mn(3,9-PC2ABn^{pMA})(H_2O)]-Cys-HER2-affibody.

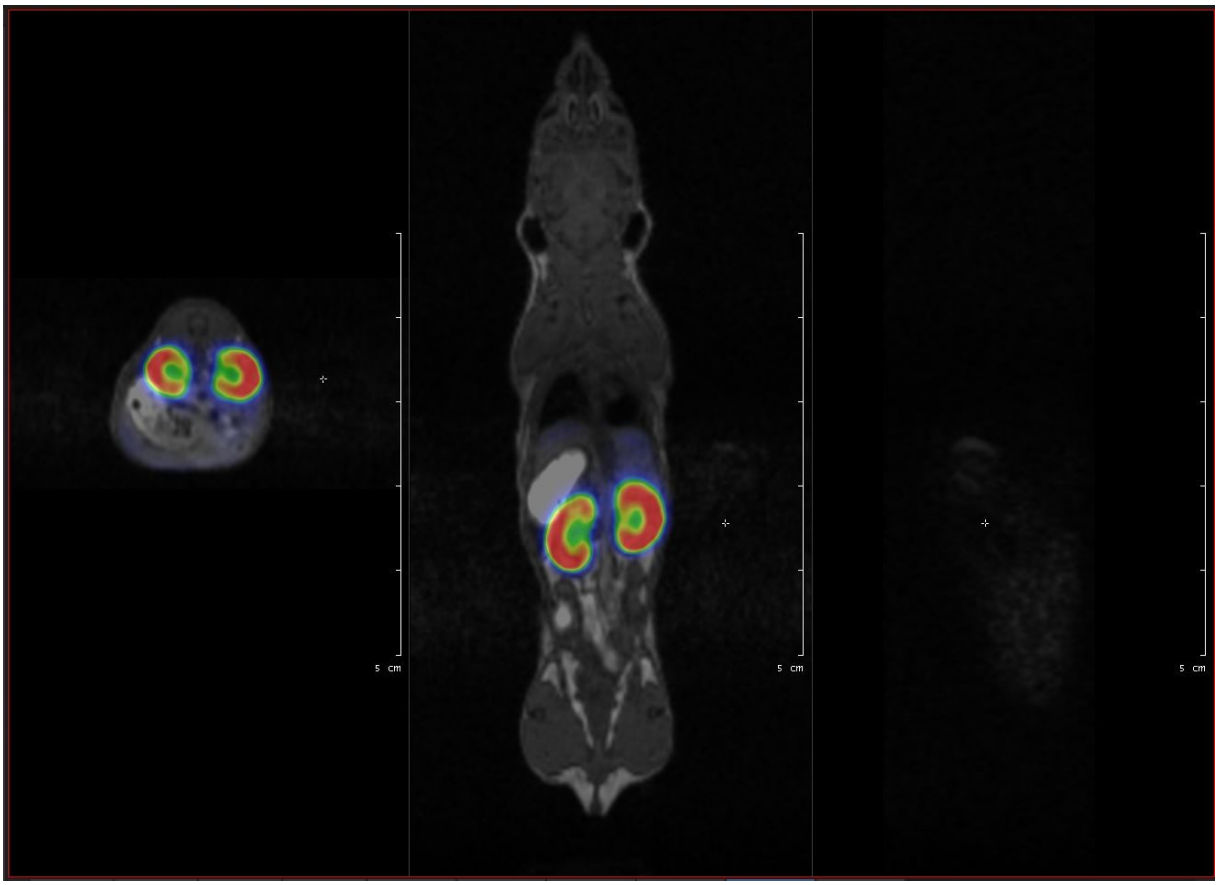

Figure S109. NanoPET/MR imaging of MDA-MB (HER2+) tumour-bearing SCID mouse (7FBJ). Representative decay-corrected coronal PET images showing slices with kidney (k) and transaxial PET images at 24 hours after the intravenous injection of [[^{52}Mn]Mn(3,9-PC2ABn^{pMA})(H_2O)]-Cys-HER2-affibody.

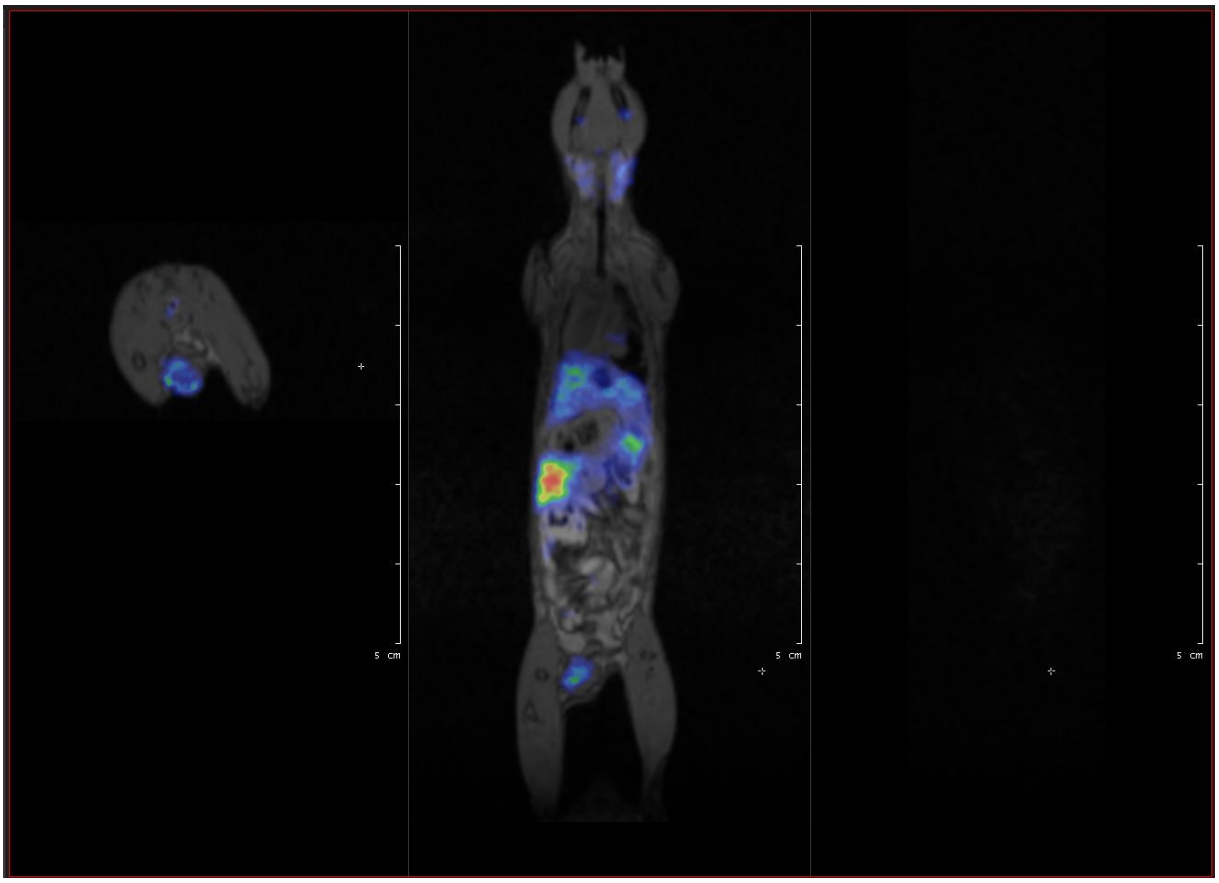

Figure S110. NanoPET/MR imaging of MDA-MB (HER2+) tumour-bearing SCID mouse (7FBJ). Representative decay-corrected coronal PET images showing slices without kidney (w/o k) (area of the breast fat pad (orthotopic)) and transaxial PET images at 72 hours after the intravenous injection of [[^{52}Mn]Mn(3,9-PC2ABn$^{p\text{MA}}$)(H_2O)]-Cys-HER2-affibody.

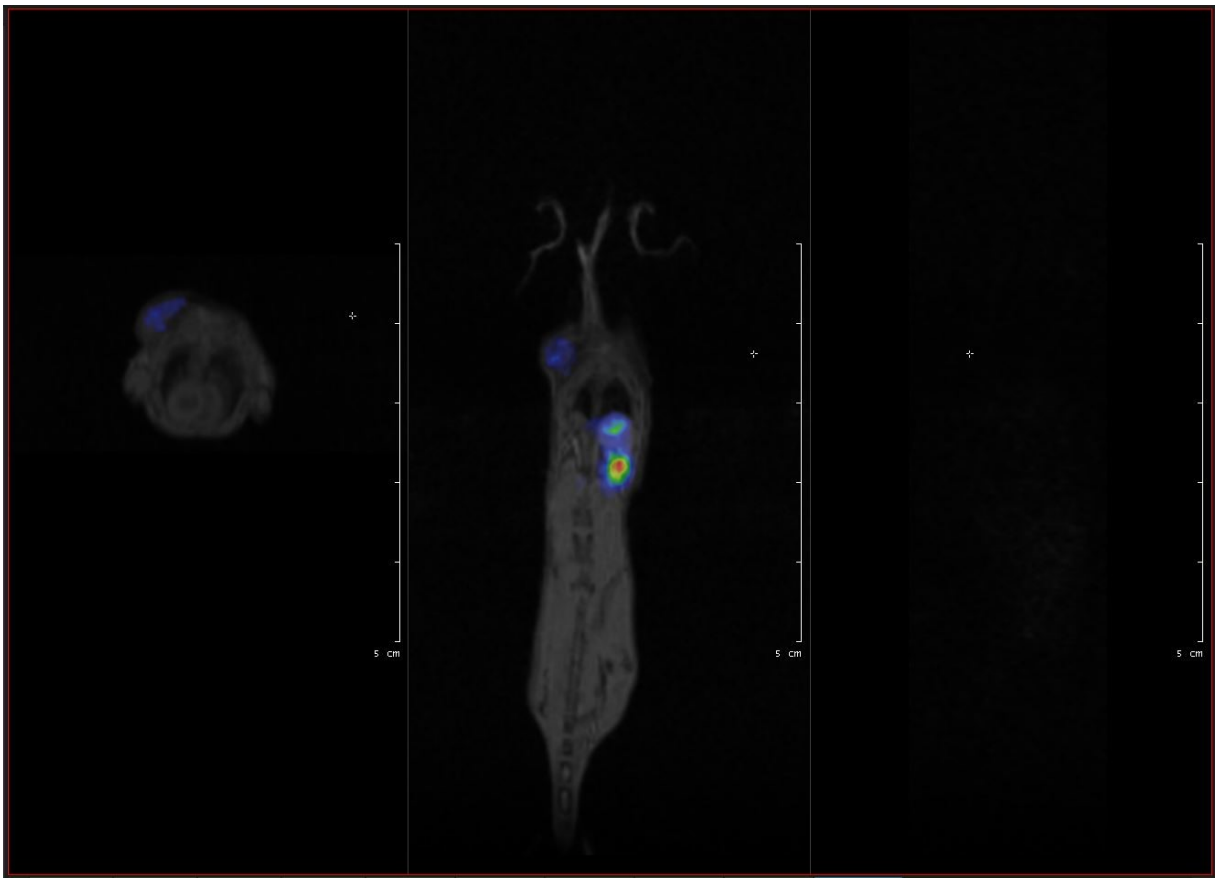

Figure S111. NanoPET/MR imaging of MDA-MB (HER2+) tumour-bearing SCID mouse (7FBJ). Representative decay-corrected coronal PET images showing slices without kidney (w/o k) (area of the shoulder (heterotopic)) and transaxial PET images at 72 hours after the intravenous injection of [[^{52}Mn]Mn(3,9-PC2ABn$^{p\text{MA}}$)(H_2O)]-Cys-HER2-affibody.

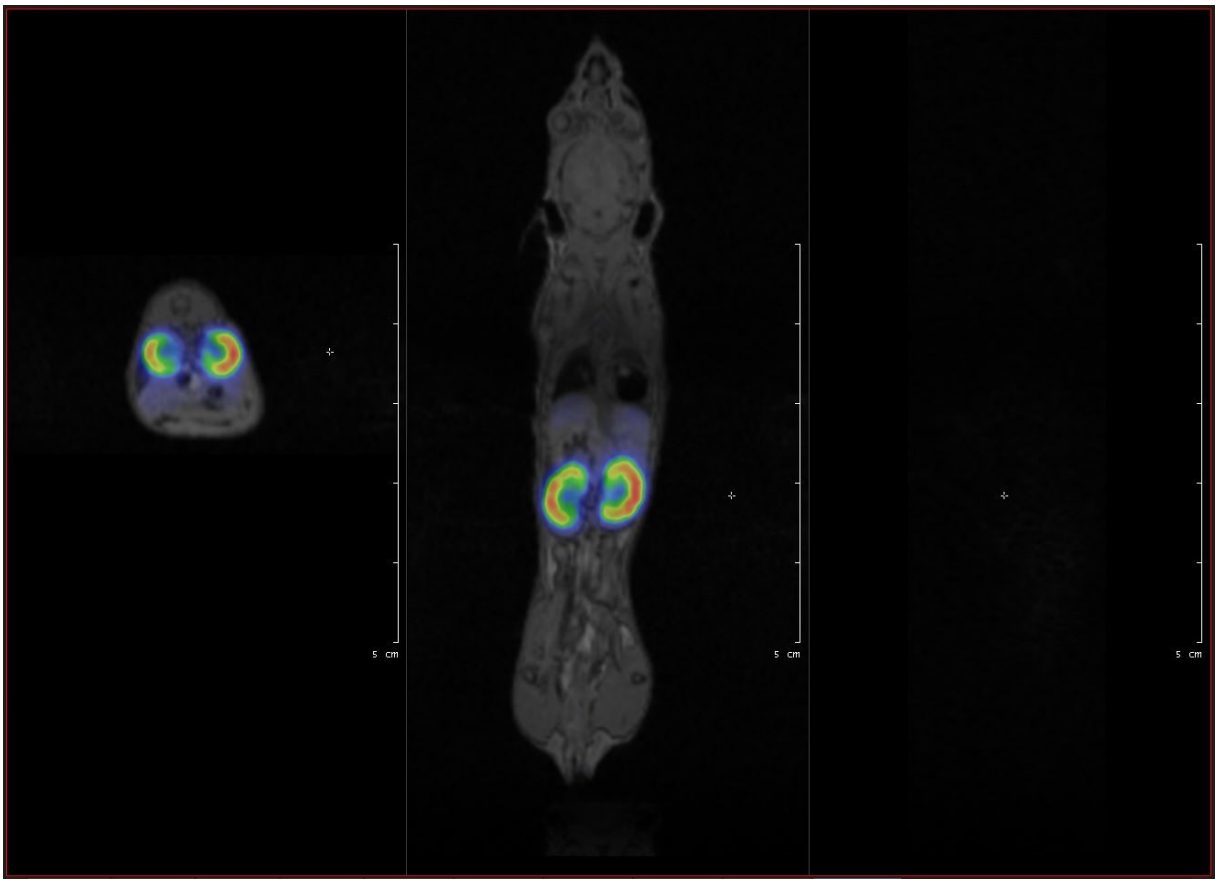

Figure S112. NanoPET/MR imaging of MDA-MB (HER2+) tumour-bearing SCID mouse (7FBJ). Representative decay-corrected coronal PET images showing slices with kidney (k) and transaxial PET images at 72 hours after the intravenous injection of [[^{52}Mn]Mn(3,9-PC2ABn^{pMA})(H_2O)]-Cys-HER2-affibody.

4T1 HER2- (1. mouse)

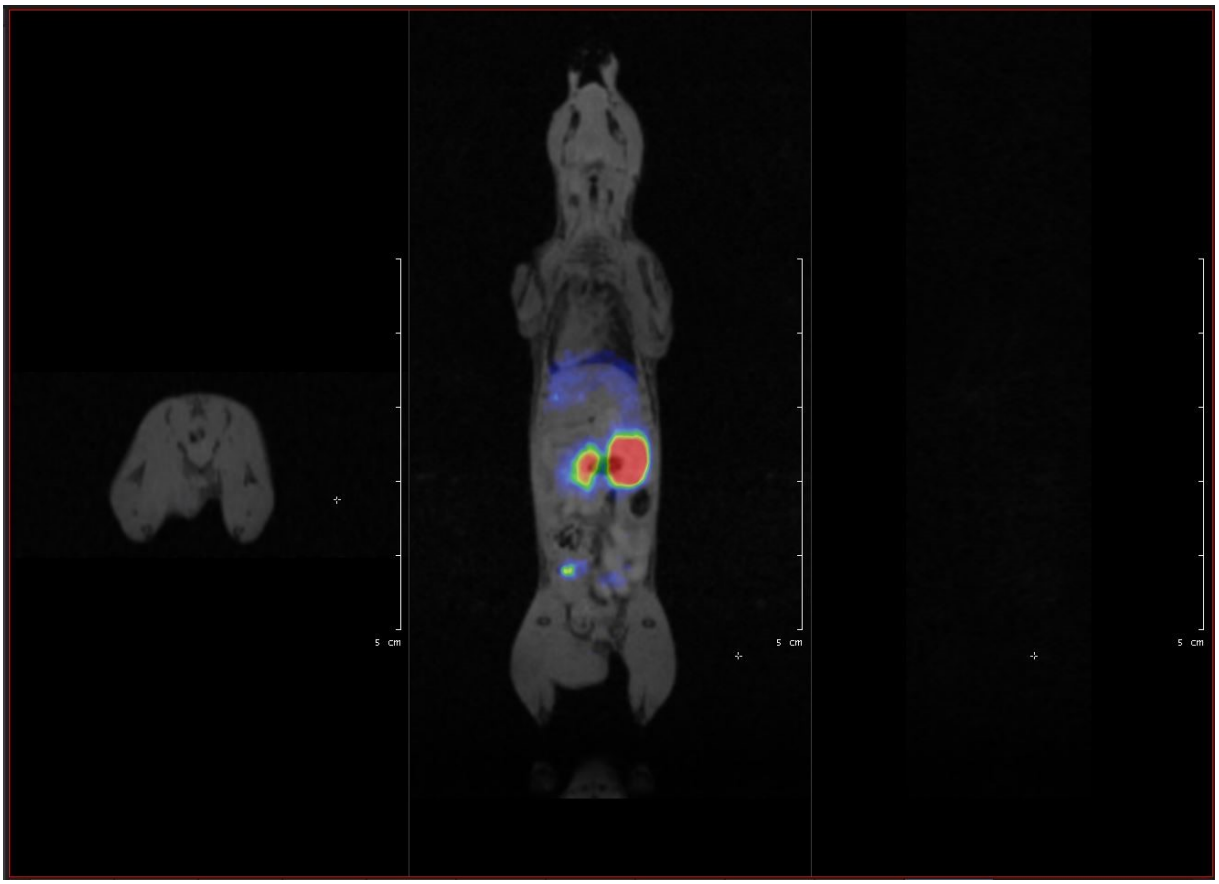

Figure S113. NanoPET/MR imaging of 4T1 (HER2-) tumour-bearing SCID mouse (5CJ). Representative decay-corrected coronal PET images showing slices without kidney (w/o k) (area of the breast fat pad (orthotopic)) and transaxial PET images at 4 hours after the intravenous injection of [[^{52}Mn]Mn(3,9-PC2ABn^{pMA})(H_2O)]-Cys-HER2-affibody.

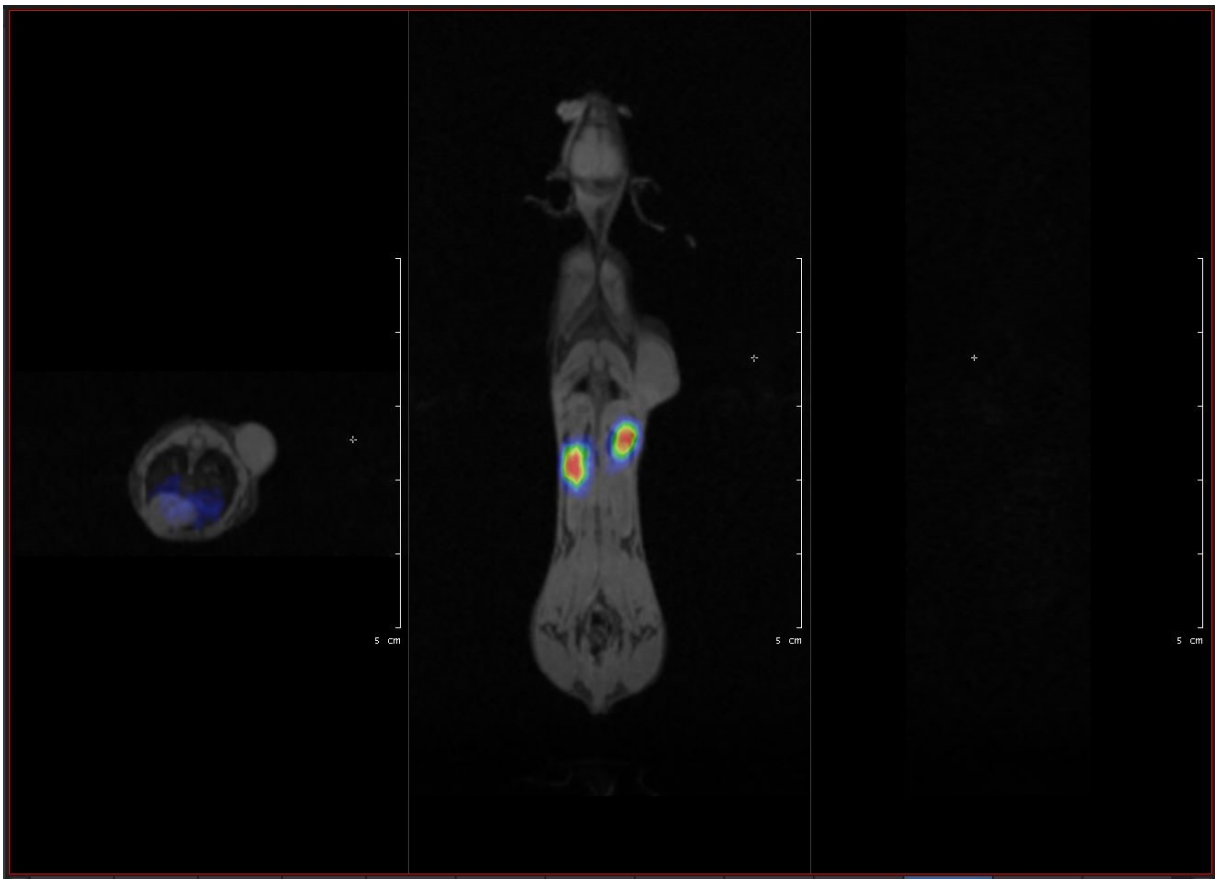

Figure S114. NanoPET/MR imaging of 4T1 (HER2-) tumour-bearing SCID mouse (5CJ). Representative decay-corrected coronal PET images showing slices without kidney (w/o k) (area of the shoulder (heterotopic)) and transaxial PET images at 4 hours after the intravenous injection of [[^{52}Mn]Mn(3,9-PC2ABn$^{p\text{MA}}$)(H_2O)]-Cys-HER2-affibody.

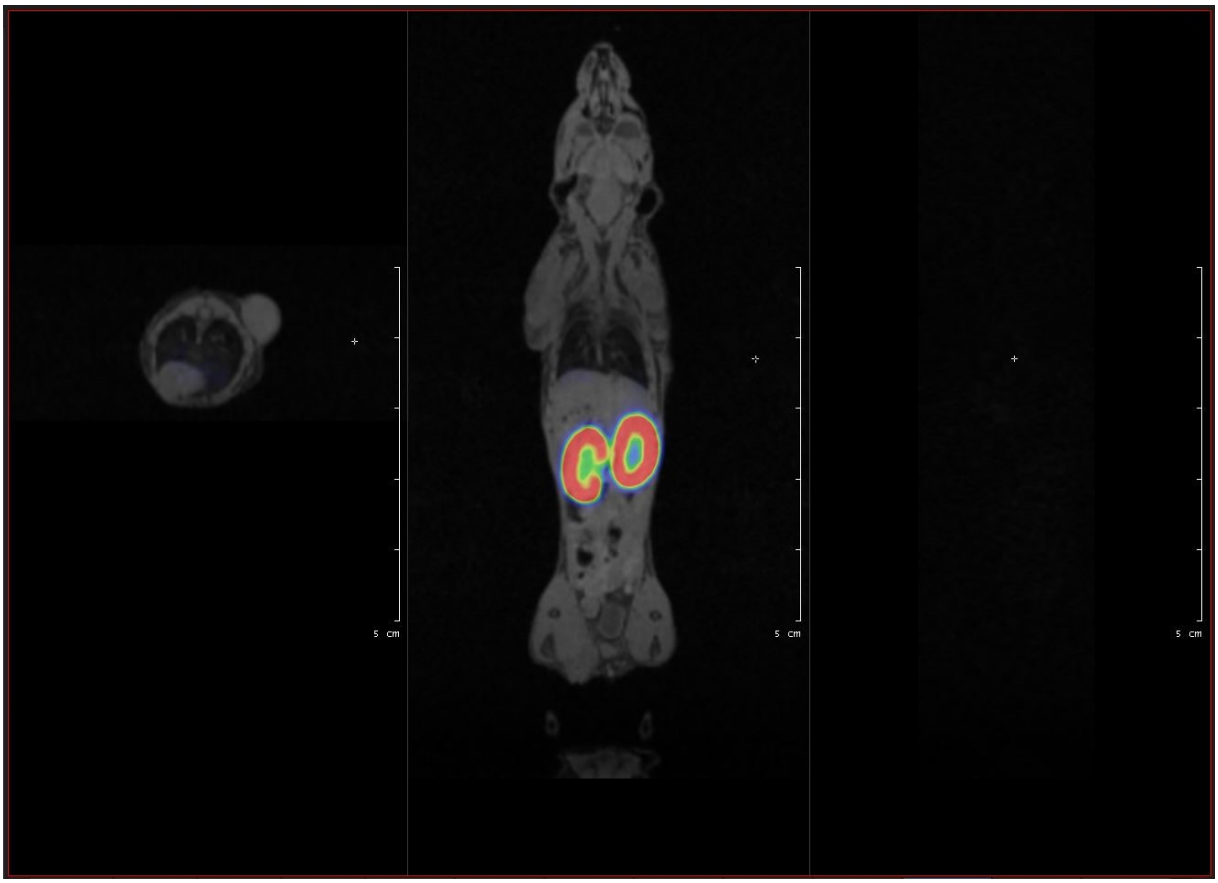

Figure S115. NanoPET/MR imaging of 4T1 (HER2-) tumour-bearing SCID mouse (5CJ). Representative decay-corrected coronal PET images showing slices with kidney (k) and transaxial PET images at 4 hours after the intravenous injection of [[^{52}Mn]Mn(3,9-PC2ABn$^{p\text{MA}}$)(H_2O)]-Cys-HER2-affibody.

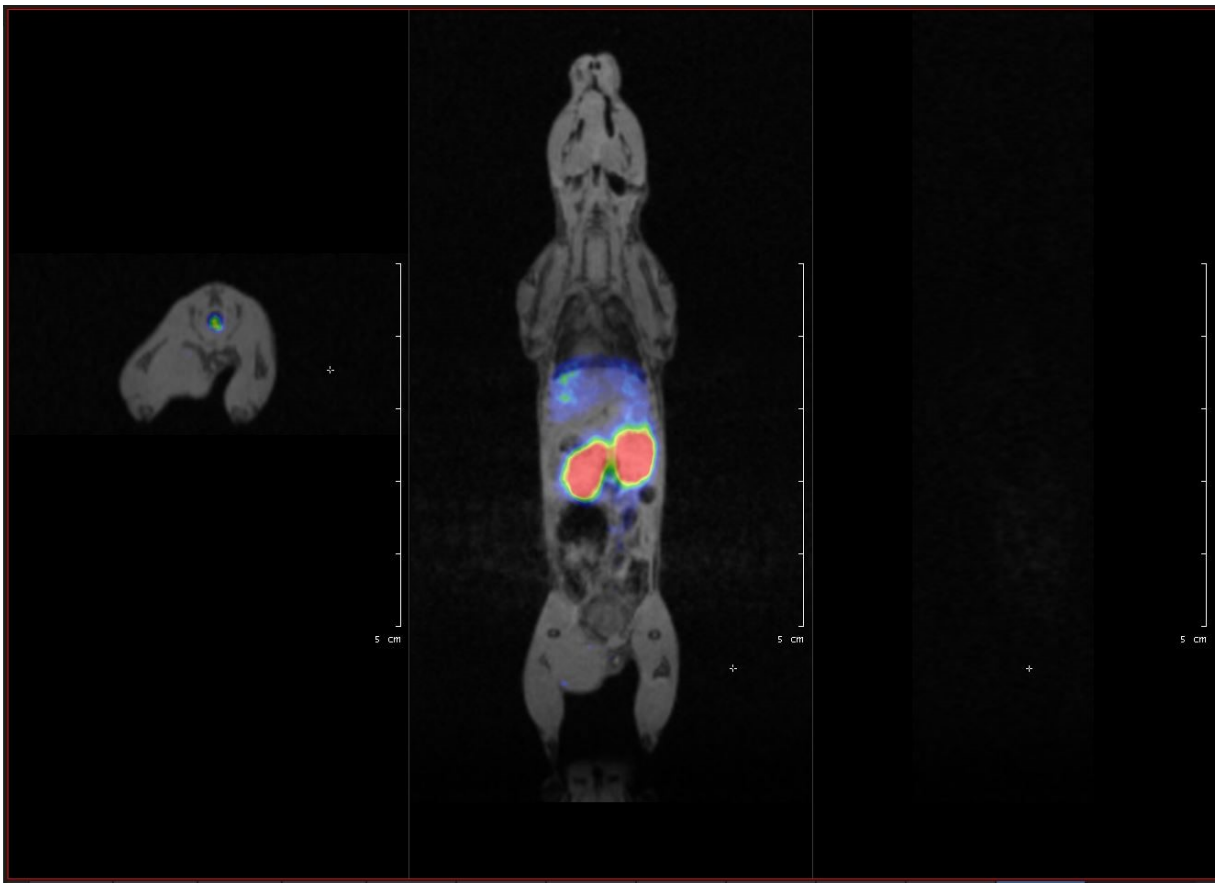

Figure S116. NanoPET/MR imaging of 4T1 (HER2-) tumour-bearing SCID mouse (5CJ). Representative decay-corrected coronal PET images showing slices without kidney (w/o k) (area of the breast fat pad (orthotopic)) and transaxial PET images at 24 hours after the intravenous injection of [[^{52}Mn]Mn(3,9-PC2ABn^{pMA})(H_2O)]-Cys-HER2-affibody.

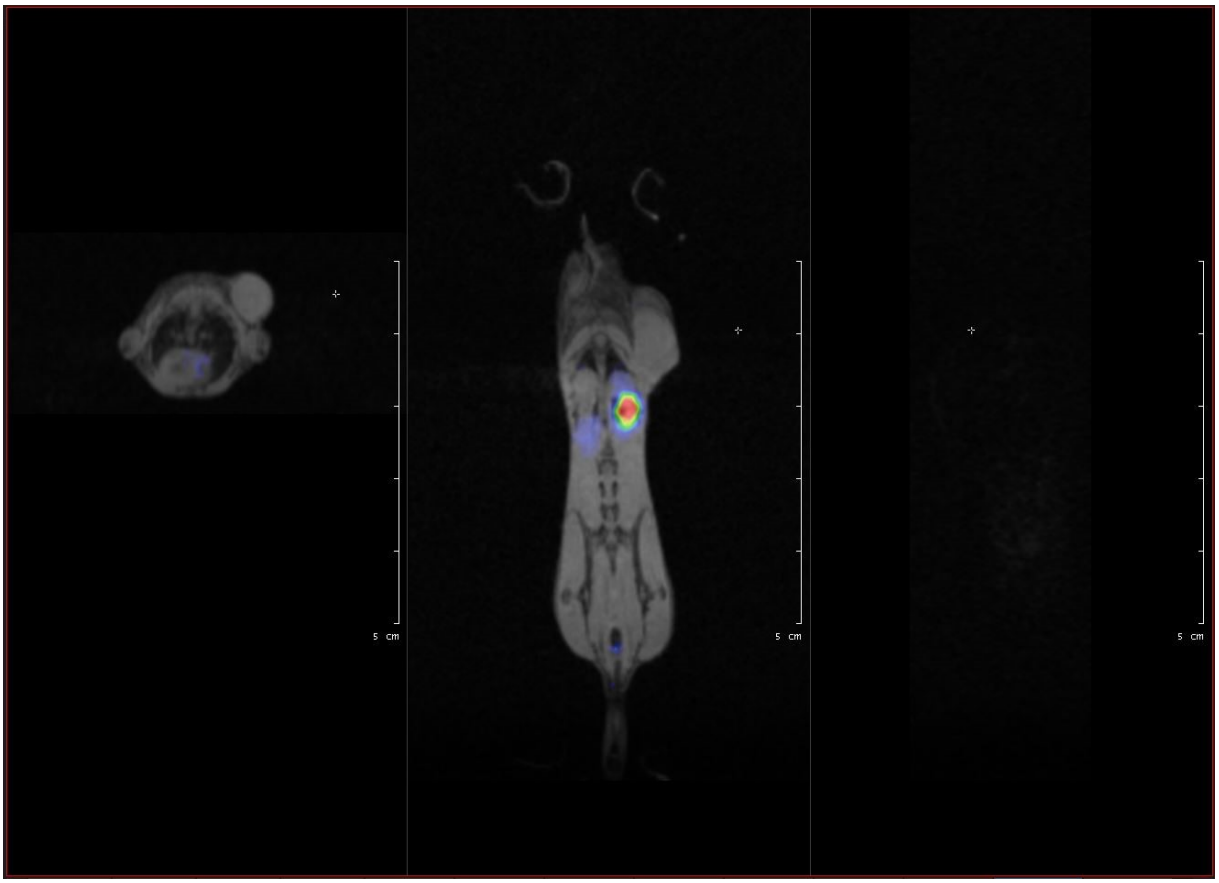

Figure S117. NanoPET/MR imaging of 4T1 (HER2-) tumour-bearing SCID mouse (5CJ). Representative decay-corrected coronal PET images showing slices without kidney (w/o k) (area of the shoulder (heterotopic)) and transaxial PET images at 24 hours after the intravenous injection of [[^{52}Mn]Mn(3,9-PC2ABn$^{p\text{MA}}$)(H_2O)]-Cys-HER2-affibody.

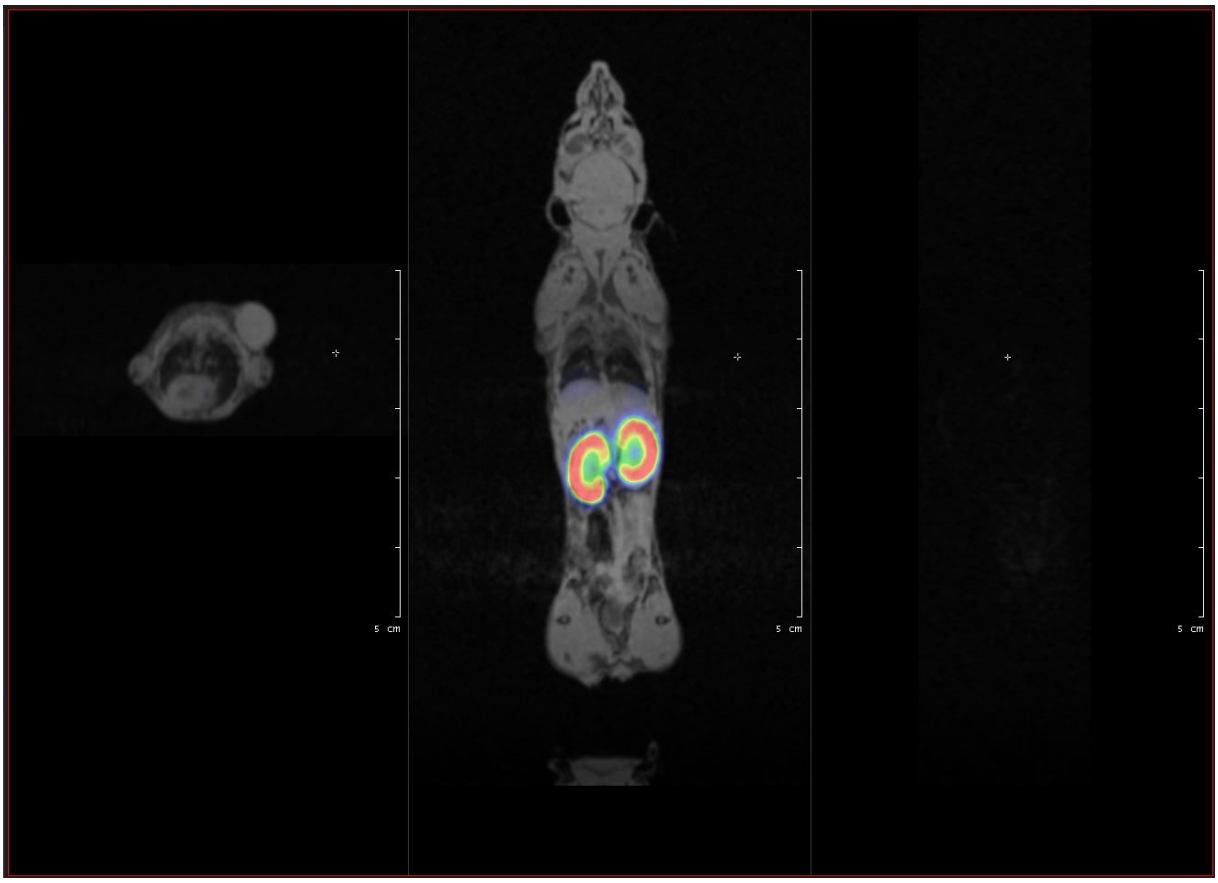

Figure S118. NanoPET/MR imaging of 4T1 (HER2-) tumour-bearing SCID mouse (5CJ). Representative decay-corrected coronal PET images showing slices with kidney (k) and transaxial PET images at 24 hours after the intravenous injection of [[^{52}Mn]Mn(3,9-PC2ABn$^{p\text{MA}}$)(H_2O)]-Cys-HER2-affibody.

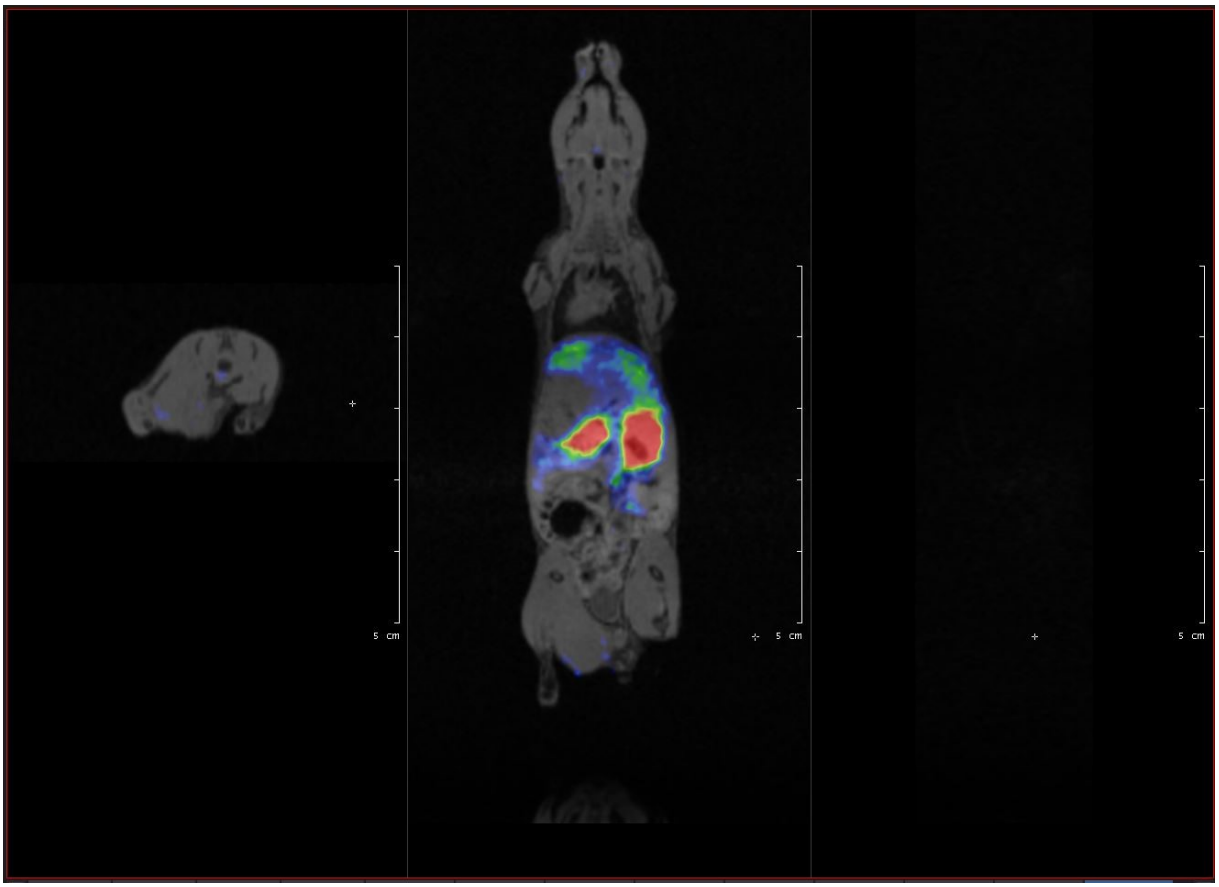

Figure S119. NanoPET/MR imaging of 4T1 (HER2-) tumour-bearing SCID mouse (5CJ). Representative decay-corrected coronal PET images showing slices without kidney (w/o k) (area of the breast fat pad (orthotopic)) and transaxial PET images at 72 hours after the intravenous injection of [[^{52}Mn]Mn(3,9-PC2ABn$^{p\text{MA}}$)(H_2O)]-Cys-HER2-affibody.

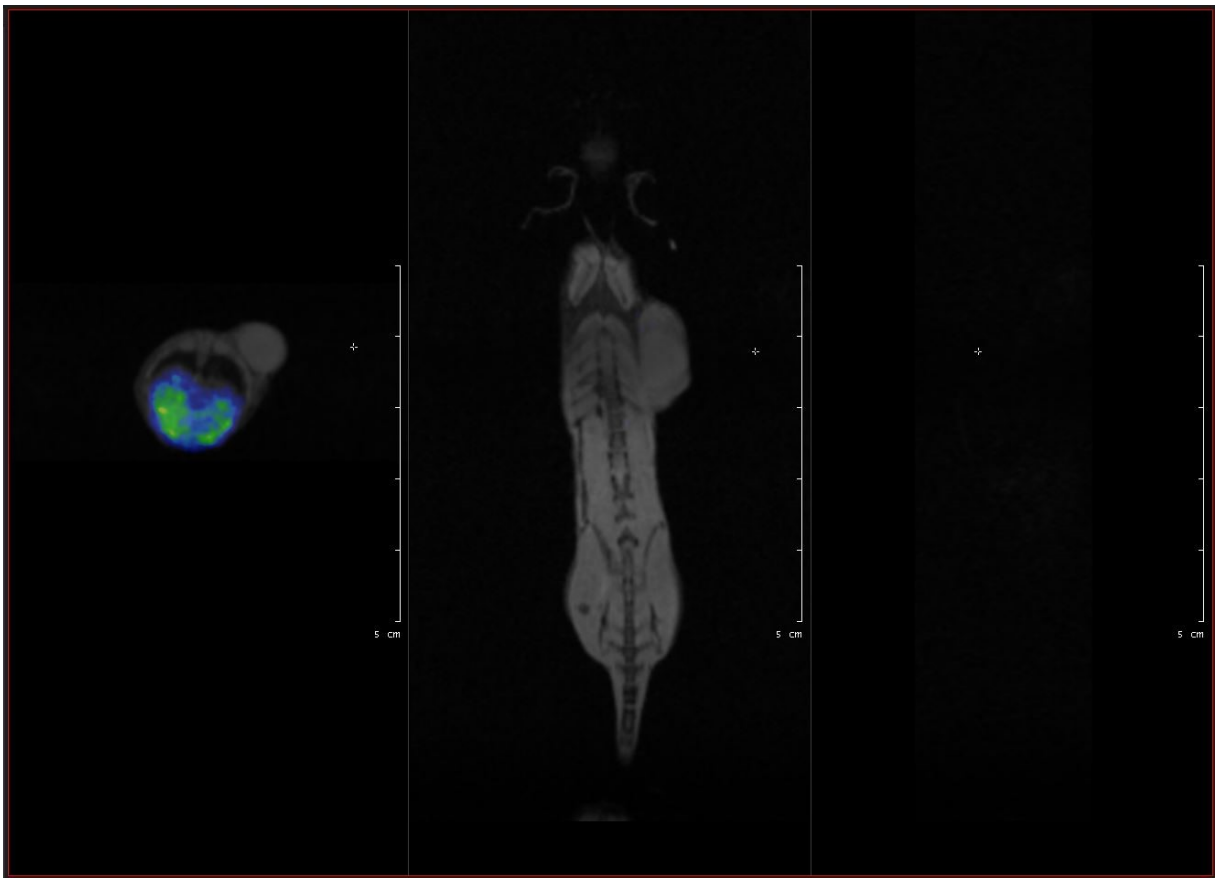

Figure S120. NanoPET/MR imaging of 4T1 (HER2-) tumour-bearing SCID mouse (5CJ). Representative decay-corrected coronal PET images showing slices without kidney (w/o k) (area of the shoulder (heterotopic)) and transaxial PET images at 72 hours after the intravenous injection of [[^{52}Mn]Mn(3,9-PC2ABn$^{p\text{MA}}$)(H_2O)]-Cys-HER2-affibody.

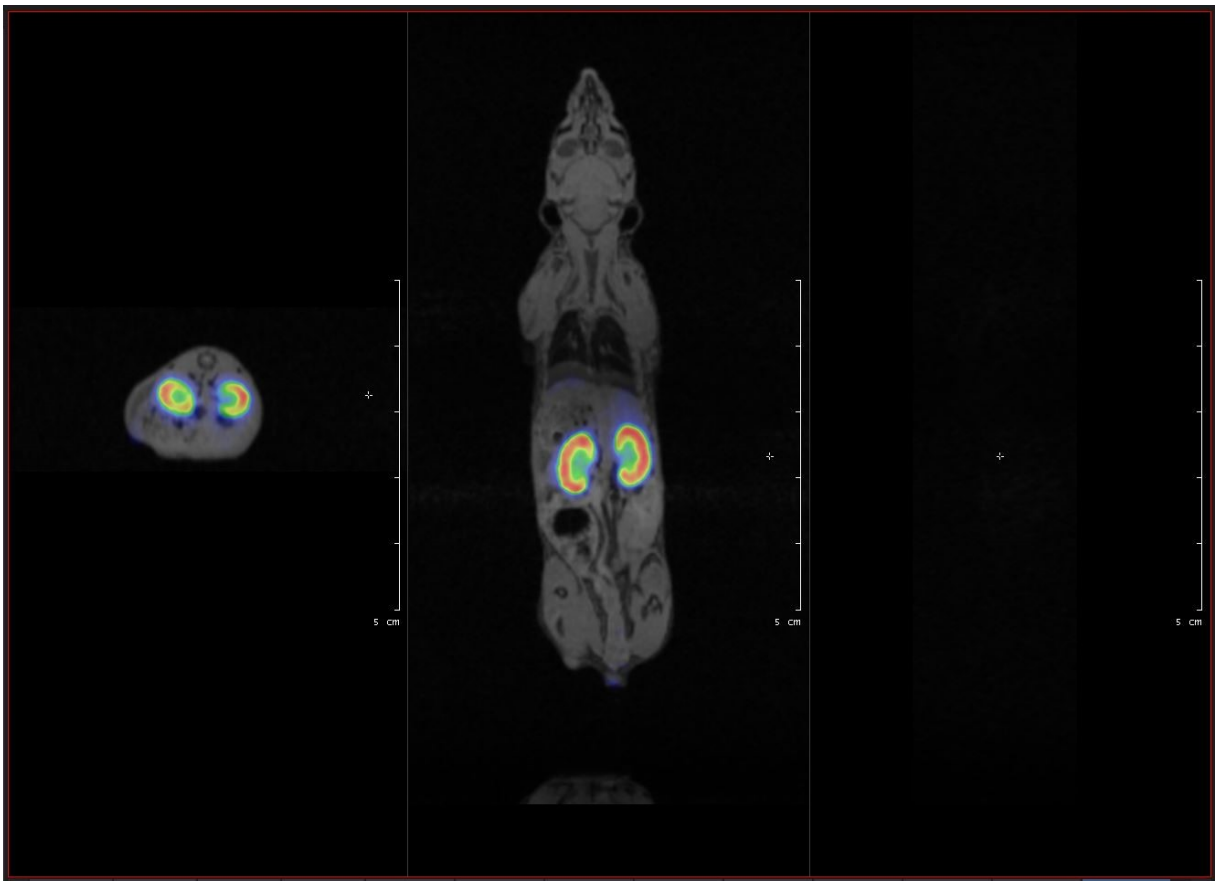

Figure S121. NanoPET/MR imaging of 4T1 (HER2-) tumour-bearing SCID mouse (5CJ). Representative decay-corrected coronal PET images showing slices with kidney (k) and transaxial PET images at 72 hours after the intravenous injection of [[^{52}Mn]Mn(3,9-PC2ABn$^{p\text{MA}}$)(H_2O)]-Cys-HER2-affibody.

4T1 HER2- (2. mouse)

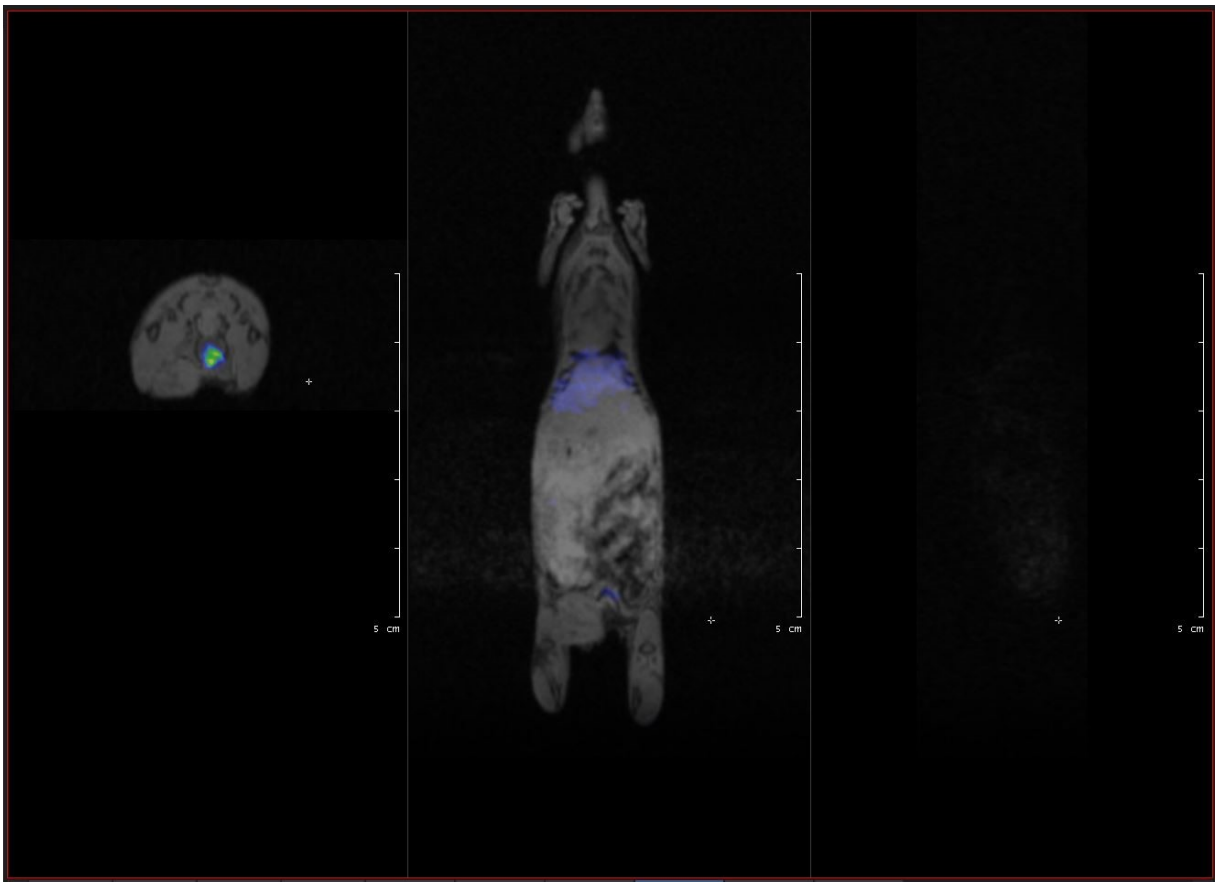

Figure S122. NanoPET/MR imaging of 4T1 (HER2-) tumour-bearing SCID mouse (5CB). Representative decay-corrected coronal PET images showing slices without kidney (w/o k) (area of the breast fat pad (orthotopic)) and transaxial PET images at 4 hours after the intravenous injection of [[^{52}Mn]Mn(3,9-PC2ABn^{pMA})(H_2O)]-Cys-HER2-affibody.

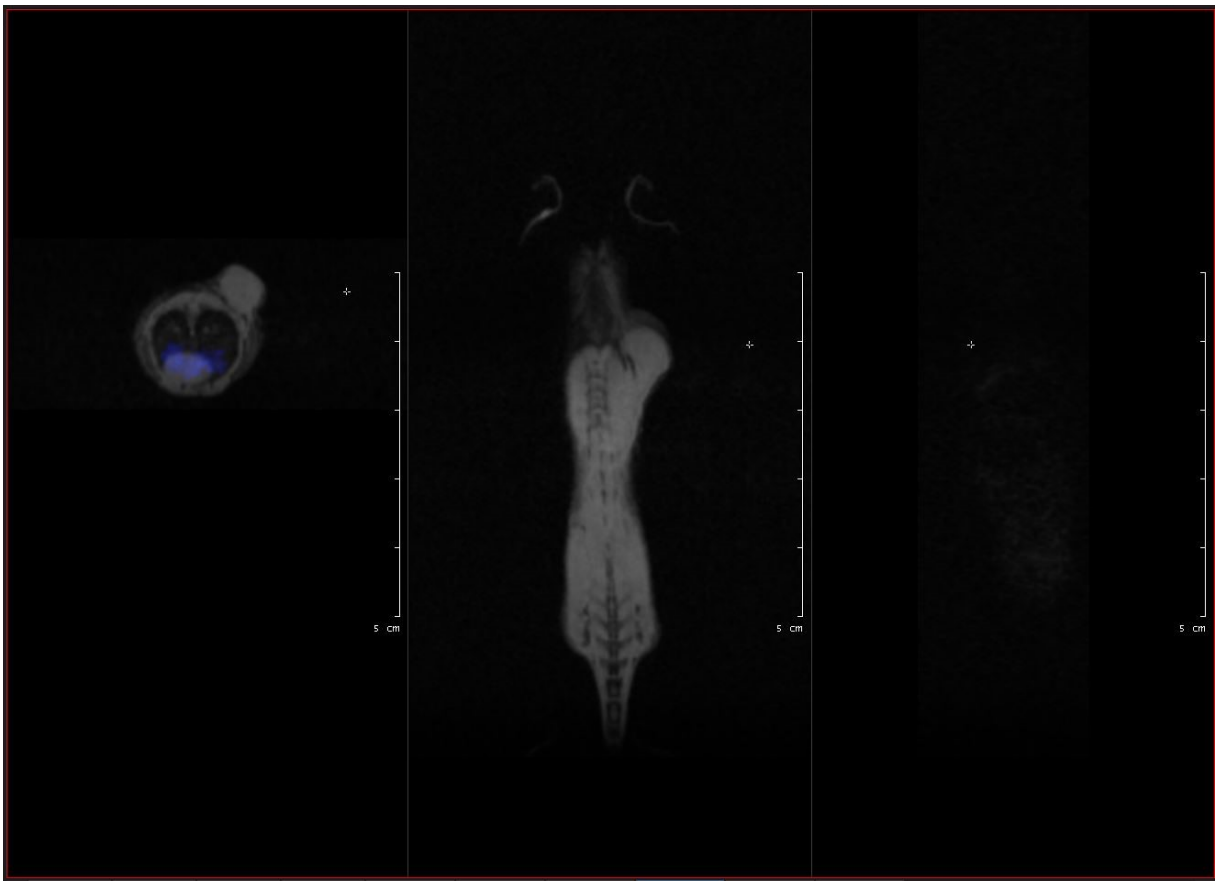

Figure S123. NanoPET/MR imaging of 4T1 (HER2-) tumour-bearing SCID mouse (5CB). Representative decay-corrected coronal PET images showing slices without kidney (w/o k) (area of the shoulder (heterotopic)) and transaxial PET images at 4 hours after the intravenous injection of [[^{52}Mn]Mn(3,9-PC2ABn^{pMA})(H_2O)]-Cys-HER2-affibody.

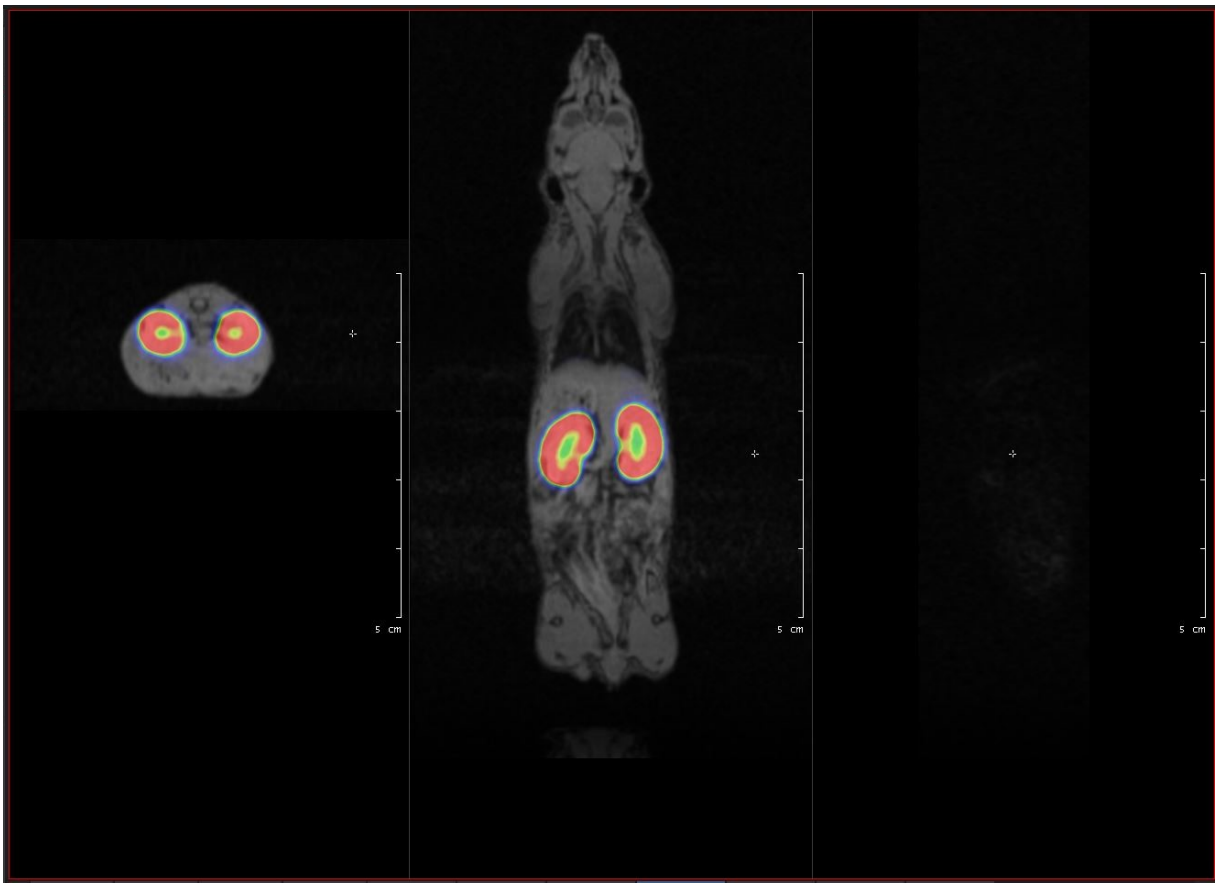

Figure S124. NanoPET/MR imaging of 4T1 (HER2-) tumour-bearing SCID mouse (5CB). Representative decay-corrected coronal PET images showing slices with kidney (k) and transaxial PET images at 4 hours after the intravenous injection of [[^{52}Mn]Mn(3,9-PC2ABn^{pMA})(H_2O)]-Cys-HER2-affibody.

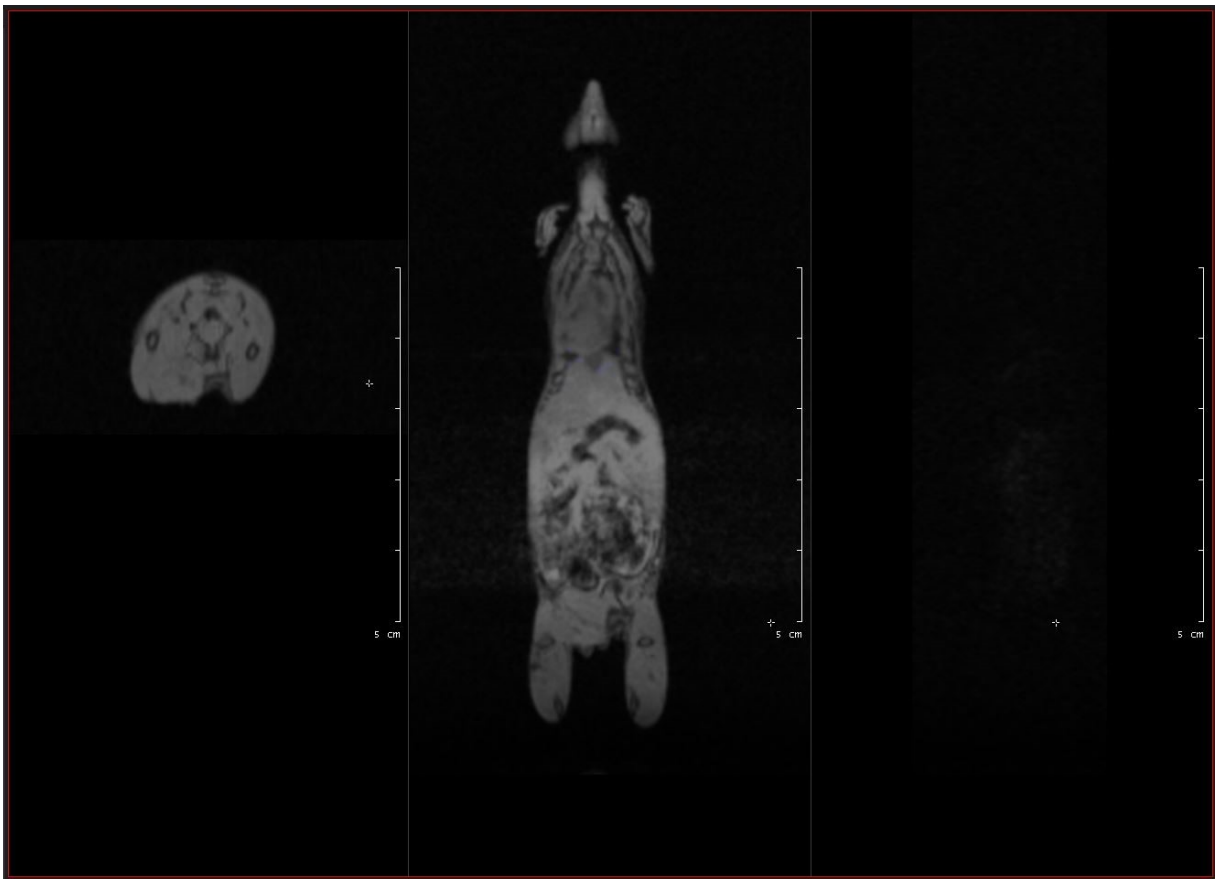

Figure S125. NanoPET/MR imaging of 4T1 (HER2-) tumour-bearing SCID mouse (5CB). Representative decay-corrected coronal PET images showing slices without kidney (w/o k) (area of the breast fat pad (orthotopic)) and transaxial PET images at 24 hours after the intravenous injection of [[^{52}Mn]Mn(3,9-PC2ABn$^{p\text{MA}}$)(H_2O)]-Cys-HER2-affibody.

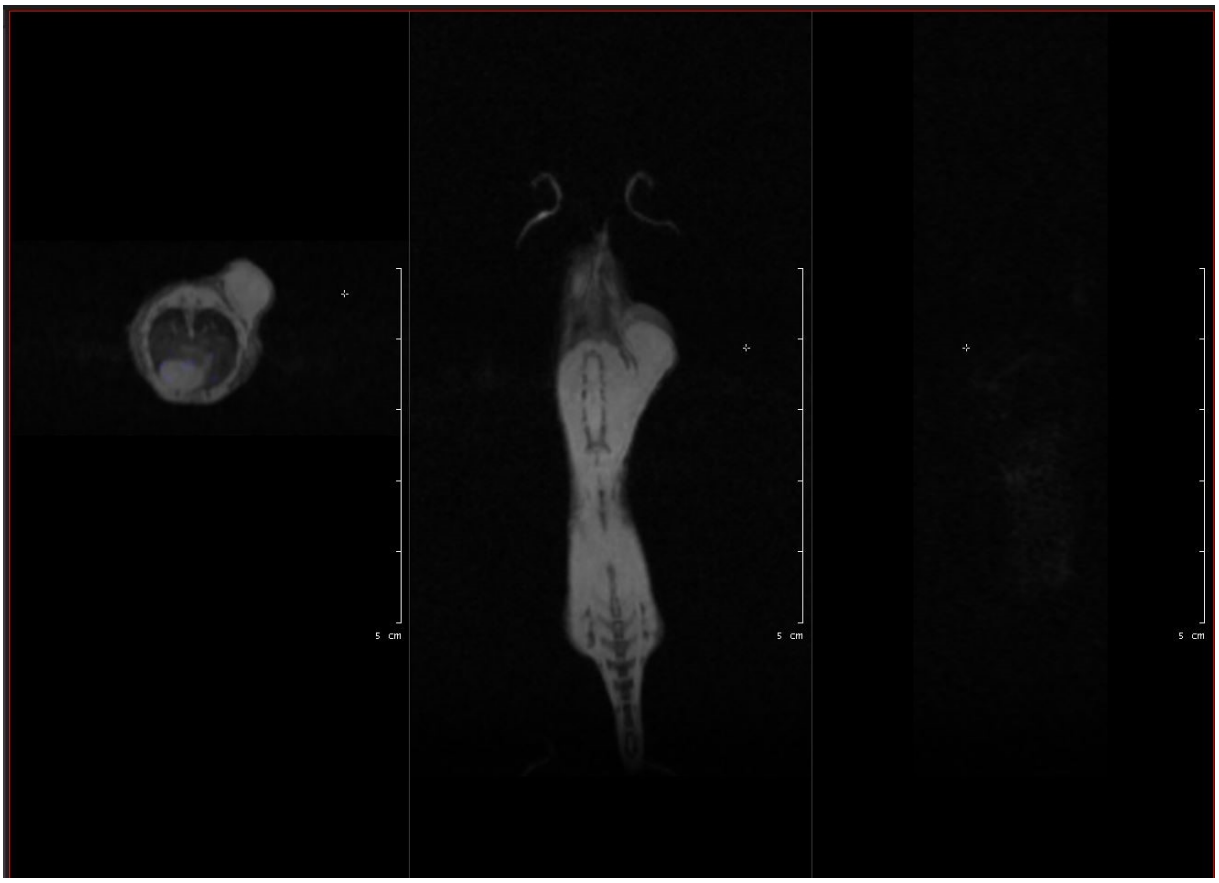

Figure S126. NanoPET/MR imaging of 4T1 (HER2-) tumour-bearing SCID mouse (5CB). Representative decay-corrected coronal PET images showing slices without kidney (w/o k) (area of the shoulder (heterotopic)) and transaxial PET images at 24 hours after the intravenous injection of [[^{52}Mn]Mn(3,9-PC2ABn$^{p\text{MA}}$)(H_2O)]-Cys-HER2-affibody.

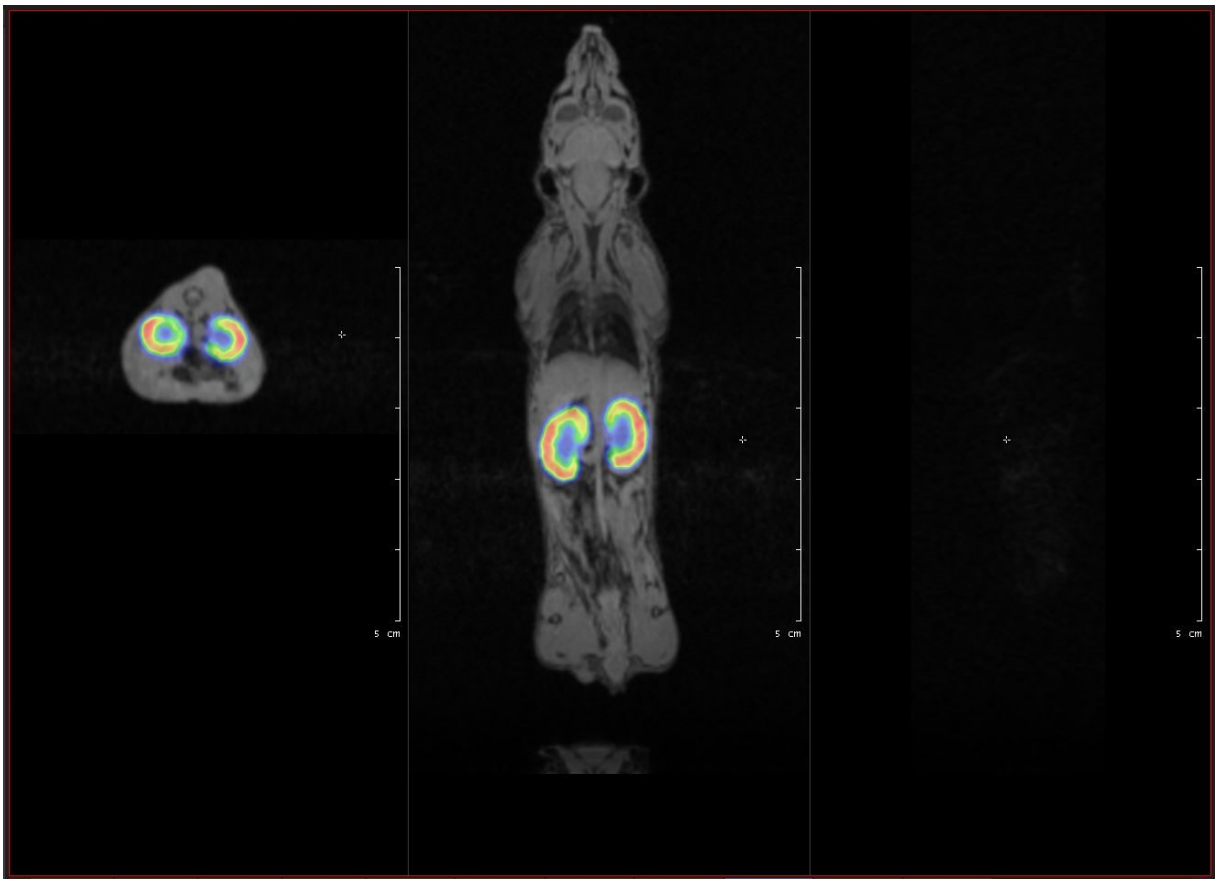

Figure S127. NanoPET/MR imaging of 4T1 (HER2-) tumour-bearing SCID mouse (5CB). Representative decay-corrected coronal PET images showing slices with kidney (k) and transaxial PET images at 24 hours after the intravenous injection of [[^{52}Mn]Mn(3,9-PC2ABn$^{p\text{MA}}$)(H_2O)]-Cys-HER2-affibody.

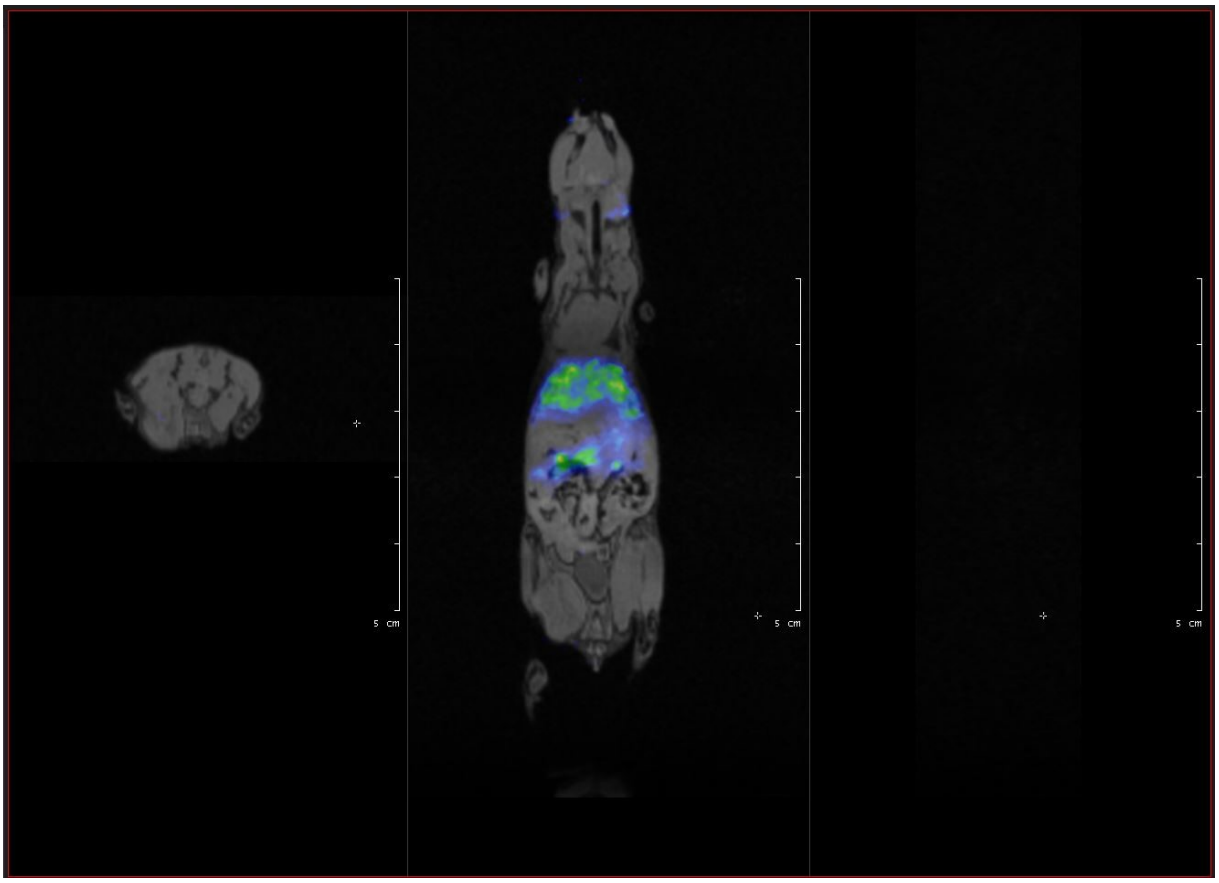

Figure S128. NanoPET/MR imaging of 4T1 (HER2-) tumour-bearing SCID mouse (5CB). Representative decay-corrected coronal PET images showing slices without kidney (w/o k) (area of the breast fat pad (orthotopic)) and transaxial PET images at 72 hours after the intravenous injection of [[^{52}Mn]Mn(3,9-PC2ABn$^{p\text{MA}}$)(H_2O)]-Cys-HER2-affibody.

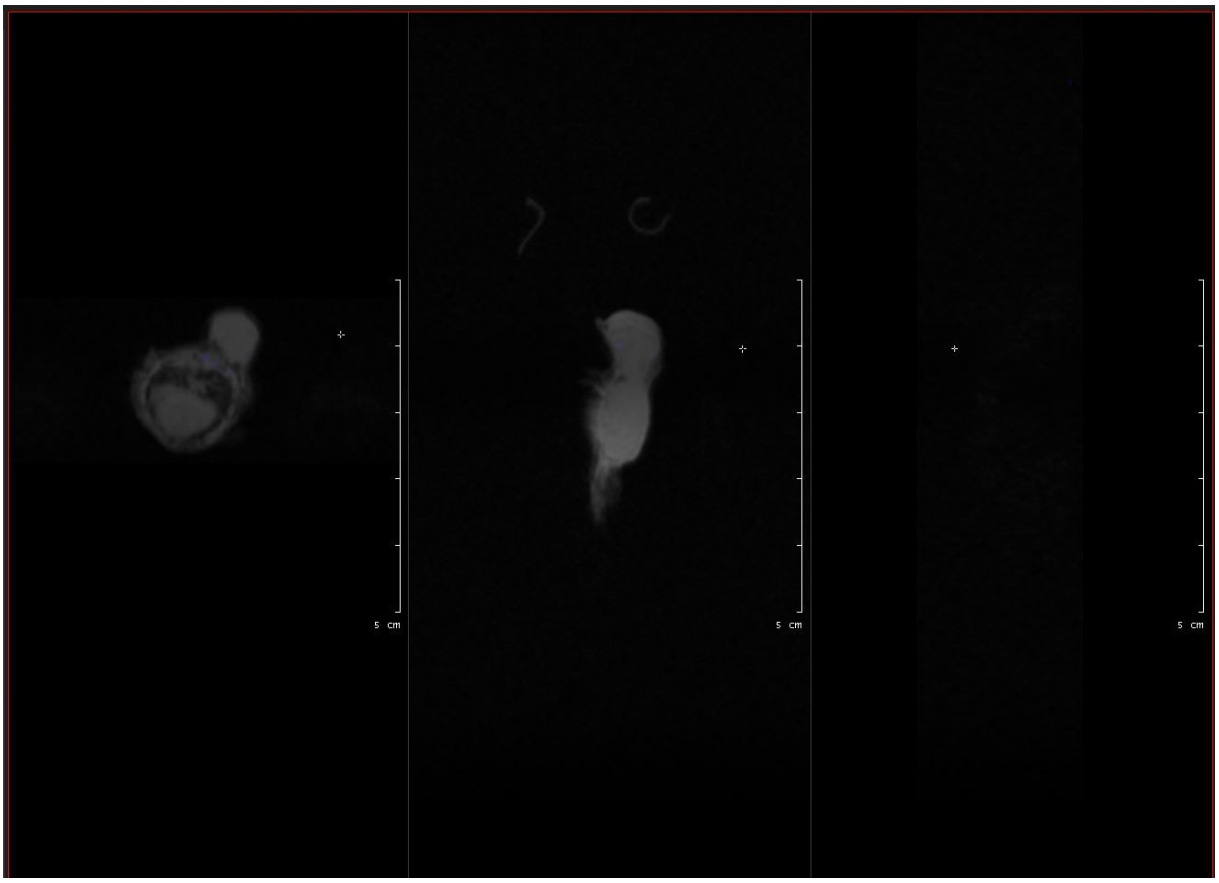

Figure S129. NanoPET/MR imaging of 4T1 (HER2-) tumour-bearing SCID mouse (5CB). Representative decay-corrected coronal PET images showing slices without kidney (w/o k) (area of the shoulder (heterotopic)) and transaxial PET images at 72 hours after the intravenous injection of [[^{52}Mn]Mn(3,9-PC2ABn$^{p\text{MA}}$)(H_2O)]-Cys-HER2-affibody.

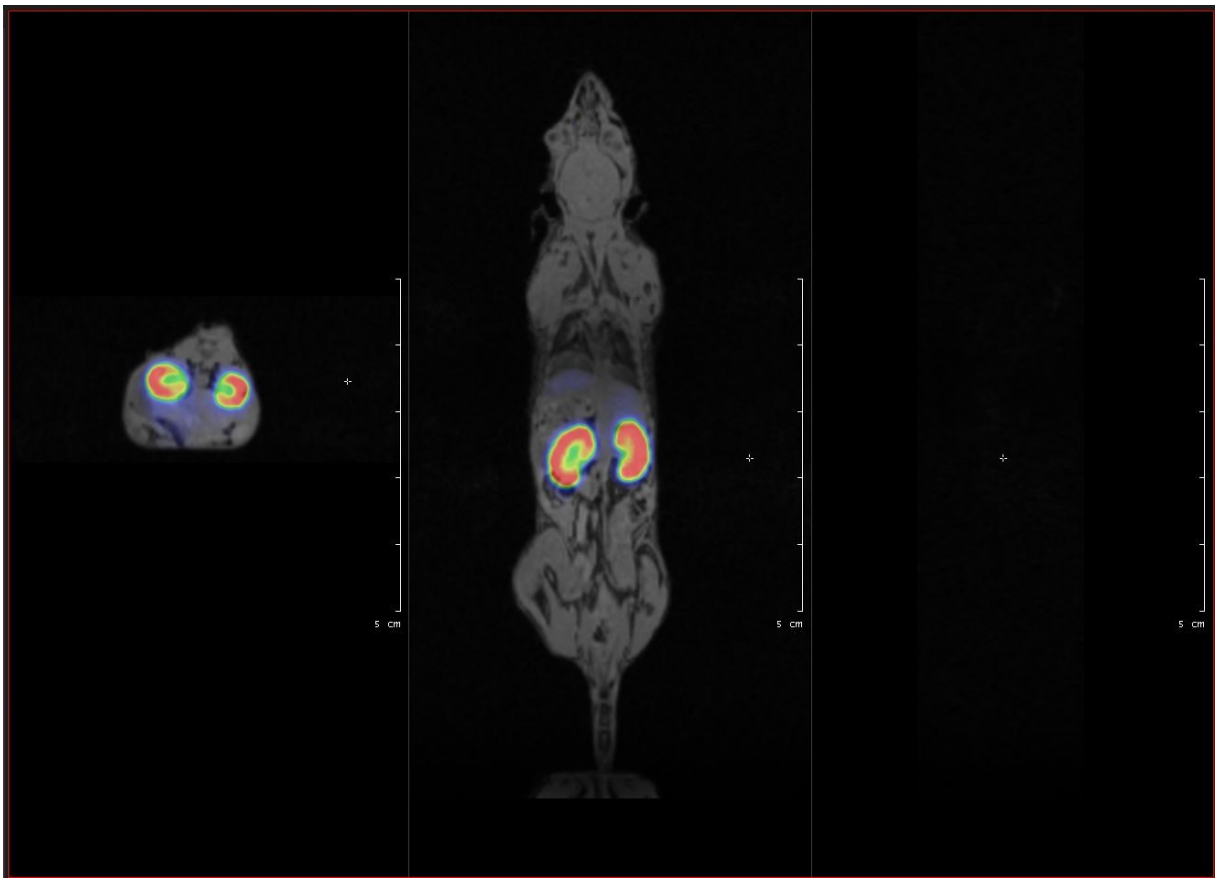

Figure S130. NanoPET/MR imaging of 4T1 (HER2-) tumour-bearing SCID mouse (5CB). Representative decay-corrected coronal PET images showing slices with kidney (k) and transaxial PET images at 72 hours after the intravenous injection of [[^{52}Mn]Mn(3,9-PC2ABn$^{p\text{MA}}$)(H_2O)]-Cys-HER2-affibody.

Table S005. The complete data sets of SUVmean from.

SUVmean								
	time (h)	heart	liver	kidney	tumour back	tumour breast	muscle	average tumour
MDA-MB (HER2+)	4	0.18	1.72	22.19	0.75	1.36	0.07	1.055
	24	0.18	1.23	16.23	0.67	1.18	0.08	0.925
	72	0.16	1.17	10.75	0.63	0.91	0.10	0.770
1. 4T1 (HER2-)	4	0.17	0.67	29.45	0.16	0.15	0.05	0.155
	24	0.07	0.42	6.70	0.09	0.11	0.06	0.100
	48	0.23	1.36	17.19	0.30	0.26	0.14	0.280
	72	0.21	1.23	17.25	0.35	0.32	0.10	0.335
2. 4T1 (HER2-)	4	0.15	0.68	22.88	0.15	0.18	0.05	0.165
	24	0.21	0.94	16.36	0.20	0.28	0.07	0.240
	48	0.14	1.37	14.89	0.26	0.27	0.11	0.265
	72	0.16	1.24	13.28	0.34	0.33	0.11	0.335

Table S006. The complete data sets of SUVmax

SUVmax								
	time (h)	heart	liver	kidney	tumour back	tumour breast	muscle	average tumour
MDA-MB (HER2+)	4	0.36	2.05	25.84	1.21	2.90	0.15	2.055
	24	0.44	1.64	20.80	0.96	1.94	0.21	1.450
	72	0.38	1.61	13.35	1.11	1.70	0.21	1.405
1. 4T1 (HER2-)	4	0.31	1.09	35.93	0.30	0.41	0.29	0.355
	24	0.18	0.62	8.57	0.21	0.59	0.17	0.400
	48	0.47	1.88	20.58	0.61	0.82	0.33	0.715
	72	0.49	1.58	19.13	0.69	0.62	0.22	0.655
2. 4T1 (HER2-)	4	0.26	1.02	28.15	0.27	0.48	0.12	0.375
	24	0.36	1.29	19.01	0.32	0.68	0.18	0.500
	48	0.34	1.91	17.38	0.46	0.55	0.21	0.505
	72	0.31	1.69	16.10	0.52	0.84	0.26	0.680

Table S007. The complete data sets of SUVmean ratio.

SUVmean ratio											
ratio	time (h)	MDA-MB (HER2+)		1. 4T1 (HER2-)		2. 4T1 (HER2-)		4T1 (HER2-) average		4T1 (HER2-) SD	
		Tumour back	Tumour breast	Tumour back	Tumour breast	Tumour back	Tumour breast	Tumour back	Tumour breast	Tumour back	Tumour breast
Tumour / Liver	4	0.43605	0.79070	0.23881	0.22388	0.22059	0.26471	0.22970	0.24429	0.01288	0.02887
	24	0.54472	0.95935	0.21429	0.26190	0.21277	0.29787	0.21353	0.27989	0.00107	0.02543
	48	-	-	0.22059	0.19118	0.18978	0.19708	0.20518	0.19413	0.02178	0.00417
	72	0.53846	0.77778	0.28455	0.26016	0.27419	0.26613	0.27937	0.26315	0.00733	0.00422
Tumour / Blood	4	4.16667	7.55556	0.94118	0.88235	1.00000	1.20000	0.97059	1.04118	0.04159	0.22461
	24	3.72222	6.55556	1.28571	1.57143	0.95238	1.33333	1.11905	1.45238	0.23570	0.16836
	48	-	-	1.30435	1.13043	1.85714	1.92857	1.58075	1.52950	0.39089	0.56437
	72	3.93750	5.68750	1.66667	1.52381	2.12500	2.06250	1.89583	1.79315	0.32409	0.38091
Tumour / Liver	4	0.03380	0.06129	0.00543	0.00509	0.00656	0.00787	0.00599	0.00648	0.00079	0.00196
	24	0.04128	0.07270	0.01343	0.01642	0.01222	0.01711	0.01283	0.01677	0.00085	0.00049
	48	-	-	0.01745	0.01513	0.01746	0.01813	0.01746	0.01663	0.00001	0.00213
	72	0.05860	0.08465	0.02029	0.01855	0.02560	0.02485	0.02295	0.02170	0.00376	0.00445
Tumour / Muscle	4	10.71429	19.42857	3.20000	3.00000	3.00000	3.60000	3.10000	3.30000	0.14142	0.42426
	24	8.37500	14.75000	1.50000	1.83333	2.85714	4.00000	2.17857	2.91667	0.95964	1.53206
	48	-	-	2.14286	1.85714	2.36364	2.45455	2.25325	2.15584	0.15611	0.42243
	72	6.30000	9.10000	3.50000	3.20000	3.09091	3.00000	3.29545	3.10000	0.28927	0.14142

References

1. H. E. Gottlieb, V. Kotlyar and A. Nudelman, NMR Chemical Shifts of Common Laboratory Solvents as Trace Impurities, *The Journal of Organic Chemistry*, 1997, **62**, 7512-7515.
2. W. D. Kim, D. C. Hrncir, G. E. Kiefer and A. D. Sherry, Synthesis, Crystal Structure, and Potentiometry of Pyridine-Containing Tetraaza Macrocyclic Ligands with Acetate Pendant Arms, *Inorganic Chemistry*, 1995, **34**, 2225-2232.
3. Z. Garda, E. Molnár, N. Hamon, J. L. Barriada, D. Esteban-Gómez, B. Váradi, V. Nagy, K. Pota, F. K. Kálmán, I. Tóth, N. Lihi, C. Platas-Iglesias, É. Tóth, R. Tripier and G. Tircsó, Complexation of Mn(II) by Rigid Pyclen Diacetates: Equilibrium, Kinetic, Relaxometric, Density Functional Theory, and Superoxide Dismutase Activity Studies, *Inorganic Chemistry*, 2021, **60**, 1133-1148.
4. L. Zekany and I. Nagypal, in *Computational Methods for the Determination of Formation Constants*, ed. D. J. Leggett, Springer US, Boston, MA, 1985, DOI: 10.1007/978-1-4684-4934-1_8, pp. 291-353.
5. E. M. Gale, I. P. Atanasova, F. Blasi, I. Ay and P. Caravan, A Manganese Alternative to Gadolinium for MRI Contrast, *Journal of the American Chemical Society*, 2015, **137**, 15548-15557.
6. G. J. Topping, P. Schaffer, C. Hoehr, T. J. Ruth and V. Sossi, Manganese-52 positron emission tomography tracer characterization and initial results in phantoms and in vivo, *Medical Physics*, 2013, **40**, 042502.
7. P. Roepstorff and J. Fohlman, Proposal for a common nomenclature for sequence ions in mass spectra of peptides, *Biomedical mass spectrometry*, 1984, **11**, 601.
8. R. S. Johnson, S. A. Martin, K. Biemann, J. T. Stults and J. T. Watson, Novel fragmentation process of peptides by collision-induced decomposition in a tandem mass spectrometer: differentiation of leucine and isoleucine, *Analytical Chemistry*, 1987, **59**, 2621-2625.
9. I. A. Papayannopoulos, The interpretation of collision-induced dissociation tandem mass spectra of peptides, *Mass Spectrometry Reviews*, 1995, **14**, 49-73.
10. J. K. Eng, A. L. McCormack and J. R. Yates, An approach to correlate tandem mass spectral data of peptides with amino acid sequences in a protein database, *Journal of the American Society for Mass Spectrometry*, 1994, **5**, 976-989.
11. D. N. Perkins, D. J. Pappin, D. M. Creasy and J. S. Cottrell, Probability-based protein identification by searching sequence databases using mass spectrometry data, *Electrophoresis*, 1999, **20**, 3551-3567.
12. J. E. Elias and S. P. Gygi, Target-decoy search strategy for increased confidence in large-scale protein identifications by mass spectrometry, *Nature Methods*, 2007, **4**, 207-214.
13. J. E. Elias and S. P. Gygi, Target-decoy search strategy for mass spectrometry-based proteomics, *Methods in molecular biology (Clifton, N.J.)*, 2010, **604**, 55-71.
14. https://www.bioinfor.com/).
15. A. I. Nesvizhskii and R. Aebersold, Interpretation of shotgun proteomic data: the protein inference problem, *Molecular & cellular proteomics : MCP*, 2005, **4**, 1419-1440.
16. A. Shevchenko, H. Tomas, J. Havli, J. V. Olsen and M. Mann, In-gel digestion for mass spectrometric characterization of proteins and proteomes, *Nature Protocols*, 2006, **1**, 2856-2860.

17. G. Petrareanu, M. C. Balasu, A. M. Vacaru, C. V. Munteanu, A. E. Ionescu, I. Matei and S. E. Szedlacsek, Phosphoketolases from Lactococcus lactis, Leuconostoc mesenteroides and Pseudomonas aeruginosa: dissimilar sequences, similar substrates but distinct enzymatic characteristics, *Applied microbiology and biotechnology*, 2014, **98**, 7855-7867.
18. Y. Perez-Riverol, A. Csordas, J. Bai, M. Bernal-Llinares, S. Hewapathirana, D. J. Kundu, A. Inuganti, J. Griss, G. Mayer, M. Eisenacher, E. Pérez, J. Uszkoreit, J. Pfeuffer, T. Sachsenberg, S. Yilmaz, S. Tiwary, J. Cox, E. Audain, M. Walzer, A. F. Jarnuczak, T. Ternent, A. Brazma and J. A. Vizcaíno, The PRIDE database and related tools and resources in 2019: improving support for quantification data, *Nucleic acids research*, 2019, **47**, D442-d450.
19. C. Gebhardt, M. Lehmann, M. M. Reif, M. Zacharias and T. Cordes, Molecular and spectroscopic characterization of green and red cyanine fluorophores from the Alexa Fluor and AF series, *bioRxiv*, 2020, DOI: 10.1101/2020.11.13.381152, 2020.2011.2013.381152.
20. K. Subik, J.-F. Lee, L. Baxter, T. Strzepek, D. Costello, P. Crowley, L. Xing, M.-C. Hung, T. Bonfiglio, D. G. Hicks and P. Tang, The Expression Patterns of ER, PR, HER2, CK5/6, EGFR, Ki-67 and AR by Immunohistochemical Analysis in Breast Cancer Cell Lines.*Journal*, 2010, **4**, 35-41.